Climate Change and Extreme Events

Climate Change and Extreme Events

Edited by

Ali Fares
College of Agriculture and Human Sciences, Prairie View A&M University, Prairie View, TX, United States

ELSEVIER

Elsevier
Radarweg 29, PO Box 211, 1000 AE Amsterdam, Netherlands
The Boulevard, Langford Lane, Kidlington, Oxford OX5 1GB, United Kingdom
50 Hampshire Street, 5th Floor, Cambridge, MA 02139, United States

Copyright © 2021 Elsevier Inc. All rights reserved.

No part of this publication may be reproduced or transmitted in any form or by any means, electronic or mechanical, including photocopying, recording, or any information storage and retrieval system, without permission in writing from the publisher. Details on how to seek permission, further information about the Publisher's permissions policies and our arrangements with organizations such as the Copyright Clearance Center and the Copyright Licensing Agency, can be found at our website: www.elsevier.com/permissions.

This book and the individual contributions contained in it are protected under copyright by the Publisher (other than as may be noted herein).

Notices
Knowledge and best practice in this field are constantly changing. As new research and experience broaden our understanding, changes in research methods, professional practices, or medical treatment may become necessary.

Practitioners and researchers must always rely on their own experience and knowledge in evaluating and using any information, methods, compounds, or experiments described herein. In using such information or methods they should be mindful of their own safety and the safety of others, including parties for whom they have a professional responsibility.

To the fullest extent of the law, neither the Publisher nor the authors, contributors, or editors, assume any liability for any injury and/or damage to persons or property as a matter of products liability, negligence or otherwise, or from any use or operation of any methods, products, instructions, or ideas contained in the material herein.

Library of Congress Cataloging-in-Publication Data
A catalog record for this book is available from the Library of Congress

British Library Cataloguing-in-Publication Data
A catalogue record for this book is available from the British Library

ISBN: 978-0-12-822700-8

For information on all Elsevier publications
visit our website at https://www.elsevier.com/books-and-journals

Publisher: Candice Janco
Acquisitions Editor: Louisa Munro
Editorial Project Manager: Alice Grant
Production Project Manager: Sujatha Thirugnana Sambandam
Cover Designer: Victoria Pearson Esser

Typeset by SPi Global, India

ELSEVIER Book Aid International Working together to grow libraries in developing countries
www.elsevier.com • www.bookaid.org

Contributors

Vidya Anderson
Climate Lab, Department of Physical & Environmental Sciences, University of Toronto Scarborough, Toronto, ON, Canada

Ripendra Awal
College of Agriculture and Human Sciences, Prairie View A&M University, Prairie View, TX, United States

Mark Anthony Ayure-Inga Agana
University of Arkansas, Fayetteville, AR, United States

Bilal M. Ayyub
Department of Civil and Environmental Engineering, Director of the Center for Technology and Systems Management, University of Maryland, College Park, MD, United States

Philip B. Bedient
Department of Civil and Environmental Engineering, Rice University, Houston, TX, United States

Normand E. Bergeron
Institut National de la Recherche Scientifique, Centre Eau Terre Environnement; Centre Interuniversitaire de Recherche sur le Saumon Atlantique, Québec City, QC, Canada

Udit Bhatia
Indian Institute of Technology Gandhinagar, Gandhinagar, India

Claudine Boyer
Institut National de la Recherche Scientifique, Centre Eau Terre Environnement, Québec City, QC, Canada

Daniel Caissie
Fisheries and Oceans Canada, Moncton, NB, Canada

Romney B. Duffey
Private, Idaho Falls, ID, United States

Zheng N. Fang
Civil Engineering, The University of Texas at Arlington, Arlington, TX, United States

Ali Fares
College of Agriculture and Human Sciences, Prairie View A&M University, Prairie View, TX, United States

Andrew J. Felton
Department of Wildland Resources and The Ecology Center, Utah State University, Logan, UT, United States

Vittorio (Victor) A. Gensini
Northern Illinois University, DeKalb, IL, United States

William A. Gough
Climate Lab; Department of Physical & Environmental Sciences, University of Toronto Scarborough, Toronto, ON, Canada

Hamideh Habibi
College of Agriculture and Human Sciences, Prairie View A&M University, Prairie View, TX, United States

Asif Ishtiaque
School for Environment and Sustainability, University of Michigan, Ann Arbor, MI, United States

Nishant Kamboj
Indian Institute of Technology Gandhinagar, Gandhinagar, India

Shahzaib Khan
Indian Institute of Technology Gandhinagar, Gandhinagar, India

Tu Dam Ngoc Le
Faculty of Architecture, MienTrung University of Civil Engineering, Tuy Hoa, Phu Yen, Vietnam

Dongfeng Li
Civil Engineering, The University of Texas at Arlington, Arlington, TX, United States

Taha B.M.J. Ouarda
Institut National de la Recherche Scientifique, Centre Eau Terre Environnement, Québec City, QC, Canada

André St-Hilaire
Institut National de la Recherche Scientifique, Centre Eau Terre Environnement; Centre Interuniversitaire de Recherche sur le Saumon Atlantique, Québec City, QC, Canada

Yating Zhang
Center for Technology and Systems Management, University of Maryland, College Park, MD, Unites States

Enrico Zio
Energy Department, Politecnico di Milano, Milano, Italy; MINE ParisTech, PSL Research University, CRC, Sophia Antipolis, France; Eminent Scholar, Department of Nuclear Engineering, College of Engineering, Kyung Hee University, Seoul, Republic of Korea

CHAPTER

Extreme events and climate change: A multidisciplinary approach

1

Ali Fares, Hamideh Habibi, and Ripendra Awal

College of Agriculture and Human Sciences, Prairie View A&M University, Prairie View, TX, United States

Introduction

An event can be identified as an extreme (weather or climate) when the weather or climate variable exceeds a threshold, close to the upper or lower ends of the usual range over a predefined duration (Seneviratne et al., 2012). Many studies showed that frequency, intensity, spatial extent, duration, and timing of heavy-to-extreme events have increased across the world, which could be because of global warming (Norouzi et al., 2019; Stott, 2016; Boo et al., 2006). Global warming/climate change effects have accelerated in recent decades (Sheffield and Wood, 2011). According to the US National Climate Assessment, over the past 50 years, the number and strength of weather-related natural catastrophes, such as major hurricanes, heat waves, floods, droughts, and torrential downpours, have increased in the United States (http://www.c2es.org/content/national-climate-assessment/).

As a result of increasing greenhouse gases from anthropogenic sources (Solomon et al., 2007), significant trends have been observed in maximum and minimum temperature extremes in many areas across the world, which cause fewer cold days and nights and more warm days and nights (Heim Jr, 2015). Safeeq et al. (2013) analyzed trends in observed temperature during 1969–2007 on the island of Oahu, Hawaii, to evaluate the spatial and temporal variability as well as quantify the relationship between local temperature and regional climate indices. Their results revealed that despite the substantial spatial and temporal variability in the temperature trends on the island, there was a 0.17 °C/decade islandwide minimum temperature increase during the four decades of their study period. The complexity of the issue of climate change and extreme events (Fares et al., 2014; Habibi and Seo, 2018) requires an interdisciplinary approach to help understand the difficulty of the problem and also to the interconnectivity between climate change and extreme events. This book uses a multidisciplinary approach in addressing extreme events under a changing climate based on an in-depth analysis of past and current conditions as well as future outlooks. In addition, it discusses the relationship between climate change and extreme events and their impact on several aspects of human daily activities and manifestations.

Climate Change and Extreme Events. https://doi.org/10.1016/B978-0-12-822700-8.00019-6
Copyright © 2021 Elsevier Inc. All rights reserved.

Overview of the chapters

The book comprises 12 chapters; after the first chapter, the rest are grouped into three complementing sections. The first section addresses temperatures and severe convective storms; the second section of the book contains chapters related to hydrological responses that give an overview of the current knowledge and future outlook of the respective topics. The third section of the book covers mitigation, adaptation measures, and governance. This section discusses the potential impacts of climate change and extreme events on ecosystem responses, lifeline infrastructures, green infrastructure, and sea-level rise. It also reports on how governance and policies are dealing with climate change and extreme events.

Weather parameters

This section covers three chapters. Chapter 2, Temperature Extremes in a Changing Climate, covers the past and projected hot temperature extremes and their expected social and environmental impacts. Surface temperature and the occurrences of hot extremes have been increasing since the preindustrial times (almost 140 years ago), which could be the consequence of global warming (Seneviratne et al., 2012; IPCC (Intergovernmental Panel on Climate Change), 2013). An in-depth overview of observed changes in temperature and its impact are discussed in the first part of the chapter. The indices and metrics commonly used for evaluating and predicting the changes in temperature extremes followed by the observational data collection and analysis are presented. Different regional and global climate models, as well as integrated and downscaling techniques, are one of the main components of understanding the future/projected temperature condition of the earth. These models and techniques are discussed in detail in the second part of the chapter. The last part of Chapter 2 gives us an overview of mitigation and adaptation strategies (e.g., reducing greenhouse gas emissions and increasing the resilience of infrastructure and critical buildings) applied across the United States. The methods for evaluation and optimization of these strategies are introduced, which help governments and stakeholders develop and implement the best climate adaptations and resiliency measures.

Changes in global air temperature affect daily temperatures of surface water bodies such as lakes, streams, and rivers throughout the year. One of the vital climate elements of aquatic ecosystems (e.g., rivers, oceans, and seas) is the water temperature because it influences most processes affecting water quality, biological activities, and marine lives, for example, fish, insects, zooplankton, and phytoplankton (Dallas, 2009). The temperature of surface water bodies determines the organisms that can tolerate such temperature and thrive in such freshwater systems. Chapter 3 gives an in-depth overview of the main physical processes that define extreme temperatures in the context of potential changes resulting from climate change because of their potential impact on decreasing aquatic species' growth and distributions. Detailed information about temperature extremes, their trends, physical processes, and how climate change may impact these processes are discussed in this chapter.

Human-caused climate change is increasing the frequency and strength of torrential downpours; these trends are predicted to continue as the earth gets warmer (Brooks, 2013); consequently, it is necessary to understand the impacts of climate change on severe thunderstorms and tornadoes, especially those that produce large hail and damaging straight winds. Chapter 4, Severe Convective Storms in a Changing Climate, summarizes the current knowledge on this topic, some of the critical questions that still need answers, and research opportunities in this area. The first part of the chapter contains a

concise summary of the present knowledge on the topic followed by a section explaining the conducive settings that induce such occurrences and their documented changeability. The following section covers the significant large-scale drivers of these events and their relations to climate variability. The chapter also includes a discussion on climate teleconnections (e.g., El Nino Southern Oscillation), which are recognized for their influence on the global weather patterns and extreme weather. In the last part of the chapter, the author discusses the latest research examining severe convective storms and their relations to climate change, with explicit attention to the convection-permitting dynamical downscaling methodology. Furthermore, the author highlights some of the cutting-edge research necessary to increase the ability to predict such events, lessen their environmental impacts, and minimize their harmful and adverse effects on human lives and resources.

Hydrological responses

Chapter 5 discusses the patterns, mechanisms, and uncertainties in the response of terrestrial net primary productivity to precipitation extremes. An in-depth overview of projected and observed increases in precipitation extremes and their links to anthropogenic-driven atmospheric warming are given in the introduction section of the chapter. The goals of the chapter and the outline of its remaining content mark the last part of the chapter's introduction section. The following section enumerates some key examples of the impacts that precipitation extremes have on ecological, social, and economic systems. The history of research and conceptual thoughts on precipitation extremes within ecology are then discussed. The woven within history is the standing debate about what is an "extreme" event. Patterns and mechanisms of ecosystem responses to precipitation extremes, with emphasis on their temporal variability, are presented in the middle sections of the chapter. Current and future research needs of forests, savannas, grasslands, deserts, and other ecosystems, including human-managed ecosystems, were discussed in the last section before the summary of the chapter. The chapter summary has an overview and key takeaways, knowledge gaps, and pathways on how to move forward.

Flood Early Warning Systems (FWS) under Changing Climate and Extreme Events is the title of the second chapter of the hydrological responses section of the book. It focuses on some of the current flood warning systems operating in the United States and introduces the basic concepts of an effective flood warning system, including rainfall monitoring systems. The chapter discusses the main components of a typical FWS, including (1) rain gauge networks and their operation platform and (2) a remotely sensed rainfall that encompasses radar systems such as Next-Generation Weather Radar (NEXRAD) and satellite systems such as Tropical Rainfall Measuring Mission, the Global Precipitation Measurement mission, and the Geostationary Operational Environmental Satellites mission. Hydrological modeling is the next important component of the FWS; it uses data of rainfall and other parameters to initiate flood warnings and estimation of their potential damages. It involves hydrologic and hydraulic software packages. One of the main takeaways is that there is a need to invest in flood warning systems improvement as a part of sustainable urban development practices and flood adaptation programs to minimize flood damages.

The impact of global warming, such as rising sea levels in response to changing weather patterns, is already affecting ecosystems, freshwater supplies, and human health. Climate change is hard to avoid; however, reducing and possibly stabilizing the substantial amount of heat-trapping gases (greenhouse gas concentrations) released into the atmosphere could lessen its most destructive impact (VijayaVenkataRaman et al., 2012; Kabisch et al., 2016). This effort is only dealing with climate

change mitigation. In recent years, the adaptation processes have been considered as a viable option to reduce the vulnerability to the predicted negative impacts of climate change (Nyong et al., 2007). It is more specific to adopt an integrated approach that combines mitigation and adaptation strategies and practices to address climate change and assure more reliable outcomes (Kabisch et al., 2016; Nyong et al., 2007).

Mitigation, adaptation, and governance

The last section of the book, mitigation, adaptation, and governance, contains six chapters. Chapter 7, Lifeline Infrastructures and Hydroclimate Extremes Climate: A Future Outlook, is the first chapter of the section. It introduces the critical gaps in knowledge and methodologies of climate and weather extreme stressors and stressed infrastructure lifelines as well as a science-based approach for resilient transportation networks under exacerbated stresses from precipitation extremes in changing climate scenarios. Natural or human-induced hazards are predictable, and best recovery strategies are adopted to ensure resiliency and robust lifeline of a given transport network due to advances in network science. This chapter has two main parts. Part I discusses the different aspects of characterizing and quantifying risks to transportation infrastructures from extreme events and their associated methodologies; supporting examples are also illustrated. In the second part of the chapter, a networked perspective on critical infrastructure is presented in the context of posthazard recovery using the Indian Railways Network spanning, serving the daily commute of the larger metropolitan area of Mumbai, as a case study.

The second chapter of the mitigation, adaptation, and governance section of this book focuses on green infrastructures and their role in mitigating extreme events under past, current, and future climate change conditions. The design and implementation of green infrastructures (e.g., greenways, parks, gardens, green roofs, woodlands, waterways, community farms, forests, and wilderness areas) could reduce greenhouse gas emissions and provide natural-based solutions to fill the gap between climate change mitigation and adaptation actions. Such infrastructures are part of a multifaceted ecosystems-based approach and an effective strategy that supports ecosystem resilience and human benefits through ecosystem services. Chapter 8 contains four parts. A systematic review of different types and applications of green infrastructures is presented in the first part of the chapter. Air pollution removal, temperature regulation, carbon sequestration, and important ecosystem services are included in this second part of the chapter, which also deals with the characteristics and categories of green infrastructures. Green infrastructure has multiple environmental and health benefits for communities, and its application can increase the health and environmental equity across communities in the face of climate change. Health and environmental equity is the topic of the third part of this chapter. The last part concentrates on the key characteristics and classifications of green infrastructure by function, in addition to its categorizing nomenclature. If green infrastructure practices are adopted globally, they could have apparent mitigating effects on climate change impacts. However, future studies are required to develop guidance for communities and decision-makers to determine and apply the most site-specific suited green infrastructures.

Adaptation to climate extremes and sea-level rise in coastal cities of developing countries is the topic of the next chapter of this section. It gives an in-depth overview of the responses of those cities to the challenges of sea-level rise under a changing climate facing their vulnerary populations and their combined mitigation and adaptation measures. Although adaptation to climate change and sea-level rise options are context-based, it is essential to share individual experiences to help other cities find

the most suitable adaptation pathways specific to their conditions. Chapter 9 has two main parts. The first part discusses the state-of-the-art of climate change adaptation in small and medium coastal cities in developing countries through characterizing coastal exposure and impacts of climate change and examining adaptation strategies to those exposures and impacts. The second part discusses how to conduct a synthesis of adaptation strategies for coastal cities, especially small and medium towns that have fewer adaptation capacities.

The content of these above-discussed chapters supports the concept that the impact of climate change is multidimensional and has a cascading effect. The success of mitigation and adaptation efforts needs the support of multiple policy actors (e.g., individual, community, and organization) at different levels of governance (i.e., global, national, regional, and local levels) to participate in climate adaptation and mitigation processes (Moser and Boykoff, 2013).

Chapter 10, titled Multilevel Governance in Climate Change Adaptation: Conceptual Clarification and Future Outlook, concentrates on the strengths and limitations of the multilevel governance concept and its role in future climate adaptation and mitigation measures and practices. This chapter provides insights on interactions among all the involved actors and their roles in deciphering the complexities of adaptation governance. Despite the need, it is essential to examine and validate the usability of the concept in relevant contexts before applying it to adaptation studies that are discussed afterward. Fundamental questions and issues that have been addressed throughout the chapter are as follows: How many levels of governance are required in climate change adaptation? Should we focus on the arrangement of multilevel networks or the processes? Would it be all right to consider only horizontal or vertical levels?

Despite the large need for a multiactor network of adaptation governance, only some climate change actions (discursively and materially) have been observed at local scales, particularly, across the United States. Although the United States has been a pioneer in climate change researches, it has not been active in writing and implementing policies in response to scientific understanding. Chapter 11 gives an overview of climate change governance in the United States, evaluates its actual position in relation to local Climate Action Plans (CAPs), and identifies the extent to which cities are engaging in GHG mitigation activities using descriptive statistics coming from a content analysis of cities' CAPs as well as interviews of local climate managers. This chapter has four main parts. Part 1 discusses the politics and policies of climate change in the United States at different levels to identify intergovernmental relations to multilevel networks in the context of climate change actions. This section also discusses specific federal level actions that have enabled or hindered climate governance in general. The second part gives an overview of the studies on climate change governance at the local level and the spatial distributions of local CAPs with the local political landscape. The third part advocates for the importance of understanding the prevailing conditions and factors that influence pioneering localities' innovation in climate governance to improve the adoption of climate change governance at the local level. The last part of this chapter assesses the position of local CAPs in GHG emissions reduction actions by analyzing preplan and postplan GHG emissions data. One of the key findings is that the number of localities across the United States that have symbolically joined climate action networks or signed the climate mitigation agreements is much more than the ones that implemented it.

Natural and human-made disasters cause failures of electrical infrastructures that would eventually affect millions of people and result in intersystems cascading failures (Pescaroli and Alexander, 2016; Zio, 2016). Thus one of the significant challenges in the design of resilient electrical infrastructures is

to understand the fragility induced by system interdependencies because it could "paralyze entire regions, with grave implications for the nation's economic and social well-being" (NIAC, 2018). For such matters, there is a substantial need to adopt a national approach to prepare for, respond to, and recover from catastrophic power outages as well as to improve our understanding of how cascading failures across critical infrastructure affect restoration and survival. The last chapter explores past and current risks to the electrical power grid due to natural hazards and recovery challenges. This chapter concentrates on the design of a national approach that includes clear plans of mitigation and adaptation from catastrophic power outages and an advanced understanding of the impact of cascading failures from critical infrastructure to power restoration and human survival. Experiences from past disasters, along with systems engineering implications, are also discussed in this chapter.

All the topics covered in this book help to understand the complexity of climate change and extreme events and their connectivity and impact on human lives. This multidisciplinary approach, as well as the in-depth analysis of past and current conditions and future outlooks, is required in addressing the extreme events under a changing climate.

References

Boo, K.O., Kwon, W.T., Baek, H.J., 2006. Change of extreme events of temperature and precipitation over Korea using regional projection of future climate change. Geophys. Res. Lett. 33 (1).

Brooks, H.E., 2013. Severe thunderstorms and climate change. Atmos. Res. 123, 129–138.

Dallas, H.F., 2009. The Effect of Water Temperature on Aquatic Organisms: A Review of Knowledge and Methods for Assessing Biotic Responses to Temperature. Water Research Commission Report KV, 213(09).

Fares, A., Awal, R., Michaud, J., Chu, P.S., Fares, S., Kodama, K., Rosener, M., 2014. Rainfall-runoff modeling in a flashy tropical watershed using the distributed HL-RDHM model. J. Hydrol. 519, 3436–3447.

Habibi, H., Seo, D.J., 2018. Simple and modular integrated modeling of storm drain network with gridded distributed hydrologic model via grid-rendering of storm drains for large urban areas. J. Hydrol. 567, 637–653.

Heim Jr., R.R., 2015. An overview of weather and climate extremes—products and trends. Weather Clim. Extrem. 10, 1–9.

IPCC (Intergovernmental Panel on Climate Change), 2013. Climate Change 2013, The Physical Science Basis. Working Group I, Cambridge University Press, London.

Kabisch, N., Frantzeskaki, N., Pauleit, S., Naumann, S., Davis, M., Artmann, M., Haase, D., Knapp, S., Korn, H., Stadler, J., Zaunberger, K., 2016. Nature-based solutions to climate change mitigation and adaptation in urban areas: perspectives on indicators, knowledge gaps, barriers, and opportunities for action. Ecol. Soc. 21 (2).

Moser, S.C., Boykoff, M.T. (Eds.), 2013. Successful Adaptation to Climate Change: Linking Science and Policy in a Rapidly Changing World. Routledge.

NIAC, 2018. Surviving a Catastrophic Power Outage. President's National Infrastructure Advisory Council, Washington, DC. Accessed at: www.dhs.gov/national-infrastructure-advisory-council.

Norouzi, A., Habibi, H., Nazari, B., Noh, S.J., Seo, D.J., Zhang, Y., 2019. Toward parsimonious modeling of frequency of areal runoff from heavy-to-extreme precipitation in large urban areas under changing conditions: a derived moment approach. Stoch. Env. Res. Risk A. 33 (7), 1263–1281.

Nyong, A., Adesina, F., Elasha, B.O., 2007. The value of indigenous knowledge in climate change mitigation and adaptation strategies in the African Sahel. Mitig. Adapt. Strateg. Glob. Chang. 12 (5), 787–797.

Pescaroli, G., Alexander, D., 2016. Critical infrastructure, panarchies and the vulnerability paths of cascading disasters. Nat. Hazards 82 (1), 175–192.

Safeeq, M., Mair, A., Fares, A., 2013. Temporal and spatial trends in air temperature on the Island of Oahu, Hawaii. Int. J. Climatol. 33 (13), 2816–2835.

Seneviratne, S., Nicholls, N., Easterling, D., Goodess, C., Kanae, S., Kossin, J., Luo, Y., Marengo, J., McInnes, K., Rahimi, M., Reichstein, M., 2012. Changes in Climate Extremes and Their Impacts on the Natural Physical Environment. IPCC.

Sheffield, J., Wood, E.F., 2011. Drought: Past Problems and Future Scenarios. Earthscan, London, p. 210.

Solomon, S., Manning, M., Marquis, M., Qin, D., 2007. Climate Change 2007—The Physical Science Basis. Working group I contribution to the fourth assessment report of the IPCC, vol. 4 Cambridge University Press.

Stott, P., 2016. How climate change affects extreme weather events. Science 352 (6293), 1517–1518.

VijayaVenkataRaman, S., Iniyan, S., Goic, R., 2012. A review of climate change, mitigation and adaptation. Renew. Sust. Energ. Rev. 16 (1), 878–897.

Zio, E., 2016. Challenges in the vulnerability and risk analysis of critical infrastructures. Reliab. Eng. Syst. Saf. 152, 137–150.

CHAPTER

Temperature extremes in a changing climate

2

Yating Zhang[a] **and Bilal M. Ayyub**[b]

Center for Technology and Systems Management, University of Maryland, College Park, MD, Unites States[a]

Department of Civil and Environmental Engineering, Director of the Center for Technology and Systems Management, University of Maryland, College Park, MD, United States[b]

Background

Temperature change

On average, the Earth's surface temperature grew by 0.85°C over the past 140 years, whereas the land generally warmed faster compared with the ocean (IPCC (Intergovernmental Panel on Climate Change), 2013). The carbon emissions from the preindustrial age to the present will continue to cause changes in the climate system, but these emissions alone will not result in global warming of 1.5°C in the 21st century (IPCC (Intergovernmental Panel on Climate Change), 2019). However, if the emission pattern is not altered, cumulative greenhouse gases can lead to a 2.6–4.8°C increase of global temperature by the end of the 21st century (IPCC (Intergovernmental Panel on Climate Change), 2013).

The annual average temperatures across the contiguous United States have risen by 0.7–1.0°C since the beginning of the 20th century, and an additional increment of 2.8–4.8°C is expected by the end of the 21st century if no mitigation action is taken. Extremely hot and cold temperatures are likely to increase more than average temperatures, meaning warm days can be hotter and cold days can be less freezing. Moreover, warm days are projected to increase, and cold days are expected to decrease in the rest of the 21st century (Vose et al., 2017).

Heat waves have become more frequent in the contiguous United States since the mid-1960s (Vose et al., 2017). A study found that the annual number of heat waves increased by 3, intensity rose by 0.5°C, and duration grew by 1 day for the average US city from the year 1961 to 2010. Meanwhile, heat wave season started 17.5 days earlier and lasted 11.5 days longer (Habeeb et al., 2015). More intense heat waves and less intense cold waves are expected in the rest of the 21st century (Vose et al., 2017).

The increase of extremely hot temperatures and heat waves is attributable to both natural and anthropogenic factors; however, the latter has led to a 1–3°C increase of maximum temperatures during heat waves over most land areas (Wehner et al., 2018). Natural factor refers to the change in solar and volcanic activities. Anthropogenic factors include greenhouse gas emissions resulting from human activities, land-use change due to urbanization, and waste heat discharges. Carbon dioxide concentration has increased by 40% since the preindustrial times, which is primarily due to fossil fuel combustion

Climate Change and Extreme Events. https://doi.org/10.1016/B978-0-12-822700-8.00001-9
Copyright © 2021 Elsevier Inc. All rights reserved.

and secondarily due to land-use change (IPCC (Intergovernmental Panel on Climate Change), 2013; EPA (Environmental Protection Agency), 2016). Methane concentration has increased by more than 100% as a result of farming and production, transmission, and distribution of natural gas and petroleum (IPCC (Intergovernmental Panel on Climate Change), 2013; EPA (Environmental Protection Agency), 2016). Nitrous oxide concentration has increased by 18% mainly due to food production (IPCC (Intergovernmental Panel on Climate Change), 2013; EPA (Environmental Protection Agency), 2016). These increased greenhouse gases absorb and re-radiate extra Sun's energy that is originally released back to space, heating the atmosphere and the Earth's surface and changing the Earth's overall climate. Also, urbanization replaces large-scale vegetation with asphalt and concrete roads, buildings, and other structures, increasing heat absorption and storage in urban surfaces during the daytime. This heat warms the surrounding environment, especially at night, exacerbating heat stress on populations during heat waves. Intense human activities release considerable heat from factories, vehicles, and air conditioners, further elevating urban temperatures in summers.

Impacts of extremely hot temperatures

Over the last two decades, extremely hot weather caused more than 8000 deaths in the United States (CDC (U.S. Centers for Disease Control and Prevention), 2019). A statistic for 43 US cities from the year 1987 to 2005 suggested that mortality risk may increase by 2.49% per 1 F (0.56°C) escalation of heat wave intensity and rise by 0.38% per 1-day increment in heat wave duration (Anderson and Bell, 2011). The elderly, children, and infants are particularly susceptible to extreme heat, and patients who take medications that affect the body's heat regulatory system are also vulnerable.

Extremely hot weather intensifies cooling energy demands and increases electrical loads on power systems. It was found that 1°C of temperature increment that starts from 18°C can result in 0.45%–4.6% rise of peak electricity load and 0.5%–8.5% growth of total electricity demand, dependent on building characteristics, climate zones, urban morphologies, and the type of energy services provided, such as fans or air conditioners (Santamouris et al., 2015). Moreover, the capacity and efficiency of power systems in generating, transmitting, and distributing electricity decrease under hot weather conditions, and thus the risk of power outages may increase in dense urban areas.

Extreme hot weather can cause asphalt melting, concrete hogging, and malfunction of signaling equipment. Modern rail infrastructure is particularly vulnerable because railroad tracks are welded to form a continuous rail that is typically several kilometers long. When such tracks expand due to intense heat stress, buckling may occur at spots of weakness. Moreover, in passenger trains, air conditioning units are typically designed to operate under 38°C, and temperatures above 38°C can result in electronic fault and serious damages to electronic units. This is the main reason for train cancellation during extremely hot days.

Extreme hot weather can deteriorate outdoor air quality because high temperatures and abundant sunshine can speed up the rate of chemical reactions, which propels the formation of ozone and fine particulate matters. Ozone in the upper atmosphere plays a key role in blocking harmful solar radiation, whereas ozone in the ground level impairs human health. During heat waves, atmospheric pressure is relatively high, which can constrain air convection and hinder the dissipation of pollutants, resulting in a dangerously high-level concentration of ozone and fine particulate matters.

Temperature extreme analysis and projection

Metrics and indices

The Expert Team on Climate Change Detection and Indices has defined a set of extreme indices for evaluating and predicting the change of temperature extremes, as shown in Table 1. These indices have been widely used in climate studies such as the fifth Intergovernmental Panel on Climate Change (IPCC) report.

Observational analysis

Collecting observation data for the atmosphere, ocean, and land-based systems is essential for scientists to understand and describe the conditions of our climate system. There are over 11,000 weather stations around the world, which measure and monitor land and atmospheric conditions. Daily weather records from observing stations in the United States are accessible from the National Centers for Environmental Information (https://www.ncdc.noaa.gov/cdo-web/datatools/findstation). Satellites, ships, and aircraft are additional approaches for data collection. The US National Ocean and Atmospheric Administration operates a constellation of geostationary and polar-orbiting satellites to collect continuous global environmental observations, including precipitation, sea surface temperature, atmospheric temperature and humidity, sea ice extent, and global vegetation. These data are archived in the Comprehensive Large Array-Data Stewardship System (https://www.avl.class.noaa.gov/saa/products/catSearch).

The UK Met Office Hadley Center has produced a range of observation datasets based on daily weather data collected from thousands of stations over six continents. The HadEX dataset has been updated twice to include a more significant number of stations and indices and to cover a more extended

Table 1 Extreme temperature indices.

Indices	Description	Usage
TN	The coldest day of a year, season, or month	Extreme projection
TX	The hottest day of a year, season, or month	Extreme projection
FD	The number of days when TN is below 0°C	Impact study
FR	The number of days when TN is above 20°C	Impact study
TN10p	The exceedance rate of days where TN is below the 10th percentile	Cold night probability estimation
TX10p	The exceedance rate of days where TX is below the 10th percentile	Cold day probability estimation
TN90p	The exceedance rate of days where TN is above the 90th percentile	Warm night probability estimation
TX90p	The exceedance rate of days where TN is below the 10th percentile	Warm day probability estimation
WSDI	The number of days in a year when TX is above the 90th percentile for 6 consecutive days or longer	Heat wave projection
CSDI	The number of days in a year when TX is below the 10th percentile for 6 consecutive days or longer	Cold wave projection

period. The latest version, HadEX3, comprises 17 extreme temperature and 12 extreme precipitation indices at a grid resolution of 1.25°×1.875°, spanning from the year 1901 to 2018 (Dunn et al., 2020). These extreme indices are calculated at around 7000 locations for temperature and 17,000 sites for precipitation. Another renowned dataset is the gridded temperature and precipitation climate extremes indices (GHCNDEX) developed by the US National Center for Atmospheric Research (NCAR). This dataset comprises 26 extreme indices from the year 1951 to the present with a grid resolution of 2.5°×2.5°. The ability to continuously update the data, either monthly or annually, makes GHCNDEX an excellent tool for climate monitoring. These datasets are widely used for climate change detection and attribution studies, climate model evaluation, and extreme climate events investigation. The quality of observation datasets is affected by instruments and data processing techniques, which are the primary sources of uncertainty. Data processing addresses the dilemma that weather stations are distributed unevenly on the globe and sparsely in some regions. Thus statistical approximation (e.g., angular distance weighting scheme) is employed to adjust those observations to a regular grid. Moreover, data processing is required for variables that are not measured directly but derived from other observations.

Data assimilation is a technique that combines observations from a wide variety of sources and model simulations to provide the best estimate of the state of a system. Various assimilation methods have been developed to support numerical weather prediction, numerical ocean prediction, land surface processes, hydrological cycle prediction, carbon cycle prediction, and so forth (Carrassi et al., 2018). In particular, climate reanalysis projects use the assimilation technique to determine the most likely climate condition in the recent past. The European Center for Medium-Range Weather Forecast (ECMWF) has generated a large number of reanalysis datasets for public use. The latest product is the fifth generation of ECMWF atmospheric reanalysis (ERA5), which includes hundreds of atmospheric, land, and oceanic climate variables from the year 1979 to within 5 days of real time. Other renowned reanalysis datasets include the National Center for Environmental Protection (NCEP) reanalysis, Japanese 55-year reanalysis, National Aeronautics and Space Administration's Modern Era Reanalysis for Research and Applications version 2, and NCEP's Climate Forecast System Reanalysis. The quality of reanalysis datasets is affected by the performance of the assimilation model, the quality and distribution of the underlying observations, and the technique used in combining heterogeneous observations into a regular grid. The uncertainty of reanalyses is generally larger than observations but smaller than model simulations. Still, it is not always the case because the accuracy of model simulations has been improved markedly in recent decades (Reichler and Kim, 2008).

Temperature projection

Global climate models

Energy balance models (the 1950s)

Energy balance models are the earliest and most basic numerical climate models, which simulate the balance between the energy entering the Earth's atmosphere from the sun and the energy released back to space. The surface temperature of the Earth is the only variable considered in these models.

Radiative convective models (the 1960s to 1970s)

Later researchers developed radiative-convective models by incorporating the vertical dimension (air convection) into energy balance models. These models can simulate energy transfer through the height of the atmosphere and calculate the temperature and humidity of different layers of the atmosphere.

General circulation models/Global climate models (the 1970s to 1980s)

The development process of the general circulation model can be divided into two stages. The early stage focused on characterizing the evolution of the dynamic and thermodynamic state of the atmosphere and ocean, respectively. The developed models can capture air and water flows and heat transfer in the atmosphere and oceans. The later stage coupled atmosphere and ocean models and named them the coupled atmosphere-ocean general circulation models (AOGCMs). The AOGCMs can simulate the exchange of heat and water between the land, atmosphere, and ocean.

Earth system models (starting from the 1990s)

To improve the understanding of how climate responds to increased greenhouse gas emissions, more complicated treatments of sea ice and land surface were included in AOGCMs, along with submodels of vegetation, ecosystems, and biogeochemical cycles. These formed the Earth system model, which includes the simulation of the carbon cycle, nitrogen cycle, atmospheric chemistry, ocean ecology, and changes in vegetation and land use.

Regional climate models

The first regional climate model (RCM) was developed in the late 1890s, and since then, regional modeling has experienced tremendous growth. Regional modeling is commonly referred to as dynamical downscaling because RCMs use the data of global climate models (GCMs) as input to generate fine, subgrid scale results. The fine-grid results can help decision-makers evaluate potential impacts of climate change on crop production, hydrology, species distribution, and such at scales of 10–50 km. The GCMs consider global circulation and large-scale forcings, such as greenhouse gases and solar radiation, whereas RCMs simulate a limited area of the Earth and account for sgrid scale forcings and processes, including complex topography, inland water bodies, and mesoscale dynamical processes.

Several RCMs have been developed and maintained as community tools for regional climate research, including the US Regional Climate Model, the US NCAR's Weather Research and Forecasting (WRF) model, the US National Center for Environmental Prediction's Eta model, Canadian Regional Climate Model, UK Met Office Hadley Centre's Regional Climate Model, German Consortium for Small-scale Modeling and Climate Limited-area Forecasting, German REgional MOdel (REMO), European Applications of Research to Operations at Mesoscale (AROME/ALADIN), Swedish Rossby Centre's atmospheric model (RCA), and Scripps Experimental Climate Prediction Center's regional spectral model (ECPC-RSM).

The Coordinated Regional Climate Downscaling Experiment (CORDEX) program was launched by the World Climate Research Program in 2009 to coordinate and advance the science and practice of regional climate modeling and downscaling. The program provided frameworks for model evaluation and climate projection and produced improved regional projections in support of the fifth and sixth IPCC reports. The projections of CORDEX cover all land areas, including the Arctic, consider various emission scenarios, and attain a high grid resolution of 50 km and even 25 km for some regions. The climate projections for North America are accessible from the Climate Gateway at the NCAR (https://www.earthsystemgrid.org/search/cordexsearch.html?nsc=true).

The uncertainty of RCMs is mostly inherited from GCMs. GCMs may produce different responses to the same climatic forcing because they are built on various physical schemes, parameterization methods, and land-ocean coupling techniques. It is worth noting that RCMs are driven by a small subset

of GCMs, and thus they do not adequately sample model uncertainty. This leads to the uncertainty associated with domain selection. Other sources of uncertainty are related to future emission scenarios, internal climate variability, and the choice of RGM.

Integrated assessment models

Integrated assessment models (IAMs) were developed over the past years by combining climate, economic, land use, and energy models through computer codes or data files that exchange information among each module. The inputs of IAMs are typically country-level population and gross domestic production based on existing or assumed future education, urbanization, and economic conditions. The outputs typically include regional-scale greenhouse gas emissions, air pollution, and aerosol emissions, energy supply and demand, and land-use and land-cover change. The models can also generate the costs of mitigation policies and the prices of fossil fuels and renewable energy, which helps to evaluate policy options that could be deployed to tackle the emission problem.

A new scenario framework, named the Shared Socioeconomic Pathway (SSP), was created to facilitate the integrated analysis of future climate impacts, vulnerabilities, and adaptation and mitigation potential, by using IAMs developed by six research groups. The scenario framework contains five SSPs (SSP1, SSP2, SSP3, SSP4, and SSP5), representing five assumed global development paths: sustainable development, middle-of-the-road development, regional rivalry, inequality, and fossil-fueled development. Sustainable development means that the world will shift toward a more sustainable path, emphasizing more inclusive development that respects perceived environmental boundaries. Middle-of-the-road development implies that the world will follow a path in which social, economic, and technological trends do not shift obviously from historical patterns. Regional rivalry scenario assumes that countries will concern more about competitiveness and security and increasingly focus on domestic or regional issues. The inequality scenario assumes increasing disparities in economic opportunity and political power in the future, which will lead to increasing inequalities and stratification both across and within countries. Fossil-fueled development means that the world will speed technology, economy, and society development and experience rapid population growth, along with the exploitation of abundant fossil fuel resources and the adoption of resource- and energy-intensive lifestyles around the world (Rahil et al., 2017).

Ensemble modeling

Coupled model intercomparison project phase five

There are roughly 30 research groups that have developed their climate models. These models are similar in the structure but different in details, such as physical schemes and the number of vertical layers. To enable a comparison between the results of different models, the Coupled Model Intercomparison Project set up these models in the same way and used the same inputs. The Coupled Model Intercomparison Project Phase Five (CMIP5) was published in the fifth IPCC climate change assessment report, incorporating the latest and most sophisticated climate model experiments worldwide. Compared to a single AOGCM, a multiple model ensemble has shown superior performance for historical climate assessment, because coupling these models can take advantage of their strengths and compensate limitations.

To address future uncertainties regarding emissions and concentrations of greenhouse gasses, aerosols, land change, and solar radiation, CMIP5 adopts four climate scenarios that are representative concentration pathway (RCP) 2.6, RCP 4.5, RCP 6.0, and RCP 8.5, corresponding to a radiative forcing of

2.6, 4.5, 6.0, and 8.5 W/m^2 by 2100, respectively. *Radiative forcing* is defined as the net change in the energy balance of the Earth system because of natural and anthropogenic substances and processes, relative to the reference year of 1750. The four scenarios assume CO_2 concentrations of 421, 538, 670, and 936 ppm by 2100, and greenhouse gas concentrations (CO_2, CH_4, N_2O) of 475, 630, 880, and 1313 ppm by 2100, respectively.

Coupled model intercomparison project phase six

The Coupled Model Intercomparison Project Phase Six (CMIP6) was initiated in 2014 to fill scientific gaps remaining in CMIP5 and address new challenges emerging in climate modeling (Eyring et al., 2016). CMIP6 has endorsed 23 model intercomparison projects involving 33 modeling groups in 16 countries and formed the basis of the sixth IPCC assessment report to be published in 2021. For climate projection, CMIP6 considers the impact of socioeconomic conditions (e.g., population, economy) on greenhouse gas emissions by linking RCPs to SSPs, which enhances the robustness of climate projections and provides better support to climate policies. Also, CMIP6 keeps four scenarios used in CMIP5 (SSP1-2.6, SSP2-4.5, SSP4-6.0, and SSP5-8.5) and adds four new scenarios (SSP1-1.9, SSP4-3.4, SSP5-3.4-OS, and SSP3-7.0) to give a wider selection of futures for scientists to simulate. CMIP6 data are open to public use and accessible from the Lawrence Livermore National Laboratory (https://esgf-node.llnl.gov/search/cmip6/).

Weighted and unweighted ensemble simulation

The CMIP5 archive contains simulations of 29 institutions and 62 models. Some of the models are similar to others because they share the same physical schemes and numerical methods. The fifth climate assessment of IPCC and the third national climate assessment considered each model to be equally likely in depicting future climate change, whereas the fourth national climate assessment of the US Global Change Research Program adopted a weighting strategy to coupling models based on their skills and independence. Sanderson et al. (2017) indicated that the overall performance of the weighted model ensemble can be better than that of model democracy, especially when selected models are significantly independent of each other. However, there is a tradeoff between model skills and model uniqueness, which may weaken the performance of weighted models. Model skills determine whether the simulation is of sufficient accuracy, whereas model uniqueness ensures that uncertainties and bias are small enough. It should be noted that the weighting varies for varied regions because the capacity of models is different in simulating the climate of different geographical regions.

Downscaling techniques

Climate change impacts regions and populations unevenly due to different geographical, socioeconomic, and technological conditions. To assess local-scale impacts, high-resolution climate data are needed. The data can be obtained using downscaling techniques that generate local detailed information based on global coarse simulation. There are two main downscaling techniques—statistical downscaling and dynamical downscaling—which can be used alone or together.

Statistical downscaling

Statistical downscaling has the advantage of inexpensive computing and is easy to use compared with dynamical methods. Moreover, statistical downscaling is capable of producing site-specific climate projections (e.g., the location of a weather station), whereas dynamical downscaling cannot provide

site-specific climate projections. Statistical downscaling is built on the assumption that the relationship between model simulation and observation is stationary, and hence the relationship derived from the historical period can be applied to projecting future conditions. The three major categories of statistical downscaling methods are linear method (e.g., delta method, simple and multiple linear regression, canonical correction analysis, singular value decomposition), weather classification (e.g., analog method, cluster analysis, artificial neural network, self-organizing map), and weather generator (e.g., Long Ashton Research Station Weather Generator, MarkSim Weather Generator, nonhomogeneous hidden Markov model). See Trzaska and Schnarr (2014) for details.

Asynchronous Regional Regression Modeling (ARRM) is one of the empirical statistical downscaling techniques, using a quantile mapping method to adjust global projections to station-based or fine grid-based observations. The ARRM assumes that two independent time series should have similar probability density functions if they describe the same variable and are at approximately the same location, such as temperatures simulated by a climate model and observed by a weather station for the same location. Three steps are required for applying ARRM to downscaling the information of GCMs. The first step is to rank the observed historical data and model-simulated historical data in an ascending sequence based on respective values regardless of timestamps, as shown in Fig. 1A. A strong correlation should be observed in a scatter plot for observations versus model simulations. The second step is to use a mathematical function to simulate the relationship between ranked observations and simulations. Fig. 1A shows a piecewise linear regression function used to fit ranked results of station observations and CMIP5 simulations. The third step is to validate the developed regression function using historical

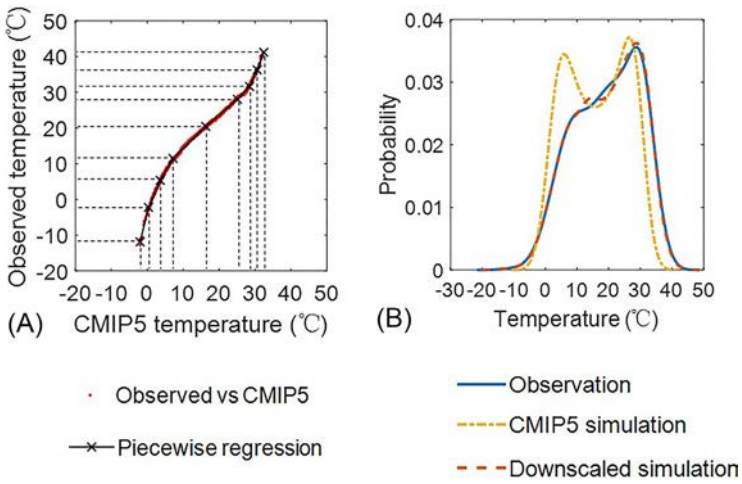

FIG. 1

Observed and simulated temperatures at the location of a weather station during 1965–2000: (A) observed versus CMIP5-simulated maximum daily temperatures and quantile mapping between observations and simulations (breakpoints representing the 1st, 10th, 25th, 50th, 75th, 90th, and 99th quantiles); (B) probability density distributions of observed, CMIP5-simulated and downscaled CMIP5-simulated temperatures.

Adapted from Zhang, Y., Ayyub, B., 2018. Urban heat projections in a changing climate: Washington, DC, case study. ASCE-ASME J. Risk Uncertainty Eng. Syst. Civ. Eng. 4(4), 04018032.

data, and the last step is to downscale model projections using the developed regression function. Fig. 1B compares CMIP5-simulated temperatures and downscaled results and demonstrates that downscaling helps capture local climate characteristics and improve the accuracy of the simulation. The major weakness of the ARRM is that the real relationship between observations and simulations can change over time, especially under different future climate conditions, which can weaken the accuracy of projections. Also, the error caused by the varied relationship cannot be measured using statistical means.

The Localized Constructed Analogs (LOCA) is a state-of-the-art downscaling technique that uses multiscale matching to improve the representation of temperature and precipitation extremes and spatial patterns in downscaled results. Multiscale matching comprises two steps. Step one selects observed days (typically 30 days), which best match the model day in a wider region around the location to be downscaled. Step two selects the single one of those observed days that best matches the model day in an immediate neighborhood of the location to be downscaled. The observed days chosen in step one are called analog days, and the location to be downscaled is called analog pool point or analog pool location, which is selected from the coarse grid. Step one requires defining the range of region that shares a similar temperature or precipitation pattern with the analog pool point, which is resolved by measuring the Pearson correlation between the analog pool point and nearby coarse-grid points. The magnitude of correlation typically decreases from one to zero as the distance from the analog pool point increases, and zero means no correlation, which forms the edge of the region. Analog days are determined in such a region by minimizing the root-mean-square differences from the model day. Once step one is completed, fine-grid analog results can be drawn from analog days at the nearest analog pool points. Step two starts with adjusting coarse-grid simulations and coarse-grid analog results to the fine grid through bicubic interpolation, and calculating the root-mean-square differences between their interpolated results, over a small square region centered on the analog pool point. Then the single day with the minimum difference is identified, and the fine-grid analog results of the single day are scaled to the model day for the region defined in step one. In downscaling temperature, the scaling is simply adding the mean difference between interpolated simulation and fine-grid analog result, whereas in downscaling precipitation, the scaling is multiplying the mean ratio of interpolated simulation to fine-grid analog result. This ensures that the extremes and spatial patterns of temperature and precipitation simulated by climate models are kept in the downscaled results. Considering that future anomalies of temperature or precipitation may exceed the range of historical variability, the LOCA method corrects downscaled projections by adding the mean difference between fine-resolution and coarse-resolution analog results. This correction is not required for downscaled historical simulations. The LOCA method can also be extended to downscale multiple climate variables at the same time by assigning a weight to each variable, which can significantly improve computing efficiency.

Dynamical downscaling

Dynamical downscaling adjusts coarse-grid simulations of GCMs to fine-grid results by using RCMs. A previous section introduced RCMs and their characteristics, and this section uses one of the RCMs to illustrate downscaling mechanisms. The WRF model is developed by the NCAR in collaboration with many research institutes and universities. The model has been improved many times since the first version came out in 2000, and its latest version WRF 4.1 was developed as a software program released last year for climate research community use. The inputs of the WRF model include three-dimensional temperature, wind speed, geopotential height, and relative or specific humidity, and two-dimensional surface pressure, mean sea level pressure, skin temperature, 2-m temperature, 2-m relative or specific

humidity, and 10-m wind speed. Optional inputs include soil temperature, soil moisture and so forth, depending on research needs. These inputs are obtained from GCMs for a domain designated by users. In addition to direct downscaling, the WRF model uses nest domains to improve the resolution of climate simulation. The grid resolution of nest domains is several times greater than that of their present domains, and thus increasing the number of nesting can exponentially improve the resolution of the innermost domain, but more computation loads are generated. The WRF model produces the results of nested domains based on the solutions of their parent domains, and hence, the outermost domain should be large enough to enable the development of a regional climate event that is usually relevant to the topography, atmosphere, and other factors in a large space.

The WRF software program provides multiple physical schemes and numerical or dynamics options for users to choose an appropriate combination and allows users to modify parameter values (e.g., urban morphology, anthropogenic heat emission) based on their research needs. The outputs of the WRF model contain all input variables at a higher spatial and temporal resolution and other statue variables such as heat fluxes. Fig. 2 shows an example of using the WRF model to downscale temperatures simulated by the Community Earth System Model version one (CESM1). The grid resolutions before and after downscaling are 0.9×1.25 degrees (approximately 100×106 km) and 4×4 km, respectively.

Although dynamical downscaling improves GCM information at a fine scale, systematic bias in GCM is prorogated to downscaled results. This can be resolved by removing the bias of GCM data before downscaling. In addition, RCM itself may produce bias, which can be corrected using statistical methods.

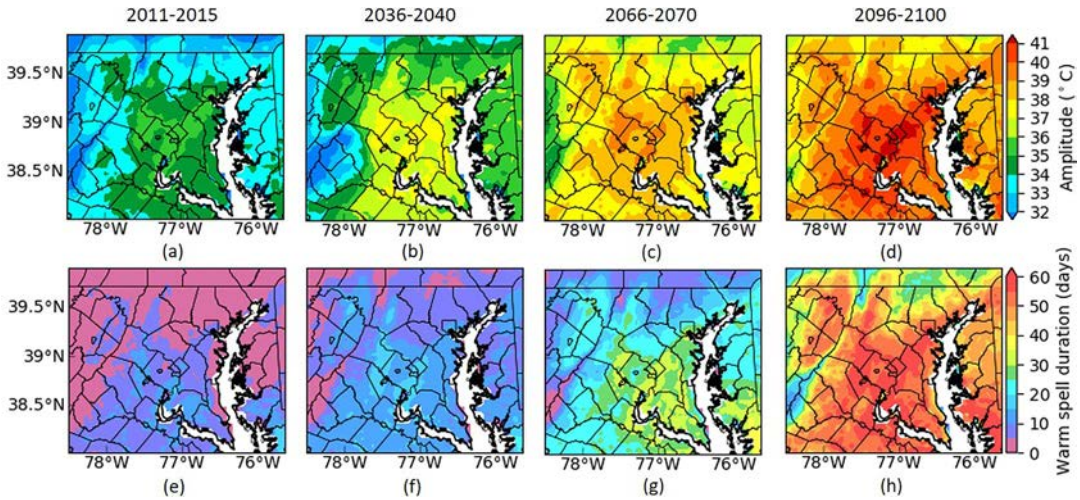

FIG. 2

Projected heat waves in the Washington DC metropolitan region for three future periods 2036–2040, 2066–2070, and 2096–2100, and the reference period 2011–2005, plotted at 4-km grid intervals. (A)–(D) Maximum temperature during heat waves; (E)–(H) Annual number of heat wave days. *Black lines* are county boundaries, and the white area is waters.

Reprinted from Zhang, Y., Ayyub, B., 2020a. Projecting heat waves temporally and spatially for local adaptations in a changing climate: Washington D.C. as a case study. Nat. Hazards, 1–20, https://doi.org/10.1007/s11069-020-04008-6.

Mitigation and adaptation strategies

Overview of mitigation and adaptation strategies

The Paris Agreement enacted in 2016 brought all nations into a common cause to prevent the rise of global temperatures this century above 2°C relative to preindustrial levels, and to make further efforts to limit the temperature increase to 1.5°C. Many US cities have evaluated the impacts of climate change on their communities and developed action plans to reduce greenhouse gas emissions. For instance, Washington DC published a sustainable plan in 2013, aiming to reduce 50% and 80% of greenhouse gas emissions in the district by the year 2032 and 2050, respectively, relative to the emission level of 2006. This plan was adjusted in 2018 to net-zero carbon footprint by 2050. Los Angeles released an action plan in 2007, intending to reduce greenhouse gas emissions to 35% below 1990 levels by the year 2030.

Climate change mitigation intends to reduce greenhouse gas emissions and concentrations in the atmosphere. The strategies employed by major US cities are as follows:

- Retrofitting existing commercial and multifamily buildings to improve their energy efficiency and reduce their reliance on fossil fuels for heating and cooling
- Implementing net-zero energy building code for new construction
- Improving energy efficiency and reducing overall consumption
- Increasing electricity generation and optimize energy distribution system
- Increasing the share of renewable energy in energy supply
- Developing renewable portfolio standards to steadily increase the use of renewable energy
- Reducing dependence on private vehicles and increasing the use of public transit
- Increasing biking and walking
- Deploying zero-emission electric vehicles

Climate change adaptation means to take appropriate action to prevent and minimize damages and to take advantage of opportunities created by such change. The strategies adopted by major US cities are as follows:

- Deploying cool roofs, green roofs, reflective pavements and other new technologies to mitigate the urban heat island effect
- Improving transportation and utility infrastructure to maintain variability during extreme weather events (e.g., heat waves, severe storm, flooding)
- Upgrading existing buildings and designing new buildings and development projects to withstand climate change impacts
- Strengthening community, social, and economic resilience to make neighborhoods and communities safer and more prepared

Strategy evaluation

The IPCC proposed a linear process for climate adaptation in its 1994 technical guidelines. This process starts with scientific analysis of climate change, including variability, then measures residual or net climate impacts after autonomous adaptations, and finally, determines adaptation needs. Subsequently introduced frameworks for climate adaptation accounted for policy criteria, population growth, economic development, and other nonclimate factors to generate accessible and affordable options.

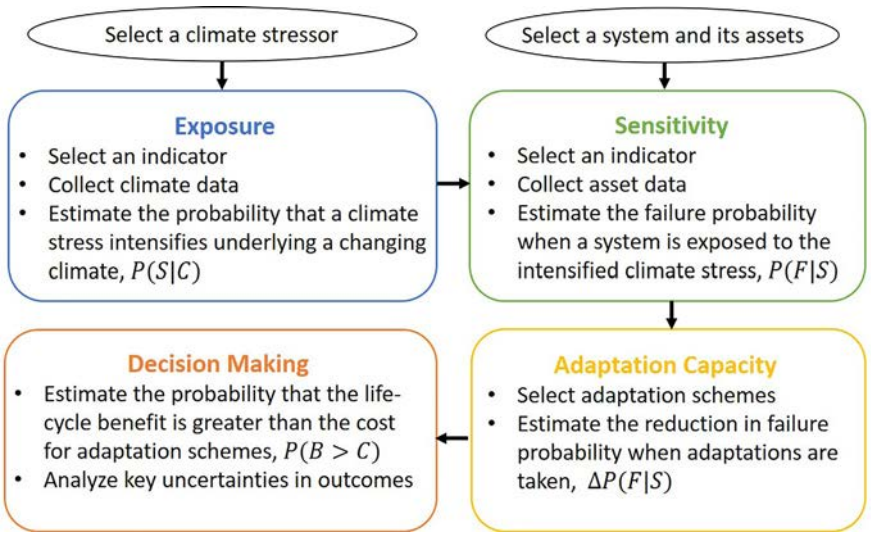
Select a climate stressor
Select a system and its assets
Exposure
Select an indicator
Collect climate data
Estimate the probability that a climate stress intensifies underlying a changing climate, P(S|C)
Sensitivity
Select an indicator
Collect asset data
Estimate the failure probability when a system is exposed to the intensified climate stress, P(F|S)
Decision Making
Estimate the probability that the life-cycle benefit is greater than the cost for adaptation schemes, P(B > C)
Analyze key uncertainties in outcomes
Adaptation Capacity
Select adaptation schemes
Estimate the reduction in failure probability when adaptations are taken, ΔP(F|S)

FIG. 3

The framework for climate adaptation planning incorporating the probabilistic risk method.

Reprinted from Zhang, Y., Ayyub, B., 2020b. Electricity system assessment and adaptation to rising temperatures in a changing climate with Washington Metro Area as a case study. ASCE J. Infrastruct. Syst. 26(2), 04020017.

A recent study incorporates a probabilistic risk method into the framework to enable quantitative assessments of adaptation options and uncertainties within outcomes, as shown in Fig. 3. The probabilistic risk method is defined by the following equation.

$$R = \sum_{t=t_0}^{n} \left[\sum_{C} \sum_{S} \sum_{F} \sum_{L} P(C)P(S|C)P(F|S)P(L|F)L \right] (1+r)^{-(t-t_0)} \tag{1}$$

where R is the net present value of climate risks. $P(C)$ is the probability that a climate-change scenario occurs. $P(S|C)$ is the probability that a stressor intensifies when climate changes. $P(F|S)$ is the probability of system failure when the stressor intensifies. $P(L|F)$ is the probability of a loss when the system fails. L is the monetized loss. r is the annual discount rate. t is the time in years starting from the year t_0. n is the number of years accounted for risk estimation.

If we consider only one climate scenario and climate stressor and one type of failure and loss, Eq. (1) can be rewritten as follows.

$$R = P(S|C) \sum_{t=t_0}^{n} [P(F|S)P(L|F)L](1+r)^{-(t-t_0)} \tag{2}$$

After taking adaption actions, the risk is reduced as follows.

$$R_{adapt} = P(S|C) \sum_{t=t_0}^{n} [(1-\Delta R)P(F|S)P(L|F)L](1+r)^{-(t-t_0)} \tag{3}$$

where ΔR is the coefficient of risk reduction due to climate adaptation, ranging between 0 and 1.

The first step of the assessment framework (Fig. 3) is selecting climate stressors and project future exposures. The climate stressor can be temperature shift, precipitation change, or sea level rise. The probability that the stressor increases under a climate scenario, $P(S|C)$, can be estimated based on the projection results of climate models supplemented with professional judgment in some cases. The second step is identifying vulnerable systems and assets and measuring the sensitivity of each system to the climate stressor. The failure probability of a system when exposed to the climate stressor, $P(F|S)$, can be estimated using historical data, model simulation results, or expert opinion elicitation. The third step is to select adaptation options and assess risk reductions associated with respective adaptation actions. Adaptation options may include deploying new techniques and equipment, developing new regulations on some industry sectors, and establishing incentive programs for some practice. The adaptation capacity of a system, $\triangle P(F|S)$, is measured as the reduction in failure probability when adaptation actions are taken. It is worth noting that adaptation capacity may vary with different geographic regions and system characteristics.

The last step is to analyze the benefit and cost of each adaptation scheme and compare and optimize these schemes. Benefit-cost analysis is widely used in the engineering decision-making process, where the benefit (B) is potential risk reduction and cost (C) is the investment made to mitigate risks. The probability that benefit is greater than the cost, $P(B > C)$, is a metric for determining whether an adaptation option is cost-effective or not. The other metrics used for decision making are net benefit ($B - C$) and benefit-to-cost ratio (B/C). Strategy comparison aims to find the option that reduces the risk in cost-effective terms within any budgetary or regulatory constraints, and optimization intends to seek the appropriate timing for the adaptation to enable the investment to be most cost-effective.

Summary and conclusions

Carbon emission from human activities has elevated global temperatures and intensified extreme heat events. The urban heat island effect further increases local temperatures and strengthens the impacts of heat waves. Heat waves can impair human health, deteriorate air quality, intensify cooling energy demands, and cause damages to the electrical power and transportation systems. Considerable efforts have been made in recent decades to improve the technology in monitoring and simulating climate change. Researchers created observation datasets (e.g., HadEX3, GHCNDEX) using daily weather data collected from thousands of stations to reveal the real climate conditions and produced reanalysis datasets (e.g., ERA5) using data assimilation methods and millions of observations to estimate the most likely climate conditions. These datasets are essential for climate change detection and attribution studies, climate model evaluation, and extreme climate events investigation.

Researchers also coupled atmosphere, ocean, vegetation, ecosystem, and biogeochemical cycle models to simulate a more complicated climate system. These modeling efforts have improved our understanding of how climate responds to increased greenhouse gas emissions. GCMs developed by different institutes and groups have been coupled to generate credible projections for temperature, precipitation, and other variables throughout the 21st century (e.g., CMIP6, CMIP5). Climate, economic, land use, and energy models have been integrated to provide important insights into the relationship between social development and climate change, which facilitates comprehensive policy analysis. Meanwhile, RCMs are coordinated to encourage global efforts on improving modeling techniques and evaluating and comparing models' performances (i.e., CORDEX). The improvement in

global and regional climate modeling will help governments and stakeholders better foresee and assess potential risks and opportunities underlying a changing climate.

Because climate impacts are distributed unevenly over different regions, a growing interest in assessing regional climate impacts and simulating regional climate change can be observed in recent studies. This drives the development of statistical downscaling methods that adjust information of GCMs to regional or local-scale results (e.g., LOCA). Moreover, governments at different levels have started to mitigate climate impacts by reducing greenhouse gas emissions and increasing the resilience of infrastructure and critical buildings. This chapter reviewed mitigation and adaptation strategies employed by major US cities and presented the methods for strategy evaluation and optimization, which represents a small portion of the state-of-the-art practice. Readers may refer to some recent review articles to gain a more comprehensive understanding.

References

Anderson, G.B., Bell, M.L., 2011. Heat waves in the United States: mortality risk during heat waves and effect modification by heat wave characteristics in 43 U.S. Communities. Environ. Health Perspect. 119 (2), 210–218.

Carrassi, A., Bocquet, M., Bertino, L., Evensen, G., 2018. Data assimilation in the geosciences: an overview of methods, issues, and perspectives. WIREs Clim. Change 9, e535. https://doi.org/10.1002/wcc.535.

CDC (U.S. Centers for Disease Control and Prevention), 2019. Underlying Cause of Death, 1999-2018 Results. CDC WONDER database (Feb. 7, 2020) http://wonder.cdc.gov/mortSQL.html.

Dunn, R.J.H., Alexander, L.V., Donat, M.G., Zhang, X., Bador, M., Yussof, M., 2020. Development of an updated global land in-situ-based dataset of temperature and precipitation extremes: HadEX3. J. Geograph. Res. Atmos. https://agupubs.onlinelibrary.wiley.com/doi/abs/10.1029/2019JD032263.

EPA (Environmental Protection Agency), 2016. Climate Change Indicators in the United States, fourth ed. https://www.epa.gov/sites/production/files/2016-08/documents/climate_indicators_2016.pdf. (June 30, 2020).

Eyring, V., Bony, S., Meehl, G.A., Senior, C.A., Stevens, B., Stouffer, R.J., Taylor, K.E., 2016. Overview of the Coupled Model Intercomparison Project Phase 6 (CMIP6) experimental design and organization. Geosci. Model Dev. 9, 1937–1958.

Habeeb, D., Vargo, J., Stone, B., 2015. Rising heat wave trends in large US cities. Nat. Hazards 76, 1651–1665.

IPCC (Intergovernmental Panel on Climate Change), 2013. Climate Change 2013, the Physical Science Basis. Working Group I, Cambridge University Press, London.

IPCC (Intergovernmental Panel on Climate Change), 2019. An IPCC Special Report on the Impacts of Global Warming of 1.5°C Above Pre-Industrial Levels and Related Global Greenhouse Gas Emission Pathways, in the Context of Strengthening the Global Response to the Threat of Climate Change, Sustainable Development, and Efforts to Eradicate Poverty. Working Group I, Cambridge University Press, London.

Rahil, K., van Vuuren, D.P., Kriegler, E., Edmonds, J., Tavoni, M., 2017. The shared socioeconomic pathways and their energy, land use, and greenhouse gas emissions implications: an overview. Glob. Environ. Chang. 42, 153–168.

Reichler, T., Kim, J., 2008. Uncertainties in the climate mean state of global observations, reanalyses, and the GFDL climate model. J. Geograph. Res. Atmos. 113. https://doi.org/10.1029/2007JD009278, D05106.

Sanderson, B.M., Wehner, M., Knutti, R., 2017. Skill and independence weighting for multi-model assessments. Geosci. Model Dev. 10, 2379–2395.

Santamouris, M., Cartalis, C., Synnefa, A., Kolokotsa, D., 2015. On the impact of urban heat island and global warming on the power demand and electricity consumption of buildings—a review. Energy Build. 98, 119–124.

Trzaska, S., Schnarr, E., 2014. A Review of Downscaling Methods for Climate Change Projections. Report, Tetra Tech ARD, Burlington, Vermont.

Vose, R.S., Easterling, D.R., Kunkel, K.E., LeGrande, A.N., Wehner, M.F., 2017. Temperature changes in the United States. In: Climate Science Special Report: Fourth National Climate Assessment, Volume I. U.S. Global Change Research Program, Washington, DC, USA, pp. 185–206.

Wehner, M., Stone, D., Shiogama, H., Wolski, P., Ciavarella, A., Christidis, N., Krishnan, H., 2018. Early 21st century anthropogenic changes in extremely hot days as simulated by the C20C+ detection and attribution multi-model ensemble. Weather Clim. Extrem. 20, 1–8.

CHAPTER

Climate change and extreme river temperature

3

André St-Hilaire[a,b], Daniel Caissie[c], Normand E. Bergeron[a,b], Taha B.M.J. Ouarda[a], and Claudine Boyer[a]

Institut National de la Recherche Scientifique, Centre Eau Terre Environnement, Québec City, QC, Canada[a] Centre Interuniversitaire de Recherche sur le Saumon Atlantique, Québec City, QC, Canada[b] Fisheries and Oceans Canada, Moncton, NB, Canada[c]

Introduction

River temperature has increasingly garnered interest both as a research topic and as a management tool in recent decades. In their literature survey, Ouellet et al. (2020) indicated that the number of publications related to water temperature and climate change increased from less than 20 in the 1990s to nearly 100 in the 2000s and 244 in the 2010–2015 period. Changes in river temperature regimes may have numerous causes and the literature suggests deforestation (Qiu et al., 2020), urbanization (Abdi et al., 2020), agriculture (Essaid and Caldwell, 2017), flow regulation (Michie et al., 2020), and climate change (Daigle et al., 2015), which is the topic of this chapter. To provide a summary of recent work on extreme temperatures in the context of an evolving climate, this chapter will first provide an overview of the physical processes that drive temperature changes in rivers and how climate change may impact these processes. This is followed by a summary of the current situation and known trends in temperature extremes. The next section synthesizes the information available on modeling and future river thermal scenarios, followed by a conclusion.

What are river thermal extremes?

Like many environmental variables, thermal extremes are multifaceted, and their definition and selection depend on the applications and/or management considerations. As such, many thermal extremes are defined as threshold exceedances. This is especially the case for fisheries management, where fisheries closures are often threshold-based (Breau and Caissie, 2013). Fish are ectotherms that have adapted to the conditions of their native rivers. For instance, salmonids are cold-water dwellers. Species of the genus *Salmo* have known temperature preferences (Eaton and Scheller, 1996). The impact of elevated temperature on those fish will depend not only on the maximum temperature that they are exposed to but also on the minimum night time temperature that allows them to recover from a thermal stress that occurred in the day. Thus both maximum and minimum thresholds need to be defined as extremes in this case. For instance, Atlantic salmon (*Salmo salar*) angling on the Miramichi River

Climate Change and Extreme Events. https://doi.org/10.1016/B978-0-12-822700-8.00011-1
Copyright © 2021 Elsevier Inc. All rights reserved.

(Canada) is closed when maximum daily summer temperature reaches 23°C and minimum temperature stays above 20°C (Caissie et al., 2017). On the west coast of North America, high temperature thresholds have been defined for many salmon populations and the notion of "chronic exposure" to these high temperature thresholds is used in fisheries management (https://www.pac.dfo-mpo.gc.ca/science/habitat/frw-rfo/reports-rapports/2019/2019-08-15/index-eng.html). Other metrics used for the management of fisheries in western North America include the highest average of maximum daily temperatures over any 7-day period (maximum weekly maximum temperature) and the highest average of mean daily temperatures over any 7-day period (maximum weekly average temperature) (Whelsh et al., 2001). In the absence of water temperature data, high thresholds of air temperature have been used to infer extreme thermal conditions. For instance, Gunn and Snucins (2010) have used a maximum daily air temperature of 30°C to define stressful conditions for brook char (*Salvelinus fontinalis*) in the Sutton River (Canada).

Similarly to low flow or drought extreme value analysis, quantifying water temperature extremes is often completed by considering them as a function of the duration of the events. This is generally quantified using degree-days, that is, the area under the curve of water temperature time series. Jeong et al. (2013) used the number of consecutive days with a maximum temperature above 25°C as an indicator of extreme conditions for Atlantic salmon in the Ouelle River (Canada).

A more holistic approach to water temperature extremes is based on a method similar to the one used by hydrologists when conducting environmental flows. The Natural Flow Paradigm Approach (Poff et al., 1997) characterizes the flow regime of a river using metrics related not only to the amplitude of discharge but also to the timing and duration of events, as well as their variability and frequency. This concept was applied in part by Steel et al. (2016) for river temperature. They investigated not only temperature minima and maxima but explored a number of metrics characterizing variance in thermal regimes, which is an important aspect of temperature extremes.

Finally, extreme water temperatures in rivers are often associated with low flow events. Consequently, extreme value analysis can be performed in a bivariate context. The so-called hot-dry events are of the utmost interest because of their overall impact on water quality (e.g., Pekárová et al., 2009).

Thermal processes affected by climate change

The main heat fluxes that define the thermal regime of rivers have been summarized in numerous studies (e.g., Caissie, 2006; Dugdale et al., 2017). The main heat input typically originates from incoming solar radiation, and the main heat loss term is typically through latent heat (evaporation). Infrared radiation can be a net input or output in the heat budget and depends in part on canopy, cloud cover, and albedo. Convection, or sensible heat, is another surface heat flux that depends in part on wind, vapor pressure, as well as air and surface water temperatures. Heat is also advected from upstream, from tributaries or groundwater seeps in river banks, and heat gains or losses can occur within the river bed (Caissie and Luce, 2017). The latter process can be complex and includes heat exchange through conduction, advection of both groundwater and hyporheic flow (Fig. 1).

Climate change studies and models are typically focused on change in atmospheric variables, and these forcing variables can sometimes be used to infer or directly estimate possible change in stream temperatures. This is typically done using a physically based model, regression equation, or other conceptual methods that would relate a change in an atmospheric forcing variable to stream temperature. The components of the atmospheric global circulation model (GCM) or regional circulation model

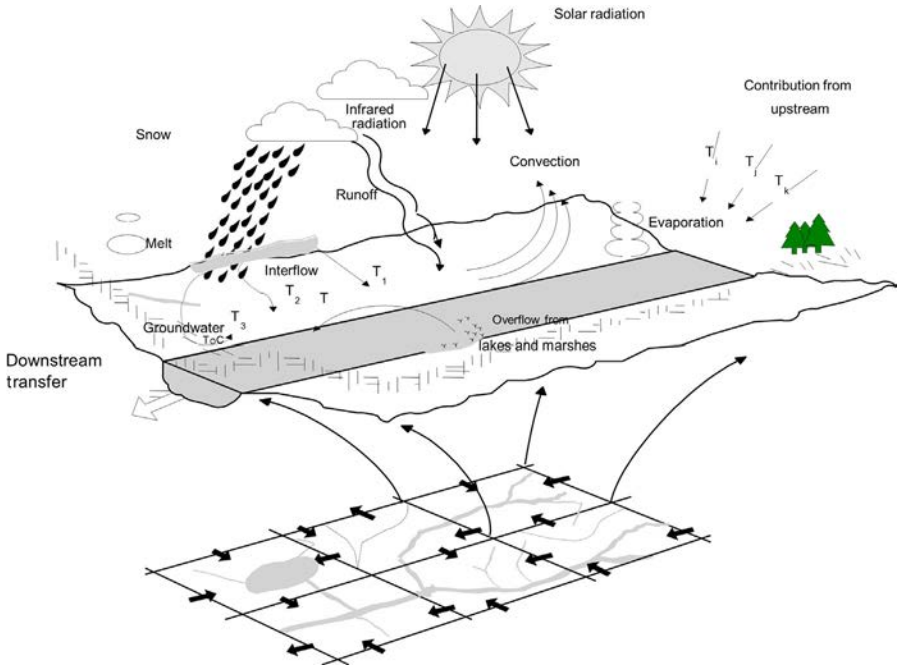

FIG. 1

The major heat fluxes in a river reach.

Adapted from St-Hilaire, A., Morin, G., El-Jabi, N., Caissie, D., 2000. Water temperature modelling in a small forested stream: implication of forest canopy and ground temperature. Can. J. Civ. Eng. 27(6), 1095-1108.

(RCM) that have a direct bearing on the energy budget of rivers have been looked at and some inferences on these important factors have been made.

Bartók et al. (2017) have studied the impact of climate change on surface solar radiation using both global climate model (using Coupled Model Intercomparison Project Phase Five [CMIP5] data) and regional model outputs (from Euro-Cordex simulations) in Europe. The different scenarios lead to different conclusions for the period 2006–2100, with a projected mean decrease of 0.6 W/m^2/decade when considering RCM outputs, but an increase of 0.4 W/m^2/decade when global climate model outputs are considered. These trends are well within the decadal oscillations observed by Sanchez-Lorenzo and Wild (2012) during the last 40 years in Switzerland. Hence, it may be difficult to conclude that possible increases in extreme water temperatures will be caused by an increase in incoming shortwave radiation.

Longwave radiation fluxes have been studied using both regional and global climate models. Wild et al. (2001) described how longwave radiation is influenced by cloud cover and moisture content, among other variables, which explains a significant part of its regional variability. Gutowsky et al. (1991) examined the impact of a doubling of atmospheric CO_2 on both incoming and outgoing surface longwave radiation. They found that changes in both fluxes are more significant than for the other terms of the heat budget. Surface incoming longwave radiation is expected to rise by 1 W/m^2 on average, but with increased absorption and feedback mechanisms, this could translate in a net increase of nearly 5 W/m^2.

Convection or sensible heat can be described as the energy exchange between two superimposed fluid layers with no phase change. In rivers, sensible heat can be a net input or a net output, depending upon the temperature gradient between the water surface and the air layer above it. We could not find studies that specifically address how convection may change with the climate in riverine environments. This is likely because climate models do not have yet the level of resolution or the appropriate scale to address this directly. However, given that this component of the heat budget is proportional to the temperature gradient and the wind speed (controlling the displacement of air masses at the river-atmosphere interface), the inference can be made on the potential impact of climate change. Global air temperature is already rising and will likely continue to rise in most regions, therefore influencing this heat flux. The likelihood of a sharper temperature gradient at the air-water interface is consequently high. This would lead to an increase in sensible heat flux from the atmosphere to the river. Most analyses related to wind and climate change focus on oceans or the energy sector. Pryor and Barthelmie (2010) reviewed wind outputs from climate models in Northern Europe and concluded that natural variability is higher than a potential net trending signal associated with climate change for this region. Fant et al. (2016) reached the same conclusion for Southern Africa. It therefore seems difficult to infer on the impact of future wind scenarios on convection in rivers.

Latent heat is generally the primary heat loss term at the rivers' surface. Again, this heat flux is dependent on a number of meteorological variables, including net radiation, wind velocity, relative humidity, and air temperature (Liu and McVicar, 2012). The combined effect of these variables leads to high local variability in evaporation trends from past data and future climate scenarios. For instance, Kay et al. (2013) found that although potential evaporation will likely show an overall increase under most climate change scenarios, there will be some months that will show an average decrease. They also mentioned that the complexity of providing clear scenarios related to latent heat is further exacerbated by the role of vegetation. Although transpiration is important to measure potential evapotranspiration over land, the impact of vegetation on river evaporation is mostly associated with the indirect impact of canopy closure as well as the available moisture above the river, which determines fetch and affects the wind function used in evaporation calculations (e.g., Maheu et al., 2014). One important aspect of the latent heat flux under climate change is that at high water temperatures, this flux can be significant and can contribute to the cooling of rivers. The so-called "evaporative cooling" of rivers can result in slower increases in river temperatures, especially at high temperatures, as reported in Mohseni and Stefan (1999). More research is required in the understanding of evaporative cooling to better quantify the thermal regime of rivers under a warming climate.

Another aspect that will be impacted by climate change is the streambed heat fluxes or exchange at the riverbed-water interface. The streambed heat flux is influenced by both conductive and advective components (i.e., groundwater). Studies have shown that the groundwater temperature will increase, however, at a slower rate than air temperature (with a lag) and as a function of depth in the ground (Kurylyk et al., 2015a). As such, shallow groundwater (which has a more significant impact on the streambed heat flux) will increase at a higher rate the deep groundwater with potential impacts on aquatic habitats, including thermal refugia (Kurylyk et al., 2015b).

Apart from possible changes in the heat fluxes at the surface and the river bed, the stream thermal regime, including the timing and amplitude of extremes, will likely be affected by changes in the snowmelt regime in many regions of the world. Lisi et al. (2015) investigated the thermal sensitivity of rivers in southwestern Alaska as a function of the snow (vs. rain) contribution to stream discharge and showed

how warmer streams and rivers typically have more significant rain contribution than cooler streams in the region. Given that the proportion of liquid precipitation is expected to increase in most northern regions of the world, the likelihood of warmer water temperature is bound to increase in those regions.

Past and current trends and shifts in observations

Given the relative paucity of river temperature data compared to air temperature, there are much fewer studies that investigated trends in the former compared to the latter. In addition, most existing studies focused on the trend in mean water temperatures. As Orr et al. (2015) pointed out in their study of river changes in the United Kingdom, most trend studies are local and include a limited number of stations. Hannah and Garner (2015) warned that even for rivers with long time series, the complexity of the physical processes involved in a river heat budget and the numerous confounding factors (e.g., deforestation, urbanization, and impoundment) might limit our ability to detect trending signals associated with climate change. However, given the clear evidence of increasing trends in air temperature around the globe, it is not surprising that studies are reporting increasing trends in water temperatures.

Nonetheless, some studies have reported significant trends in the past (Webb, 1996; Webb and Nobilis, 2007). For example, Webb (1996) summarized some of the earlier studies on trends in river temperature time series and stated that during the past century in Europe, river temperature increased by 0.1°C/decade, but also listed a number of potential drivers other than climate change (e.g., urbanization and agriculture). Letcher et al. (2016) investigated trends in mean water temperatures in four rivers located in western Massachusetts, United States (a third-order main stem and three second-order tributaries), and found a mean trend of 0.63°C/decade. Ptak et al. (2019) calculated trends for mean temperatures from four stations on the Warta River in Poland and found increasing trends varying between 0.1 and 0.3°C/decade for the period 1960–2009. Hrdinka et al. (2015) assessed the impact of climate change in rivers of the Czech Republic and found an average increase in stream temperature of 1.15°C over 28 years.

One approach used to partially compensate for the relative paucity of long water temperature time series is to extend existing time series through relatively simple statistical models. Soto (2016) used a nonlinear regression between water temperature and air temperature to complete time series for the period 1950–2013 in Spain. They found a mean trend of 0.16°C/decade for 11 rivers in the study area. Isaak et al. (2017) used a multivariate regression that included both climatic and physiographic predictors to quantify water temperature changes in a 2500-km river network in central Idaho. They found an average mean stream increase of 0.28°C/decade, whereas temperature maxima increased by 0.35°C/decade. Islam et al. (2019) used the Air2Stream hybrid (deterministic/stochastic) model (Toffolon and Piccolroaz, 2018) to investigate 17 sites in the Fraser River Basin in western Canada and found that summer water temperatures increased by an average of nearly 1.0°C during the period 1950–2015.

A more comprehensive study was conducted by Adrien et al. (2020) for the whole of the Swiss Alps with over 50 drainage basins. Positive trends in mean water temperature were found over the last 50 years for all seasons, with an average increase of 0.37 ± 0.11°C/decade for mean water temperature. They also observed increasing air temperatures, decreasing precipitation, which resulted in decreasing mean discharge. One of the few studies dealing with water temperature extremes was also conducted in Switzerland by Piccolroaz et al. (2018), who looked at the response of water temperature to heatwaves.

They calculated the number of days with daily water temperature anomalies during the summer period >90th percentile and found increasing trends in low-land, regulated, and snow-fed rivers. The cumulative degree-days of average temperature anomalies were also tested for long-term trends in the summer and were found to be significant (outliers corresponding to summer during which important heat waves have occurred). Another study looked at trends in water temperature means, maxima, and minima worldwide at fine spatial resolution (10 km) by using a 1D model to simulate water temperatures (Wanders et al., 2019). Their simulations showed that annual maxima have increased by 0.62°C/decade, whereas minima increased by 0.45°C/decade during the 1960–2014 period.

There are few studies that have looked at water temperature extremes through frequency analyses, which is often used for extreme value analysis in hydrology and climatology. A study was conducted by Caissie et al. (2020), who used a peaks-over-threshold approach. This method is appealing, given that most management and ecological concerns related to river temperature are threshold exceedances. Using a 21-year long time series of water temperature from the Miramichi River (Canada), they found the 0.01 exceedance probability for daily maximum river temperature was 32.7°C. This study was completed under the hypothesis of stationarity (i.e., no temporal trend in the time series of maxima). Nonstationary peaks-over-threshold methods exist (e.g., Thiombiano et al., 2017) and could be used to assess future maximum water temperature quantiles in the context of climate change.

River thermal modeling and scenarios at global, regional, and local scales

A number of studies have investigated the impact of climate change on the thermal regime of rivers. In general, the approach is similar to methods used to generate different scenarios of environmental variables that are likely affected or going to be affected by climate change, that is, the implementation of a cascade of mathematical models, that is, outputs of one model feeding into another. In general, GCMs or RCMs that use GCM for boundary conditions provide meteorological outputs such as air temperature and precipitations, which have been extensively analyzed for potential biases (e.g., Workru et al., 2020). Fewer studies have examined other meteorological outputs from climate models that are required for heat budget calculations such as wind, humidity, and cloud cover. These climate model outputs are subsequently fed in other models that will, in turn, calculate or estimate future water temperature scenarios.

Three main types of temperature models have been applied: (1) deterministic models are based on the explicit mathematical representation of physical processes that define heat fluxes; (2) empirical models that rely on the statistical relationship between predictor(s) and water temperature; and (3) hybrid models that combine the two approaches. In all three cases the models need to be calibrated against historical data before they can be used to generate future scenarios.

Empirical models have often been used because of their relative simplicity and because they typically require fewer inputs than deterministic models. Most applications of empirical models are site specific. For instance, Mohseni et al. (2003) used a linear and a nonlinear (sigmoid) regression with air temperature as the independent variable to investigate maximum weekly stream temperature at 764 stations in the United States using a doubling of CO2 concentrations as a future scenario. They showed an average decrease of 20% (from 80% to 60%) of the probability of exceedance of 30°C. Jeong et al. (2013) used the so-called stochastic model of Caissie et al. (1998) for 18 sites on the Ouelle River (Canada). In this model, the stream water temperature is expressed by the sum of a seasonal component (sine function) and a residual component (autoregressive function). They used five different

combinations of GCM-RCM with three different greenhouse gas emission scenarios to generate future water temperature scenarios for the 2046–2065 scenarios. They compared low-order streams to the river main stem in this drainage basin. They concluded that seven tributaries could still be used as cool-water refugia for Atlantic salmon (*S. salar*), whereas in the main stem and in three tributaries, stressful conditions will occur for this species. Daigle et al. (2015) used the same model as well as an artificial neural network to investigate future water scenarios on three eastern Canadian rivers. Ten different climate change scenarios were used to provide meteorological inputs to these two models. They computed six extreme temperature metrics (7-day maximum, percent of maximum temperature >24°C, percent of maximum temperature >28°C, duration of consecutive days with maximum >24, timing of first daily maximum >24°C daily, and percent minimum >20°C). Among the predicted changes, they noted important increases in occurrence and duration of >24°C and >28°C temperature events in the river's main stems.

Parra et al. (2012) constructed a statistical model for maximum water temperature using air temperature as a predictor. By using air temperature as the input variable (from climate model outputs) into this statistical tool, they produced future maximum water temperature scenarios and mapped a possible reduction of 12% in suitable thermal habitat for brown trout (*Salmo trutta*) in the Mediterranean region.

Arismendi et al. (2014) criticized the use of simple regression models to infer possible changes in river temperatures associated with climate change (especially for short time scale, i.e., daily or weekly). They stated that these approaches may have a relatively limited ability to link both air and water temperatures because the underlying heat fluxes are distinctive in each medium and vary spatially and through time. It could be argued that these challenges are true for all models; however, simpler models could prove valuable in the short term (<20 years) where extrapolation into the future is limited.

Also, deterministic models may prove valuable in understanding important underlying physical processes and heat fluxes observed under climate change. For example, Morrison et al. (2002) coupled the UBC hydrological model with a one-dimensional temperature advection-dispersion model to investigate the impacts of climate change on both flow and water temperature of the Fraser River (Canada). Their projections indicated that for the period 2070–2099, peak flows would decrease by 18% and that summer mean water temperature would increase by about 2°C. Most importantly, temperatures exceeding 20°C were predicted to occur ten times more frequently.

Morid et al. (2020) proposed a deterministic modeling framework that combines the Soil and Water Assessment Tool and International River Interface Cooperative models to investigate climate change impacts on the Kikuchi River in Japan. They predicted water temperatures under two climate change scenarios that were subsequently used in a fish habitat model. They were able to generate scenarios of habitat degradation associated with increased water temperature.

Wondzell et al. (2019) used the deterministic Heat Source model to investigate the potential confounding impacts of climate change, riparian shading, and discharge on the temperature of the Middle Fork John Day River (Oregon, United States). In total, 36 scenarios combining future changes in air temperature, stream discharge decrease, and riparian vegetation shading were compared. They concluded that shade from riparian vegetation had the largest influence on the 7-day average daily maximum temperature.

Although many studies forecast possible increases in river temperature, some indicate more variability than others. Kwak et al. (2017) modeled future water temperature scenarios in a relatively small impounded system, the Fourchue River (QC, Canada) using the CEQUEAU hydrological and water temperature model, with meteorological inputs from the CMIP5 GCMs and two more or less optimistic

greenhouse gas emission scenarios. Results of this study indicated that water temperature in June would increase by as much as 0.7°C over the 2050 horizon. In contrast, September water temperature could decrease by more than 0.2°C due to an increase in predicted discharge for the same period.

At the global scale, van Vliet et al. (2013) coupled a hydrological and thermal model at the global scale and investigated bivariate extreme events: the so-called hot-dry events that combine low flows and high water temperatures. They mapped areas, where low flows are likely to decrease on average by 25% and water temperatures are likely to rise by more than 2°C and found that the area where these combined extremes could occur covers 18% of the globe and include regions with high human population density, such as China and the United States.

Future work

In recent years, a number of important water temperature databases have been constructed (see Ouellet et al., 2020, for a partial list). As these databases are being populated, more analytical and modeling work on extreme temperatures will become feasible. For instance, the Canadian RivTemp database (www.rivtemp.ca; Boyer et al., 2016) includes a relatively large number of stations (>600) across Eastern Canada. However, the majority of these stations have relatively short (i.e., <5 years) records. Such short records preclude the implementation of traditional tools used for extreme value analyses such as frequency analysis. Trend analyses are impossible to complete on such short records but will also be of interest once the record length has sufficiently increased.

Although trend detection in river temperature data has been commonly performed, shift detection is rarely done. Nevertheless, shifts can occur for a number of natural or human-made reasons, including groundwater emergence, up-stream controls, or the development of a beaver dam, for instance. It is also possible to observe shifts in the long-term annual mean values, for instance, and these can be due to the impact of low-frequency climate oscillation phenomena, for instance. Global climate circulation has a direct impact on air temperature and precipitation, among other variables, and therefore, influences river temperature also. These oscillatory phenomena can lead to the detection of shifts and apparent trends in the series when the series is not long enough. What can be detected statistically as a trend may in fact be a correlation with one or a number of climate oscillation indices (see, for instance, Ouarda et al., 2014. The separation of climate change and climate variability signals in hydro-climatic variables remains a topic of much work and needs also to be looked at for river temperature data. Bayesian regression-based change detection procedures (see, for instance, Seidou et al., 2007) can be practical tools to detect and attribute changes in river temperature series. They are also perfect tools to model the evolution of river temperature data as a function of air temperature.

River temperature phenomena are multivariate in nature as it is possible to focus on a number of variables other than mean water temperatures (maxima and minima, daily ranges between maxima and minima, exceedances above or values below thresholds, extremes considered over a certain period of time, etc.). It is hence also important to use multivariate trend and shift detection techniques (see, for instance, Chebana et al., 2017) to study the evolution of river temperature characteristics. For instance, although the trends in the maximum and minimum daily river temperatures may be statistically insignificant, the change in the daily min-max range may be significant with substantial impacts on fish habitat.

Future work can also focus on the use of a number of advanced statistical techniques for the development of improved predictions of future river temperature regimes. These would include, for instance, covariate-based models (frequency models in which the parameters are a function of covariates that represent time or the status of a relevant climate oscillation indices) or wavelet- or inverse wavelet-based techniques. It is also worthwhile to use empirical mode decomposition techniques (Lee and Ouarda, 2011) to develop long-term estimates of river temperatures that take into consideration climate variability and change. Functional data analysis is gaining popularity and its use for the forecasting of hydro-climatic variables was shown to lead to improved performances (for instance, Curceac et al., 2019). Future work should also focus on the application of FDA for the forecasting and prediction of river temperature in the context of climate change. Better forecasting capacity will become especially important for fisheries management, given that the limit of adequate habitat of many warm-water fish species will likely shift further north, thereby expanding their territory and inducing competition with native species (Sharma et al., 2007).

It would also be interesting to develop a temperature-duration-curve context, similar to the flow-duration-curve framework (Castellarin et al., 2013), to transfer river temperature information from gauged to ungauged sites and to fill in missing data in the context of a changing climate. Some researchers investigated the development of regional hydrological estimation approaches that take into consideration climate change signal. It would be curious to investigate the applicability of these approaches to river temperature regionalization. Most previous work has focused on mean and extreme values of river temperature, but it would also be important to investigate the evolution of the variance of river temperature data in the context of climate change. Finally, previous work has also shown that not only the parameters of the distribution but the whole parent distribution of hydro-climatic variables changes in the context of climate change. It would be important to investigate this hypothesis for river temperature data, as it would have significant impacts on the environment and the habitat of aquatic species.

Conclusions

This review of river temperature extremes provides a summary of the research completed in the past few decades. Water temperature extremes are most often defined in terms of either threshold exceedances or in terms of maxima for a given duration.

The main physical processes that define extreme temperatures were reviewed in the context of potential changes associated with climate change. Many of the main heat fluxes driving water temperature changes will likely change in the future; however, local variability may be as important as the trending signal over the next decades. Heat flux terms that are associated (and calculated) with air temperature are predicted to increase. Evaporative cooling may become even more important than currently as a regulating mechanism for river temperature.

Most trend analyses performed on historical data were conducted on mean river temperatures. They indicate significant positive trends in many parts of the world, including North America and Europe, where trends vary between 0.1 and 0.4°C/decade.

Modeling future thermal scenarios has been mostly done at local scales, on one or few watersheds at a time. The modeling tools are quite varied and include statistical, deterministic, and hybrid models. In some cases, the number of inputs required to generate water temperature scenarios is extensive and

some of the climate model outputs required need to be further examined for essential variables other than air temperature used to estimate water temperature and potential biases. Nonetheless, increases in water temperature of up to 2°C are projected by some modeling studies, as well as an increase of the frequency of occurrence of relatively high temperatures for the 2100 horizon.

References

Abdi, R., Endreny, T., Nowak, D., 2020. A model to integrate urban river thermal cooling in river restoration. J. Environ. Manag. 258 (March). https://doi.org/10.1016/j.jenvman.2019.110023, 110023.

Adrien, M., Brauchli, T., Lehning, M., Schaefli, B., Huwald, H., 2020. Stream temperature and discharge evolution in Switzerland over the last 50 years: annua and seasonal behaviour. Hydrol. Earth Syst. Sci. 24 (1), 115–142. https://doi.org/10.5194/hess-24-115-2020.

Arismendi, I., Safeeq, M., Dunham, J.B., Johnson, S.L., 2014. Can air temperature be used to project influences of climate change on stream temperature? Environ. Res. Lett. 9 (8). https://doi.org/10.1088/1748-9326/9/8/084015, 084015.

Bartók, B., Wild, M., Folini, D., Lüthi, D., Kotlarski, S., Schär, C., Vautard, R., Jerez, S., Imecs, Z., 2017. Projected changes in surface solar radiation in CMIP5 global climate models and in EURO-CORDEX regional climate models for Europe. Clim. Dyn. 49 (7–8), 2665–2683. https://doi.org/10.1007/s00382-016-3471-2.

Boyer, C., Andre, S.-H., Allen Curry, R., Caissie, D., Gillis, C.-A., 2016. Technical Report: RivTemp: A Water Temperature Network for Atlantic Salmon Rivers in Eastern Canada. Water News, Canadian Water Association Newsletter, Spring edition.

Breau, C., Caissie, D., 2013. Adaptive management strategies to protect salmon (Salmo salar) under environmentally stressful conditions. DFO Can. Sci. Adv. Secr. Res. Doc. 2012/164. ii+14 p.

Caissie, D., 2006. The thermal regime of rivers: a review. Freshw. Biol. 51 (8), 1389–1406. https://doi.org/10.1111/j.1365-2427.2006.01597.x.

Caissie, D., Luce, C.H., 2017. Quantifying streambed advection and conduction heat fluxes: quantifying streambed heat fluxes. Water Resour. Res. 53 (2), 1595–1624. https://doi.org/10.1002/2016WR019813.

Caissie, D., El-Jabi, N., St-Hilaire, A., 1998. Stochastic modelling of water temperatures in a small stream using air to water relations. Can. J. Civ. Eng. 25 (2), 250–260.

Caissie, D., Thistle, M.E., Benyahya, L., 2017. River temperature forecasting: case study for little Southwest Miramichi River (New Brunswick, Canada). Hydrol. Sci. J. 62 (5), 683–697. https://doi.org/10.1080/02626667.2016.1261144.

Caissie, D., Ashkar, F., El-Jabi, N., 2020. Analysis of air/river maximum daily temperature characteristics using the peaks over threshold approach. Ecohydrology 13 (1). https://doi.org/10.1002/eco.2176.

Castellarin, A., Camorani, G., Brath, A., 2013. Predicting annual and long-term flow-duration curves in ungauged basins. Adv. Water Resour. 30 (4), 937–953.

Chebana, F., Aissia, M.A.B., Ouarda, T.B.M.J., 2017. Multivariate shift testing for hydrological variables, review, comparison and application. J. Hydrol. 548, 88–103.

Curceac, S., Ternynck, C., Ouarda, T.B.M.J., Chebana, F., Dabo-Niang, S., 2019. Short-term air temperature forecasting using Nonparametric Functional Data Analysis and SARMA models. Environ. Model. Softw. 111, 394–408.

Daigle, A., Jeong, D.I., Lapointe, M.F., 2015. Climate change and resilience of tributary thermal refugia for salmonids in eastern Canadian Rivers. Hydrol. Sci. J. 60 (6), 1044–1063. https://doi.org/10.1080/02626667.2014.898121.

Dugdale, S.J., Hannah, D.M., Malcolm, I.A., 2017. River temperature modelling: a review of process-based approaches and future directions. Earth Sci. Rev. 175 (December), 97–113. https://doi.org/10.1016/j.earscirev.2017.10.009.

Eaton, J.G., Scheller, R.M., 1996. Effects of climate warming on fish thermal habitat in streams of the United States. Limnol. Oceanogr. 41 (5), 1109–1115. https://doi.org/10.4319/lo.1996.41.5.1109.

Essaid, H.I., Caldwell, R.R., 2017. Evaluating the impact of irrigation on surface water—groundwater interaction and stream temperature in an agricultural watershed. Sci. Total Environ. 599–600 (December), 581–596. https://doi.org/10.1016/j.scitotenv.2017.04.205.

Fant, C., Adam Schlosser, C., Strzepek, K., 2016. The impact of climate change on wind and solar resources in Southern Africa. Appl. Energy 161 (January), 556–564. https://doi.org/10.1016/j.apenergy.2015.03.042.

Gunn, J., Snucins, E., 2010. Brook Charr mortalities during extreme temperature events in Sutton River, Hudson Bay Lowlands, Canada. Hydrobiologia 650 (1), 79–84. https://doi.org/10.1007/s10750-010-0201-3.

Gutowsky, W., Gutzer, D., Wang, W.-C., 1991. Surface energy balances of three general circulation models: implications for simulating regional climate change. J. Clim. 4, 121–134.

Hannah, D.M., Garner, G., 2015. River water temperature in the United Kingdom: changes over the 20th century and possible changes over the 21st century. Prog. Phys. Geogr. 39 (1), 68–92. https://doi.org/10.1177/0309133314550669.

Hrdinka, T., Vlasák, P., Havel, L., Mlejnská, E., 2015. Possible impacts of climate change on water quality in streams of the Czech Republic. Hydrol. Sci. J. 60 (2), 192–201. https://doi.org/10.1080/02626667.2014.889830.

Isaak, D.J., Wenger, S.J., Peterson, E.E., Ver Hoef, J.M., Nagel, D.E., Luce, C.H., Hostetler, S.W., et al., 2017. The NorWeST summer stream temperature model and scenarios for the Western U.S.: a crowd-sourced database and new geospatial tools foster a user community and predict broad climate warming of rivers and streams: stream climates in the Western U.S. Water Resour. Res. 53 (11), 9181–9205. https://doi.org/10.1002/2017WR020969.

Islam, S.U., Hay, R.W., Déry, S.J., Booth, B.P., 2019. Modelling the impacts of climate change on riverine thermal regimes in Western Canada's Largest Pacific Watershed. Sci. Rep. 9 (1), 11398. https://doi.org/10.1038/s41598-019-47804-2.

Jeong, D.I., Daigle, A., St-Hilaire, A., 2013. Development of a stochastic water temperature model and projection of future water temperature and extreme events in the Ouelle River Basin (Canada). River Res. Appl. 29 (7), 805–821. https://doi.org/10.1002/rra.2574.

Kay, A.L., Bell, V.A., Blyth, E.M., Crooks, S.M., Davies, H.N., Reynard, N.S., 2013. A hydrological perspective on evaporation: historical trends and future projections in Britain. J. Water Clim. Change 4 (3), 193–208. https://doi.org/10.2166/wcc.2013.014.

Kurylyk, B.L., MacQuarrie, K.T.B., Caissie, D., McKenzie, J.M., 2015a. Shallow groundwater thermal sensitivity to climate change and land cover disturbances: derivation of analytical expressions and implications for stream temperature modeling. Hydrol. Earth Syst. Sci. 19, 2469–2489.

Kurylyk, B.L., MacQuarrie, K.T.B., Linnansaari, T., Cunjak, R.A., Allen Curry, R., 2015b. Preserving, augmenting, and creating cold-water thermal refugia in rivers: concepts derived from research on the Miramichi river, New Brunswick (Canada): preserving, augmenting, and creating cold-water thermal Refugia in rivers. Ecohydrology 8 (6), 1095–1108. https://doi.org/10.1002/eco.1566.

Kwak, J., St-Hilaire, A., Chebana, F., Kim, G., 2017. Summer season water temperature modeling under the climate change: case study for Fourchue River, Quebec, Canada. Water 9 (5), 346. https://doi.org/10.3390/w9050346.

Lee, T., Ouarda, T.B.M.J., 2011. Prediction of climate nonstationary oscillation processes with empirical mode decomposition. J. Geophys. Res. Atmos. 16 (D6).

Letcher, B.H., Hocking, D.J., O'Neil, K., Whiteley, A.R., Nislow, K.H., O'Donnell, M.J., 2016. A hierarchical model of daily stream temperature using air-water temperature synchronization, autocorrelation, and time lags. PeerJ 4 (February). https://doi.org/10.7717/peerj.1727, e1727.

Lisi, P.J., Schindler, D.E., Cline, T.J., Scheuerell, M.D., Walsh, P.B., 2015. Watershed geomorphology and snowmelt control stream thermal sensitivity to air temperature: water source and stream thermal regimes. Geophys. Res. Lett. 42 (9), 3380–3388. https://doi.org/10.1002/2015GL064083.

Liu, Q., McVicar, T.R., 2012. Assessing climate change induced modification of penman potential evaporation and runoff sensitivity in a large water-limited basin. J. Hydrol. 464–465 (September), 352–362. https://doi.org/10.1016/j.jhydrol.2012.07.032.

Maheu, A., Caissie, D., St-Hilaire, A., El-Jabi, N., 2014. River evaporation and corresponding heat fluxes in forested catchments. Hydrol. Process. 28 (23), 5725–5738. https://doi.org/10.1002/hyp.10071.

Michie, L.E., Hitchcock, J.N., Thiem, J.D., Boys, C.A., Mitrovic, S.M., 2020. The effect of varied dam release mechanisms and storage volume on downstream river thermal regimes. Limnologica. https://doi.org/10.1016/j.limno.2020.125760, 125760.

Mohseni, O., Stefan, H.G., 1999. Stream temperature/air temperature relationship: a physical interpretation. J. Hydrol. 218, 128–141.

Mohseni, O., Stefan, H.G., Eaton, J.G., 2003. Global warming and potential changes in fish habitat in U.S. streams. Clim. Chang. 59 (3), 389–409. https://doi.org/10.1023/A:1024847723344.

Morid, R., Shimatani, Y., Sato, T., 2020. An integrated framework for prediction of climate change impact on habitat suitability of a river in terms of water temperature, hydrological and hydraulic parameters. J. Hydrol. https://doi.org/10.1016/j.jhydrol.2020.124936, 124936.

Morrison, J., Quick, M., Foreman, M., 2002. Climate change in the Fraser river watershed: flow and temperature projections. J. Hydrol. 263 (1), 230–244.

Orr, H.G., Simpson, G.L., Clers, S.d., Watts, G., Hughes, M., Hannaford, J., Dunbar, M.J., et al., 2015. Detecting changing river temperatures in England and Wales: river temperature change. Hydrol. Process. 29 (5), 752–766. https://doi.org/10.1002/hyp.10181.

Ouarda, T.B.M.J., Charron, C., Niranjan Kumar, K., Marpu, P.R., Ghedira, H., Molini, A., Khayal, I., 2014. Evolution of the rainfall regime in the United Arab Emirates. J. Hydrol. 514, 258–270.

Ouellet, V., St-Hilaire, A., Dugdale, S., Hannah, D., Ouellet-Proulx, S., 2020. Challenges and Opportunities for Water Temperature Research and Pratice. Submitted to Science of the Total Environment.

Parra, I., Almodóvar, A., Ayllón, D., Nicola, G.G., Elvira, B., 2012. Unravelling the effects of water temperature and density dependence on the spatial variation of brown trout (Salmo trutta) body size. Can. J. Fish. Aquat. Sci. 69, 821–832.

Pekárová, P., Onderka, M., Pekár, J., Rončák, P., Miklánek, P., 2009. Prediction of water quality in the Danube river under extreme hydrological and temperature conditions. J. Hydrol. Hydromech. 57 (1), 3–15. https://doi.org/10.2478/v10098-009-0001-5.

Piccolroaz, S., Toffolon, M., Robinson, C., Siviglia, A., 2018. Exploring and quantifying river thermal response to heatwaves. Water 10 (8), 1098. https://doi.org/10.3390/w10081098.

Poff, N.L.R., Allan, J.D., Bain, M.B., Karr, J.R., Prestegaard, K.L., Richter, B.D., Sparks, R.E., Stromberg, J.C., 1997. The natural flow regime. Bioscience 47 (11), 769–784. https://doi.org/10.2307/1313099.

Pryor, S.C., Barthelmie, R.J., 2010. Climate change impacts on wind energy: a review. Renew. Sust. Energ. Rev. 14 (1), 430–437. https://doi.org/10.1016/j.rser.2009.07.028.

Ptak, M., Sojka, M., Kałuża, T., Choiński, A., Nowak, B., 2019. Long-term water temperature trends of the Warta river in the years 1960–2009. Ecohydrol. Hydrobiol. 19 (3), 441–451. https://doi.org/10.1016/j.ecohyd.2019.03.007.

Qiu, H., Hamilton, S.K., Phanikumar, M.S., 2020. Modeling the effects of vegetation on stream temperature dynamics in a large, mixed land cover watershed in the great lakes region. J. Hydrol. 581 (February), 124283. https://doi.org/10.1016/j.jhydrol.2019.124283.

Sanchez-Lorenzo, A., Wild, M., 2012. Decadal variations in estimated surface solar radiation over Switzerland since the late 19th century. Atmos. Chem. Phys. 12 (18), 8635–8644. https://doi.org/10.5194/acp-12-8635-2012.

Seidou, O., Asselin, J.J., Ouarda, T.B.M.J., 2007. Bayesian multivariate linear regression with application to change point models in hydrometeorological variables. Water Resour. Res. 43 (8).

Sharma, S., Jackson, D.A., Minns, C.K., Shuter, B.J., 2007. Will northern fish populations be in hot water because of climate change? Glob. Chang. Biol. 13, 2052–2064.

Soto, B., 2016. Assessment of trends in stream temperatures in the north of the Iberian Peninsula using a nonlinear regression model for the period 1950-2013: stream temperatures in the Iberian Peninsula. River Res. Appl. 32 (6), 1355–1364. https://doi.org/10.1002/rra.2971.

Steel, A.E., Sowder, C., Peterson, E.E., 2016. Spatial and temporal variation of water temperature regimes on the Snoqualmie river network. J. Am. Water Resour. As. 52 (3), 769–787. https://doi.org/10.1111/1752-1688.12423.

Thiombiano, A.N., El Adlouni, S., St-Hilaire, A., Ouarda, T.B.M.J., El-Jabi, N., 2017. Nonstationary frequency analysis of extreme daily precipitation amounts in Southeastern Canada using a peaks-over-threshold approach. Theor. Appl. Climatol. 129 (1–2), 413–426. https://doi.org/10.1007/s00704-016-1789-7.

Toffolon, M., Piccolroaz, S., 2018. A hybrid model for river water temperature as a function of air temperature and discharge. Environ. Res. Lett. 10 (11), 114011.

van Vliet, M.T.H., Franssen, W.H.P., Yearsley, J.R., Ludwig, F., Haddeland, I., Lettenmaier, D.P., Kabat, P., 2013. Global river discharge and water temperature under climate change. Glob. Environ. Chang. 23 (2), 450–464. https://doi.org/10.1016/j.gloenvcha.2012.11.002.

Wanders, N., Vliet, M.T.H., Wada, Y., Bierkens, M.F.P., Beek, L.P.H.(.R.)., 2019. High-resolution global water temperature modeling. Water Resour. Res. 55 (4), 2760–2778. https://doi.org/10.1029/2018WR023250.

Webb, B., 1996. Trends in stream and river temperature. Hydrol. Process. 10 (2), 205–226.

Webb, B., Nobilis, F., 2007. Long-term changes in river temperature and the influence of climatic and hydrological factors. Hydrol Sci J. 52 (1), 74–85. https://doi.org/10.1623/hysj.52.1.74.

Whelsh, H., Hodjson, J.R., Harvey, B.C., Roche, M.F., 2001. Distribution of juvenile coho salmon in relation to water temperatures in tributaries of the Mattole River, California. N. Am. J. Fish. Manag. 21 (3), 464–470.

Wild, M., Ohmura, A., Gilgen, H., 2001. Evaluation of downward longwave radiation in general circulation models. J. Clim. 14 (15), 3227–3239.

Wondzell, S.M., Diabat, M., Haggerty, R., 2019. What matters most: are future stream temperatures more sensitive to changing air temperatures, discharge, or riparian vegetation? J. Am. Water Resour. Assoc. 55 (1), 116–132. https://doi.org/10.1111/1752-1688.12707.

Workru, G., Teferi, E., Batinder, A., DIile, Y., 2020. Statistical bias correction of regional climate model simulations for climate change projection in the Jemma Sub-Basin, Upper Blue Nile Basin of Ethiopia. Theor. Appl. Climatol. 139, 1569–1588.

CHAPTER

Severe convective storms in a changing climate

4

Vittorio (Victor) A. Gensini
Northern Illinois University, DeKalb, IL, United States

The 40-year period from 1980 to 2019 observed 258 distinct billion-dollar weather- and climate-related disasters (NCEI, 2020). Of those, ~44% (113 disasters) were the result of severe convective storms (SCSs), with consumer price index-adjusted losses exceeding $230 billion and more than 1500 fatalities. SCSs lead the way in percent frequency of billion-dollar disasters, with tropical cyclones placing a distant second (17%). Despite a significant increase in contiguous United States (CONUS) SCS (tornadoes, large hail, damaging convective wind gusts) reports over the past three decades (Tippett et al., 2015), research indicates that environmental control factors (e.g., convective available potential energy [CAPE] and 0–6 km deep-layer wind shear) have exhibited little to no annual trend (Gensini and Ashley, 2011; Robinson et al., 2013). This recent inflation in SCS reports has been extensively documented (Doswell III and Burgess, 1988; Grazulis, 1993; Brooks and Doswell III, 2001; Brooks and Doswell III, 2002; Verbout et al., 2006; Doswell, 2007). Thus the recent increase in losses from severe thunderstorms (Changnon, 2001) and tornadoes (Brooks and Doswell III, 2001; Changnon, 2009) may be attributed to societal and economic changes rather than an increase in SCS frequency (Bouwer, 2011). Increases in SCS losses are demonstrated by examining the trend in billion-dollar severe storm events since 1980 (Fig. 1).

Given the socioeconomic importance of these events, this chapter will explore the landscape of SCSs in a changing climate, highlighting what scientists know, what scientists desire to know, and avenues for potential research to push scientific understanding forward. The chapter starts with a brief overview of current trends in SCS events before explaining the environments that support such phenomena and their recorded variability. Next, some of the major large-scale drivers of SCS events as they relate to climate variability are discussed. This includes discussion of the so-called climate teleconnections (e.g., El Nino Southern Oscillation) that are known to influence global weather patterns and have an influence on extreme weather. Finally, the latest research in attempting to study SCS events and climate change is examined, with specific emphasis on the convection-permitting dynamical downscaling methodology. Throughout the chapter, future areas ripe for research productivity will be highlighted in an effort to guide readers toward cutting-edge research that will be needed to reduce uncertainty associated with the future landscape of these costly extreme weather events.

Climate Change and Extreme Events. https://doi.org/10.1016/B978-0-12-822700-8.00007-X
Copyright © 2021 Elsevier Inc. All rights reserved.

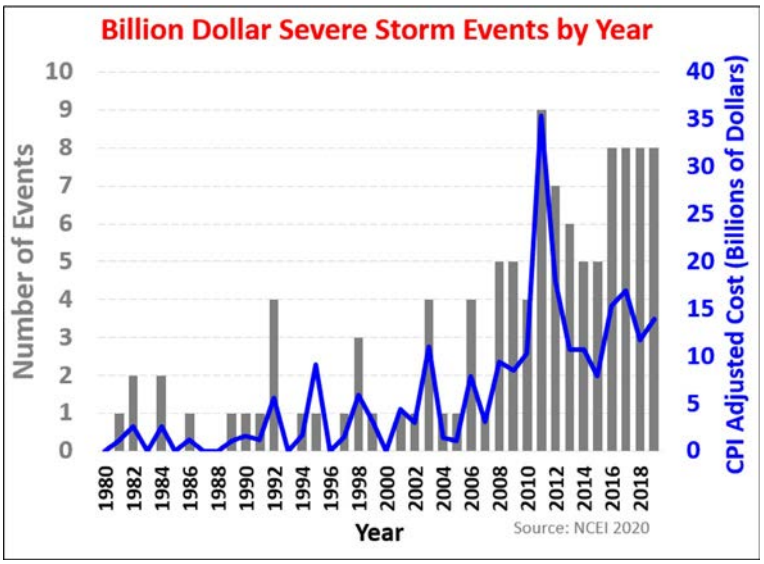

FIG. 1

Number of US billion-dollar severe convective storm events (bars; left axis) and associated cost since 1980.
Data source: NCEI, 2020. Billion-Dollar Weather and Climate Disasters: Overview. https://www.ncdc.noaa.gov/billions/.

Observations and trends

Recent trends in global and United States temperature have provoked questions about the impact on frequency, intensity, timing, and location of SCS events. When removing nonmeteorological factors, it is shown that the annual frequency of United States SCS through the most reliable portions of the historical record (roughly starting around 1950) has remained relatively constant (Verbout et al., 2006; Kunkel et al., 2013; Tippett et al., 2015). The most notable trends in SCS frequency are associated with increasing annual variability and a recent tendency for more tornadoes on any given tornado day (Brooks et al., 2014; Tippett et al., 2016). There has also been a measurable shift in the annual timing of tornado season, but it is currently unknown if this is due to rising global temperatures or natural variability (Long and Stoy, 2014; Lu et al., 2015). Temporally, the average annual number of US tornado reports more than doubles over the lifetime of the modern SCS record (1950 to current), with most of this increase associated with weak tornadoes (those rated [E]F0 on the [enhanced] Fujita scale; Doswell III et al., 2009). Similarly, CONUS hail and damaging convective wind gust reports have increased by an order of magnitude through the same reporting period (Tippett et al., 2015). Increases in all SCS hazards appear to be nonmeteorological in origin (Verbout et al., 2006; Allen and Tippett, 2015; Edwards et al., 2018). However, there are aspects of SCS reports that are less affected by such nonmeteorological factors. Examples include annual significant tornado frequency (those rated [E]F2 or greater), the number of annual days with significant hail reports (diameter $\geq \approx 5$ cm), and measured severe convective wind gusts (Allen and Tippett, 2015; Tippett et al., 2015; Edwards et al., 2018). For tornadoes, the aggregate consensus indicates that frequency has remained relatively constant through the most reliable portions of the climatological record (Verbout et al., 2006; Kunkel et al., 2013;

Tippett et al., 2015; Long et al., 2018; Potvin et al., 2019). Trends have been noted, however, in the temporal variability (Brooks et al., 2014; Tippett, 2014; Farney and Dixon, 2015; Guo et al., 2016) and spatial locations of tornado (Gensini and Brooks, 2018; Moore and McGuire, 2019) and hail (Tang et al., 2019) reports. A clearer consensus about spatio-temporal trends in damaging convective wind gusts has yet to emerge in the literature (Gensini et al., 2020a, b).

Environments

Observed reporting deficiencies have motivated researchers to focus on developing and analyzing derived atmospheric indices relating environmental conditions to tornado occurrence. Such indices are often used in an ingredients-based approach commonly used in operational weather forecasting (Johns and Doswell III, 1992). A derived covariate representing the background atmospheric state may be preferable to SCS reports for climatological studies. For example, it has been shown that variables such as storm relative helicity and convective precipitation adequately represent United States monthly tornado frequency (Tippett, 2014; Gensini and Bravo de Guenni, 2019). Reports are subject to a human reporting process, whereas environmental covariates allow for an objective model-derived climatology. This is typically done by mining historical reanalysis datasets. However, one major limitation of the covariate methodology for SCS reports is the lack of accounting for a thunderstorm initiation metric. It is well documented that SCSs occur in environments characteristic of adequate vertical wind shear, relatively high surface water vapor mixing ratios, directional change in the lowest 1 km of tropospheric wind, and low static stability (Rasmussen and Blanchard, 1998; Rasmussen, 2003). Yet, even with a supportive atmosphere, thunderstorms may not form in the absence of an initial lifting mechanism needed to commence the convective process (i.e., convective initiation). The space and time scales of various lifting sources are often below the spatial scale of current reanalysis observation capabilities, and thus, not accounted for by most covariate environmental metrics. This often leads to an overestimation of favorable SCS environments and a lack of explanatory capability regarding observed SCS reports (Hoogewind et al., 2017). Still, these "convective environments" are extremely useful in understanding the global climatologies of SCSs.

Studies using the background convective environment have typically resulted in the formation of spatial-statistical models using various forms of regression techniques. As an example, Poisson regression has demonstrated skill in explaining the variance associated with monthly tornado frequency by using an observation-based covariate of monthly averaged atmospheric parameters (Tippett et al., 2012, 2014). A Bayesian hierarchical approach and an inhomogeneous Poisson process have also been used to explain the variance of tornado frequency at various spatio-temporal scales using convective environments (Cheng et al., 2016; Gensini and Bravo de Guenni, 2019). Similar work has also been done over North America for large hail reports to estimate hailstone diameter and/or frequency from the convective environment (Jewell and Brimelow, 2009; Allen et al., 2015).

SCSs and climate change

There is a growing body of literature (numerous studies cited in the Intergovernmental Panel on Climate Change Fifth Assessment Report [IPCC AR5]) describing the potential large-scale changes in sensible weather conditions in the 21st century (Pachauri et al., 2014). The IPCC AR5 report states

that heavy precipitation events (another aspect of SCSs) are likely to increase in frequency during the 21st century. The report, however, makes broad generalizations regarding regional thunderstorm activity (Tippett et al., 2015), admitting that SCS frequency is highly variable and sensitive to remote (teleconnections) and local forcings (Diffenbaugh et al., 2008; Kendon et al., 2014). Compounding these issues, the report generally relied on coarse-resolution GCMs, which cannot currently resolve phenomena below the spatial dimension of meso-β (20–200 km; Stevens and Bony, 2013). Thus more research is needed to reduce this uncertainty in SCS activity projections, and dynamical downscaling to convection-permitting resolution will be a viable methodology for this problem for the foreseeable future due to the proposed Coupled Model Intercomparison Project Phase 6 model suite horizontal grid spacings (Eyring et al., 2016).

Preliminary research suggests that environmental controls related to SCSs (e.g., CAPE) will increase in response to elevated greenhouse forcing (Del Genio et al., 2007; Trapp et al., 2007, 2009; Van Klooster and Roebber, 2009; Diffenbaugh et al., 2013; Gensini et al., 2014, Seeley and Romps, 2015; Hoogewind et al., 2017). Despite this evidence, climate change assessments have largely avoided any conclusions regarding potential changes of SCSs in a future climate (see discussions in Alley, 2007, Karl et al., 2009 and Brooks, 2013). This is primarily due to problems with the historical record of observed SCS reports, the link between SCS reports and associated environmental controls, and the large spatial scale in which GCMs operate relative to SCSs. Although more SCS environments could mean more events in the future, such environments indicate periods when the atmosphere is favorable for organized SCSs, not that it will necessarily occur due to the convective initiation problem discussed earlier. To mitigate this deficiency, recent research has turned to the use of convection-permitting dynamical downscaling in an attempt to resolve storm-scale features that are important for the assessment of SCSs.

Convection-permitting dynamical downscaling

The effect of future climatic change on severe thunderstorm occurrence can also be explicitly modeled via dynamical downscaling. These analyses use coarse-resolution global climate models or reanalysis data as initial and lateral boundary conditions to drive regional convective-allowing models through dynamical downscaling to produce realistic simulations of SCSs (Trapp et al., 2011; Robinson et al., 2013; Gensini and Mote, 2014, 2015; Prein et al., 2017; Trapp and Hoogewind, 2016; Hoogewind et al., 2017; Liu et al., 2017; Trapp et al., 2019). This process is similar to that used in short-range numerical weather prediction. These recent simulations have been found to reasonably reproduce observations of rainfall and convective hazards (Trapp et al., 2011; Bukovsky and Karoly, 2011; Robinson et al., 2013; Lackmann, 2013; Gensini and Mote, 2014, 2015; Hoogewind et al., 2017; Trapp et al., 2019) to replicate meso-γ (i.e., $\leq$10-km horizontal scale) processes critical to the development and evolution of the convection that produces SCSs (e.g., supercell thunderstorms).

A growing number of studies have produced future regional climate model simulations at convection-permitting scales (Rasmussen et al., 2011, 2014; Kendon et al., 2012; Harding et al., 2013; Lauer et al., 2013; Mahoney et al., 2013; Prein et al., 2013; Prein et al., 2017). However, few studies have examined the potential for future SCS change using this explicit downscaling methodology. Gensini and Mote (2015) used the Community Climate System Model 3 (Collins et al., 2006) and the Weather Research and Forecasting (WRF) model (Powers et al., 2017) to explicitly simulate SCSs for past and future periods during the months of March, April, and May. Of note was the increase in the

overall mean of SCS activity, but also an increase in the interannual variability (more high-frequency SCS seasons; more low-frequency SCS seasons). In addition, the spatial areas of greatest SCS increase were noted in already vulnerable regions (Ashley, 2007). Hoogewind et al. (2017) expanded this research (also using WRF) to the annual cycle, finding similar results using a different integration technique, different convection-permitting microphysics, and a different parent GCM from the Coupled Model Intercomparison Project Phase 5 model suite. Although these studies used different approaches and largely came to the same conclusions, they still only represent two experiments attempting to understand the potential for change in the CONUS SCSs. Regarding specific SCS hazards, Mahoney et al. (2013) produced high-resolution WRF simulations (1.33 km) over Colorado and examined how hailstorm frequency and intensity may change in the future, and they found that for warm-season extreme precipitation events, hail reaching the surface was significantly decreased owing to the increased height of the melting level. These three studies discuss the need for more research focused on dynamical downscaling to further asses SCS activity. It should be noted that a horizontal grid spacing of 3 or 4 km is much too coarse to resolve specific SCS phenomena. Instead, convection-permitting configurations for these purposes rely heavily on the detection of rotating updrafts in a favorable atmospheric environment to explain variability in SCS frequency (Potvin and Flora, 2015). This has been demonstrated to be an effective approach given our understanding of the theory behind the atmospheric ingredients present during the time of observed severe weather (e.g., adequate tropospheric wind shear, high surface water vapor mixing ratios, surface air parcel buoyancy).

Explicit dynamical downscaling approaches to detect and track SCS activity rely on extracting synthetic (i.e., surrogate) SCS events from within the convective-allowing model, using severe weather reports for calibration guidance. For example, composite RADAR reflectivity factor, maximum updraft velocity, and 2- to 5-km updraft helicity have been used to serve as a climatological proxy for SCS events (Trapp et al., 2011; Robinson et al., 2013; Gensini and Mote, 2014, 2015; Hoogewind et al., 2017; Trapp et al., 2019). Also, RCMs using a convection-permitting configuration have a well-documented ability to produce guidance products shown to be skillful for detecting various SCS hazards, such as tornado path length (Clark et al., 2013), hail size (Adams-Selin and Ziegler, 2016; Gagne et al., 2017), and total severe weather probabilities (Sobash et al., 2011; Sobash et al., 2016). Tracking, on the other hand, detects such synthetic events with the added complexity of associating these objects with time that can be done in an automated fashion if researchers understand the underlying assumptions of image processing theory. Tracking of mesoscale convective systems from observed RADAR data is a good example of what is possible when applying convolutional neural network techniques on meteorological data (Haberlie and Ashley, 2018).

Such explicit storm-tracking procedures have known issues with identifying (segmentation) and associating objects between time steps (tracking), especially when handling splitting and merging events (Lakshmanan and Smith, 2010). To address this issue, supervised machine learning models have shown utility in nonparametric classification of precipitation areas in previous research (Gagne et al., 2009; Haberlie and Ashley, 2018). During supervised classification (e.g., decision trees), expert labeling of a subset of objects is performed, and the features common to each classification type (mean intensity, geometry, temporal characteristics, etc.) are used to assign types to the complete dataset. Decision tree classifiers, such as the random forest classifier (Breiman, 2001), are widely used in many applications because they are relatively easy to interpret, can provide an objective assessment of the relative importance various attributes have on the classification decision, and can perform as well as more complicated classifiers (Gagne et al., 2009; Ahijevych et al., 2016). After the random forest

classifier is trained, it provides more efficient classifications compared with other approaches. These, and other forms of, machine learning techniques will be vital to weather and climate researchers who want to identify, extract, and examine hazards within their dynamically downscaled simulations. These types of methods are already becoming popular in day-to-day weather forecasts made through numerical weather prediction. Finally, "pseudo global warming" approaches (Lackmann, 2013; Trapp and Hoogewind, 2016; Liu et al., 2017; Prein et al., 2017) and one-dimensional cloud models (Brimelow et al., 2017) have also been tested for purposes of assessing potential future changes in various SCS phenomena. These studies have shown great promise for assessing the potential for storm-scale changes due to climate change.

Drivers of interannual variability

As weather forecast skill continues to improve (Bauer et al., 2015), especially in the extended range (Wanders and Wood, 2016; Tian et al., 2017; Vigaud et al., 2017; Wang and Robertson, 2019), demand from stakeholders is growing rapidly for forecasts that cover the intraseasonal (or subseasonal) window, typically defined as the period spanning 2 weeks to 2 months into the future (Robertson et al., 2015; Schubert et al., 2002). This is particularly true for SCSs given the significant impacts (an average of more than $10 billion per year) on many economic and societal sectors (Simmons and Sutter, 2013; NCEI, 2020; Smith and Matthews, 2015). Recent research has shown some skill in forecasting US tornado and hail frequency at various lead times in the intraseasonal period (Allen et al., 2015; Lepore et al., 2017; Baggett et al., 2018; Lepore et al., 2018; Gensini and Tippett, 2019). The few contemporary demonstrations of forecast skill for SCS events at subseasonal lead times are likely a testament to the increasing accuracy of global numerical weather prediction models (Bauer et al., 2015) and our increased understanding of weather and climate factors that explain the variance in atmospheric intraseasonal frequency. For example, climatological studies have identified both spatial and temporal clustering behaviors in periods of high tornado frequency (Verbout et al., 2006; Trapp, 2014), and we now know that some weather and climate mode oscillations have strong links to US tornado and hail frequency.

Examining sources of planetary and synoptic scale variability on SCS frequency is an emerging field of research. These climate-mesoscale interactions are necessary to understand the physical reasons for years that experience abnormally high and low frequencies of SCSs. There has been little research, for example, exploring the potential climate and large-scale dynamical contributions as to why there were a record number of tornadoes in April 2011, whereas subsequent years produced abnormally low frequencies (Brooks et al., 2014). More recently, the peak of the 2018 SCS season exhibited some of the lowest tornado frequencies in the modern reporting era. In the following year, the period 17–29 May 2019 was among the most active periods of severe weather the United States has experienced in decades. Although 2019 data are still preliminary, at least 225 tornadoes occurred during this 13-day stretch, more than doubling the 1986–2016 average for this period (105). In total, 757 tornado warnings were issued by National Oceanic and Atmospheric Administration (NOAA's) National Weather Service, and seven fatalities were reported. This late-May period contributed significantly to the fourth highest monthly (E)F1+ tornado count (202) on record for May since reliable tornado counts began in the early 1950s (Gensini et al., 2019). Although some research and media reports using solely observed tornado statistics have pointed to climate change as the source of this variability, an alternate

hypothesis is that the variability may result from the projection of demonstrated (or perhaps unknown) climate teleconnections on CONUS SCS frequency. More research will be needed to examine various modes of climate variability on SCS frequency, but some demonstrated sources of forcing for CONUS SCS are the Madden-Julian oscillation (MJO), global earth-relative atmospheric angular momentum (AAM), and El-Niño Southern Oscillation (ENSO).

They are briefly summarized, given our current understanding in relation to CONUS SCS activity:

ENSO—Previous research has demonstrated that a statistically robust physical connection exists between ENSO, classified by Niño 3.4, and the large-scale environmental conditions favorable to SCSs over the CONUS during the winter and spring months (Cook and Schaefer, 2008; Lee et al., 2013; Allen et al., 2015; Cook et al., 2017; Allen et al., 2018; Molina et al., 2018). Using environmental indices that simulate the expected number of hail or tornado events, El Niño events resulted in fewer tornadoes and hail events over the central plains, contrasting an increasing frequency that was shifted eastward in La Niña conditions. Analyzing anomalous activity in the indices and observations relative to climatology, nearly all La Niña seasons are associated with frequencies greater than 100% of climatology and provide the few observed cases above 175%. Seasons with frequency below 75% of climatology are nearly exclusively associated with moderate to strong El Niño conditions. There is however a high degree of variability that cannot be explained by ENSO phase alone, which is highlighted by considering the annual cycle of El Niño and La Niña years. The mean annual cycle of CONUS large hail and tornado reports by fraction of reports per calendar day suggests that both El Niño and La Niña can modify the frequency of CONUS SCSs and lead to earlier and later shifts in the seasonal peak, respectively, but individual years can vary substantially within each phase (Allen et al., 2018).

MJO—The MJO (Madden and Julian, 1971; Madden and Julian, 1972) is the leading mode of intraseasonal variability of the tropical atmosphere. Since its discovery in the 1960s, the MJO has remained a topic of substantial scientific interest because of its extensive interactions with many components of the Earth-climate system, including those in regions beyond the tropics, such as the CONUS. Indeed, the MJO has been shown to modulate US atmospheric circulation (Seo and Son, 2012; Roundy et al., 2010; Lorenz and Hartmann, 2006; L'Heureux and Higgins, 2008; Riddle et al., 2013; Jiang et al., 2017), surface temperature (Vecchi and Bond, 2004; Zhou et al., 2012; Yao et al., 2011; Seo et al., 2016; Barrett, 2019), daily rainfall (Donald et al., 2006; Becker et al., 2011; Jones et al., 2011; Jones and Carvalho, 2012; Zhou et al., 2012; DelSole et al., 2017), atmospheric rivers (Mundhenk et al., 2018), and cloud-to-ground lightning (Abatzoglou and Brown, 2009; Tippett and Koshak, 2018). Over the warm equatorial waters of the tropical Indian and western Pacific Oceans, the MJO manifests itself as a large-scale convective anomaly. Its most basic feature consists of an eastward-moving region of deep convective clouds and heavy precipitation bounded on both the west and east by regions of suppressed convection and minimal precipitation. Zonal circulations connect the two regions, with lower troposphere (near 850 hPa) anomalous westerly (easterly) winds to the west (east) of the deep convection; in the upper troposphere (near 200 hPa), the circulation anomalies are reversed (Madden and Julian, 1972; Madden and Julian, 1994; Zhang, 2005; Zhang, 2013). In the Eastern Hemisphere, the convective signal moves eastward around 5 m s^{-1}. As the MJO reaches the Western Hemisphere and progresses over cooler ocean waters, the deep convection tends to dissipate. However, the signal remains coherent in fields of upper and lower troposphere winds and velocity potential (Knutson and Weickmann, 1987; Weickmann and Khalsa, 1990) and moves eastward at a faster 15 m s^{-1}. These circulation and convection anomalies have been observed to circumnavigate the tropics from 30 to 60 days and that is the time scale we will focus on here.

One of the most commonly used metrics for both locating the MJO geographically and defining the intensity of MJO convective activity is the real-time multivariate MJO (RMM) index of Wheeler and Hendon (2004). The daily RMM index is a combined outgoing longwave radiation (OLR)- and circulation-based index that is created from the leading empirical orthogonal functions (EOFs) of daily OLR, 200- and 850-hPa zonal wind fields. Although the RMM index is used widely in operational settings because of its real-time updates and simplicity of interpretation, it has known shortcomings. Notably, higher-frequency synoptic variability can project onto the RMM index (Roundy et al., 2009), which may then indicate westward MJO propagation or other uncharacteristic features. In addition, the RMM index has been demonstrated to exhibit a bias toward zonal wind observations over OLR observations, meaning shifts in large-scale convection and precipitation associated with the MJO may not be projected well onto the index (Straub, 2013). To account for those biases, daily MJO intensity and location can be quantified using another recently developed MJO index, the OLR MJO index (OMI; Kiladis et al., 2014), which is based on an EOF analysis of only bandpass-filtered OLR to project MJO strength and geographic position onto a phase space similar to the RMM. The OMI quantifies the MJO based on its convective anomalies, which can be an advantage over the RMM index. However, because of its focus on OLR, the OMI can miss MJO-driven circulation features. To account for these strengths and weaknesses, we will analyze the MJO in this proposed work using both the daily RMM and OMI indices, both of which are freely available online and cover the period from 1979 to current.

The tropical MJO has profound connections to weather in the extratropics because its hallmark convective heating can act as a Rossby wave source into the extratropics (Hoskins and Karoly, 1981; Sardeshmukh and Hoskins, 1988; Jin and Hoskins, 1995; Bladé and Hartmann, 1995; Roundy, 2012). It is this pathway to the extratropics that forms the foundation of our proposed work to better understand the MJO's relationship to SCS activity. In one of the first studies to examine the possible connection of CONUS severe weather frequency to the MJO, Thompson and Roundy (2013) showed that violent tornado days (i.e., 24-h periods with at least six tornadoes rated $\geq$EF2 on the enhanced Fujita [EF] scale, McDonald et al., 2010) tend to be more frequent when the MJO convection is over the Indian Ocean. In a parallel study, Barrett and Gensini (2013) found that that tornado-day likelihood varied by MJO phase, and on days when the MJO convection was active and over the Western Hemisphere and Africa, the likelihood of a tornado day increased to 51% in April (12% above climatology) and 72% in May (8% above climatology). Building on this work, Barrett and Henley (2015) found dipole-like patterns in CONUS hail-day anomalies in April and May for many active MJO phases, some more positive and some more negative, and with significant spatial variability across the US hail-day anomalies ranged from -10% to $+8\%$ with respect to the long-term climatology, again suggesting a potentially significant modulation of SCSs by the MJO. Together, Barrett and Gensini (2013), Thompson and Roundy (2013), and Barrett and Henley (2015) indicated that severe storms tend to occur to the east and south of intraseasonally evolving negative geopotential height anomalies, a pattern that favors ascent, strong instability, and significant deep-layer wind shear. The spatial structures suggest that MJO influence on both tornadoes and hail occurs on the synoptic and mesoscale.

Several other studies have extended these initial results by testing whether researchers can use the MJO as a subseasonal forecast tool for US tornado occurrence (Baggett et al., 2018; Moore and McGuire, 2020). These studies have raised new and unanswered questions regarding the MJO's role as a modulator of SCS variability, particularly with respect to the possible physical pathway by which it does so. For example, nearly 90% of the tornado activity in May 2019 occurred during phases 8 and 1 of the MJO (Fig. 2), during an extension, collapse, and retrogression (Breeden and Martin, 2019; Winters

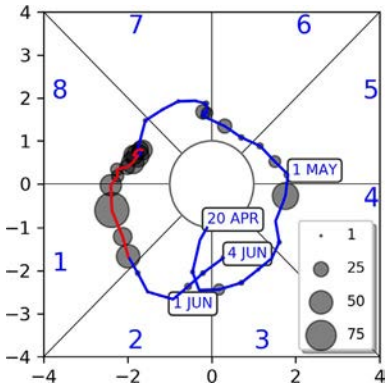

FIG. 2

Evolution of the Wheeler and Hendon (2004) MJO index from 20 April to 4 June 2019 *(blue line). Red line* represents the period 17 to 29 May 2019. *Grey circles* indicate the number of preliminary tornado reports each day. Calculated following Gensini et al. (2019).

et al., 2019) of the north Pacific jet stream. These 8-1-2 MJO phase transitions seem to be common among studies that have examined significant tornado outbreaks in the United States (Thompson and Roundy, 2013; Barrett and Gensini, 2013; Gensini and Marinaro, 2016; Tippett, 2018). The late April to early June 2019 event happened to be rather strong and well forecasted (Gensini et al., 2019; Gensini et al., 2020a, b), leading to the intraseasonal "Forecast of Opportunity" that motivates much of such research. However, as discussed above, there remains a gap in our understanding of the physical processes by which the MJO may modulate SCS activity in the United States. We hypothesize here that AAM may be a key bridge (Zhang, 2013) by which we can detect, describe, and anticipate the strength and timing of the tropical-extratropical connection.

AAM—Broadly, AAM is an important metric for describing planetary-scale changes in the global circulation due to tropical convection, extratropical dynamics, and surface torques. Changes in AAM can modulate jet stream structure, evolution, orientation, and Rossby wave dispersion in the midlatitudes. AAM forcing terms were brought together using a global synoptic-dynamic model (Weickmann and Berry, 2007), which evolved into real-time monitoring of global relative AAM (MR) and global relative AAM tendency (dMR/dt) following a previously established definition of MR (Weickmann and Sardeshmukh, 1994). The global wind oscillation (GWO) was later defined using MR and dMR/dt standardized anomalies (Weickmann and Berry, 2009). The relationship of GWO to CONUS SCS was first explored in a case study where a specific GWO stage was identified and used to forecast a mid and upper tropospheric thermal trough in the southwestern United States 2 weeks in advance, which resulted in hazardous convective weather (Weickmann and Berry, 2009). Using this framework, several new studies have used various metrics of AAM and the GWO as a covariate to SCS frequency (Gensini and Allen, 2018; Gensini and Marinaro, 2016; Moore, 2018). Using the GWO to explain Rossby wave dispersion and modulation of downstream tropospheric flow is of interest to researchers here, especially when other climate signals (like the MJO) are in weak or neutral regimes.

This area of climate teleconnection research (i.e., linking large-scale climate variability to mesoscale extreme weather events) is emerging. Scientists do not yet fully understand all the intricacies that

these modes of variability force on the general and local-scale circulations. For example, it has been suggested that Arctic sea-ice may play a role in modulating US tornado frequency (Trapp and Hoogewind, 2018). It is likely that in the next 10–15 years, scientists will have a much greater understanding of these sources of variability using machine learning and artificial intelligence. This is due to the large amount of training data required to generalize weather and climate regimes that are either favorable or unfavorable for SCS events. As our climatological datasets grow, and computational performance continues to increase, we will no doubt gain a greater understanding of the role of these (and other) important modes of weather and climate variability.

Future research

Forecasting of SCS events

In the United States, the NOAA's Storm Prediction Center (SPC) issues areal outlooks for SCS at lead times spanning 1–8 days. At such lead times, an ingredients-based approach (Johns and Doswell III, 1992) is often used in the forecast process. These ingredients include low static stability, high-surface water vapor mixing ratios, a lifting mechanism (e.g., a boundary or orographic feature) to get air parcels to the level of free convection, and adequate deep-layer vertical wind shear (Rasmussen, 2003; Rasmussen and Blanchard, 1998) to promote organized convection. More recently, storm-scale outputs from convection-permitting models provide short-range (e.g., 12–36 h) forecast guidance (Gallo et al., 2016; Gallo et al., 2018).

Accurately forecasting severe weather events remains a challenging task, but skill of SPC days 1–3 forecasts for SCSs has been increasing since the mid-1990s (Herman et al., 2018; Hitchens and Brooks, 2012; Hitchens and Brooks, 2014; Hitchens et al., 2013). Less attention has been given to forecast guidance at medium to extended lead times (e.g., 4–14 days), but there is evidence that deterministic forecasts from a numerical weather prediction ensemble can make skillful forecasts for tornado and large hail occurrence into the week 2 lead window. There are also emerging indications that tornado and hail frequencies are predictable on subseasonal to seasonal time scales (Lepore et al., 2017; Lepore et al., 2018; Gensini et al., 2019; Gensini et al., 2020a, b; Miller et al., 2020), especially those that appear to be related to the so-called forecasts of opportunity associated with some of the aforementioned modes of weather and climate variability.

A promising avenue for future forecasting of SCS events, especially as it relates to longer lead-time forecasts, is the blending of dynamical numerical weather prediction solutions with statistical techniques (e.g., self-organizing maps for weather regime classification). Because we know that dynamical forecast skill wanes in a linear fashion with time, forecasts can be weighted as a function of lead time. Additional incorporation of atmospheric teleconnection indices may allow for a weighting approach that could leverage the best of both forecast techniques and allow for more skillful prediction (versus a climatological baseline forecast) of SCS events as many as 3–4 weeks in advance.

Climate change and SCS

Significant amounts of future research are needed if scientists are to increase understanding of the impacts climate change may play on SCS frequency, intensity, and location. This research is likely to be optimally focused on the use of convection-permitting dynamical downscaling and novel machine

learning methods to extract features from copious amounts of climate model simulation data. In addition, newly available global reanalysis datasets may permit a greater understanding of the variability of SCS in space and time. This is particularly important to explain the year-to-year natural variability that is likely a function of the impacts of weather and climate teleconnections on the general circulation.

To get a full understanding of the potential for change, a large suite of ensemble simulations will be necessary. This may include multimodel (e.g., several parent GCMs driving the local simulations), multiple representations of microphysics and other parameterization schemes, and stochastic perturbations to the model state to understand sensitivity. Given current computational limitations, this has not been done to date. It will be particularly important to understand any of the potential biases that are present in the GCMs, as they are passed to the downscaled simulations. Until GCMs are simulated at cloud-resolving scale, there will continue to be a need for dynamical downscaling.

One, perhaps underappreciated, aspect of the potential for future changes in SCSs is related to the changing human-built environment. Ignoring the potential influence from climate change for a moment, economic losses associated with SCS events will continue to increase in future years, primarily due to the expanding footprint of the built environment (Ashley and Strader, 2016). It is noted that the impacts associated with projected 21st century increases in SCS frequency are outweighed by projected growth in the human-built environment. However, the combination of an increase in risk and exposure could lead to a threefold increase in tornado disaster potential (Strader et al., 2017a, b). Thus it is important to continue monitoring the presented physical trends in tornado frequency and recognize that they have consequences for increases in tornado disaster potential.

References

Abatzoglou, J.T., Brown, T.J., 2009. Influence of the Madden–Julian oscillation on summertime cloud-to-ground lightning activity over the continental United States. Mon. Weather Rev. 137, 3596–3601.

Adams-Selin, R.D., Ziegler, C.L., 2016. Forecasting hail using a one-dimensional hail growth model within WRF. Mon. Weather Rev. 144, 4919–4939.

Ahijevych, D., Pinto, J.O., Williams, J.K., Steiner, M., 2016. Probabilistic forecasts of mesoscale convective system initiation using the random forest data mining technique. Weather Forecast. 31, 581–599.

Allen, J.T., Tippett, M.K., 2015. The characteristics of United States hail reports: 1955-2014. Electron. J. Severe Storms Meteor. 10.

Allen, J.T., Tippett, M.K., Sobel, A.H., 2015. Influence of the El Niño/Southern Oscillation on tornado and hail frequency in the United States. Nat. Geosci. 8, 278–283.

Allen, J.T., Molina, M.J., Gensini, V.A., 2018. Modulation of annual cycle of tornadoes by El Niño–Southern Oscillation. Geophys. Res. Lett. 45, 5708–5717.

Alley, R.A.C., 2007. Summary for Policymakers. Cambridge University Press, pp. 1–18.

Ashley, W.S., 2007. Spatial and temporal analysis of tornado fatalities in the United States: 1880–2005. Weather Forecast. 22, 1214–1228.

Ashley, W.S., Strader, S.M., 2016. Recipe for disaster: how the dynamic ingredients of risk and exposure are changing the tornado disaster landscape. Bull. Am. Meteorol. Soc. 97, 767–786.

Baggett, C.F., Nardi, K.M., Childs, S.J., Zito, S.N., Barnes, E.A., Maloney, E.D., 2018. Skillful subseasonal forecasts of weekly tornado and hail activity using the Madden-Julian Oscillation. J. Geophys. Res. Atmos. 123, 12661–612675.

Barrett, B.S., 2019. Connections between the Madden–Julian Oscillation and surface temperatures in winter 2018 over eastern North America. Atmos. Sci. Lett. 20, e869.

Barrett, B.S., Gensini, V.A., 2013. Variability of Central United States April–May tornado day likelihood by phase of the Madden-Julian Oscillation. Geophys. Res. Lett. 40, 2790–2795.
Barrett, B.S., Henley, B.N., 2015. Intraseasonal variability of hail in the contiguous United States: relationship to the Madden–Julian Oscillation. Mon. Weather Rev. 143, 1086–1103.
Bauer, P., Thorpe, A., Brunet, G., 2015. The quiet revolution of numerical weather prediction. Nature 525, 47–55.
Becker, E.J., Berbery, E.H., Higgins, R.W., 2011. Modulation of cold-season US daily precipitation by the Madden–Julian oscillation. J. Clim. 24, 5157–5166.
Bladé, I., Hartmann, D.L., 1995. The linear and nonlinear extratropical response of the atmosphere to tropical intraseasonal heating. J. Atmos. Sci. 52, 4448–4471.
Bouwer, L.M., 2011. Have disaster losses increased due to anthropogenic climate change? Bull. Am. Meteorol. Soc. 92, 39–46.
Breeden, M., Martin, J.E., 2019. Evidence for nonlinear processes in fostering a North Pacific jet retraction. Q. J. R. Meteorol. Soc. 145, 1559–1570.
Breiman, L., 2001. Random forests. Mach. Learn. 45, 5–32.
Brimelow, J.C., Burrows, W.R., Hanesiak, J.M., 2017. The changing hail threat over North America in response to anthropogenic climate change. Nat. Clim. Change 7 (7), 516–522.
Brooks, H.E., 2013. Severe thunderstorms and climate change. Atmos. Res. 123, 129–138.
Brooks, H.E., Doswell III, C.A., 2001. Normalized damage from major tornadoes in the United States: 1890–1999. Weather Forecast. 16, 168–176.
Brooks, H.E., Doswell III, C.A., 2002. Deaths in the 3 may 1999 Oklahoma City tornado from a historical perspective. Weather Forecast. 17, 354–361.
Brooks, H.E., Carbin, G.W., Marsh, P.T., 2014. Increased variability of tornado occurrence in the United States. Science 346, 349–352.
Bukovsky, M.S., Karoly, D.J., 2011. A regional modeling study of climate change impacts on warm-season precipitation in the Central United States. J. Clim. 24, 1985–2002.
Changnon, S.A., 2001. Damaging thunderstorm activity in the United States. Bull. Am. Meteorol. Soc. 82, 597–608.
Changnon, S.A., 2009. Tornado losses in the United States. Nat. Hazard. Rev. 10, 145–150.
Cheng, V.Y., Arhonditsis, G.B., Sills, D.M., Gough, W.A., Auld, H., 2016. Predicting the climatology of tornado occurrences in North America with a Bayesian hierarchical modeling framework. J. Clim. 29, 1899–1917.
Clark, A.J., et al., 2013. Tornado pathlength forecasts from 2010 to 2011 using ensemble updraft helicity. Weather Forecast. 28, 387–407.
Collins, W.D., et al., 2006. The community climate system model version 3 (CCSM3). J. Clim. 19, 2122–2143.
Cook, A.R., Schaefer, J., 2008. The relation of El Niño–Southern oscillation (ENSO) to winter tornado outbreaks. Mon. Weather Rev. 136, 3121–3137.
Cook, A.R., Leslie, L.M., Parsons, D.B., Schaefer, J.T., 2017. The impact of El Niño–southern Oscillation (ENSO) on winter and early spring US tornado outbreaks. J. Appl. Meteorol. Climatol. 56, 2455–2478.
Del Genio, A.D., Yao, M.S., Jonas, J., 2007. Will moist convection be stronger in a warmer climate? Geophys. Res. Lett. 34.
DelSole, T., Trenary, L., Tippett, M.K., Pegion, K., 2017. Predictability of week-3–4 average temperature and precipitation over the contiguous United States. J. Clim. 30, 3499–3512.
Diffenbaugh, N.S., Trapp, R.J., Brooks, H., 2008. Does global warming influence tornado activity? Eos Trans. AGU 89 (53), 553–554.
Diffenbaugh, N.S., Scherer, M., Trapp, R.J., 2013. Robust increases in severe thunderstorm environments in response to greenhouse forcing. Proc. Natl. Acad. Sci. 110, 16361–16366.
Donald, A., et al., 2006. Near-global impact of the Madden-Julian Oscillation on rainfall. Geophys. Res. Lett. 33.
Doswell, C.A., 2007. Small sample size and data quality issues illustrated using tornado occurrence data. Electron. J. Severe Storms Meteor. 2.

Doswell III, C.A., Burgess, D.W., 1988. On some issues of United States tornado climatology. Mon. Weather Rev. 116, 495–501.
Doswell III, C.A., Brooks, H.E., Dotzek, N., 2009. On the implementation of the enhanced Fujita scale in the USA. Atmos. Res. 93, 554–563.
Edwards, R., Allen, J.T., Carbin, G.W., 2018. Reliability and climatological impacts of convective wind estimations. J. Appl. Meteorol. Climatol. 57, 1825–1845.
Eyring, V., Bony, S., Meehl, G.A., Senior, C.A., Stevens, B., Stouffer, R.J., Taylor, K.E., 2016. Overview of the Coupled Model Intercomparison Project Phase 6 (CMIP6) experimental design and organization. Geosci. Model Dev. (Online) 9.
Farney, T.J., Dixon, P.G., 2015. Variability of tornado climatology across the continental United States. Int. J. Climatol. 35, 2993–3006.
Gagne, D.J., McGovern, A., Brotzge, J., 2009. Classification of convective areas using decision trees. J. Atmos. Ocean. Technol. 26, 1341–1353.
Gagne, D.J., McGovern, A., Haupt, S.E., Sobash, R.A., Williams, J.K., Xue, M., 2017. Storm-based probabilistic hail forecasting with machine learning applied to convection-allowing ensembles. Weather Forecast. 32, 1819–1840.
Gallo, B.T., Clark, A.J., Dembek, S.R., 2016. Forecasting tornadoes using convection-permitting ensembles. Weather Forecast. 31, 273–295.
Gallo, B.T., Clark, A.J., Smith, B.T., Thompson, R.L., Jirak, I., Dembek, S.R., 2018. Blended probabilistic tornado forecasts: combining climatological frequencies with NSSL–WRF ensemble forecasts. Weather Forecast. 33, 443–460.
Gensini, V.A., Allen, J.T., 2018. US hail frequency and the global wind oscillation. Geophys. Res. Lett. 45 (3), 1611–1620.
Gensini, V.A., Ashley, W.S., 2011. Climatology of potentially severe convective environments from the North American Regional Reanalysis. Electron. J. Severe Storms Meteor. 6.
Gensini, V.A., Bravo de Guenni, L., 2019. Environmental covariate representation of seasonal US tornado frequency. J. Appl. Meteorol. Climatol. 58, 1353–1367.
Gensini, V.A., Brooks, H.E., 2018. Spatial trends in United States tornado frequency. NPJ Clim. Atmos. Sci. 1, 1–5.
Gensini, V.A., Marinaro, A., 2016. Tornado frequency in the United States related to global relative angular momentum. Mon. Weather Rev. 144, 801–810.
Gensini, V.A., Mote, T.L., 2014. Estimations of hazardous convective weather in the United States using dynamical downscaling. J. Clim. 27, 6581–6589.
Gensini, V.A., Mote, T.L., 2015. Downscaled estimates of late 21st century severe weather from CCSM3. Clim. Chang. 129, 307–321.
Gensini, V.A., Tippett, M.K., 2019. Global ensemble forecast system (GEFS) predictions of days 1–15 US tornado and hail frequencies. Geophys. Res. Lett. 46, 2922–2930.
Gensini, V.A., Ramseyer, C., Mote, T.L., 2014. Future convective environments using NARCCAP. Int. J. Climatol. 34, 1699–1705.
Gensini, V.A., Gold, D., Allen, J.T., Barrett, B.S., 2019. Extended US tornado outbreak during late May 2019: a forecast of opportunity. Geophys. Res. Lett. 46, 10150–10158.
Gensini, V.A., Barrett, B.S., Allen, J.T., Gold, D., Sirvatka, P., 2020a. The extended-range tornado activity forecast (ERTAF) project. Bull. Am. Meteorol. Soc.
Gensini, V.A., Haberlie, A.M., Marsh, P.T., 2020b. Practically perfect hindcasts of severe convective storms. Bull. Am. Meteorol. Soc. 101.
Grazulis, T.P., 1993. A 110-year perspective of significant tornadoes. Geophys. Monogr. Ser. 79, 467–474.
Guo, L., Wang, K., Bluestein, H.B., 2016. Variability of tornado occurrence over the continental United States since 1950. J. Geophys. Res. Atmos. 121, 6943–6953.

Haberlie, A.M., Ashley, W.S., 2018. A method for identifying midlatitude mesoscale convective systems in radar mosaics. Part I: segmentation and classification. J. Appl. Meteorol. Climatol. 57, 1575–1598.
Harding, K.J., Snyder, P.K., Liess, S., 2013. Use of dynamical downscaling to improve the simulation of Central US warm season precipitation in CMIP5 models. J. Geophys. Res. Atmos. 118 (22), 12522–12536.
Herman, G.R., Nielsen, E.R., Schumacher, R.S., 2018. Probabilistic verification of Storm Prediction Center convective outlooks. Weather Forecast. 33, 161–184.
Hitchens, N.M., Brooks, H.E., 2012. Evaluation of the Storm Prediction Center's day 1 convective outlooks. Weather Forecast. 27, 1580–1585.
Hitchens, N.M., Brooks, H.E., 2014. Evaluation of the Storm Prediction Center's convective outlooks from day 3 through day 1. Weather Forecast. 29, 1134–1142.
Hitchens, N.M., Brooks, H.E., Kay, M.P., 2013. Objective limits on forecasting skill of rare events. Weather Forecast. 28, 525–534.
Hoogewind, K.A., Baldwin, M.E., Trapp, R.J., 2017. The impact of climate change on hazardous convective weather in the United States: insight from high-resolution dynamical downscaling. J. Clim. 30, 10081–10100.
Hoskins, B.J., Karoly, D.J., 1981. The steady linear response of a spherical atmosphere to thermal and orographic forcing. J. Atmos. Sci. 38, 1179–1196.
Jewell, R., Brimelow, J., 2009. Evaluation of Alberta hail growth model using severe hail proximity soundings from the United States. Weather Forecast. 24, 1592–1609.
Jiang, Z., Feldstein, S.B., Lee, S., 2017. The relationship between the Madden–Julian oscillation and the North Atlantic oscillation. Q. J. R. Meteorol. Soc. 143, 240–250.
Jin, F., Hoskins, B.J., 1995. The direct response to tropical heating in a baroclinic atmosphere. J. Atmos. Sci. 52, 307–319.
Johns, R.H., Doswell III, C.A., 1992. Severe local storms forecasting. Weather Forecast. 7, 588–612.
Jones, C., Carvalho, L.M., 2012. Spatial–intensity variations in extreme precipitation in the contiguous United States and the Madden–Julian oscillation. J. Clim. 25, 4898–4913.
Jones, C., Carvalho, L.M., Gottschalck, J., Higgins, W., 2011. The Madden–Julian oscillation and the relative value of deterministic forecasts of extreme precipitation in the contiguous United States. J. Clim. 24, 2421–2428.
Karl, T.R., Melillo, J.M., Peterson, T.C., Hassol, S.J., 2009. Global Climate Change Impacts in the United States. Similar work has also been done over North America for large hail reports to estimate hailstone diameter and/or frequency from the convective environment (Jewell and Brimelow 2009; Allen et al. 2), Cambridge University Press.
Kendon, E.J., Roberts, N.M., Senior, C.A., Roberts, M.J., 2012. Realism of rainfall in a very high-resolution regional climate model. J. Clim. 25, 5791–5806.
Kendon, E.J., Roberts, N.M., Fowler, H.J., Roberts, M.J., Chan, S.C., Senior, C.A., 2014. Heavier summer downpours with climate change revealed by weather forecast resolution model. Nat. Clim. Chang. 4, 570–576.
Kiladis, G.N., Dias, J., Straub, K.H., Wheeler, M.C., Tulich, S.N., Kikuchi, K., et al., 2014. A comparison of OLR and circulation-based indices for tracking the MJO. Mon. Weather Rev. 142 (5), 1697–1715.
Knutson, T.R., Weickmann, K.M., 1987. 30–60 day atmospheric oscillations: composite life cycles of convection and circulation anomalies. Mon. Weather Rev. 115, 1407–1436.
Kunkel, K.E., et al., 2013. Monitoring and understanding trends in extreme storms: state of knowledge. Bull. Am. Meteorol. Soc. 94, 499–514.
L'Heureux, M.L., Higgins, R.W., 2008. Boreal winter links between the Madden–Julian oscillation and the Arctic oscillation. J. Clim. 21, 3040–3050.
Lackmann, G.M., 2013. The south-central US flood of May 2010: present and future. J. Clim. 26, 4688–4709.
Lakshmanan, V., Smith, T., 2010. An objective method of evaluating and devising storm-tracking algorithms. Weather Forecast. 25, 701–709.
Lauer, A., Zhang, C., Elison-Timm, O., Wang, Y., Hamilton, K., 2013. Downscaling of climate change in the Hawaii region using CMIP5 results: On the choice of the forcing fields. J. Clim. 26 (24), 10006–10030.

Lee, S.-K., Atlas, R., Enfield, D., Wang, C., Liu, H., 2013. Is there an optimal ENSO pattern that enhances large-scale atmospheric processes conducive to tornado outbreaks in the United States? J. Clim. 26, 1626–1642.
Lepore, C., Tippett, M.K., Allen, J.T., 2017. ENSO-based probabilistic forecasts of March–May US tornado and hail activity. Geophys. Res. Lett. 44, 9093–9101.
Lepore, C., Tippett, M.K., Allen, J.T., 2018. CFSv2 monthly forecasts of tornado and hail activity. Weather Forecast. 33, 1283–1297.
Liu, C., et al., 2017. Continental-scale convection-permitting modeling of the current and future climate of North America. Clim. Dyn. 49, 71–95.
Long, J.A., Stoy, P.C., 2014. Peak tornado activity is occurring earlier in the heart of "Tornado Alley". Geophys. Res. Lett. 41, 6259–6264.
Long, J.A., Stoy, P.C., Gerken, T., 2018. Tornado seasonality in the southeastern United States. Weather Clim. Extrem. 20, 81–91.
Lorenz, D.J., Hartmann, D.L., 2006. The effect of the MJO on the North American monsoon. J. Clim. 19, 333–343.
Lu, M., Tippett, M., Lall, U., 2015. Changes in the seasonality of tornado and favorable genesis conditions in the Central United States. Geophys. Res. Lett. 42, 4224–4231.
Madden, R.A., Julian, P.R., 1971. Detection of a 40–50 day oscillation in the zonal wind in the tropical Pacific. J. Atmos. Sci. 28, 702–708.
Madden, R.A., Julian, P.R., 1972. Description of global-scale circulation cells in the tropics with a 40–50 day period. J. Atmos. Sci. 29, 1109–1123.
Madden, R.A., Julian, P.R., 1994. Observations of the 40–50-day tropical oscillation—a review. Mon. Weather Rev. 122, 814–837.
Mahoney, K., Alexander, M., Scott, J.D., Barsugli, J., 2013. High-resolution downscaled simulations of warm-season extreme precipitation events in the Colorado front range under past and future climates. J. Clim. 26, 8671–8689.
McDonald, J.R., Mehta, K.C., Smith, D.A., Womble, J.A., 2010. The enhanced Fujita scale: development and implementation. In: Forensic Engineering 2009: Pathology of the Built Environment, pp. 719–728.
Miller, D.E., Wang, Z., Trapp, R.J., Harnos, D.S., 2020. Hybrid prediction of weekly tornado activity out to week 3: utilizing weather regimes. Geophys. Res. Lett., e2020GL087253.
Molina, M.J., Allen, J.T., Gensini, V.A., 2018. The Gulf of Mexico and ENSO influence on subseasonal and seasonal CONUS winter tornado variability. J. Appl. Meteorol. Climatol. 57, 2439–2463.
Moore, T.W., 2018. Annual and seasonal tornado activity in the United States and the global wind oscillation. Clim. Dyn. 50 (11–12), 4323–4334.
Moore, T.W., McGuire, M.P., 2019. Using the standard deviational ellipse to document changes to the spatial dispersion of seasonal tornado activity in the United States. NPJ Clim. Atmos. Sci. 2, 1–8.
Moore, T.W., McGuire, M.P., 2020. Tornado-days in the United States by phase of the Madden–Julian oscillation and global wind oscillation. Clim. Dyn. 54, 17–36.
Mundhenk, B.D., Barnes, E.A., Maloney, E.D., Baggett, C.F., 2018. Skillful empirical subseasonal prediction of landfalling atmospheric river activity using the Madden–Julian oscillation and quasi-biennial oscillation. NPJ Clim. Atmos. Sci. 1, 1–7.
NCEI, 2020. Billion-Dollar Weather and Climate Disasters: Overview. NOAA. https://www.ncdc.noaa.gov/billions/.
Pachauri, R.K., Allen, M.R., Barros, V.R., Broome, J., Cramer, W., Christ, R., et al., 2014. Climate change 2014: synthesis report. Contribution of Working Groups I, II and III to the fifth assessment report of the Intergovernmental Panel on Climate Change. IPCC, p. 151.
Potvin, C.K., Broyles, C., Skinner, P.S., Brooks, H.E., Rasmussen, E., 2019. A Bayesian hierarchical modeling framework for correcting reporting bias in the US tornado database. Weather Forecast. 34, 15–30.
Potvin, C.K., Flora, M.L., 2015. Sensitivity of idealized supercell simulations to horizontal grid spacing: implications for warn-on-forecast. Mon. Weather Rev. 143 (8), 2998–3024.

Powers, J.G., Klemp, J.B., Skamarock, W.C., Davis, C.A., Dudhia, J., Gill, D.O., et al., 2017. The weather research and forecasting model: overview, system efforts, and future directions. Bull. Am. Meteorol. Soc. 98 (8), 1717–1737.

Prein, A.F., Holland, G.J., Rasmussen, R.M., Done, J., Ikeda, K., Clark, M.P., Liu, C.H., 2013. Importance of regional climate model grid spacing for the simulation of heavy precipitation in the Colorado headwaters. J. Clim. 26, 4848–4857.

Prein, A.F., Rasmussen, R.M., Ikeda, K., Liu, C., Clark, M.P., Holland, G.J., 2017. The future intensification of hourly precipitation extremes. Nat. Clim. Chang. 7, 48–52.

Rasmussen, E.N., 2003. Refined supercell and tornado forecast parameters. Weather Forecast. 18, 530–535.

Rasmussen, E.N., Blanchard, D.O., 1998. A baseline climatology of sounding-derived supercell andtornado forecast parameters. Weather Forecast. 13, 1148–1164.

Rasmussen, R., et al., 2011. High-resolution coupled climate runoff simulations of seasonal snowfall over Colorado: a process study of current and warmer climate. J. Clim. 24, 3015–3048.

Rasmussen, R., et al., 2014. Climate change impacts on the water balance of the Colorado headwaters: high-resolution regional climate model simulations. J. Hydrometeorol. 15, 1091–1116.

Riddle, E.E., Stoner, M.B., Johnson, N.C., L'Heureux, M.L., Collins, D.C., Feldstein, S.B., 2013. The impact of the MJO on clusters of wintertime circulation anomalies over the North American region. Clim. Dyn. 40, 1749–1766.

Robertson, A.W., Kumar, A., Peña, M., Vitart, F., 2015. Improving and promoting subseasonal to seasonal prediction. Bull. Am. Meteorol. Soc. 96, ES49–ES53.

Robinson, E.D., Trapp, R.J., Baldwin, M.E., 2013. The geospatial and temporal distributions of severe thunderstorms from high-resolution dynamical downscaling. J. Appl. Meteorol. Climatol. 52, 2147–2161.

Roundy, P., 2012. Tropical–extratropical interactions. In: Lau, W.K.-M., Waliser, D.E. (Eds.), Intraseasonal variability in the Atmosphere-Ocean Climate System. Springer.

Roundy, P.E., Schreck III, C.J., Janiga, M.A., 2009. Contributions of convectively coupled equatorial Rossby waves and Kelvin waves to the real-time multivariate MJO indices. Mon. Weather Rev. 137, 469–478.

Roundy, P.E., MacRitchie, K., Asuma, J., Melino, T., 2010. Modulation of the global atmospheric circulation by combined activity in the Madden–Julian oscillation and the El Niño–Southern Oscillation during boreal winter. J. Clim. 23, 4045–4059.

Sardeshmukh, P.D., Hoskins, B.J., 1988. The generation of global rotational flow by steady idealized tropical divergence. J. Atmos. Sci. 45, 1228–1251.

Schubert, S., Dole, R., vandenDool, H., Suarez, M., Waliser, D., 2002. Prospects for improved forecasts of weather and short-term climate variability on subseasonal (2-week to 2-month) times scales. In: Technical Report Series on Global Modeling and Data Assimilation. vol. 23. NASA/TM.

Seeley, J.T., Romps, D.M., 2015. The effect of global warming on severe thunderstorms in the United States. J. Clim. 28, 2443–2458.

Seo, K.-H., Son, S.-W., 2012. The global atmospheric circulation response to tropical diabatic heating associated with the Madden–Julian oscillation during northern winter. J. Atmos. Sci. 69, 79–96.

Seo, K.-H., Lee, H.-J., Frierson, D.M., 2016. Unraveling the teleconnection mechanisms that induce wintertime temperature anomalies over the northern hemisphere continents in response to the MJO. J. Atmos. Sci. 73, 3557–3571.

Simmons, K., Sutter, D., 2013. Economic and Societal Impacts of Tornadoes. Similar work has also been done over North America for large hail reports to estimate hailstone diameter and/or frequency from the convective environment (Jewell and Brimelow 2009; Allen et al. 2), Springer Science & Business Media.

Smith, A.B., Matthews, J.L., 2015. Quantifying uncertainty and variable sensitivity within the US billion-dollar weather and climate disaster cost estimates. Nat. Hazards 77, 1829–1851.

Sobash, R.A., Kain, J.S., Bright, D.R., Dean, A.R., Coniglio, M.C., Weiss, S.J., 2011. Probabilistic forecast guidance for severe thunderstorms based on the identification of extreme phenomena in convection-allowing model forecasts. Weather Forecast. 26, 714–728.

Sobash, R.A., Schwartz, C.S., Romine, G.S., Fossell, K.R., Weisman, M.L., 2016. Severe weather prediction using storm surrogates from an ensemble forecasting system. Weather Forecast. 31, 255–271.
Stevens, B., Bony, S., 2013. What are climate models missing? Science 340, 1053–1054.
Strader, S.M., Ashley, W.S., Pingel, T.J., Krmenec, A.J., 2017a. Observed and projected changes in United States tornado exposure. Weather Clim. Soc. 9, 109–123.
Strader, S.M., Ashley, W.S., Pingel, T.J., Krmenec, A.J., 2017b. Projected 21st century changes in tornado exposure, risk, and disaster potential. Clim. Chang. 141, 301–313.
Straub, K.H., 2013. MJO initiation in the real-time multivariate MJO index. J. Clim. 26 (4), 1130–1151.
Tang, B.H., Gensini, V.A., Homeyer, C.R., 2019. Trends in United States large hail environments and observations. NPJ Clim. Atmos. Sci. 2, 1–7.
Thompson, D.B., Roundy, P.E., 2013. The relationship between the Madden–Julian oscillation and US violent tornado outbreaks in the spring. Mon. Weather Rev. 141, 2087–2095.
Tian, D., Wood, E.F., Yuan, X., 2017. CFSv2-based sub-seasonal precipitation and temperature forecast skill over the contiguous United States. Hydrol. Earth Syst. Sci. 21, 1477–1490.
Tippett, M.K., 2014. Changing volatility of US annual tornado reports. Geophys. Res. Lett. 41, 6956–6961.
Tippett, M.K., 2018. Robustness of relations between the MJO and US tornado occurrence. Mon. Weather Rev. 146, 3873–3884.
Tippett, M.K., Koshak, W.J., 2018. A baseline for the predictability of US cloud-to-ground lightning. Geophys. Res. Lett. 45, 10,719–710,728.
Tippett, M.K., Allen, J.T., Gensini, V.A., Brooks, H.E., 2015. Climate and hazardous convective weather. Curr. Climate Change Rep. 1, 60–73.
Tippett, M.K., Lepore, C., Cohen, J.E., 2016. More tornadoes in the most extreme US tornado outbreaks. Science 354, 1419–1423.
Tippett, M.K., Sobel, A.H., Camargo, S.J., 2012. Association of US tornado occurrence with monthly environmental parameters. Geophys. Res. Lett. 39 (2).
Tippett, M.K., Sobel, A.H., Camargo, S.J., Allen, J.T., 2014. An empirical relation between US tornado activity and monthly environmental parameters. J. Clim. 27 (8), 2983–2999.
Trapp, R.J., 2014. On the significance of multiple consecutive days of tornado activity. Mon. Weather Rev. 142, 1452–1459.
Trapp, R.J., Diffenbaugh, N.S., Gluhovsky, A., 2009. Transient response of severe thunderstorm forcing to elevated greenhouse gas concentrations. Geophys. Res. Lett. 36 (1).
Trapp, R.J., Hoogewind, K.A., 2016. The realization of extreme tornadic storm events under future anthropogenic climate change. J. Clim. 29, 5251–5265.
Trapp, R.J., Hoogewind, K.A., 2018. Exploring a possible connection between US tornado activity and Arctic Sea ice. NPJ Clim. Atmos. Sci. 1, 1–8.
Trapp, R.J., Diffenbaugh, N.S., Brooks, H.E., Baldwin, M.E., Robinson, E.D., Pal, J.S., 2007. Changes in severe thunderstorm environment frequency during the 21st century caused by anthropogenically enhanced global radiative forcing. Proc. Natl. Acad. Sci. 104, 19719–19723.
Trapp, R.J., Robinson, E.D., Baldwin, M.E., Diffenbaugh, N.S., Schwedler, B.R., 2011. Regional climate of hazardous convective weather through high-resolution dynamical downscaling. Clim. Dyn. 37, 677–688.
Trapp, R.J., Hoogewind, K.A., Lasher-Trapp, S., 2019. Future changes in hail occurrence in the United States determined through convection-permitting dynamical downscaling. J. Clim. 32, 5493–5509.
Van Klooster, S.L., Roebber, P.J., 2009. Surface-based convective potential in the contiguous United States in a business-as-usual future climate. J. Clim. 22, 3317–3330.
Vecchi, G.A., Bond, N.A., 2004. The Madden-Julian Oscillation (MJO) and northern high latitude wintertime surface air temperatures. Geophys. Res. Lett. 31.
Verbout, S.M., Brooks, H.E., Leslie, L.M., Schultz, D.M., 2006. Evolution of the US tornado database: 1954–2003. Weather Forecast. 21, 86–93.

Vigaud, N., Robertson, A.W., Tippett, M.K., 2017. Multimodel ensembling of subseasonal precipitation forecasts over North America. Mon. Weather Rev. 145, 3913–3928.
Wanders, N., Wood, E.F., 2016. Improved sub-seasonal meteorological forecast skill using weighted multi-model ensemble simulations. Environ. Res. Lett. 11, 094007.
Wang, L., Robertson, A.W., 2019. Week 3–4 predictability over the United States assessed from two operational ensemble prediction systems. Clim. Dyn. 52, 5861–5875.
Weickmann, K., Berry, E., 2007. A synoptic–dynamic model of subseasonal atmospheric variability. Mon. Weather Rev. 135, 449–474.
Weickmann, K., Berry, E., 2009. The tropical Madden–Julian oscillation and the global wind oscillation. Mon. Weather Rev. 137, 1601–1614.
Weickmann, K., Khalsa, S., 1990. The shift of convection from the Indian Ocean to the western Pacific Ocean during a 30–60 day oscillation. Mon. Weather Rev. 118, 964–978.
Weickmann, K.M., Sardeshmukh, P.D., 1994. The atmospheric angular momentum cycle associated with a Madden–Julian oscillation. J. Atmos. Sci. 51, 3194–3208.
Wheeler, M.C., Hendon, H.H., 2004. An all-season real-time multivariate MJO index: development of an index for monitoring and prediction. Mon. Weather Rev. 132 (8), 1917–1932.
Winters, A.C., Keyser, D., Bosart, L.F., 2019. The development of the North Pacific jet phase diagram as an objective tool to monitor the state and forecast skill of the upper-tropospheric flow pattern. Weather Forecast. 34, 199–219.
Yao, W., Lin, H., Derome, J., 2011. Submonthly forecasting of winter surface air temperature in North America based on organized tropical convection. Atmosphere-Ocean 49, 51–60.
Zhang, C., 2005. Madden-julian oscillation. Rev. Geophys. 43.
Zhang, C., 2013. Madden–Julian oscillation: bridging weather and climate. Bull. Am. Meteorol. Soc. 94, 1849–1870.
Zhou, S., L'Heureux, M., Weaver, S., Kumar, A., 2012. A composite study of the MJO influence on the surface air temperature and precipitation over the continental United States. Clim. Dyn. 38, 1459–1471.

CHAPTER

5

Response of terrestrial net primary productivity to precipitation extremes: Patterns, mechanisms, and uncertainties

Andrew J. Felton

Department of Wildland Resources and The Ecology Center, Utah State University, Logan, UT, United States

Introduction

Changes to precipitation extremes

Emissions from human activity have increased the concentration of carbon dioxide (CO_2) in the atmosphere by nearly 50% since the beginning of the industrial revolution in the 19th century.

The most certain climatic change of this dramatic increase in atmospheric CO_2 is an increase in global mean temperatures (IPCC, 2013). However, rising temperatures also have implications for patterns of precipitation (PPT). Warmer temperatures increase the water vapor saturation point and water holding capacity of the atmosphere and are now intensifying the global water cycle (Huntington, 2006; Dannenberg et al., 2019). This intensification of the water cycle is consistently predicted to increase the temporal variability of PPT patterns and, by extension, the frequency and magnitude of PPT extremes (IPCC, 2013; Cook et al., 2015; Diffenbaugh et al., 2015; Swain et al., 2018; USGCRP, 2018).

Future changes to PPT extremes are predicted to occur at both inter- and intraannual timescales (Fig. 1). At interannual (year-to-year) timescales, increased frequencies and magnitudes of extreme wet and dry years are expected (Williams et al., 2015; Cook et al., 2015; Fig. 1A). At intraannual timescales (within-years), PPT is forecast to be progressively delivered in fewer, larger, and more intense daily PPT events, with longer dry intervals between PPT events (Knapp et al., 2008; IPCC, 2013; Myhre et al., 2019; Fig. 1B). These two timescales of PPT extremes, and how terrestrial net primary productivity (NPP) responds to them, are the focus of this chapter. Given the strong control water places on plant growth globally, plant-water relationships and NPP may be particularly vulnerable to increases in PPT extremes (Reyer et al., 2013). Thus, a critical need has emerged to better anticipate the consequences of such unprecedented changes to how water is delivered to terrestrial ecosystems.

Climate Change and Extreme Events. https://doi.org/10.1016/B978-0-12-822700-8.00010-X
Copyright © 2021 Elsevier Inc. All rights reserved.

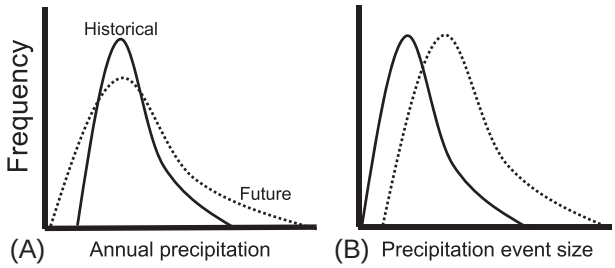

FIG. 1

A schematic of the two key projected changes in precipitation (PPT) extremes. In both cases, the *solid line* depicts the historical distribution, whereas the *dotted line* depicts the future distribution expected with climate change, (A) Depicts expected changes at interannual timescales and shows the typical skewed frequency distributed of annual PPT, but with future increases in the frequencies of greater magnitude wet and dry years and, thus, annual PPT extremes and (B) Depicts anticipated shifts in intraannual PPT dynamics, and specifically PPT event size, with an intensified water cycle; PPT is projected to be delivered in larger and fewer events. A secondary consequence of this is an increased length of dry intervals between PPT events. Both dimensions of changes to intraannual PPT patterns are important for ecosystem functioning but differentially so in xeric versus mesic ecosystems.

Precipitation extremes and the carbon cycle

Carbon cycling within terrestrial ecosystems is strongly regulated by climate and, especially, PPT. Large positive or negative deviations in PPT from average conditions—extremes—can, thus, substantially influence the terrestrial carbon cycle. These effects of PPT extremes on the carbon cycle, however, propagate through space, time, and levels of biological organization to produce complex emergent dynamics (Smith, 2011; Reichstein et al., 2013; Niu et al., 2014; Frank et al., 2015; Van de Pol et al., 2017), with consequences for the functioning of both ecological and human systems.

Drought provides an excellent example to highlight emergent dynamics of PPT extremes on the carbon cycle through a plant's perspective. Drought-induced water stress initiates a suite of physiological changes and adjustments within individual plants (McDowell et al., 2011; Reyer et al., 2013; Niu et al., 2014; Gupta et al., 2020). A proximate consequence of these changes is closure of stomatal pores on leaves to limit water losses from transpiration; however, this occurs at the general cost of reduced plant photosynthesis and, thus, carbon uptake. If this reduction in leaf-level carbon uptake and transpiration of individual plants is even somewhat consistent across individuals and canopies within an ecosystem, an abrupt change to the land-atmosphere exchange of water and CO_2 could result. This is especially consequential if rates of plant and soil microbial respiration (carbon losses to atmosphere) are relatively less reduced than photosynthesis (carbon inputs to ecosystem), which most likely underpins evidence of some terrestrial ecosystems shifting from sinks to sources of CO_2 to the atmosphere because of climatic variability (Ciais et al., 2005; Hoover et al., 2016; Biederman et al., 2017).

If the spatial extent of PPT extremes is sufficiently large, short-term plant responses and abrupt changes to the terrestrial carbon cycle can propagate to produce signatures on the global carbon cycle. For example, the 2003 European heat wave and drought wiped out 4 years of carbon sequestration and produced a net source of CO_2 to the atmosphere (Ciais et al., 2005). By contrast, sustained increases in

PPT associated with La Niña conditions over semiarid regions of Australia, South America, and southern Africa resulted in a record land CO_2 sink in 2011 (Poulter et al., 2014). Thus PPT extremes—both wet and dry—drive considerable temporal variability in carbon cycling at a global scale, the magnitude of which is claimed to be comparable to the magnitude of the global terrestrial carbon sink (Reichstein et al., 2013; Zscheischler et al., 2013).

If the magnitude of PPT extremes is sufficiently large, initial plant physiological adjustments to stress may progress to hydraulic failure, reduced carbohydrate reserves, and reduced pathogen resistance that pushes plants past a mortality threshold (McDowell et al., 2011; Anderegg et al., 2015a; Powers et al., 2020). Vegetation mortality events could lead to committed and chronic reductions in carbon uptake, the duration of which is contingent on the recovery potential of vegetation, which may be especially consequential in forests (Reichstein et al., 2013) because of their longer demographic return intervals and large carbon stocks and sink potentials (Pan et al., 2011). How other global environmental changes that promote terrestrial carbon uptake, such as CO_2 fertilization from human emission (Keenan et al., 2013) and consequent lengthening of growing seasons with climatic warming (Hufkens et al., 2016), interact with PPT extremes remains unclear but critical to unravel. The effect of increasing PPT extremes on plant and terrestrial ecosystem functioning poses among the largest uncertainties to the fate of the growth rate in atmospheric CO_2 and, by extension, the velocity of climate change over the 21st century.

PPT extremes effects on carbon cycling are relevant not only to unmanaged terrestrial ecosystems but to social-ecological systems such as intensively managed croplands and livestock production systems as well. For example, livestock production systems—dependent on rain-fed forage production—occur in globally expansive water-limited regions where PPT variability can be high and damaging to plant growth (Sloat et al., 2018). And despite the ability for humans to intervene in agricultural systems, such as through irrigation, PPT extremes—and specifically drought alone—produce more crop losses than all pathogens combined and have resulted in roughly 30 billion dollars of economic losses over the past decade alone (Gupta et al., 2020).

The challenges that PPT extremes present also occur within the context of a paradox; human demand for water is expected to increase globally, but the future availability of water resources with climate change is uncertain (Fisher et al., 2017). For example, a two-decade megadrought that rivals those of medieval times is ongoing in the desert southwestern United States (Williams et al., 2020); a region with scarce water resources and high human population growth (Mackun, 2019). And globally, intensifying human water consumption is intensifying drought conditions (Wada et al., 2013). This is especially problematic in less economically developed regions of the world, such as central Africa, where social vulnerability to PPT extremes may be particularly high, given direct dependencies on agriculture (Ahmadalipour et al., 2019). Thus even a small change to the frequency and magnitude of PPT extremes could have considerable implications for the global carbon cycle, the climate system, and agricultural production, implying consequences for natural and human systems alike.

Defining an extreme climate event

Three general definitions have emerged for how ecologists define extreme climatic events (Table 1) and, by extension, PPT extremes. The first is the climatic perspective. In this case, if a PPT event exceeds a certain statistical threshold for a given timescale (e.g., the 5th or 95th percentiles of a distribution), that PPT event may be deemed "extreme" (Hoover et al., 2014; Felton et al., 2019a,b).

Table 1 Proposed definitions for how to define an extreme climatic event.

Perspective	Definition	Citation
Climatic	"The occurrence of a value of a weather or climate variable above (or below) a threshold value near the upper (or lower) ends of the range of observed values of the variable (typically 5% or 10%)"	IPCC (2013)
Biotic	"An episode in which the acclamatory capacities of an organism are substantially exceeded"	Gutschick and BassiriRad (2003)
Integrative	"An episode or occurrence in which a statistically rare or unusual climatic period alters ecosystem structure and/or function well outside the bounds of what is considered typical or normal variability"	Smith (2011)

The climatic perspective proposes to define an event from a statistical perspective with respect to the historic climatic distribution of a region, for example, the 100-year precipitation record. The biotic perspective proposes that an extreme climatic event is a set of climatic conditions—irrespective of whether they are statistically extreme—which produces extreme biological responses. The integrative perspective proposes that an extreme climatic event is both statistically extreme climatic occurrence(s) that pushes the functioning of a system beyond historic levels of variability. Thus there must both be an extreme occurrence of weather and an extreme ecosystem response.

An advantage of the climatic definition is that it allows for standardization of climatic extremity across ecosystems that have different climatic baselines (Slette et al., 2019). The second is the biotic perspective (Reyer et al., 2013). In this case, only climatic conditions—irrespective of whether they are statistically extreme—which elicit large biological responses should be considered "extreme" (Gutschick and BassiriRad, 2003). An advantage of this approach is that it provides a pathway toward understanding what single or combination of climatic conditions actually produce large changes to ecosystem functioning. Motivated to reconcile the climatic and biotic perspectives, others have advocated for a third definition: an integrative perspective (Smith, 2011; Reichstein et al., 2013). This perspective suggests that an extreme climate event occurs when a statistically extreme climatic event, or constellation of climatic events, alters ecosystem functioning beyond typical levels of variability (Table 1).

To date, ecologists have not adopted a single definition of what constitutes an extreme climate event. More problematic is that ecologists often don't define what they mean when they discuss climatic extremity in reporting research results (e.g., drought; Slette et al., 2019). The continuation of this debate and its resolution are important if ecologists seek to systematically compare the increasingly large pool of research findings on the impacts of PPT extremes. The lack of agreement on an operational definition of climatic extremity is a broader reflection of the symptomatically wide range of ways ecologists approach studying ecosystems, even when the research questions are ultimately quite similar.

This chapter focuses on the response of terrestrial net primary productivity (NPP) to PPT extremes. Focusing this chapter on NPP is desirable for several reasons. First, NPP—as the rate at which plants synthesize CO_2 into chemical energy and incorporate it into new biomass (after accounting for respiration)—is a central ecosystem function that influences process ranging from energy flow within ecosystems, the land-atmosphere exchange of CO_2, to global agricultural production. Second, NPP is a common currency and response variable in ecosystems ecology research that is also estimated in a variety of ways, from the clipping of plant biomass in the field to remotely sensed observations from satellites in space. Thus NPP's prevalence as a measured and multiscale response variable facilitates

integrating insights across research studies, methodological approaches, and spatial scales. Global-scale monitoring platforms of the Earth system, achieved through satellite remote sensing, also largely focus on NPP or components of it (Running et al., 2004). Finally, there is both basic and applied rationale to understand the controls of NPP, given its central role in plant growth within natural and managed systems. And at a global scale, NPP is often limited or colimited by water availability (Churkina and Running, 1998).

The goal of this chapter is to provide a broad scientific basis for understanding NPP responses to PPT extremes that can help guide future research. Within this context, the rest of this chapter is devoted to three key objectives. The first objective is to integrate key components of our knowledge on how NPP responds to PPT extremes. From this integration comes the second objective, which is to identify key areas of uncertainty in our knowledge. And, thus, the third goal is to generate recommendations for future research, both in terms of key knowledge gaps and potential ways to address them.

Patterns and mechanisms of net primary productivity responses to PPT extremes

Interannual timescales

Patterns of NPP sensitivity to interannual precipitation across ecosystems

Annual PPT is highly variable, both across the land surface and through time. On a relative basis, the most temporally variable interannual PPT patterns tend to exist in the driest ecosystems. A common observation is, thus, that the interannual variability of PPT tends to decrease as the long-term average PPT increases (Knapp and Smith, 2001; Davidowitz, 2002; Fatichi et al., 2012). In addition, the driest ecosystems on earth also tend to have the largest relative deviations in PPT (Knapp et al., 2015a). However, the ecosystems that have the most variable PPT patterns are not necessarily the most sensitive to interannual variation in PPT. And in many terrestrial ecosystems, interannual variation in NPP (expressed as the coefficient of variation) is higher than interannual variation in PPT (Knapp and Smith, 2001; Hsu and Adler, 2014). Thus variation and extremes in annual PPT may not necessarily correlate with variation and extremes in NPP (Smith, 2011).

Anticipating patterns of NPP responses to interannual-scale PPT extremes concerns, in large part, how resource limitation and vegetation attributes interact. Multiple resource colimitation theory predicts a joint control of NPP by water, light, and soil nutrients. Thus the relative control of a given resource on NPP concerns demands relative to supply (Eskelinen and Harrison, 2015). This prediction stems from the agricultural principle Liebig's law of the minimum, which states that crop productivity is most constrained by the single most limiting resource at any given time (Danger et al., 2008). With respect to NPP responses to PPT extremes, this theory predicts that, as average water limitation of NPP decreases, and as mean annual PPT increases, the sensitivity of NPP to interannual variation PPT extremes should decrease (Fig. 2). Implicit in this prediction is the role of average ecosystem water availability as a central arbiter of PPT-NPP interactions. A specific prediction of this theory would be that NPP in humid tropical forests should be less sensitive to interannual PPT extremes than mesic (sufficient moisture) grasslands, and NPP in mesic grasslands should be less sensitive than xeric (dry) deserts.

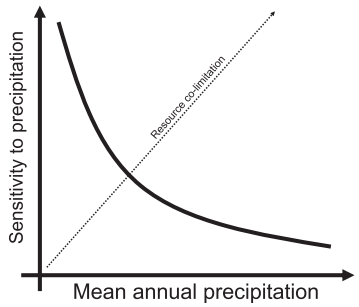

FIG. 2

Hypothesized relationship for ecosystem sensitivity to temporal variation in precipitation (PPT) with mean annual PPT based on the dynamics of multiple limiting resources. In short, as mean annual PPT increases, ecosystem processes are expected to be increasingly limited by resources other than water. Thus the frequency in which net primary productivity (NPP) is colimited by resources other than water, such as soil nutrients or light, is expected to increase as average water availability increases. As a consequence, the sensitivity of NPP to temporal variation in PPT—and potentially PPT extremes—may decrease as mean annual PPT increases. This schematic is largely inspired by the ideas and cross-biome analysis discussed in Huxman et al. (2004a).

In a groundbreaking study using long-term, observational aboveground NPP data spanning deserts to forests, Huxman et al., 2004a found a monatomic decrease in NPP sensitivity (grams of NPP per mm of PPT) to interannual PPT variability with increasing mean annual PPT, in support of the predictions of multiple resource colimitation theory (Fig. 2). This finding also supported the general expectation that historically "wetter" ecosystems, where NPP is likely more limited by light or soil nutrients, should be less sensitive to interannual variation in PPT than "drier" ecosystems. More recent remote sensing-based work, using the normalized vegetation difference index (e.g., greenness) as a proxy for NPP, found a strikingly similar cross-biome pattern as that observed by Huxman et al. (2004a) (Fig. 2), where desert NPP was more sensitive to interannual PPT variability than forest NPP (Maurer et al., 2020).

For PPT extremes, Knapp et al. (2015b) tested the predictions of multiple resource colimitation theory within a single grassland biome but across multiple ecosystems with respect to NPP responses to the 2012 central US regional drought. Here, NPP in xeric grasslands was more sensitive to drought than in mesic grasslands, supporting predictions of multiple resource colimitation theory. Similarly, in forests, a metaanalysis of 50 studies and over 100 tree species showed that the greatest prevalence of drought-induced tree morality occurs in populations at the driest ranges of their distribution (Anderegg et al., 2019). These individuals may be particularly vulnerable to drought if they function close to a physiological threshold, as was observed with tree mortality patterns in a seasonally dry tropical forest (Powers et al., 2020). Thus evidence points to plant populations, communities, and ecosystem types at the dry ends of their climatic distributions being the most sensitive to future increases in PPT extremes and specifically drought.

However, even if light or soil nutrients are not limiting, NPP could be constrained by vegetation attributes. For example, plants adapted to frequent water limitation in xeric ecosystems may be less-sensitive PPT extremes, such as drought (Grime et al., 2000), because conservative water use strategies or drought tolerance would presumably be favored in regions with frequent drought. And the opposite could also be true that have evolved in humid regions where conservative water use may not be important, observed in some tropical trees (Zuleta et al., 2017). Recent work using satellite imagery of vegetation cover suggests that the spatial pattern of a monotonic decrease in NPP sensitivity to

PPT variability as mean annual PPT does not always hold, and, thus, that multiple resource colimitation theory likely offers an incomplete framework to predict patterns of NPP sensitivity to PPT extremes across large gradients of average water availability. Specifically, there is evidence that the sensitivity of NPP to temporal PPT variability appears to first *increase* as mean annual PPT increases in the driest regions until a peak is reached and then subsequently decreases (Hu et al., 2018).

The mechanism for the initial increase in temporal NPP sensitivity to PPT variability with mean annual PPT is likely, in part, related to vegetation structure. Despite the dominant control of water on xeric ecosystem NPP (Noy-Meir, 1973), low vegetation densities and high bare ground in deserts can constrain NPP responses to PPT (Yahdjian and Sala, 2006; Reichmann et al., 2013). In the most water-limited regions on Earth, such as deserts, vegetation may counterintuitively not respond strongly to variation in PPT (Fernández, 2007). A combination of low and unpredictable PPT patterns—much of which is lost through abiotic pathways—often selects for vegetation structures with low growth rates, conservative water use strategies, or deeper rooting depths to access more stable soil moisture pools. These attributes of vegetation would reduce the apparent sensitivity of NPP to PPT extremes in the driest ecosystems on earth. Thus regions with the lowest mean annual PPT may harbor a fundamental "vegetation constraint" in their responses to interannual PPT extremes.

Experimental and observational studies suggest that low vegetation densities (e.g., meristematic, tiller, or leaf area) within an ecosystem can constrain NPP responses to PPT increases in the Patagonian Steppe, Southwestern US deserts, and central US semiarid grasslands (Lauenroth and Sala, 1992; Yahdjian and Sala, 2006; Reichmann et al., 2013). Across ecosystems of the central US great plains, meristematic densities increase with mean annual PPT (Dalgleish and Hartnett, 2006). Thus some have hypothesized a dominant control of demographic mechanisms of NPP sensitivity in the driest ecosystems (Hu et al., 2018). Gradual increases in vegetation densities and greater total NPP potential as mean annual PPT increases can, in turn, increase NPP sensitivity to temporal variation in PPT across space. By contrast, resource colimitation may constrain NPP responses to PPT at the wet end of the mean annual PPT gradient, which is consistent with the observations of Huxman et al., 2004a. Biomes located between these two extremes of average water availability, perhaps where shallow-rooted grasslands often dominate vegetation cover—is where ecosystem NPP was originally documented to be the most temporally variable (Knapp and Smith, 2001). And more recent cross-biome work that combined remote sensing, field data, and modeling found that the highest fraction of precipitation used for plant transpiration—another metric of sensitivity—occurred in between extremes of high and low mean aridity (Good et al., 2017). Thus shifts in the control of vegetation production potentials and resource colimitation on NPP responses to PPT variability and extremes may occur across spatial gradients of mean annual PPT.

The implication is that predicting patterns in NPP sensitivity to PPT extremes must collectively consider the dynamics of multiple limiting resources and vegetation structure. Water-limited ecosystems where NPP is dominated by vegetation with low growth potentials and meristematic densities, such as shrub-dominated deserts, should not be highly sensitivity to PPT extremes. Ecosystems dominated by vegetation with high growth potentials, but that are not limited by water availability, such as mesic forests, should also be relatively insensitive to PPT extremes. By contrast, water-limited ecosystems dominated by vegetation with high growth potentials, such as mesic grasslands, should be highly sensitive to PPT variability and extremes (Huxman et al., 2004a). This supports the idea of a "mesic maximum" for identifying terrestrial ecosystems with the most temporally variable NPP (Knapp and Smith, 2001) and for anticipating ecosystem and biome sensitivity to interannual PPT extremes across gradients of water availability (Good et al., 2017). Thus a unimodal rather than monotonic relationship between NPP sensitivity to PPT extremes and mean annual PPT is proposed (Fig. 3).

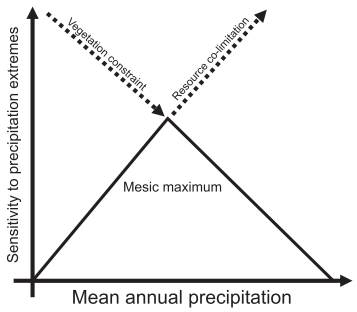

FIG. 3

A unimodal relationship between ecosystem sensitivity to precipitation (PPT) extremes and mean annual PPT is proposed. In the driest ecosystems, net primary productivity is proposed to be strongly constrained by meristematic densities, leaf area, and life history traits of vegetation that in turn limit the magnitude of NPP responses to temporal variation in PPT and, by extension, PPT extremes. This emphasizes a control of biotic mechanisms in the driest regions on Earth. However, as average water availability increases, so too does the capacity for NPP to respond to PPT, which coincides with a decline in the magnitude of constraint that vegetation attributes impose of NPP. A mesic maximum is proposed in which growth potentials of vegetation, water limitation, and PPT variable converge to result the highest sensitivities and greatest variabilities of NPP. Subsequent to this, the magnitude of constrain that other resource imposes on NPP increases, and the sensitivity of NPP to PPT extremes is thought to decrease. This schematic is largely inspired by the ideas and findings discussed in the cross-biome analysis of Knapp and Smith (2001) and Good et al. (2017).

A key issue—one repeated throughout this chapter—with our understanding of patterns of NPP sensitivity to interannual PPT is that much of our understanding is rooted in observational, "opportunistic" studies. Although naturally occurring PPT extremes have greatly advanced our understanding of ecosystem-to global-scale responses of primary productivity dynamics (Ciais et al., 2005; Poulter et al., 2014; Zscheischler et al., 2014), the relatively infrequent nature of their occurrence still poses a challenge. Limited representation of extreme PPT years in observational datasets lends a certain degree of uncertainty in extrapolating NPP responses to historical PPT variability to predicted increases in the magnitude of PPT extremes with climate change.

Dynamics of within-ecosystem NPP responses to PPT extremes

Increasing magnitudes of wet and dry PPT extremes are widely expected to result in nonlinear NPP responses to PPT within ecosystems (Knapp et al., 2017; Felton et al., 2019a,b). A linear relationship between interannual PPT and NPP holds across many terrestrial ecosystems, and when there is evidence for nonlinear relationships, these nonlinearities are weak (Hsu et al., 2012). Identifying when nonlinear responses emerge is critical for anticipating impacts to both the mean and variability of NPP with increasing magnitudes of PPT extremes (Fig. 4). For example, if increases in wet and dry PPT extremes shift a PPT-NPP relationship to saturating (concave-down), future increases in PPT variability and extremes will reduce average NPP because droughts reduce NPP more than wet years increase NPP. By contrast, if a linear PPT-NPP relationship still holds under extremes, future increases in PPT extremes may increase the variability of NPP, with smaller impacts to average NPP.

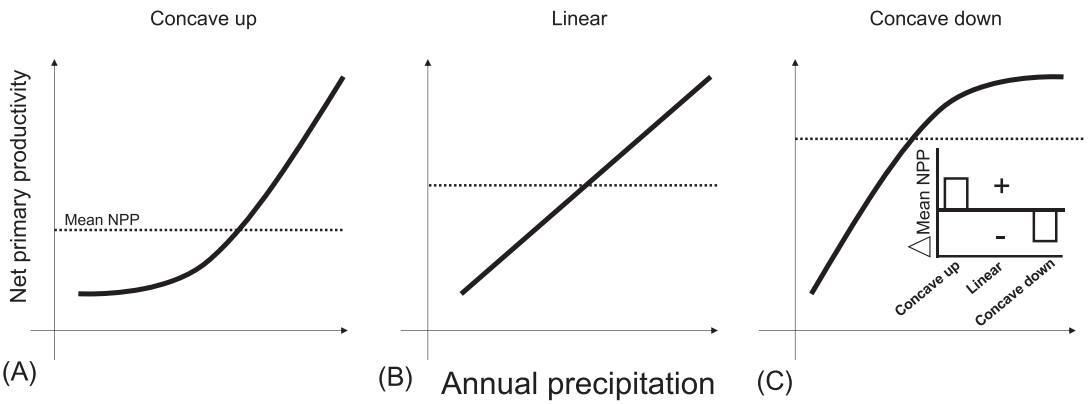

FIG. 4

Forms of within-ecosystem net primary productivity (NPP) responses to interannual variation in PPT. (A) Depicts a nonlinear "concave-up" NPP response to PPT, in which NPP responses to extreme wet years are larger than the driest years, denoted as "positive asymmetry." Such types of responses may be most common when mean NPP is relatively low *(horizontal dashed lines)*, (B) Depicts a linear form of NPP responses to interannual variation in PPT. This is argued to be the most common NPP response dynamic because nonlinear PPT-NPP statistical models often do not perform better than linear models, (C) Depicts a nonlinear "concave-down" or saturating NPP response dynamic, in which NPP reductions during the driest years are largest than increase during extreme wet years, denoted as "negative asymmetry." Such types of responses may be most common ecosystems with relatively high mean rates of NPP (C: inset). Because of asymmetries in NPP responses to wet and dry conditions, nonlinear forms of NPP responses to PPT could result in long-term reductions in average NPP if increases in PPT variability and extremes do occur. By contrast, linear PPT-NPP relationship would have minimal impacts to average NPP but could result in larger increases NPP variability.

One reason for the hypothesis of nonlinear NPP responses to PPT extremes is that ecosystems are known to be differentially sensitive to wet versus dry years, a prerequisite for nonlinear NPP responses to PPT. This differential sensitivity to wet and dry years is denoted as a response "asymmetry," which can be positive or negative. In positive asymmetry, the increases in NPP during wet years are greater than the decreases during dry years (Fig. 4A). Mechanisms for positive asymmetry could include soil moisture carryover effects from previous years that buffer NPP during dry years and/or high growth potentials of vegetation. Positive asymmetry to PPT extremes is widely observed in field studies within short-statured ecosystems such as grasslands (Wilcox et al., 2017), and coupled remote sensing-modeling work suggests pulse-response behavior of vegetation to wet episodes is also apparent in semi-arid regions with low mean NPP, such as in Australia (Haverd et al., 2017). However, PPT-gradient experiments in some ecosystems, such as grasslands, suggest that the magnitude of positive asymmetry may not be strong enough to produce a clear nonlinear PPT-NPP relationship, even when NPP responses to PPT extremes are considered (Felton et al., 2019a,b).

Negative asymmetry arises when drought-induced reductions in NPP are relatively greater than NPP increases during wet years (Fig. 4C). Mechanisms include multiple resource colimitation during wet years (e.g., by light or nutrients), high drought sensitivity of vegetation, or increased water losses (e.g., runoff, leaching) from the ecosystems during wet years. Negative asymmetry is, to date, claimed

to be less frequently observed than positive asymmetry (Knapp et al., 2017). However, observational work using tree-ring records in forests across the conterminous United States observed negative asymmetry (Dannenberg et al., 2019). Remotely sensed estimates of gross primary productivity anomalies revealed that much of the variability in continental-scale primary productivity is derived from drought-induced productivity reductions or "negative" anomalies (Zscheischler et al., 2014). Other remote sensing work suggests that saturating PPT-NPP responses—and thus negative asymmetry—do occur and are most common in regions with low solar radiation or soil nutrients (Ye et al., 2018). A global-scale modeling study further suggested negative asymmetric responses of ecosystem productivity to soil moisture variation may drive declines in global terrestrial carbon uptake near the middle of the 21st century (Green et al., 2019).

In total, evidence for hypothesized nonlinearities in NPP to responses to PPT, at least at interannual timescales, is to date surprisingly limited and ultimately equivocal. The diversity of results from empirical studies reflects contingency in within-ecosystems drivers of NPP as opposed to exploring broader spatial patterns. One hypothesis is that ecosystems have not been exposed to PPT deviations of sufficient magnitude because much of our understanding of within-ecosystem responses of NPP to interannual PPT is derived from observational datasets of PPT and NPP with limited occurrences of extremes. Indeed, a recent data synthesis concluded that extreme drought only elicits extreme responses in gross primary productivity about ~15% of the time (Zhang et al., 2019). Thus there appears to be a prevalence of "mismatches" between extremes in PPT and extremes in within-ecosystem responses of primary productivity.

Mismatches could be because of contingency in plant community dynamics. Changes to plant community structure—such as species or functional diversity—are an indirect pathway by which PPT extremes can impact NPP. For example, in semiarid grassland, maintenance of linear NPP responses to PPT under wet and dry PPT extremes was found to be driven by plant community structural changes in response to extreme wet conditions through seed bank mobilization of a forb species (Felton et al., 2019a). Theory also predicts, and empirical evidence supports, the expectation that biodiversity can stabilize NPP in response to wet and dry PPT extremes (Isbell et al., 2015). Community-level stabilizing mechanisms related to biodiversity, such as compensatory and asynchronous responses among species to PPT extremes (Jentsch et al., 2011), are widely documented to stabilize NPP responses to drought across multiple ecosystem types (Felton and Smith, 2017). Finally, above versus belowground NPP may be differentially sensitive to wet versus dry PPT extremes, further obscuring the impacts of PPT extremes on NPP (Zhang et al., 2017). These plant community dynamics underscore the contingent nature in which terrestrial NPP responds to PPT extremes.

Mismatches may also be because of the characteristics of interannual PPT extremes, such as their magnitude (e.g., percent deviation from mean PPT), duration (e.g., 1 versus 3 years), or direction (wet versus dry). For example, experimental work imposing multiple magnitudes of drought found that only the most extreme drought produced an "extreme" NPP response in the Tibetan Plateau (Zhang et al., 2019). Other drought experiments have shown that only in the second year of a multiyear drought were extreme reductions in NPP observed (Hoover et al., 2014). Multiyear wet periods are known to be especially critical for fostering plant germination, establishment, and NPP in deserts (Peters et al., 2014). And multiple recent synthesis study also suggests different ecosystem and vegetation types, such as grasslands versus forests, vary in their sensitivity to different drought durations (Gao et al., 2019). For example, a recent cross-biome synthesis of ecosystem flux and remotely sensed primary productivity data found productivity in arid regions to be more sensitive to drought duration than humid regions, a difference that land surface models failed to adequately capture (Orth et al., 2020). If and how NPP

asymmetries and nonlinearities emerge will also depend on corresponding asymmetry in wet or dry PPT extremes with respect to both their magnitude and frequency because it is unrealistic to assume an even distribution of wet and dry PPT extremes in space, time, and magnitude. Moreover, the seasonality, size, and timing of individual PPT events can also impact NPP (Knapp et al., 2002; Yaseef et al., 2010), which only heightens the need to understand the role of increasing *intraannual* PPT extremes.

Intraannual timescales

Focusing assessments on NPP responses to annual PPT amounts precludes a full understanding of how PPT impacts terrestrial NPP. For example, the timing of vegetation activity, that is, phenology, is often tuned to use PPT delivered during specific temporal windows (Sala et al., 1997; Craine et al., 2012; Lauenroth et al., 2014). Thus many terrestrial ecosystems are likely to be highly sensitive to shifts in PPT patterns within years, perhaps even independent of changes to annual or average PPT amounts. Understanding how ecosystems respond to such changes in intraannual PPT is critical because PPT is consistently predicted to be delivered in fewer but larger downpour events, with longer intervening dry periods between PPT events (IPCC, 2013, Fourth US National Climate Assessment).

A conceptual model based on historical ecosystem water balance has been proposed to provide a basis for anticipating how NPP may be impacted by larger and fewer PPT events across different ecosystems (Knapp et al., 2008). Much like xeric and mesic ecosystems might be expected to be differentially sensitive to interannual PPT extremes, so is historical water balance expected to underpin patterns of how more frequent downpours and intervening droughts impact terrestrial NPP. Interestingly, the different dimensions of such increased intraannual PPT—intermittent drought versus more intense downpours—are expected to differentially impact NPP in xeric versus mesic ecosystems, further emphasizing the role of average water availability as an arbiter of PPT-NPP interactions and NPP responses to PPT extremes.

Xeric ecosystems typically exist in a state of chronic water stress, where low average soil moisture in the upper soil layers are transiently relieved through relatively small PPT events. Xeric regions also typically have high atmospheric evaporative demand, and, thus, a substantial portion of PPT events, which typically only puncture shallow soil layers, is lost to evaporation (Noy-Meir, 1973) and may even result in pulsed losses of CO_2 through transient stimulation soil microbial respiration (Parton et al., 2012). In many xeric ecosystems, small PPT events ($\sim$5 mm) are the most common event size class (Huxman et al., 2004b). And globally, the presence of large PPT events increases during extreme wet years and may even define a wet year (Knapp et al., 2015a), signifying their general historic rarity during normal or dry years. In contrast to smaller PPT events, large PPT events result in soil water penetrating to deeper soil layers where water is less subject to immediate evaporation in xeric ecosystems. In general, this change to the location of soil moisture increases both the amount and duration of plant available water. As a consequence, a shift toward fewer and larger PPT events is expected to increase NPP within xeric ecosystems (Knapp et al., 2008).

In mesic ecosystems, water balances are sufficiently positive such that plant water stress is relatively infrequent. In mesic ecosystems, intraannual PPT regimes are expected to lower soil moisture through increased durations of dry intervals between PPT events. Thus in contrast to xeric ecosystems, it is the increased length of dry intervals that may be most important for impacting NPP in mesic ecosystems. Larger and more intense PPT may also increase the amount of PPT lost to abiotic pathways, which could include evaporation from the canopy and soil surface, percolation of water below the rooting zone, and runoff. Considering the potential for increased abiotic losses of PPT in concert with

longer intervening dry periods, the general effect of fewer and larger PPT events in mesic systems may be a decrease in NPP (Knapp et al., 2008).

Empirical studies offer some support for these expectations (Heisler-White et al., 2009). Early experimental work in mesic grassland found that fewer and larger PPT events reduced NPP through reductions in soil moisture and increases in plant water stress (Knapp et al., 2002; Fay et al., 2003). But later work in this same ecosystem found relatively weak or minimal impacts (Wilcox et al., 2015), and that the negative impacts may diminish during wet years (Felton et al., 2020). An experiment in semiarid grassland found that fewer and larger PPT events increased primary productivity through increases in soil moisture and reductions in plant water stress (Heisler-White et al., 2008), with a similar result observed in desert grassland (Thomey et al., 2011). These observations are supported through ecosystem flux assessments, which have shown that large PPT events promote carbon uptake in semiarid regions (Parton et al., 2012). The generality of these previously discussed findings is restricted to shallow-rooted ecosystems and, thus, are challenged by uncertainties related to characteristics that will vary in other ecosystem types.

Variation in vegetation structure and climate obscure predictions of NPP responses to more extreme intraannual PPT regimes based on ecosystem water balance. How responses may differ within ecosystems dominated by other vegetation types, such as shrublands and forests, where aboveground vegetation cover and rooting depths differ greatly, remains less clear. Given the pulse-driven nature of NPP responses to PPT in shallow-rooted systems such as grasslands (Lauenroth et al., 2014), NPP in herbaceous-dominated ecosystems may be particularly sensitive to intraannual PPT changes in the near term. In the long-term, there is empirical evidence to suggest that more extreme PPT patterns may promote the abundance and productivity of deeper-rooted species, such as shrubs, in both deserts and grasslands by placing more soil moisture in deeper soil layers (Gherardi and Sala, 2015; Sala et al., 2015).

Implications for forests are less clear. The strong constraint of other resources on NPP, such as light, nitrogen, and phosphorus (Norby et al., 2010; Fleischer et al., 2019), and sufficient soil moisture could mean that more frequent deluges would more likely impose frequent physiological stress through oxygen deprivation in waterlogged soils (Pedersen et al., 2020). This mechanism could still reduce NPP. Moreover, dry and semiarid forests—where PPT inputs are generally low—may be a particularly vulnerable forest type to more extreme intraannual PPT patterns through increased drought stress (Anderegg et al., 2019; Dannenberg et al., 2019). However, there is evidence that large PPT events during the cool season can account for nearly 25% of annual PPT in some forests, which can stabilize soil water availability in the main rooting zone (e.g., 20–40 cm Yaseef et al., 2010). Other work has shown that, globally, tree growth is most sensitive to intraannual droughts during the dry seasons (Huang et al., 2018), when soil water perhaps becomes most limiting to growth. Indeed, the response of NPP to intraannual PPT is not only a question of *where* vegetation access water in the soil profile but also *when*.

A second contingency is, thus, the timing of the larger PPT events (Reyer et al., 2013). Studies have observed that the timing of intraannual PPT variability—for both droughts and large PPT events—is a critical component for how intraannual PPT patterns impact NPP (Craine et al., 2012). The timing of intraannual drought also clearly matters across biomes (Dietrich and Smith, 2016; Denton et al., 2017; Huang et al., 2018). Depending on whether or not droughts or deluges occur during a sensitive time period for plant growth, the impacts of more extreme intraannual PPT patterns could theoretically be exacerbated, reduced, or have negligible impacts on NPP. For example, an ecosystem flux study in forests found that large carbon uptake during the spring—enhanced by warming—preceding an extreme drought during summer partially mitigated drought-induced reductions productivity (Wolf

et al., 2016). Such "phenological mismatches" at the intraannual timescale could also potentially underpin mismatches between ecosystem responses and PPT extremes at interannual timescales, underscoring the need to elucidate the interactive effects of increasing intra and interannual PPT extremes on NPP.

Intra and interannual interactions

A discussion about how the timing and distribution of PPT events impacts NPP dynamics raises questions as to how projected increases in intraannual PPT variability may impact PPT-NPP interactions at interannual timescales. The interactive effects of intra and interannual PPT extremes on NPP remain surprisingly underexplored. This is despite a clear influence of certain dimensions of intraannual PPT variability, such as PPT seasonality, on magnitudes of interannual PPT variability globally (Fatichi et al., 2012). And in some ecosystems, the presence of larger PPT events can influence not only annual variability in PPT but also NPP variability (Lauenroth and Sala, 1992). Impacts of changes to intra and interannual PPT extremes on NPP are, thus, likely to be nonexclusive. One hypothesis is that the impact of more extreme intraannual PPT patterns may depend on annual PPT amounts. Specifically, the influence of larger and fewer PPT events could theoretically be dampened during extreme wet years.

As soil water reaches saturation, increased abiotic water losses, resource colimitation, or production, constrains of vegetation may increase, and NPP responses to variation in PPT event size may be muted. But as years become drier, the realized effect of more extreme intraannual PPT patterns of NPP may become apparent (Fig. 5) because water moves closer to becoming the primary resource limiting

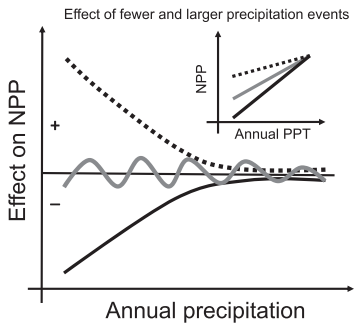

FIG. 5

Hypothesized interactions of intra- and interannual precipitation variability on NPP and their implications for interannual precipitation-productivity relationships. In every scenario, the influence of larger and fewer PPT events is expected to have minimal impacts during years of high annual PPT as soil water becomes saturated. As years become drier and water moves closer to becoming a primary resource limiting net primary productivity (NPP), the effect of larger and fewer PPT events is proposed to become clarified. Larger and fewer events could exacerbate NPP reductions during dry years through longer dry intervals (*solid black line*; Felton et al., 2020) have minimal effects *(solid gray line)* or provide a "drought rescue" effect that would alleviate drought stress during dry years *(dotted line)*. Each interaction type would therein alter the slope and intercepts of temporal relationships between interannual PPT and NPP primarily through how NPP is altered during years of low annual PPT. However, cross-ecosystem tests of this hypothesis are needed.

NPP. The magnitude and direction of these interactions would have clear implications for relationships between NPP and interannual PPT (Fig. 5 inset). For example, a negative interaction during dry years would increase NPP sensitivity to PPT, whereas a positive interaction would reduce NPP sensitivity to PPT.

Uncertainties and pathways forward

Do we know enough about terrestrial NPP responses to PPT extremes? No. But in the past two decades, our knowledge on this topic has grown significantly. Part of this reflects an increased urgency to understand and predict the ecological consequences of increases in PPT extremes. Another part of this reflects the temporal maturation and computational advancements in the datasets and tools ecologists use to study terrestrial ecosystems. Furthermore, core areas of uncertainties in our understanding NPP responses to PPT extremes are outlined. Research approaches for studying ecosystem responses to PPT extremes are also suggested. Improvements in these areas will build off of the significant advances made within the past two decades.

Uncertainties

Characteristics of precipitation extremes

It is frequently observed that PPT extremes do not produce large, extreme, or nonlinear ecosystem responses (Jentsch et al., 2011; Zhang et al., 2019; Felton et al., 2019a,b). A first step toward understanding these mismatches may involve deeper consideration of the characteristics of PPT extremes themselves. The relative influence of different characteristics of PPT extremes across different ecosystems, such as their timing, duration, and return intervals, is unclear. We also know little about how the impacts of interannual PPT extremes may interact with increases in the size of PPT events within years (Fig. 5). Large PPT events could either "rescue" ecosystem functioning during drought (Yaseef et al., 2010), exacerbate drought effects (Felton et al., 2020), or have no discernable impact (Fig. 5). In general, the influence of these interactions on ecosystem functioning likely depends on average water availability, vegetation structure, and the timing of PPT events. Unraveling the independent and interactive effects of these characteristics of PPT extremes on ecosystem functioning will be critical toward linking different components of PPT extremes to large changes in ecosystem functioning.

Plant community dynamics and change

Plant community dynamics are perhaps the greatest—but least predictable—indirect driver of how PPT extremes will impact of terrestrial ecosystem functioning and NPP. Plant community dynamics can transiently stabilize NPP in response to PPT extremes (Jentsch et al., 2011; Felton and Smith, 2017), but the longer-term dynamics, such as species reordering and shifts in dominance, are unclear and perhaps unpredictable. Prolonged droughts can reduce the abundance and productivity of shallow-rooted vegetation in drylands (Winkler et al., 2019). And a shift toward PPT regimes with larger PPT events and greater PPT variability could promote deeper-rooted vegetation (Jones et al., 2016; Gherardi and Sala, 2015). Observed and predicted tree mortality events, largely due to extreme drought, also pose large uncertainties for anticipating the future structure and functioning of forests (Breshears et al., 2005).

Anticipating structural changes, particularly in forests, could involve identification of climatic thresholds among species in plant water use physiologies (Hammond et al., 2019). For example, tree species maintain the xylem pressures closer to a mortality threshold (hydraulic safety margin) are documented to be more vulnerable to drought (Powers et al., 2020), and forests with higher hydraulic diversity among species are documented to be more resistant to drought (Anderegg et al., 2019). Recent work suggests hydraulic trait compositions of some forests may be shifting toward drought-tolerant species (Trugman et al., 2020). Feedbacks between how plant community dynamics impact terrestrial ecosystem functioning are not only a product of direct responses to PPT extremes during the event but also how the structure and function of vegetation following a PPT extreme (Tilman and El Haddi, 1992; Hoover et al., 2014).

Recovery dynamics

This chapter has focused on the *response* of NPP to PPT extremes. However, understanding and projecting the long-term dynamics (e.g., multidecadal) of ecosystem functioning requires consideration of *recovery* dynamics follow PPT extremes. Recent work suggests that recovery of NPP following PPT extremes, such as drought, can vary with long-term climatic conditions such as mean annual PPT (Stuart-Haëntjens et al., 2018). There is also growing evidence that NPP in herbaceous-dominated ecosystems, such as grasslands, can recover rapidly from extreme drought (Hoover et al., 2014; Wilcox et al., 2020), and that drought recovery times may be longest in tropical regions and northern-latitude ecosystems (Schwalm et al., 2017). Understanding such recovery dynamics in a multiscale fashion—from species physiology, carbon allocation, to ecosystem fluxes—will be especially important in forested ecosystems (Kannenberg et al., 2019), with long-lived species that have slower demographic rates and recovery horizons (Reichstein et al., 2013). But evidence also suggests lags in NPP recovery are widespread across biomes, from forests (Anderegg et al., 2015b) to deserts (Yahdjian and Sala, 2006), although the underlying mechanisms of recovery may differ among different biomes (Sala et al., 2012; Kannenberg et al., 2019). Finally, the degree to which NPP increases during extreme wet years can compensate NPP losses during drought, and how more frequent droughts—and, thus, shorter return intervals—impact NPP responses to future droughts is unclear. Focusing on these temporal dynamics is important because projected increases in PPT extremes are a consequence of projected increases in temporal PPT variability (Swain et al., 2018).

Interaction with other climatic and global change drivers

How the ecosystem impacts of PPT extremes may be modulated by other concurrent global change drivers, such as rising atmospheric CO_2, atmospheric aridity, and nitrogen deposition, is also unclear. For example, rising atmospheric CO_2 may increase water use efficiency of ecosystems through its influence on plant physiology (Keenan et al., 2013), but concurrent increases in atmospheric aridity may counteract this positive effect through similar mechanisms (Yuan et al., 2019; Grossiord et al., 2020). Regardless, it is virtually certain that rising temperatures will exacerbate drought effects and increase drought risk over the 21st century (Diffenbaugh et al., 2015). Modeling work also suggests the benefits of rising CO_2 on plant physiology and productivity may diminish by mid-century and give way to the negative influence of increasing soil moisture variability (Green et al., 2019). Indeed, NPP responses to PPT extremes—particularly within semiarid region—can produce signatures on the global carbon cycle through anomalies in land CO_2 sinks and sources (Poulter et al., 2014; Ma et al., 2016). Thus future increases in PPT extremes could increase variability in the global carbon cycle, particularly

if ongoing aridification expands the global extent of semiarid regions (Yao et al., 2020). Competing impacts of PPT extremes with other global change drivers, and how they impact terrestrial primary productivity, may perhaps be the greatest uncertainty in our ability to predict how the land surface will feed back to climate change over the course of the 21st century.

Pathways forward

Cross-site distributed experiments

Limited cohesion in ecological research—from defining a climatic extreme to experimental study design—heightens the challenge of anticipating the ecological consequences of increasing PPT extremes. Advances in global-scale remote sensing platforms (Running et al., 2004) and cross-ecosystem data collection initiatives (Hobbie et al., 2003) have promoted generality and data synthesis in ecological research. However, mechanistic experiments are best suited to empirically simulate novel climatic conditions and produce empirical data about ecosystem responses.

Ecological experiments simulating PPT extremes and variability have grown considerably over the past two decades (Fay et al., 2000; Yahdjian and Sala, 2002; Jentsch et al., 2007; Gherardi and Sala, 2013; Asbjornsen et al., 2018), but there has been limited cohesion in this growth, with ecologists often proceeding independently with site-specific research conducted on short-term funding cycles. The result can be a scattershot of how PPT extremes are imposed, what data are collected, and the duration of the experiments. A lack of cohesion can call into question the comparability of research findings and, thus, the ability to synthesize research results.

To achieve a more general understanding of ecosystem responses to PPT extremes, ecologists should consider embracing a cohesive, collaborative, and global-scale approach to studying and experimentally imposing PPT extremes. One idea is a network approach of coordinated distributed experiments. Although this is not a new idea, echoing its need is warranted. The nutrient network—a cross-ecosystem global scale nutrient and herbivore experiment—provides a template for how to achieve this, both in execution and magnitude of research output (https://nutnet.org; Borer et al., 2014). Standardized research protocols (e.g., data collection and experimental design), which also incorporate site-based knowledge and logistics (Asbjornsen et al., 2018), offer multiple benefits. Standard research protocols and a common mission and research question add creditability toward achieving comparability and generality in research findings across ecosystems.

For PPT extremes, the International Drought Experiment (DroughtNet; https://drought-net.colostate.edu) provides a contemporary, ongoing example. In this global scale, coordinated distributed experiment, researchers are imposing 1 in 100-year droughts for at least 4 years to unravel patterns of drought sensitivity through time and across terrestrial ecosystems. And much like the highly successful and ongoing Long-Term Ecological Research Network in the United States (https://lternet.edu), these cross-ecosystem initiatives leave room for additional research to address ecosystem-specific research questions.

Future changes to PPT extremes will include factors other than droughts, however, such as increased prevalence of extreme wet years and large PPT events. Cross-ecosystem experiments and networks addressing these facets of climate change are also warranted. Typically, climate change experiments have involved few-factor designs (e.g., a treatment and ambient control). Such experiments can produce information on the relative effect of a PPT extreme relative to a control treatment;

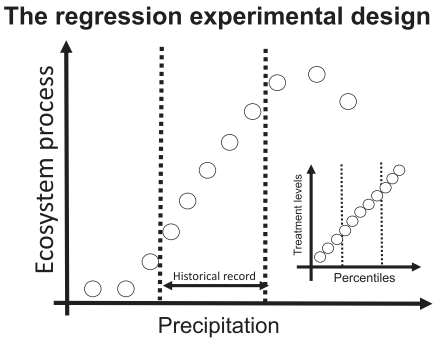

FIG. 6

The regression experiment. The regression-based approach to experimental design involves imposing a continuous treatment gradient (e.g., precipitation) to produce a surface response of a continuous variable (e.g., net primary productivity). Specific to precipitation (PPT) extremes research, the inset shows how PPT amounts could be guided by historical PPT percentiles (*vertical dashed lines* in both main and inset figure), and, thus, the treatment gradient could include PPT levels with restricted to and beyond the historic climate record. This type of experimental design would then allow empirical tests of the hypothesized emergence of nonlinear ecosystem responses under magnitudes of PPT extremity with no recent historic analog that is also amenable to being incorporated into ecosystems models.

however, they provide limited information on how wet and dry PPT extremes could lead to nonlinear dynamics of ecosystem functioning (Fig. 3).

For over a decade, ecologists have advocated for regression-based experimental designs (Cottingham et al., 2005; Gotelli and Ellinson, 2013) when the two variables of interest are continuous (e.g., PPT and NPP). These experimental designs can test for nonlinearities and threshold response of ecosystem processes (e.g., NPP) to PPT extremes (Fig. 6) at both intra and interannual timescales, and also the interactions between these two timescales of PPT change (Fig. 5). And because the output is a continuous response gradient, it is argued that regression experiments produce datasets that are better suited for integration with computational models (Cottingham et al., 2005).

Improving ecosystem models with ecological experiments

Process-based (or mechanistic) models that couple the land and atmosphere are among the primary means by which predictions are made concerning the response and feedbacks of the land surface to climate change (Green et al., 2019). However, our ability to mechanistically model plant responses to PPT extremes, from individuals to ecosystems, is uncertain (Wu et al., 2018; Kolus et al., 2019). Variation among different models in their assumptions of parameters and key ecosystem processes, such as the physiological mechanisms and thresholds of plant responses to water stress (Trugman et al., 2018), has produced uncertainty for projecting terrestrial ecosystem responses to PPT extremes.

One recent idea to address model limitations and uncertainties is to use in situ experiments. Experiments can produce data that can (1) empirically constrain model parameters and (2) serve as an empirical benchmark by which to compare modeling outputs (Fig. 7). However, models can repeat empirical patterns based off of the wrong process-based assumptions. To address this, modeling

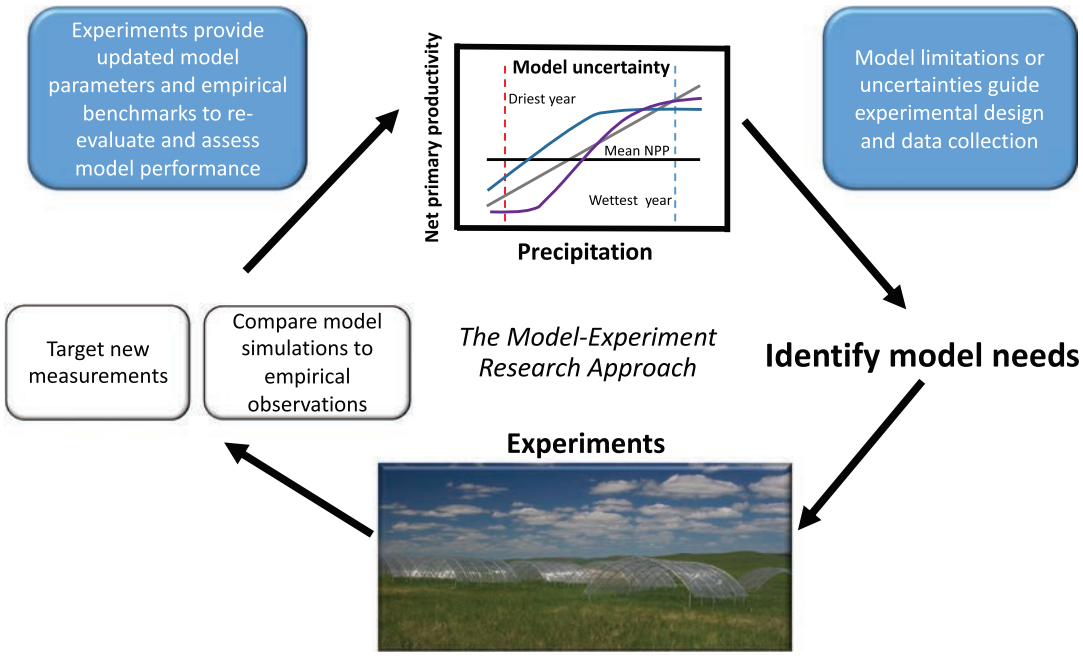
Experiments provide updated model parameters and empirical benchmarks to re-evaluate and assess model performance
Model uncertainty
Driest year
Mean NPP
Wettest year
Net primary productivity
Precipitation
Model limitations or uncertainties guide experimental design and data collection
Target new measurements
Compare model simulations to empirical observations
The Model-Experiment Research Approach
Identify model needs
Experiments

FIG. 7

The model-experiment research approach. Uncertainties in current process-based ecosystem models present an opportunity to guide the design of experiments. The data produced from these experiments are useful in multiple regards. First, results from experiments can serve as an empirical benchmark to compare with model simulations. Second, the data from experiments can be used to empirically constrain model parameters for key variables. Third, because different models employ different assumptions about ecosystem processes, such as how plants respond to drought stress, experiments can serve as an empirical test of different modeling assumptions. This cyclical interactions continually result in new insights about model performance and directions for model improvements and associated experiments. Regression-based experimental approaches are particularly useful in this regard.

assumptions for a given process—which often vary across models—can be treated as a hypothesis that can be empirically tested with experiments (Medlyn et al., 2015). This assumption-based approach provides a roadmap for how experiments and models can cyclically interact and, by extension, how models can be iteratively improved using empirical data produced from experiments. Regression experiments are useful for this approach in general, and for PPT extremes in particular. This is because simulation of ecosystems processes in models are highly dynamic and, thus, can exhibit nonlinear response dynamics to environment drivers at multiple biological, temporal, and spatial scales (Walker et al., 2017; Wu et al., 2018; Green et al., 2019). Such a multiscale perspective will be vital toward improving our ability to anticipate the consequences of intensified PPT extremes for the functioning of terrestrial ecosystems and the services we as humans derive from them.

Summary

Climate change forecasts of increases in PPT extremes at both inter and intraannual timescales have driven ecologists to increasingly study the consequences for terrestrial ecosystem functioning in general and NPP in particular. Conceptual models of the sensitivity of terrestrial NPP to PPT extremes are fundamentally based in how mean ecosystem water availability mediates PPT-NPP interactions. One expectation is that NPP in dry regions will be more sensitive to PPT extremes than wet regions, and much evidence supports this expectation. However, contingencies in within-ecosystem characteristics, such as vegetation structure and plant community dynamics, along with the characteristics of PPT extremes themselves, such as their timing, also influence NPP responses to PPT extremes. Much of our understanding about how NPP responds to PPT is based on observational datasets with limited representation of PPT extremes, which may not be predictive of responses to PPT extremes with no historic analog. And although the increasing prevalence of field experiments imposing PPT extremes has sought to address this, limited cohesion across experimental studies poses a challenge in extracting generality from them. Within this context, cross-site distributed experimental networks, regression-based experimental designs and having these experiments guided by uncertainties in process-based models show promise to produce a more predictive understanding of ecosystem responses to PPT extremes.

References

Ahmadalipour, A., Moradkhani, H., Castelletti, A., Magliocca, N., 2019. Future drought risk in Africa: integrating vulnerability, climate change, and population growth. Sci. Total Environ. https://doi.org/10.1016/j.scitotenv.2019.01.278.

Anderegg, W.R.L., et al., 2015a. Tree mortality predicted from drought-induced vascular damage. Nat. Geosci. https://doi.org/10.1038/ngeo2400.

Anderegg, W.R.L., et al., 2015b. Pervasive drought legacies in forest ecosystems and their implications for carbon cycle models. Science (80-). https://doi.org/10.1126/science.aab1833.

Anderegg, W.R.L., Anderegg, L.D.L., Kerr, K.L., Trugman, A.T., 2019. Widespread drought-induced tree mortality at dry range edges indicates that climate stress exceeds species' compensating mechanisms. Glob. Chang. Biol. https://doi.org/10.1111/gcb.14771.

Asbjornsen, H., et al., 2018. Guidelines and considerations for designing field experiments simulating precipitation extremes in forest ecosystems. Methods Ecol. Evol. https://doi.org/10.1111/2041-210X.13094.

Biederman, J.A., et al., 2017. CO_2 exchange and evapotranspiration across dryland ecosystems of southwestern North America. Glob. Chang. Biol. https://doi.org/10.1111/gcb.13686.

Borer, E.T., et al., 2014. Herbivores and nutrients control grassland plant diversity via light limitation. Nature. https://doi.org/10.1038/nature13144.

Breshears, D.D., et al., 2005. Regional vegetation die-off in response to global-change-type drought. Proc. Natl. Acad. Sci. U. S. A. https://doi.org/10.1073/pnas.0505734102.

Churkina, G., Running, S.W., 1998. Contrasting climatic controls on the estimated productivity of global terrestrial biomes. Ecosystems 1 (2), 206–215.

Ciais, P., et al., 2005. Europe-wide reduction in primary productivity caused by the heat and drought in 2003. Nature. https://doi.org/10.1038/nature03972.

Cook, B.I., Ault, T.R., Smerdon, J.E., 2015. Unprecedented 21st century drought risk in the American Southwest and Central Plains. Sci Adv. https://doi.org/10.1126/sciadv.1400082.

Cottingham, K.L., Lennon, J.T., Brown, B.L., 2005. Knowing when to draw the line: designing more informative ecological experiments. Front. Ecol. Environ. https://doi.org/10.1890/1540-9295(2005)003[0145:KWTDTL]2.0.C0;2.

Craine, J.M., et al., 2012. Timing of climate variability and grassland productivity. Proc. Natl. Acad. Sci. U. S. A. https://doi.org/10.1073/pnas.1118438109.

Dalgleish, H.J., Hartnett, D.C., 2006. Below-ground bud banks increase along a precipitation gradient of the North American great plains: A test of the meristem limitation hypothesis. New Phytol. https://doi.org/10.1111/j.1469-8137.2006.01739.x.

Danger, M., Daufresne, T., Lucas, F., Pissard, S., Lacroix, G., 2008. Does Liebig's law of the minimum scale up from species to communities? Oikos. https://doi.org/10.1111/j.1600-0706.2008.16793.x.

Dannenberg, M.P., Wise, E.K., Smith, W.K., 2019. Reduced tree growth in the semiarid United States due to asymmetric responses to intensifying precipitation extremes. Sci. Adv. https://doi.org/10.1126/sciadv.aaw0667.

Davidowitz, G., 2002. Does precipitation variability increase from mesic to xeric biomes? Glob. Ecol. Biogeogr. https://doi.org/10.1046/j.1466-822X.2002.00271.x.

Denton, E.M., Dietrich, J.D., Smith, M.D., Knapp, A.K., 2017. Drought timing differentially affects above- and belowground productivity in a mesic grassland. Plant Ecol. https://doi.org/10.1007/s11258-016-0690-x.

Dietrich, J.D., Smith, M.D., 2016. The effect of timing of growing season drought on flowering of a dominant C4 grass. Oecologia. https://doi.org/10.1007/s00442-016-3579-4.

Diffenbaugh, N.S., Swain, D.L., Touma, D., Lubchenco, J., 2015. Anthropogenic warming has increased drought risk in California. Proc. Natl. Acad. Sci. U. S. A. https://doi.org/10.1073/pnas.1422385112.

Eskelinen, A., Harrison, S.P., 2015. Resource colimitation governs plant community responses to altered precipitation. Proc. Natl. Acad. Sci. U. S. A. https://doi.org/10.1073/pnas.1508170112.

Fatichi, S., Ivanov, V.Y., Caporali, E., 2012. Investigating interannual variability of precipitation at the global scale: is there a connection with seasonality? J. Clim. https://doi.org/10.1175/JCLI-D-11-00356.1.

Fay, P.A., Carlisle, J.D., Knapp, A.K., Blair, J.M., Collins, S.L., 2000. Altering rainfall timing and quantity in a mesic grassland ecosystem: design and performance of rainfall manipulation shelters. Ecosystems. https://doi.org/10.1007/s100210000028.

Fay, P.A., Carlisle, J.D., Knapp, A.K., Blair, J.M., Collins, S.L., 2003. Productivity responses to altered rainfall patterns in a C 4-dominated grassland. Oecologia. https://doi.org/10.1007/s00442-003-1331-3.

Felton, A.J., Smith, M.D., 2017. Integrating plant ecological responses to climate extremes from individual to ecosystem levels. Philos. Trans. R. Soc. B Biol. Sci. https://doi.org/10.1098/rstb.2016.0142.

Felton, A.J., Knapp, A.K., Smith, M.D., 2019a. Carbon exchange responses of a mesic grassland to an extreme gradient of precipitation. Oecologia. https://doi.org/10.1007/s00442-018-4284-2.

Felton, A.J., Zavislan-Pullaro, S., Smith, M.D., 2019b. Semiarid ecosystem sensitivity to precipitation extremes: weak evidence for vegetation constraints. Ecology. https://doi.org/10.1002/ecy.2572.

Felton, A.J., Slette, I.J., Smith, M.D., Knapp, A.K., 2020. Precipitation amount and event size interact to reduce ecosystem functioning during dry years in a mesic grassland. Glob. Chang. Biol. https://doi.org/10.1111/gcb.14789.

Fernández, R.J., 2007. On the frequent lack of response of plants to rainfall events in arid areas. J. Arid Environ. https://doi.org/10.1016/j.jaridenv.2006.07.004.

Fisher, J.B., et al., 2017. The future of evapotranspiration: global requirements for ecosystem functioning, carbon and climate feedbacks, agricultural management, and water resources. Water Resour. Res. https://doi.org/10.1002/2016WR020175.

Fleischer, K., et al., 2019. Amazon forest response to CO_2 fertilization dependent on plant phosphorus acquisition. Nat. Geosci. https://doi.org/10.1038/s41561-019-0404-9.

Frank, D., et al., 2015. Effects of climate extremes on the terrestrial carbon cycle: concepts, processes and potential future impacts. Glob. Chang. Biol. https://doi.org/10.1111/gcb.12916.

Gao, J., Zhang, L., Tang, Z., Wu, S., 2019. A synthesis of ecosystem aboveground productivity and its process variables under simulated drought stress. J. Ecol. https://doi.org/10.1111/1365-2745.13218.

Gherardi, L.A., Sala, O.E., 2013. Automated rainfall manipulation system: a reliable and inexpensive tool for ecologists. Ecosphere. https://doi.org/10.1890/ES12-00371.1.

Gherardi, L.A., Sala, O.E., 2015. Enhanced precipitation variability decreases grass- and increases shrub-productivity. Proc. Natl. Acad. Sci. U. S. A. https://doi.org/10.1073/pnas.1506433112.

Good, S.P., Moore, G.W., Miralles, D.G., 2017. A mesic maximum in biological water use demarcates biome sensitivity to aridity shifts. Nat. Ecol. Evol. https://doi.org/10.1038/s41559-017-0371-8.

Gotelli, N.J., Ellinson, A.M., 2013. A Primer of Ecological Statistics., https://doi.org/10.1017/CBO9781107415324.004.

Green, J.K., et al., 2019. Large influence of soil moisture on long-term terrestrial carbon uptake. Nature. https://doi.org/10.1038/s41586-018-0848-x.

Grime, J.P., et al., 2000. The response of two contrasting limestone grasslands to simulated climate change. Science (80-). https://doi.org/10.1126/science.289.5480.762.

Grossiord, C., et al., 2020. Plant responses to rising vapor pressure deficit. New Phytol. https://doi.org/10.1111/nph.16485.

Gupta, A., Rico-Medina, A., Caño-Delgado, A.I., 2020. The physiology of plant responses to drought. Science (80-). https://doi.org/10.1126/science.aaz7614.

Gutschick, V.P., BassiriRad, H., 2003. Extreme events as shaping physiology, ecology, and evolution of plants: toward a unified definition and evaluation of their consequences. New Phytol. https://doi.org/10.1046/j.1469-8137.2003.00866.x.

Hammond, W.M., et al., 2019. Dead or dying? Quantifying the point of no return from hydraulic failure in drought-induced tree mortality. New Phytol. https://doi.org/10.1111/nph.15922.

Haverd, V., Ahlström, A., Smith, B., Canadell, J.G., 2017. Carbon cycle responses of semi-arid ecosystems to positive asymmetry in rainfall. Glob. Chang. Biol. https://doi.org/10.1111/gcb.13412.

Heisler-White, J.L., Knapp, A.K., Kelly, E.F., 2008. Increasing precipitation event size increases aboveground net primary productivity in a semi-arid grassland. Oecologia. https://doi.org/10.1007/s00442-008-1116-9.

Heisler-White, J.L., Blair, J.M., Kelly, E.F., Harmoney, K., Knapp, A.K., 2009. Contingent productivity responses to more extreme rainfall regimes across a grassland biome. Glob. Chang Biol. https://doi.org/10.1111/j.1365-2486.2009.01961.x.

Hobbie, J.E., Carpenter, S.R., Grimm, N.B., Gosz, J.R., Seastedt, T.R., 2003. The US long term ecological research program. Bioscience. https://doi.org/10.1641/0006-3568(2003)053[0021,tulter]2.0.co;2.

Hoover, D.L., Knapp, A.K., Smith, M.D., 2014. Resistance and resilience of a grassland ecosystem to climate extremes. Ecology. https://doi.org/10.1890/13-2186.1.

Hoover, D.L., Knapp, A.K., Smith, M.D., 2016. The immediate and prolonged effects of climate extremes on soil respiration in a mesic grassland. J. Geophys. Res. G Biogeosci. https://doi.org/10.1002/2015JG003256.

Hsu, J.S., Adler, P.B., 2014. Anticipating changes in variability of grassland production due to increases in inter-annual precipitation variability. Ecosphere. https://doi.org/10.1890/ES13-00210.1.

Hsu, J.S., Powell, J., Adler, P.B., 2012. Sensitivity of mean annual primary production to precipitation. Glob. Chang. Biol. https://doi.org/10.1111/j.1365-2486.2012.02687.x.

Hu, Z., et al., 2018. Shifts in the dynamics of productivity signal ecosystem state transitions at the biome-scale. Ecol. Lett. https://doi.org/10.1111/ele.13126.

Huang, M., Wang, X., Keenan, T.F., Piao, S., 2018. Drought timing influences the legacy of tree growth recovery. Glob. Chang. Biol. https://doi.org/10.1111/gcb.14294.

Hufkens, K., et al., 2016. Productivity of North American grasslands is increased under future climate scenarios despite rising aridity. Nat. Clim. Chang. https://doi.org/10.1038/nclimate2942.

Huntington, T.G., 2006. Evidence for intensification of the global water cycle: review and synthesis. J. Hydrol. https://doi.org/10.1016/j.jhydrol.2005.07.003.

Huxman, T.E., et al., 2004a. Convergence across biomes to a common rain-use efficiency. Nature. https://doi.org/10.1038/nature02561.

Huxman, T.E., et al., 2004b. Precipitation pulses and carbon fluxes in semiarid and arid ecosystems. Oecologia. https://doi.org/10.1007/s00442-004-1682-4.

IPCC, 2013. Working Group I Contribution to the IPCC Fifth Assessment Report, Climate Change 2013: The Physical Science Basis. IPCC.

Isbell, F., et al., 2015. Biodiversity increases the resistance of ecosystem productivity to climate extremes. Nature. https://doi.org/10.1038/nature15374.

Jentsch, A., Kreyling, J., Beierkuhnlein, C., 2007. A new generation of climate-change experiments: events, not trends. Front. Ecol. Environ. https://doi.org/10.1890/1540-9295(2007)5[365:ANGOCE]2.0.CO;2.

Jentsch, A., et al., 2011. Climate extremes initiate ecosystem-regulating functions while maintaining productivity. J. Ecol. https://doi.org/10.1111/j.1365-2745.2011.01817.x.

Jones, S.K., Collins, S.L., Blair, J.M., Smith, M.D., Knapp, A.K., 2016. Altered rainfall patterns increase forb abundance and richness in native tallgrass prairie. Sci. Rep. https://doi.org/10.1038/srep20120.

Kannenberg, S.A., et al., 2019. Linking drought legacy effects across scales: from leaves to tree rings to ecosystems. Glob. Chang. Biol. https://doi.org/10.1111/gcb.14710.

Keenan, T.F., et al., 2013. Increase in forest water-use efficiency as atmospheric carbon dioxide concentrations rise. Nature. https://doi.org/10.1038/nature12291.

Knapp, A.K., Smith, M.D., 2001. Variation among biomes in temporal dynamics of aboveground primary production. Science (80-). https://doi.org/10.1126/science.291.5503.481.

Knapp, A.K., et al., 2002. Rainfall variability, carbon cycling, and plant species diversity in a mesic grassland. Science (80-). https://doi.org/10.1126/science.1076347.

Knapp, A.K., et al., 2008. Consequences of more extreme precipitation regimes for terrestrial ecosystems. Bioscience. https://doi.org/10.1641/b580908.

Knapp, A.K., et al., 2015a. Characterizing differences in precipitation regimes of extreme wet and dry years: implications for climate change experiments. Glob. Chang Biol. https://doi.org/10.1111/gcb.12888.

Knapp, A.K., et al., 2015b. Differential sensitivity to regional-scale drought in six central US grasslands. Oecologia. https://doi.org/10.1007/s00442-015-3233-6.

Knapp, A.K., Ciais, P., Smith, M.D., 2017. Reconciling inconsistencies in precipitation-productivity relationships: implications for climate change. New Phytol. https://doi.org/10.1111/nph.14381.

Kolus, H.R., et al., 2019. Land carbon models underestimate the severity and duration of drought's impact on plant productivity. Sci. Rep. https://doi.org/10.1038/s41598-019-39373-1.

Lauenroth, W.K., Sala, O.E., 1992. Long-term forage production of North American shortgrass steppe. Ecol. Appl. https://doi.org/10.2307/1941874.

Lauenroth, W.K., Schlaepfer, D.R., Bradford, J.B., 2014. Ecohydrology of dry regions: storage versus pulse soil water dynamics. Ecosystems. https://doi.org/10.1007/s10021-014-9808-y.

Ma, X., et al., 2016. Drought rapidly diminishes the large net CO_2 uptake in 2011 over semi-arid Australia. Sci. Rep. https://doi.org/10.1038/srep37747.

Mackun, P., 2019. About 14.6 million people live in 40 counties in five states. In: United States Census Bur US For Serv.

Maurer, G.E., Hallmark, A.J., Brown, R.F., Sala, O.E., Collins, S.L., 2020. Sensitivity of primary production to precipitation across the United States. Ecol. Lett. https://doi.org/10.1111/ele.13455.

McDowell, N.G., et al., 2011. The interdependence of mechanisms underlying climate-driven vegetation mortality. Trends Ecol. Evol. https://doi.org/10.1016/j.tree.2011.06.003.

Medlyn, B.E., et al., 2015. Using ecosystem experiments to improve vegetation models. Nat. Clim. Chang. https://doi.org/10.1038/nclimate2621.

Myhre, G., et al., 2019. Frequency of extreme precipitation increases extensively with event rareness under global warming. Sci. Rep. https://doi.org/10.1038/s41598-019-52277-4.
Niu, S., et al., 2014. Plant growth and mortality under climatic extremes: an overview. Environ. Exp. Bot. https://doi.org/10.1016/j.envexpbot.2013.10.004.
Norby, R.J., Warren, J.M., Iversen, C.M., Medlyn, B.E., McMurtrie, R.E., 2010. CO_2enhancement of forest productivity constrained by limited nitrogen availability. Proc. Natl. Acad. Sci. U. S. A. https://doi.org/10.1073/pnas.1006463107.
Noy-Meir, I., 1973. Desert ecosystems: environment and producers. Annu. Rev. Ecol. Syst. https://doi.org/10.1146/annurev.es.04.110173.000325.
Orth, R., Destouni, G., Jung, M., Reichstein, M., 2020. Large-scale biospheric drought response intensifies linearly with drought duration in arid regions. Biogeosciences. https://doi.org/10.5194/bg-17-2647-2020.
Pan, Y., et al., 2011. A large and persistent carbon sink in the world's forests. Science (80-). https://doi.org/10.1126/science.1201609.
Parton, W., et al., 2012. Impact of precipitation dynamics on net ecosystem productivity. Glob. Chang. Biol. https://doi.org/10.1111/j.1365-2486.2011.02611.x.
Pedersen, O., Sauter, M., Colmer, T.D., Nakazono, M., 2020. Regulation of root adaptive anatomical and morphological traits during low soil oxygen. New Phytol. https://doi.org/10.1111/nph.16375.
Peters, D.P.C., Yao, J., Browning, D., Rango, A., 2014. Mechanisms of grass response in grasslands and shrublands during dry or wet periods. Oecologia. https://doi.org/10.1007/s00442-013-2837-y.
Poulter, B., et al., 2014. Contribution of semi-arid ecosystems to interannual variability of the global carbon cycle. Nature. https://doi.org/10.1038/nature13376.
Powers, J.S., et al., 2020. A catastrophic tropical drought kills hydraulically vulnerable tree species. Glob. Chang. Biol. https://doi.org/10.1111/gcb.15037.
Reichmann, L.G., Sala, O.E., Peters, D.P.C., 2013. Precipitation legacies in desert grassland primary production occur through previous-year tiller density. Ecology. https://doi.org/10.1890/12-1237.1.
Reichstein, M., et al., 2013. Climate extremes and the carbon cycle. Nature. https://doi.org/10.1038/nature12350.
Reyer, C.P.O., et al., 2013. A plant's perspective of extremes: terrestrial plant responses to changing climatic variability. Glob. Chang. Biol. https://doi.org/10.1111/gcb.12023.
Running, S.W., et al., 2004. A continuous satellite-derived measure of global terrestrial primary production. Bioscience. https://doi.org/10.1641/0006-3568(2004)054[0547:acsmog]2.0.co;2.
Sala, O.E., Lauenroth, W.K., Golluscio, R.A., 1997. Plant functional types in temperate semiarid regions.pdf. In: Plant Funct Types Their Relev to Ecosyst Prop Glob Chang.
Sala, O.E., Gherardi, L.A., Reichmann, L., Jobbágy, E., Peters, D., 2012. Legacies of precipitation fluctuations on primary production: theory and data synthesis. Philos. Trans. R. Soc. B Biol. Sci. https://doi.org/10.1098/rstb.2011.0347.
Sala, O.E., Gherardi, L.A., Peters, D.P.C., 2015. Enhanced precipitation variability effects on water losses and ecosystem functioning: differential response of arid and mesic regions. Clim. Change. https://doi.org/10.1007/s10584-015-1389-z.
Schwalm, C.R., et al., 2017. Global patterns of drought recovery. Nature. https://doi.org/10.1038/nature23021.
Slette, I.J., et al., 2019. How ecologists define drought, and why we should do better. Glob. Chang. Biol. https://doi.org/10.1111/gcb.14747.
Sloat, L.L., et al., 2018. Increasing importance of precipitation variability on global livestock grazing lands. Nat. Clim. Chang. https://doi.org/10.1038/s41558-018-0081-5.
Smith, M.D., 2011. An ecological perspective on extreme climatic events: a synthetic definition and framework to guide future research. J. Ecol. https://doi.org/10.1111/j.1365-2745.2011.01798.x.
Stuart-Haëntjens, E., et al., 2018. Mean annual precipitation predicts primary production resistance and resilience to extreme drought. Sci. Total Environ. https://doi.org/10.1016/j.scitotenv.2018.04.290.

Swain, D.L., Langenbrunner, B., Neelin, J.D., Hall, A., 2018. Increasing precipitation volatility in twenty-first-century California. Nat. Clim. Chang. https://doi.org/10.1038/s41558-018-0140-y.

Thomey, M.L., et al., 2011. Effect of precipitation variability on net primary production and soil respiration in a Chihuahuan desert grassland. Glob. Chang. Biol. https://doi.org/10.1111/j.1365-2486.2010.02363.x.

Tilman, D., El Haddi, A., 1992. Drought and biodiversity in grasslands. Oecologia. https://doi.org/10.1007/BF00317226.

Trugman, A.T., Medvigy, D., Mankin, J.S., Anderegg, W.R.L., 2018. Soil moisture stress as a major driver of carbon cycle uncertainty. Geophys. Res. Lett. https://doi.org/10.1029/2018GL078131.

Trugman, A.T., Anderegg, L.D.L., Shaw, J.D., Anderegg, W.R.L., 2020. Trait velocities reveal that mortality has driven widespread coordinated shifts in forest hydraulic trait composition. Proc. Natl. Acad. Sci. https://doi.org/10.1073/pnas.1917521117.

USGCRP, 2018. In: Reidmiller, D.R., Avery, C.W., Easterling, D.R., Kunkel, K.E., Lewis, K.L.M., Maycock, T.K., Stewart, B.C. (Eds.), Impacts, Risks, and Adaptation in the United States: Fourth National Climate Assessment, Volume II. U.S. Global Change Research Program, Washington, DC, USA, p. 1515 pp, https://doi.org/10.7930/NCA4.2018.

Van de Pol, M., Jenouvrier, S., Cornelissen, J.H.C., Visser, M.E., 2017. Behavioural, ecological and evolutionary responses to extreme climatic events: challenges and directions. Philos. Trans. R. Soc. B Biol. Sci. https://doi.org/10.1098/rstb.2016.0134.

Wada, Y., Van Beek, L.P.H., Wanders, N., Bierkens, M.F.P., 2013. Human water consumption intensifies hydrological drought worldwide. Environ. Res. Lett. https://doi.org/10.1088/1748-9326/8/3/034036.

Walker, A.P., et al., 2017. The impact of alternative trait-scaling hypotheses for the maximum photosynthetic carboxylation rate (Vcmax) on global gross primary production. New Phytol. https://doi.org/10.1111/nph.14623.

Wilcox, K.R., von Fischer, J.C., Muscha, J.M., Petersen, M.K., Knapp, A.K., 2015. Contrasting above- and belowground sensitivity of three Great Plains grasslands to altered rainfall regimes. Glob. Chang. Biol. https://doi.org/10.1111/gcb.12673.

Wilcox, K.R., et al., 2017. Asymmetric responses of primary productivity to precipitation extremes: a synthesis of grassland precipitation manipulation experiments. Glob. Chang. Biol. https://doi.org/10.1111/gcb.13706.

Wilcox, K.R., et al., 2020. Rapid recovery of ecosystem function following extreme drought in a South African savanna grassland. Ecology. https://doi.org/10.1002/ecy.2983.

Williams, A.P., et al., 2015. Contribution of anthropogenic warming to California drought during 2012-2014. Geophys. Res. Lett. https://doi.org/10.1002/2015GL064924.

Williams, A.P., et al., 2020. Large contribution from anthropogenic warming to an emerging North American megadrought. Science (80-). https://doi.org/10.1126/science.aaz9600.

Winkler, D.E., Belnap, J., Hoover, D., Reed, S.C., Duniway, M.C., 2019. Shrub persistence and increased grass mortality in response to drought in dryland systems. Glob. Chang. Biol. https://doi.org/10.1111/gcb.14667.

Wolf, S., et al., 2016. Warm spring reduced carbon cycle impact of the 2012 US summer drought. Proc. Natl. Acad. Sci. U. S. A. https://doi.org/10.1073/pnas.1519620113.

Wu, D., et al., 2018. Asymmetric responses of primary productivity to altered precipitation simulated by ecosystem models across three long-term grassland sites. Biogeosciences. https://doi.org/10.5194/bg-15-3421-2018.

Yahdjian, L., Sala, O.E., 2002. A rainout shelter design for intercepting different amounts of rainfall. Oecologia. https://doi.org/10.1007/s00442-002-1024-3.

Yahdjian, L., Sala, O.E., 2006. Vegetation structure constrains primary production response to water availability in the patagonian steppe. Ecology 87 (4), 952–962.

Yao, J., et al., 2020. Accelerated dryland expansion regulates future variability in dryland gross primary production. Nat. Commun. https://doi.org/10.1038/s41467-020-15515-2.

Yaseef, N.R., Yakir, D., Rotenberg, E., Schiller, G., Cohen, S., 2010. Ecohydrology of a semiarid forest: partitioning among water balance components and its implications for predicted precipitation changes. Ecohydrology. https://doi.org/10.1002/eco.65.

Ye, J.S., Pei, J.Y., Fang, C., 2018. Under which climate and soil conditions the plant productivity-precipitation relationship is linear or nonlinear? Sci. Total Environ. https://doi.org/10.1016/j.scitotenv.2017.10.203.

Yuan, W., et al., 2019. Increased atmospheric vapor pressure deficit reduces global vegetation growth. Sci. Adv. https://doi.org/10.1126/sciadv.aax1396.

Zhang, F., et al., 2017. Net primary productivity and its partitioning in response to precipitation gradient in an alpine meadow. Sci. Rep. https://doi.org/10.1038/s41598-017-15580-6.

Zhang, F., et al., 2019. When does extreme drought elicit extreme ecological responses? J. Ecol. https://doi.org/10.1111/1365-2745.13226.

Zscheischler, J., Mahecha, M.D., Harmeling, S., Reichstein, M., 2013. Detection and attribution of large spatio-temporal extreme events in Earth observation data. Ecol. Inform. https://doi.org/10.1016/j.ecoinf.2013.03.004.

Zscheischler, J., et al., 2014. A few extreme events dominate global interannual variability in gross primary production. Environ. Res. Lett. https://doi.org/10.1088/1748-9326/9/3/035001.

Zuleta, D., Duque, A., Cardenas, D., Muller-Landau, H.C., Davies, S.J., 2017. Drought-induced mortality patterns and rapid biomass recovery in a terra firme forest in the Colombian Amazon. Ecology. https://doi.org/10.1002/ecy.1950.

CHAPTER

Flood early warning systems under changing climate and extreme events

6

Dongfeng Li[a], Zheng N. Fang[a], and Philip B. Bedient[b]

Civil Engineering, The University of Texas at Arlington, Arlington, TX, United States[a] Department of Civil and Environmental Engineering, Rice University, Houston, TX, United States[b]

Introduction

Flooding is one of the costliest and most common natural disaster in the United States and around the globe. It claims lives, presents dangers to infrastructure and public safety, inflicts financial losses on individuals and communities, and strains the government agencies that provide flood response and relief. It caused 4586 fatalities between 1959 and 2005 (Ashley and Ashley, 2008). From 1980 to 2020, flood damages totaled $150 billion throughout the United States (NOAA National Centers for Environmental Information (NCEI), 2020). On average, flood damages account for a third of the annual economic losses due to natural disasters worldwide. In Europe, floods have caused at least 700 deaths, the displacement of about half a million people, and at least 28 billion US dollars in insured economic losses since 2000 (European Environment Agency, 2018). The flood-associated damages will inevitably increase along with the frequency of floods under the current trend of the global temperature increases. According to the Intergovernmental Panel on Climate Change (IPCC), an increase in the average global temperature will likely lead to changes in precipitation and atmospheric moisture, including shifts toward more extreme precipitation during storms (Intergovernmental Panel on Climate Change, 2013). Flooding is increasing both globally and nationwide. In the Central United States, 158 (20%) of the 774 US Geological Survey (USGS) stream gauges exhibit statistically significant changes in the magnitude of flood peaks over the time period of 1962–2011, and of these, 101 (13% of the total number) are characterized by a trend toward increasing flood magnitude, with many of them concentrated in the Greater Chicago area (Mallakpour and Villarini, 2015). Given the changing climate, the design standard for flood control infrastructure has also increased across the United States. The National Oceanic and Atmospheric Administration (NOAA's) Hydrometeorological Design Studies Center has updated precipitation frequency estimates (with 90% confidence intervals) for many states with the NOAA Atlas 14 analysis, which is the official US Government source of precipitation frequency estimates (Perica et al., 2018). For instance, as a result of the NOAA Atlas 14 analysis recently performed for the State of Texas, the rainfall amount of the 100-year 24-h design storm event in Harris County, Texas, has been increased from 12.4–13.5 in. to 16–18 in., a nearly 30% increase. Increased rainfall has been observed at the majority of the rain gauges used in the most recent NOAA

Climate Change and Extreme Events. https://doi.org/10.1016/B978-0-12-822700-8.00002-0
Copyright © 2021 Elsevier Inc. All rights reserved.

Atlas 14 analysis, implying that flooding problems would be exacerbated with the limited capacity of stormwater and flood control systems. Collins et al. (2013) provide climate change projections indicating that rainfall volumes will continue to increase in the 21st century.

Rainfall with a higher intensity and longer duration will lead to a higher frequency of flood events. Within the hydrologic cycle, water is continuously transported from the oceans to the atmosphere, to land, and back to the oceans through hydrologic processes: condensation, precipitation, interception, surface flow runoff, infiltration, percolation, transpiration, storage, and evaporation. A flood is generally defined as a temporary increase in the surface flow resulting from additional precipitation higher than the infiltration capacity. Floods can also be triggered by failures of dams, levees, or other structures that retain water. The risks posed by future flood events are significant, given population growth and change in land-use patterns, proximities of populations to coastlines, expanded development of urban areas in both coastal and inland, environmental degradation, and climate change (Kahn, 2005). Great floods have been found to be increasing in the 20th century (Milly et al., 2002). In 2018, flooding affected more people than any other disaster types over the world (Centre for Research on the Epidemiology of Disasters (CRED), 2019).

Flood damage resulting from typhoons, hurricanes, torrential rainfall, and urban flash flood is increasing over time; thus, obtaining accurate and reliable flood predictions is a valuable strategy for disaster mitigation. Many existing flood control infrastructure was designed decades ago with a low threshold of rainfall amount, and it would be prohibitively costly to update all outdated structural flood control infrastructure. An increasing number of communities have realized that an accurate and timely warning system can provide information to significantly reduce the risks of disaster. Predicting floods is the key component of an effective early warning system, giving governments, businesses, and individuals precious lead time to evacuate and protect their assets. The United Nations Office for Disaster Risk Reduction (UNDRR) (2018) defines an early warning system as "an integrated system of hazard monitoring, forecasting and prediction, disaster risk assessment, communication and preparedness activities systems and processes that enable individuals, communities, governments, businesses and others to take timely actions to reduce disaster risks in advance of hazardous events". Essentially the function of a flood warning system (FWS) is to "collect, handle, analyze, and disseminate hydrologic information, ideally in real time, for the purpose of providing accurate advance warnings of an impending flood event." (United Nations Office for Disaster Risk Reduction, 2018).

With this fundamental function, modern FWSs have evolved to meet the specific needs of different clients, regions, and nations. These systems range from basic river gauge monitoring networks to complex forecasting systems that employ radar rainfall data and advanced computer modeling techniques to produce lead times fluctuating from hours to days. The organizations that oversee these FWSs vary significantly in terms of complexity, size, and scope (Smith et al., 2016a, b).

The United States and many other countries across the globe have foreseen the benefits of FWSs and have implemented their flood forecasting systems to reduce loss of life and economic damages. For example, the European Flood Awareness System operated in the European Response and Coordination Centre provides complementary flood early warning information up to 10 days in advance on a continental scale and regional hydrological services to different national authorities (Smith et al., 2016a, b). In the Netherlands the rivers Rhine and Meuse are forecasted by a "Flood Early Warning System Rivers" (FEWS Rivieren) platform simulating the amount of water entering the Netherlands via these rivers and the relevant river water levels (Ebel and Beckers, 2010). In Japan, a team of researchers from the Institute of Industrial Science, the University of Tokyo, and the Japan Aerospace Exploration

Agency have developed a new system-Today's Earth Japan (TE-Japan) for forecasting flood events. Of the 57 levees that broke during Typhoon Hagibis (2019), TE-Japan successfully alerted 54 of them with a sufficient lead time of just under 33 h on average (Today's Earth Developing Group, 2020).

In this chapter, we will focus on the current FWSs operated in the United States starting with a general introduction of FWSs, including the basic concepts of FWSs, followed by the gauge network with its operation platform, the remote sensing technology of rainfall for FWS rainfall information, and the hydrologic and hydraulic modeling as the core engines of the FWSs.

FWS concept and methodology

Both the National Weather Service (NWS) and the emergency management community recognize the importance of FWSs for protecting lives and livelihoods. Communities across the country have created FWSs to warn areas of flood danger and to provide NWS with critical rainfall, stream levels, and other hydrometeorological data. A successful FWS has three key components as introduced in Parker (2017): (1) input data from rainfall, river, and catchment information, (2) hydrologic and hydraulic modeling processes, and (3) warning dissemination as shown in Fig. 1. The fundamental benefit of a flood warning program is to provide an increased lead time for watches and warnings at locations subject to flood risk. The information can be used to predict whether a flood is about to occur, when it will arrive, and how severe it will be. Organizations and individuals will then be given timely notices by the system so they can protect themselves and their properties from potential floods.

An effective, real-time FWS should be based on the regular collection of local rainfall, stream level, and streamflow data through a gauge network and precipitation measurements. A modern real-time

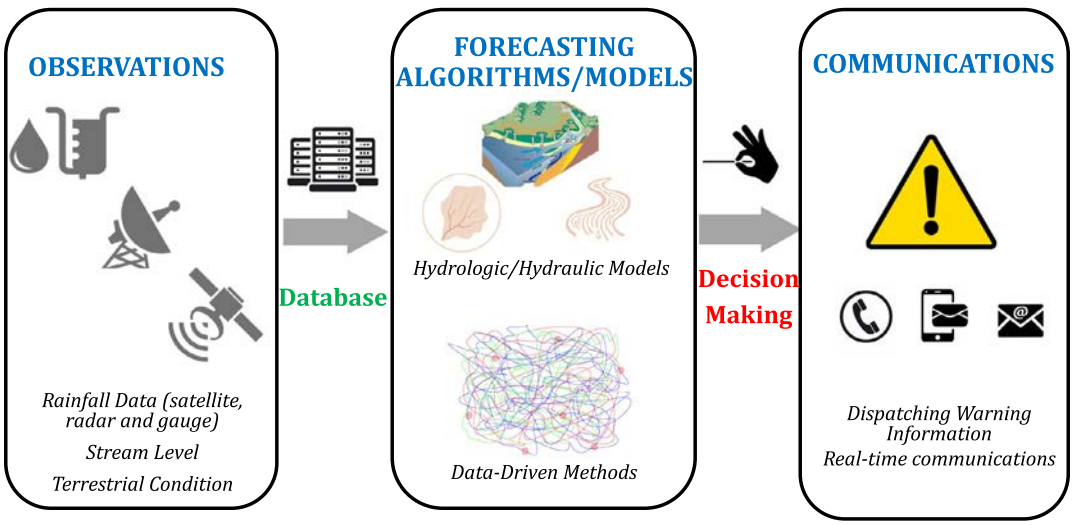

FIG. 1

Flood ALERT system-concept.

monitoring system with telemetry capabilities can make data collection easier—and, in many cases, more cost-effective—while allowing for the fastest possible response to flooding events.

Gauge network hardware and software

In an FWS the most important forcing input is the real-time hydrometeorological observations to monitor the precipitation process provided by an automatic station gauge network, weather radar, or satellite system. Gauges have two primary functions—sensing and communicating. Sensing involves the detection of an "event," which is the smallest unit of measurement desired, and communicating involves reporting the event to a user location. The most common and economic rain gauge is the telemetric tipping bucket gauge as shown in Fig. 2. The tipping bucket gauge consists of a collector funnel with a knife edge that diverts water. The mechanism is so designed that one alternate tip of the bucket occurs for each 0.01 in. (0.0254 cm) of rainfall accumulation. A magnet is attached to the tipping bucket, which, as the bucket tips, actuates a magnetic switch to signal the accumulation to the data logger communicating through the transmitter (National Weather Service (NWS), 2012). The same gauge station that reports rainfall can also be interfaced with other sensors to collect and communicate information such as stream level and temperature. Streamflow records from stream gauges are also needed as a reference to calibrate watershed models, verify forecasts from models, or trigger alarms

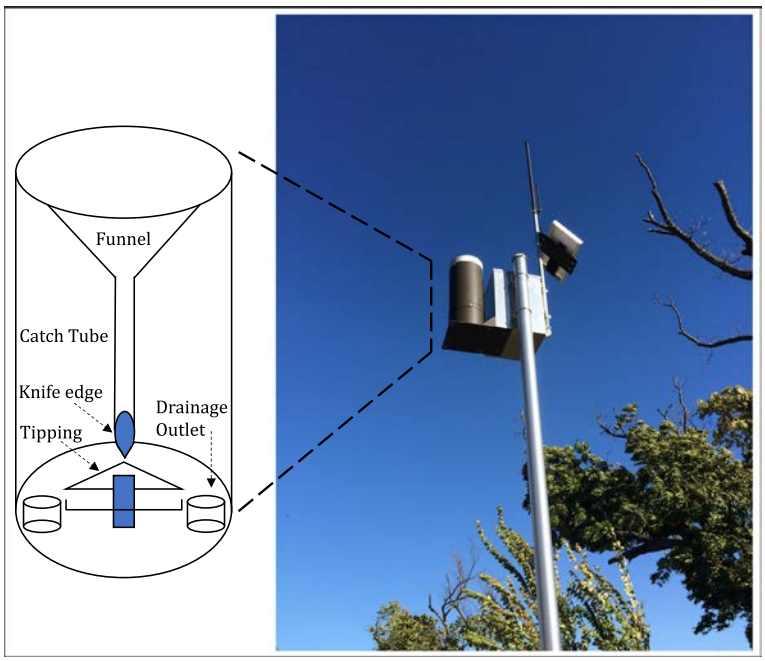

FIG. 2

A telemetric tipping bucket rain gauge and its schematic design graph located near Belt Line Road in Grand Prairie, Texas.

when flooding is impending or occurring. One of the most common ways of measuring the relative height of streams is through an underwater tube contained in the stream gauge. The level of pressure is measured to calculate the height of the water above the tube. Stage values can be converted into discharge values if a rating curve has been established for the stream at that location (Nielsen and Norris, 2007). In the United States, stream gauges are primarily operated and maintained by the USGS, but most are funded in partnership with one or more of about 1400 federal, state, and local agencies, or organizations.

For FWSs, data from rain and stream gauge are being transferred through satellite signals and processed in a nearly real-time mode on software platforms. The automated local evaluation in real-time system is the most widely adopted platform. It is a common FWS configuration that consists of automated event-reporting meteorological and hydrologic sensors, communications equipment, and computer software and hardware. Systems typically display both textual and graphical information and can be used in combination with other data to show geospatial flood inundation (National Weather Service (NWS), 2012).

Remote sensing precipitation measurement methods

Precipitation measurements from rain gauges are relatively accurate at the point scale (Villarini et al., 2008). However, the configurations of rain gauge network density and instrument precision can introduce great uncertainties to flood prediction. In addition, the gauge network can only cover relatively small areas instead of an entire basin (Michelson, 2004) and needs to be interpolated to fill the coverage gap (Ly et al., 2013). Radar is able to cover a larger spatial area than a point-based rain gauge network. Radar techniques have assisted weather predictions for over 50 years and have been used in hydrological applications for around two decades. In the United States, since 1994, the NWS has installed the Next Generation Weather Radar (NEXRAD) system with 160 WSR-88D radars across the United States with their coverage shown in Fig. 3 (NOAA National Center of Environmental Information (NCEI), 2019). Fig. 3A shows the NEXRAD radar network coverage for the United States continent, and Fig. 3B shows the reflectivity of Hurricane Harvey (2017) when making landfall. For NEXRAD the rain rate is converted from the composite reflectivity maps using the common Z (intensity)-R (reflectivity) relation. For more than two decades the NEXRAD precipitation products have undergone a series of improvements and been applied to many hydrometeorological studies, hydrologic analysis research, remote sensing validation, and flood forecasting operations (Krajewski and Smith, 2002). NEXRAD data are viewed as one of the most reliable and stable rainfall information sources in the flooding operations and research communities. For example, the San Antonio River Authority uses a 15-min raw NEXRAD product as the precipitation input to a probability-distributed model to simulate runoff for a real-time FWS in Bexar County, Texas. Radar technology has also been used in many other countries as the main source of precipitation estimates for input in hydrological modeling of FWSs (Moore et al., 2005; Liechti et al., 2013).

Along with radar precipitation measurement, satellite rainfall products have also been applied in many different flood-related studies and flood warning operations on regional and national levels (Nikolopoulos et al., 2013). Almost 25 years have elapsed since satellite data were first used in attempts to estimate rainfall. Satellite measurements of precipitation have made considerable advancements during the last two decades, mainly through the Tropical Rainfall Measuring Mission, the Global Precipitation Measurement mission, and the recent Geostationary Operational Environmental Satellite

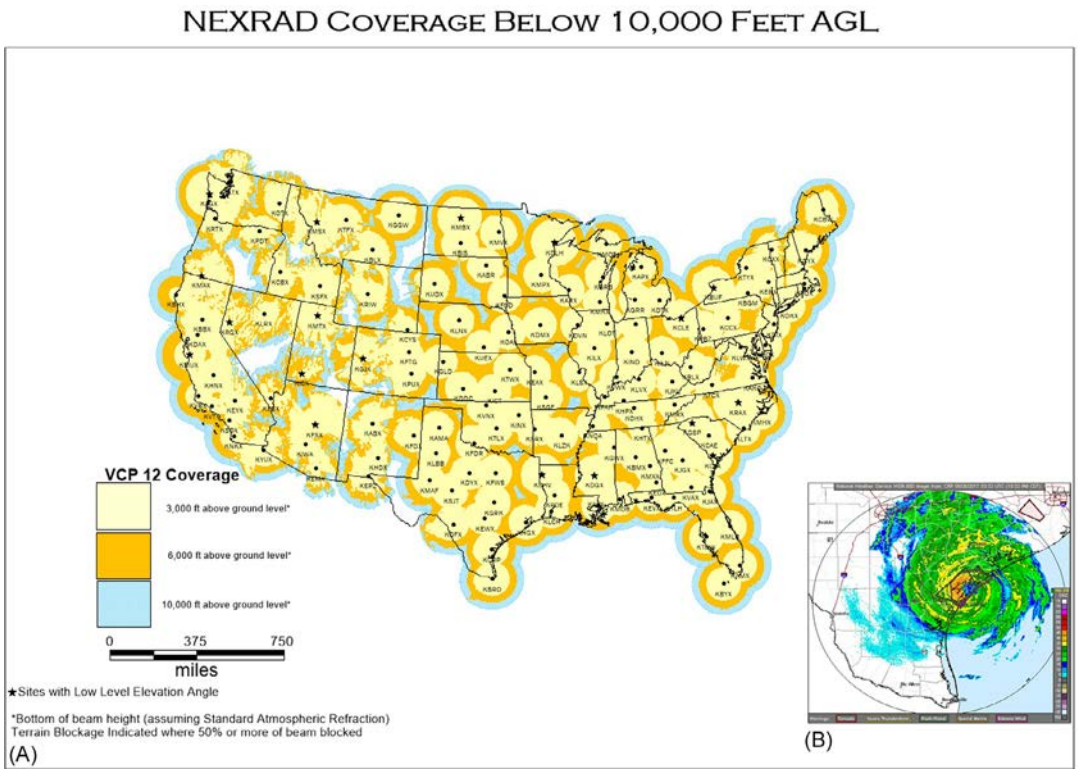

FIG. 3

(A) NEXRAD Radar network coverage below 10,000 ft AGL in CONUS and (B) RADAR base reflective map during Harvey.

Part (A) from National Weather Service [NWS], https://roc.noaa.gov/WSR88D/Maps.aspx, Accessed 3 July 2020 and (B) from NWS Corpus Christi, Texas, https://radar.weather.gov/radar.php?rid=CRP&product=NOR&overlay=11111111&loop=no, Accessed 28 August 2017.

(GOES) mission (Kuligowski et al., 2016, Chad et al., 2018, National Aeronautics and Space Administration (NASA), 2020a, b).

Hydrologic and hydraulic modeling

To provide lead time for the warning and potential damages estimation from floods, engineers and scientists typically use hydrologic and hydraulic (H&H) software packages for the modeling processes as shown in Fig. 4. Using precipitation data from different sources along with evaporation and infiltration processes incorporated, hydrologic and hydraulic models can simulate rainfall-runoff processes to predict the river water levels and flooding extent in a well-tested way for reducing the flooding. A hydrologic model (either lumped or distributed) normally involves two main components: a rainfall-runoff estimator and a routing scheme. Water is routed using a routing equation in lumped models

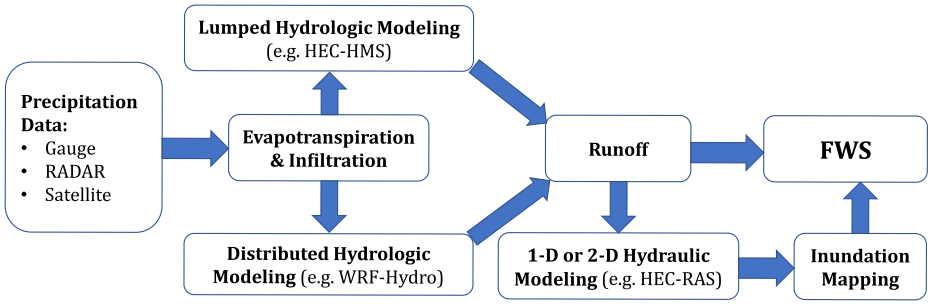

FIG. 4

Hydrologic and hydraulic modeling processes flow chart for FWS.

(Sacramento Soil Moisture Accounting [SAC-SMA], hydrologic modeling system [HEC-HMS]) or through a cell "conceptual" channel system in distributed models (Weather Research and Forecasting Model Hydrological modeling system [WRF-Hydro]). Then, river and channel hydraulics are simulated through hydraulic models such as HEC-RAS and Gridded Surface/Subsurface Hydrologic Analysis (US Army Corps of Engineers), MIKE FLOOD (Danish Hydraulic Institute), BreZo (Sanders & Begnudelli), or LISFLOOD-FP (University of Bristol).

The SAC-SMA model of the National Weather Service River Forecast System has typically been applied as a lumped model to simulate runoff within a basin. Among all H/H models, the SAC-SMA is a well-tested continuous soil moisture accounting model with spatially lumped parameters. The model divides the basin into lower and upper zones at different depths and defines the distribution of moisture, that is, tension water components (driven by evapotranspiration and diffusion) and free water components (driven by gravitational forces) in each of these two zones through a set of parameters. The model uses precipitation and evapotranspiration time series input, along with parameters on soil moisture states and the basin's relative permeability to estimate the amount of water that enters, is stored in, and leaves the basin (National Weather Service (NWS), 2016). The SAC-SMA model is currently used by different NWS River Forecasting Centers as the main tool to predict flow rate during flood forecasting operation.

The WRF-Hydro was developed by NOAA as a community-based, open source, model coupling framework designed to link multiscale process models of the atmosphere and terrestrial hydrology. It is both a standalone hydrological modeling architecture and a coupling architecture for coupling with atmospheric models. The model is able to provide a land-atmosphere modeling capability and prediction of major water cycle components such as streamflow and inundation across different spatial and temporal scales (Gochis et al., 2020). WRF-Hydro model output can supply forecasters and decision makers with locations and timing of rapid river stage increase as well as the duration of high waters and inundation while accounting for landscape dynamics essential to flood risks. The model has been used by the National Water Center, serving as the core engine for the new National Water Model (NWM).

The HEC-HMS, a lumped hydrologic model, is designed to simulate the complete hydrologic processes of dendritic watershed systems. The software includes many traditional hydrologic analysis procedures such as infiltration, unit hydrographs, and hydrologic routing. It includes procedures necessary for continuous simulation, including evapotranspiration, snowmelt, and soil moisture accounting. HEC-HMS is widely used for flood frequency studies, engineering design applications, environmental

studies, systems operation, and flow forecasting (Hydrologic Engineering Center (HEC), 2013). The Hydrologic Engineering Center-River Analysis System (HEC-RAS) is an integrated package that simulates the hydraulics of water flow through natural rivers and other channels. The basic computational procedure of HEC-RAS for steady flow is based on the solution of the one-dimensional energy and momentum equation. For unsteady flow, HEC-RAS solves the one-dimensional dynamic Saint Venant Equation using an implicit, finite difference method. It is capable of modeling subcritical, supercritical, and mixed flow regime along with the effects of bridges, culverts, weirs, and structures. In HEC-RAS Version 5.0, two-dimensional hydrodynamic routing within the unsteady flow analysis was added to the HEC-RAS packages (Hydrologic Engineering Center (HEC), 2016). Hydrologic Engineering Center-Real Time Simulation is the public version of the Corps Water Management System, which serves as a robust platform to provide hydrologic and hydraulic simulations in real time by integrating hydrologic simulation from HEC-HMS and hydraulic simulation from HEC-RAS. As shown in Fig. 5, it is a comprehensive data acquisition and HEC-HMS for short-term decision support of water control operations or flood forecasting in real time (Hydrologic Engineering Center (HEC), 2017).

Apart from traditional hydrologic and hydraulic models, many DD models have also emerged and been used in flood-related studies, such as statistical models for flood frequency analysis and Bayesian forecasting models for predicting long-term floods. With the recent development of machine learning (ML) models, DD methods demonstrate vast potential to handle short-term prediction along with an

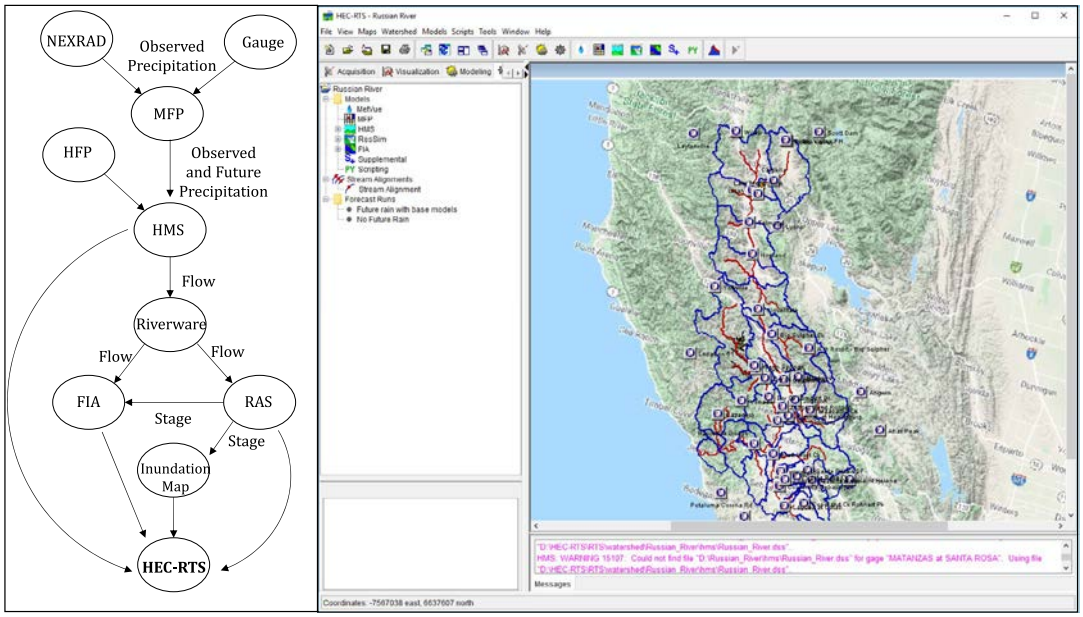

FIG. 5

(A) HEC-RTS schematic data flow and (B) User interface from an example project of the Russian River.

From HEC-RTS software, 2020.

improvement in complexity of the usage, computation cost, and robustness of the method. Many ML algorithms, for example, artificial neural networks, support vector machine, and decision tree (DT), are reported to be effective for both short-term and long-term flood forecasts that can be applied in the flood forecasting applications (Mosavi et al., 2018; Shen, 2018).

With H/H computation models providing a flood forecast in terms of peak, timing and magnitude, and real-time precipitation measurements from gauge network, radar, or satellite, FWSs are able to function as a real-time communication tool to disseminate the critical forecast information to government and the general public. To help readers learn FWS methodology and technology in real examples and understand FWSs in a comprehensive way, several operational FWSs in the United States are introduced in the following sections, including the observational flood monitoring systems, the radar-based FWSs, and the DD FWSs.

Flood monitoring system

Despite appearing relatively antiquated with the recent advances of weather forecast systems, gauging networks are still the most common flood warning practice in many areas. Typically, these systems consist of a network of interconnected stream and rain gauges and automatically disseminate alerts when weather parameters, flow volumes, or river stages exceed prespecified threshold values. In the United States, one of the principal gauge-based FWSs is the USGS's National Water Information System (NWIS), which is a comprehensive and distributed application that supports the acquisition, processing, and long-term storage of water data. Nationally, the system displays real-time, recent, and past streamflow conditions at 10,526 sites nationwide (United States Geological Survey (USGS), 2020). The data relayed through the GOES system are processed automatically in near real time, and in many cases, current data are available online within minutes. On a web graphical interface (https://waterdata.usgs.gov/nwis/rt), a map of colored dots depicts streamflow conditions as a percentile, which is computed from the period of record for the current day of the year. For individual gauges, users can see the time-series plot of discharge over the past 7 days or any other customized range that is available. Water Alert, a real-time, personalized flood alert system (FAS), is available on the NWIS as well. Users are able to select specific gauges and register to receive notification parameters such as rainfall accumulation and gauge height (stage). The system can email or text message daily or hourly updates of the gauge as well as send emergency notification when parameter values exceed a user-defined threshold.

Compared to the national water level monitoring program, local flood warning programs can be extremely effective with close communication between local agencies and their residents. Local programs are most valuable where flooding occurs quickly following heavy rains. These programs have also been credited with preventing unnecessary evacuations and other overreactions in cases where floods threatened but did not occur. In particularly flood-prone urban areas, existing USGS infrastructure is often augmented with additional gauges in a localized FWS. For example, a monitoring network known as the Harris County FWS in Houston, Texas, has a total of 175 local gauges that are operated and maintained by the Harris County Flood Control District (HCFCD). Gauge data are made public through a graphical user interface on the HCFCD website (https://www.harriscountyfws.org/?View=full). Fig. 6 shows an example of the website snapshots during Hurricane Harvey (2017). Compared with the USGS NWIS, not only can local FWSs provide increased data resolution, but also the

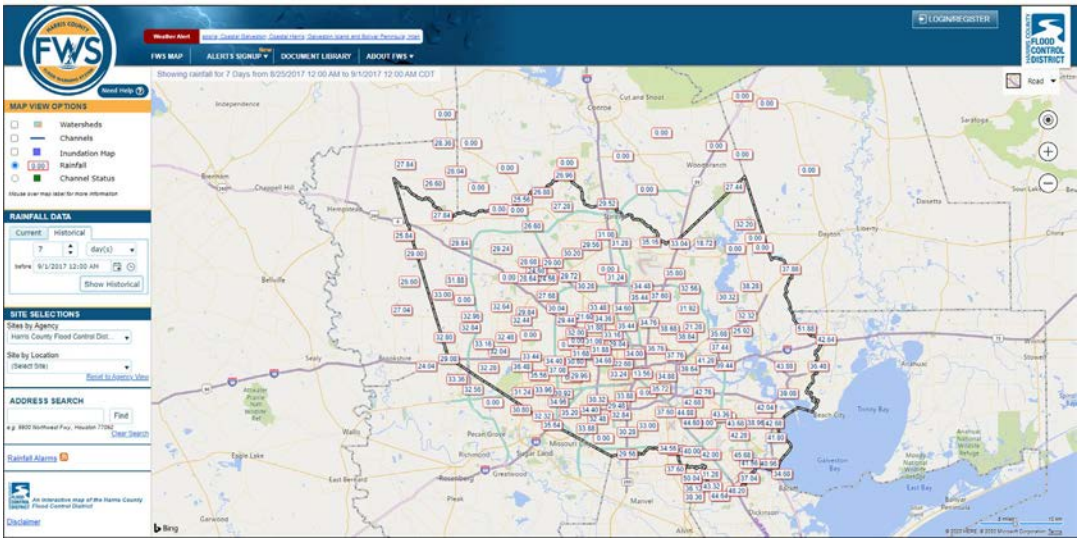

FIG. 6

The HCFCD Flood Warning System snapshot during Hurricane Harvey (2017).

From Harris County Flood Control District [HCFCD], https://www.harriscountyfws.org/, Accessed 25 June 2020.

ability to tailor gauge placements to vulnerabilities in each urban area. Selecting proper station locations ensures that critical infrastructure is monitored, allowing emergency officials to respond more intelligently and efficiently to an emerging crisis.

The HCFCD Flood Warning System offers an alert feature that allows residents to subscribe to receive email and/or text alerts that report near real-time rainfall and water levels. Residents can customize alerts and notifications in their particular areas of interest. The inundation mapping feature of the HCFCD Flood Warning System provides current channel inundation information transmitted by water level gauge locations, which have been used to produce estimated inundation extents for several storm events. The technology behind the inundation mapping tool runs continuously to provide live inundation extents during a flood event to depict the current flood extent.

Although not on the forefront of flood warning technology, river gauge-based FASs are still being used extensively, providing valuable advisory of the locations of occurring or imminent flood conditions, establishing a flood warning function baseline. The networks serve important roles in many flood management organizations.

Radar-based FWSs

Compared with the river gauge flood monitoring system, the radar-based FWSs provide a higher spatial resolution, increased coverage, and improved lead time. However, there are still many uncertainties and inaccuracies in the radar products. The radar-based FWSs can provide a relatively sufficient lead time for flood emergency management with a capability of updating forecasts in a refined computation

interval for a spatial coverage. In this section, examples of three scales of radar-based FWSs are introduced: the continental level (NWM), state/regional level (Iowa Flood Information System [IFIS]), and city/community/watershed level (Texas Medical Center-Rice University Flood Alert System).

National water model

The NWM is a new tool that simulates and forecasts how water moves throughout rivers and streams in the United States. The NWM uses data from more than 8000 USGS gauges to simulate conditions for 2.7 million locations in the contiguous United States. It simulates the water cycle with mathematical representations of the different processes on an hourly forecast. This complex representation of physical processes such as snowmelt and infiltration and movement of water through the soil layers varies significantly with changing elevations, soils, vegetation types, and a host of other variables. In addition, extreme variability in precipitation over short distances and times can lead to the response in rivers and streams to change quickly.

The core of the NWM system is the National Center for Atmospheric Research-supported WRF-Hydro model. WRF-Hydro ingests forcing from a variety of sources, including two different radar precipitation datasets. Forcings include Multi-Radar/Multi-Sensor System precipitation data, Stage IV Multisensor Precipitation Estimator radar gauge-observed precipitation data, and Numerical Weather Prediction (NWP) forecast data. Considering the large uncertainties in the NWP forecast, the radar data are the main operational precipitation input. For the land-surface process, WRF-Hydro is configured to use the Noah-Multiparameterization Land Surface Model. Separate water routing modules perform diffusive wave surface routing and saturated subsurface flow routing on a 250-m grid, and Muskingum-Cunge channel routing down National Hydrography Dataset (NHDPlusV2) stream reaches. River analyses and forecasts are provided across a domain encompassing the CONUS and additional hydrologically contributing areas as shown in the user interface in Fig. 7. The NWM is run in six CONUS configurations: Standard Analysis (3-h look-back); Extended Analysis (28-h look-back); Long-Range Analysis (12-h look-back); Short-Range Forecast: 18-h deterministic (single value) forecast; Medium-Range Forecast: seven-member ensemble forecasts out to 10 days; and Long-Range Forecast: 30-day four-member ensemble forecast. The USGS streamflow observations are assimilated into the analysis and assimilation configuration. All analyses and forecast configurations benefit from the inclusion of over 5000 reservoirs as one of the key features in NWM (Office of Water Prediction (OWP), 2020).

Iowa flood information system

At the state level, the IFIS has been used as a mature product and major FWS tool in the State of Iowa for over the past 10 years. During this time, development has been continuous and infused with the state-of-the-art technologies. The data analytics and visualization capabilities along with critical flood information in the IFIS have supported flood risk management and disaster preparedness and response efforts in Iowa. The IFIS is the real-time flood warning tool that Iowa Flood Center (IFC) uses for providing the real-time access to up-to-the-minute data on river and stream levels, precipitation, flood inundation maps, flood alert, and communicating flooding risks with communities. Over 500 bridge-mounted stream-stage sensors are being monitored in the IFIS to keep track of water levels in real time as a flood warning module. Hydrodynamic modeling software is used to simulate river and floodplain flows for conditions ranging from near bank-full to above the 0.2% annual chance flood event as flood

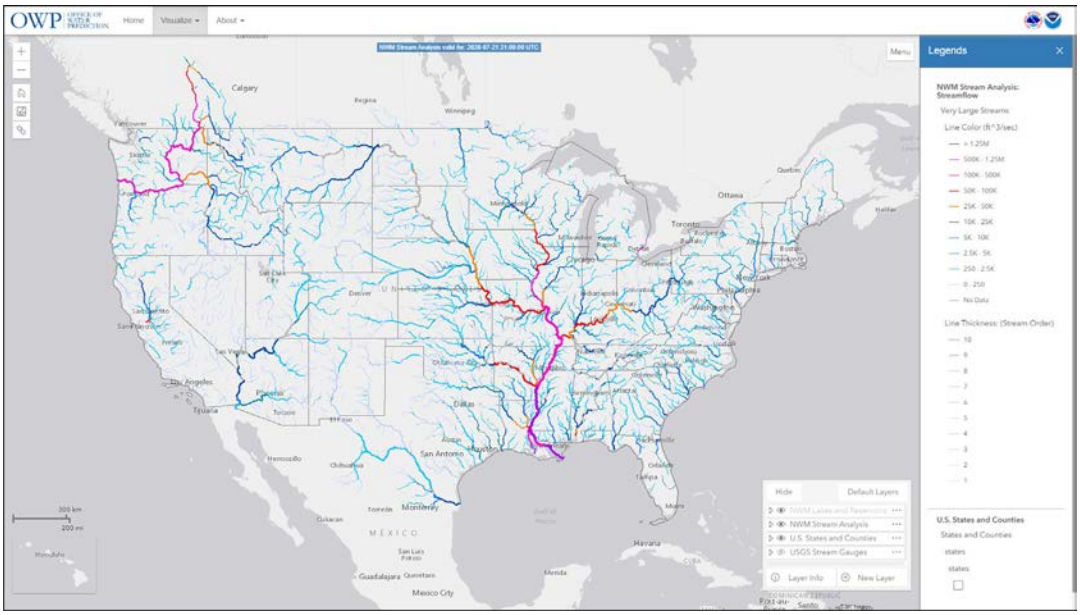

FIG. 7

User interface of National Water Model.

From Office of Water Prediction [OWP], https://water.noaa.gov/map, Accessed 2 July 2020.

inundation maps, which are displayed on the IFIS associated with various rainfall levels. The inundation models are validated using measured water surface profiles and high-water marks.

Major components of the IFIS include rainfall and evapotranspiration inputs and a rainfall-runoff distributed model with streamflow routing parameters that were calibrated using historical flood events. Streamflow predictions are communicated to the public through IFIS. The forecasting system makes hydrologic predictions for all streams in Iowa, whereas the IFIS makes predictions for some 2000 points on the river network. The statewide rainfall intensity and accumulation maps are updated every 5 min, processing Level II data from the seven NEXRAD radars covering Iowa. For rainfall-runoff process, the IFIS mainly focuses on the hillslope runoff process. The real-time forecasting program is a mixture of C and Python and performed using the IFC's ASYNCH numerical solvers, and PostgreSQL's library is used for access to the IFC Central Database. Every 15 min, rainfall estimates are pulled from the IFC Central Database and the corresponding 10-day streamflow are forecasted (Demir et al., 2018; Krajewski et al., 2017).

Texas Medical Center-Rice University flood alert system

Although the FWSs on a regional or national level are able to provide accurate and timely flood warnings at a county level for most areas in the nation, they have difficulties in providing precise warning information for small urban catchments due to the rapid runoff, limited response time, and system effectiveness for complex computer simulations. For especially time-sensitive, flood-prone critical

infrastructure within urban areas, a customized watershed level FWS is greatly demanded due to its increased effectiveness. One of such FWS has been in operations for a highly urbanized watershed in Houston, Texas, which has been credited with saving scores of lives and preventing millions of dollars of damage. This flood alert system (FAS) was developed by the Texas Medical Center (TMC) and Rice University for Brays Bayou (334 km^2), which is one of the most urbanized watersheds in Texas. The system has been using NEXRAD radar to provide flood warning messages for several critical infrastructures in the watershed for over 20 years and has successfully predicted streamflow with reliable lead time for flood warnings. The main function of the FAS is to provide flood warnings for a highly urbanized subwatershed (11.6 km^2) of Brays Bayou called Harris Gully, which contains many high-value entities, including Hermann Park, Rice University, and TMC.

During the 20 years of operations, the FAS has evolved into its fifth generation (FAS5), which is a mature product that has gone through rigorous evaluations. By employing gauge calibrated radar rainfall data into the models (Vieux and Vieux, 2005), the FAS5 is able to provide TMC emergency personnel with more accurate flow estimates and flood forecasts with 2–3 h of lead time. The FAS is also one of the pioneering flood forecasting tools that can provide hydraulic prediction information through a Flood Plain Map Library. Over the past decades, the FAS (i.e., FAS5 [TMC]) has been found to better predict shapes, peak values, and peak timings for more intense storm events compared with small and/or moderate events (Bedient et al., 2003; Fang et al., 2008; Fang et al., 2011; Fang et al., 2014). Table 1 summarizes the history of FAS upgrades in the past 20 years.

The system has been tested through many different major flood events in Houston, including Tropical Storm Allison in 2001 (Vieux and Bedient, 2004) and Hurricane Harvey in 2017. During this off-the-chart event, the FAS4 was able to provide the prompt forecasted information, past rainfall, and real-time monitoring. It served as a key information source to decision makers and emergency personnel. Throughout the entire event, the system was operating on a 5-min frequency and updating the simulated peak and estimated peak moment for Brays Bayou. The system continued simulating the watershed hydrologic response and providing essential information to the emergency management team. Fig. 8 demonstrates the satisfactory performance of FAS4 during Hurricane Harvey based on the snapshots of the simulated hydrographs recorded at the six time steps compared with the observations. According to the TMC's President and CEO, Bill McKeon, FAS4 provided reliable, prompt, and accurate warning information to the TMC, allowing the hospitals to shut their floodgates and evacuate basement garages before the flood hit (The Dallas Morning News, 2017). This helped the TMC maintain the power system and

Table 1 FAS update history in the past 20 years.

Time	Updates
1997	FAS1 initiated with Rating Curve method
2003	FAS2 updated with hydrologic simulation (HEC-1)
2004	Radar technology implemented in FAS2
2008	FAS3 updated with new hydrologic parameters (HEC-HMS)
2008	FAS3 updated with a Floodplain Map Library (FPML)
2016	FAS4 updated with a mobile version and an updated hydrologic model
2017	FAS4 tested on Hurricane Harvey
2020	FAS4 updated to FAS5

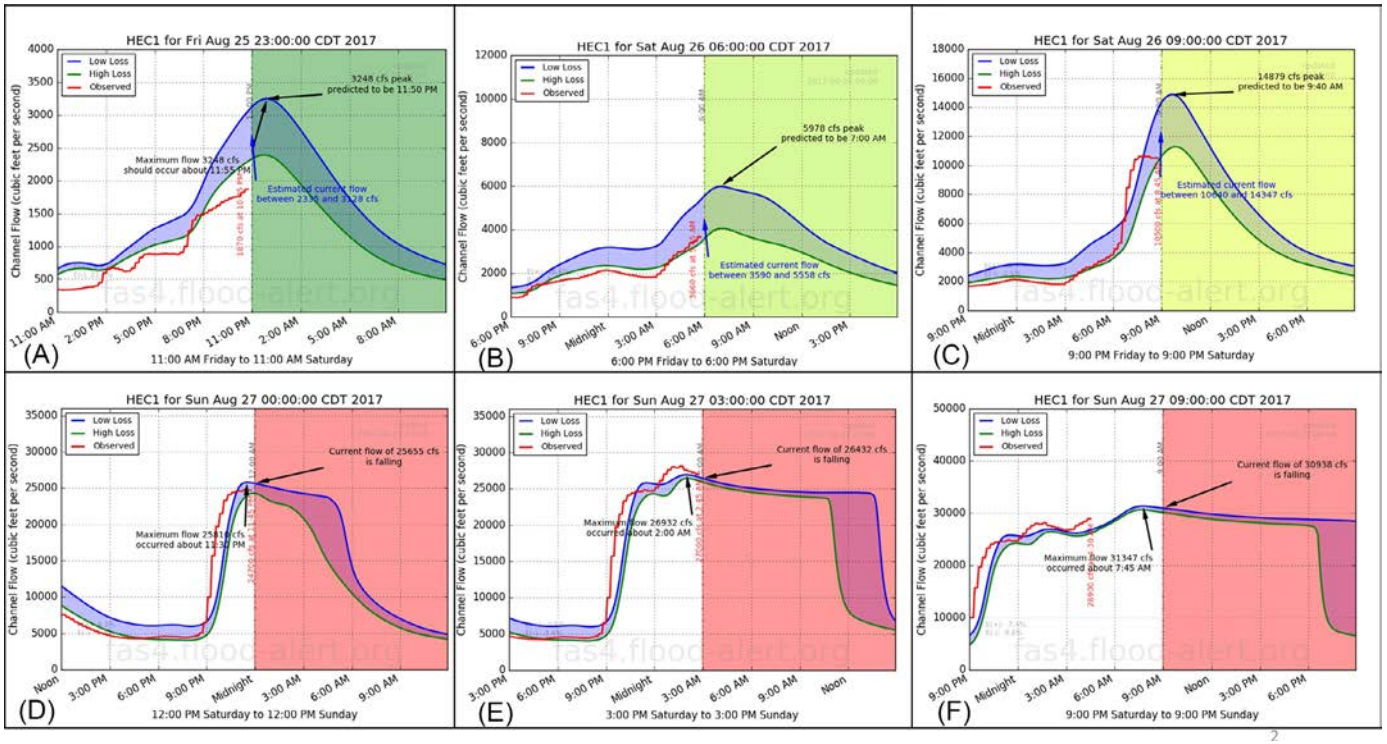
HEC1 for Fri Aug 25 23:00:00 CDT 2017
Low Loss
High Loss
Observed
3248 cfs peak predicted to be 11:50 PM
Maximum flow 3248 cfs should occur about 11:55 PM
Estimated current flow between 2330 and 3228 cfs
Channel Flow (cubic feet per second)
(A)
11:00 AM Friday to 11:00 AM Saturday
HEC1 for Sat Aug 26 06:00:00 CDT 2017
5978 cfs peak predicted to be 7:00 AM
Estimated current flow between 3590 and 5558 cfs
(B)
6:00 PM Friday to 6:00 PM Saturday
HEC1 for Sat Aug 26 09:00:00 CDT 2017
14879 cfs peak predicted to be 9:40 AM
Estimated current flow between 10440 and 14347 cfs
(C)
9:00 PM Friday to 9:00 PM Saturday
HEC1 for Sun Aug 27 00:00:00 CDT 2017
Current flow of 25655 cfs is falling
(D)
12:00 PM Saturday to 12:00 PM Sunday
HEC1 for Sun Aug 27 03:00:00 CDT 2017
Current flow of 26432 cfs is falling
Maximum flow 26932 cfs occurred about 2:00 AM
(E)
3:00 PM Saturday to 3:00 PM Sunday
HEC1 for Sun Aug 27 09:00:00 CDT 2017
Current flow of 30938 cfs is falling
Maximum flow 31347 cfs occurred about 7:45 AM
(F)
9:00 PM Saturday to 9:00 PM Sunday

FIG. 8

FAS4-simulated hydrograph vs. observation at six time step during Harvey.

From Rice University/TMC Flood Alert System [FAS], http://fas4.flood-alert.org/#Home:Home, Accessed 3 September 2017.

continue caring for patients throughout the record rainfall caused by Hurricane Harvey. Certainly, accurate and reliable performance observed during Hurricane Harvey (2017) has proven that FAS4 is essential to local officials in this location. The technology and methodology used in FAS have inspired communities to implement similar tools and systems in other flood-prone areas over the nation.

Data-driven FWS

Compared with traditional hydrologic and hydraulic models, DD methods show significant capability to simplify the complex atmosphere-land surface-ground water interactions and provide insights directly from the data. The methods are similar to empirical functions and do not reflect on physics-based phenomenon, but they do provide several benefits: the setup and update processes are automatic; small number of physical parameters of watersheds are required; and outputs can reach high accuracy with a low computation power requirement. For many small communities that cannot afford resources for a highly integrated, complex FWS, DD-based FWSs show great potential for providing vital flood forecasting information at a relatively low cost.

Traditional DD approaches such as the nomograph and rating curve methods are useful to provide flood warnings, but they are not suitable and capable of handling large watersheds with varied characteristics. Fortunately, recent advances of ML in nonlinear interactions and computational complexity can enhance the DD approach of FAS flood forecasting. One such example of the FAS improved by the ML algorithm is a system developed for White Oak Bayou, one of the urban watersheds in Houston, Texas. The system uses eXtreme Gradient Boosted (XGBoost) DT models as the core engine. Advantages of this core engine are that the input variables do not need to be scaled to a common range and that the iterative nature of the model fits the extreme event nature of stage prediction, where traditional models tend to predict extreme events poorly without particular care.

The system is developed by taking advantage of a combination of 32 rain gauges and 12 stage gauges with a 5-min time interval records from 2010 to 2019 as the input. The training and validation sets are 70% vs. 22.5% of the total numbers of the rainfall events with Hurricane Harvey (2017) labeled as validation data. The overfitting issues are controlled with a test dataset (7.5% of the whole set). Different sets of predetermined lead time (5, 10, … to 120 min) forecast models are tested with the 30-min model predictions reaching a root-mean-square error of 0.810 and a KGE of 0.996 for one flood event in the validation set as shown in Fig. 9A. This is more than sufficient for confidence in the model's ability to predict 30 min into the future. A limitation of a fixed 30-min forecast model is that predictions can only be reliably made with this model for exactly 30 min ahead. To overcome this limitation, a combination of forecast models are trained with different forecast windows and can be used jointly as a comprehensive FAS, as an example shown in Fig. 9B. In a comprehensive system, all models make predictions simultaneously in real time, and then, if one or more models predict stage above some critical stage threshold, the reported system's lead time is the smallest forecast window out of the models that predict above the threshold. This combination approach is justified because predictions closer to the current are generally more accurate, have less variability, and require greater urgency than predictions further into the future. By combining multiple ML models into a comprehensive system, a variable amount of lead time until a flood event can be calculated and reported in real time. Although more research is still required for ML models to surpass physics-based models in terms of raw prediction ability, the authors believe that ML models like XGBoost are at present a valuable tool and show great potential to aid the decision-making process of emergency managers in flood alert prediction.

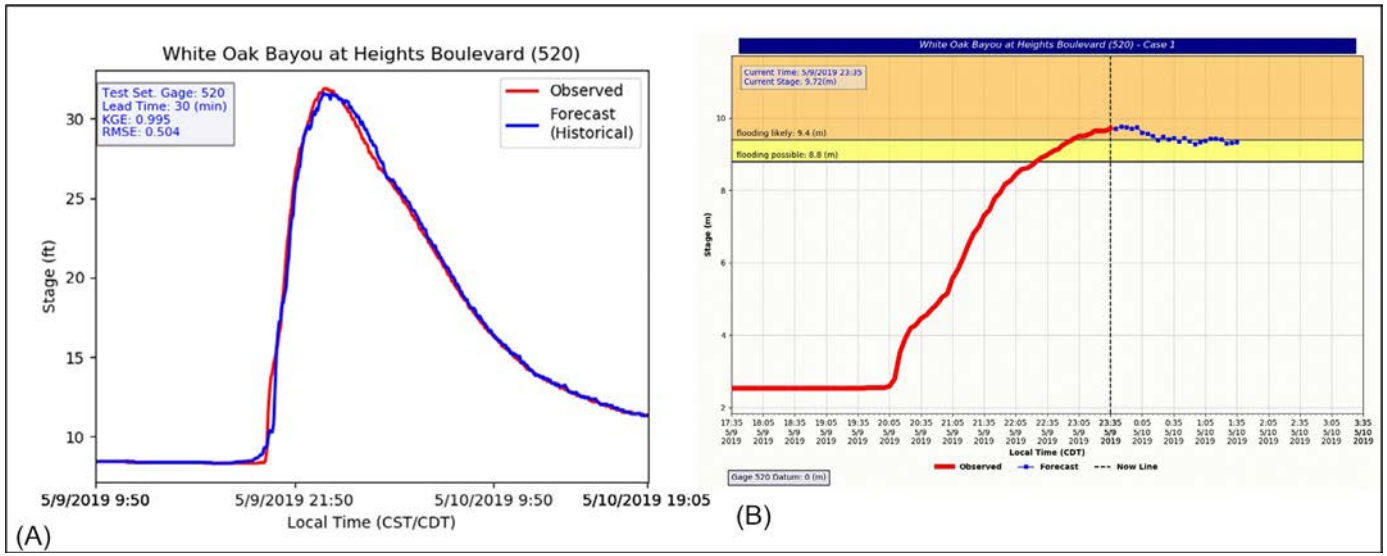

FIG. 9

(A) Machine Learning Flood Warning System (FWS) 30-min forecast plot vs. observation and (B) Different lead time forecasts combined operational FWS in White Oak Bayou, Houston, Texas.

Communications

Communication is also one of the main components of FWSs, and robust hazard communication strategy is possibly the most cost-effective countermeasure against natural hazards (United Nations International Strategy for Disaster Reduction (UNISDR), 2006). During the last two decades, flood management has also evolved, with a greater responsibility now placed on at-risk communities to better understand their risk and take protective actions to develop flood resilience both before and during flooding events. Consequently, communicating flood risk has become an increasingly central part of developing flood resilience and for both long-term and short-term FWSs. The government agencies are still striving to improve how they communicate threats to the public who often form the weak link and are also the most vulnerable group in flood mitigation. Flood risk communication specifically in FWSs encompasses two phases: (1) identifying areas at risk of flooding and (2) letting those at risk know when flooding is likely to occur. Both phases are crucial to helping those at risk prepare for, anticipate, and act to lessen the consequences of flood events. Flood inundation maps have shown enormous potential in flood risk communication when used properly for FWS applications. During flooding, there are also several general rules to focus on to improve efficiency and avoid confusion: simplicity, accuracy, and positiveness (Federal Emergency Management Agency (FEMA), 2019). With proper communication between government agencies, affected groups, and journalists, the flood risk and damages could be considerably reduced (Rollason et al., 2018; Associated Programme on Flood Management, 2015).

Challenges and future of FWSs

Regarding the anticipation of floods, the general flood warning community faces several difficulties for future improvements, including technical, financial, and social challenges. There are various technical challenges at national, regional, and local levels to operating FWSs: data collection and integration, synthesis, management; the hydrologic modeling process; warning dissemination and communication networks; and others. One of the most common technical issues is the performance of the models used for flood forecasting. In operational flood forecasting, modeling-related challenges involve improving the accuracy of forecasts by accounting for uncertainties in input data, modeling approaches, model simplifications, and the output quantification. Nearly half of the flood forecasters (survey responses) mentioned that the models they use for producing early warnings were not accurate or advanced enough for the flood forecasting purpose. The erroneous or false alarms can affect public perception of magnitude and timing of floods, leading to missed warnings of flood disasters. Inadequate and poor management of hydrological networks and/or temporary shutdown due to equipment damage, weather, or financial issues is another main challenge that adversely impacts the performance of FWSs (Perera et al., 2019).

Many technical issues faced by operational systems are related to financial challenges. Funding limitations challenge the sustainability of FWSs by causing discontinuous operations, reduced budget for upgrading or advancements, and insufficient recruitment and training of staff and personnel. Even with an efficient FWS, losses will only be maximally mitigated if the communities at risk have adequate infrastructure to receive warnings. Hence the strategies in place and regular organizational awareness programs such as drills, seminars, and trainings in preparedness and evacuation are crucial,

especially in developing and least-developed countries where highly vulnerable communities have low literacy rates (Perera et al., 2019).

Despite the challenges outlined, many advancements in the technologies and flood awareness and preparedness program help improve FWSs to make better predictions and mitigate flood losses. With improved data quality and availability, better data management systems, incorporating and integrating advanced technologies and methods into "basic" FWSs, and closer coordination between agencies and different levels of governments, FWSs show a promising future in mitigating and preventing flood damages.

Summary and conclusions

Among any natural disaster events, flooding presents the greatest danger to infrastructure, private property, and public safety. FWSs, of one type within nonstructural flood risk management methods, have been widely adopted worldwide at different levels of spatial scale to reduce the risk of damage and loss of lives in the case of an impending flood as a preventive measure. Over the past two decades, FWSs have evolved to meet the specific needs of different clients, regions, and nations, differing significantly in complexity, size, and scope. FWSs range from basic gauge monitoring networks to complex forecasting platforms that employ radar and satellite precipitation data and computer modeling techniques to produce lead times of flood spanning from hours to days. Along with introducing several real examples of FWSs at various levels, this chapter establishes a broad overview of basic concepts of FWSs, gauge networks, rainfall measurements, and hydrologic and hydraulic computer modeling.

When nature is uncooperative, the best approaches are to take both defensive approaches such as building traditional flood potential infrastructure and proactive approaches such as using and updating FWSs based on most-up-to-date information and technology. Structural solutions alone are not able to solve flooding problems because it is impossible to foresee the long-term future and unrealistic to keep increasing the design standard of flood protection. Although flooding occurrences will inevitably increase, the best option to mitigate potential damages to life and properties is to obtain accurate and timely warnings for emergency management officials. Although many existing FWSs vary in size, complexity, and forecasting ability, they are all designed to provide critical warnings to communities as great life-saving tools. With recent advances in computer technologies, hydrologic models, forecast accuracy, and lead time, the authors believe that a continued investment in and global adoption of FWSs will be a sustainable method to minimize flood damages to the greatest extent.

References

Ashley, S.T., Ashley, W.S., 2008. Flood fatalities in the United States. J. Appl. Meteorol. Climatol. 47, 805–818. https://doi.org/10.1175/2007JAMC1611.1.

Associated Programme on Flood Management, 2015. The Role of The Media in Flood Management. https://www.floodmanagement.info/publications/tools/Tool_22_The_Role_of_the_Media_in_Flood_Management.pdf.

Bedient, P.B., Holder, A., Benavides, J., Vieux, B., 2003. Radar-based flood warning system applied to TS Allison. ASCE J. Hydraul. Eng. 8 (6), 308–318.

Centre for Research on the Epidemiology of Disasters (CRED), 2019. Natural Disasters Report 2018. https://reliefweb.int/report/world/flooding-affected-more-people-2018-any-other-disaster-type-report-shows.

Chad, F., Ghebreyesus, D., Sharif, H.O., 2018. Assessment of the performance of satellite-based precipitation products for flood events across diverse spatial scales using gssha modeling system. Geosciences 8 (5), 186. https://doi.org/10.3390/geosciences8060191.

Collins, M., Knutti, R., Arblaster, J., Dufresne, J.-L., Fichefet, T., Friedlingstein, P., Gao, X., Gutowski, W.J., Johns, T., Krinner, G., Shongwe, M., Tebaldi, C., Weaver, A.J., Wehner, M., 2013. Long-term climate change: projections, commitments and irreversibility. In: Stocker, T.F., Qin, D., Plattner, G.-K., Tignor, M., Allen, S. K., Boschung, J., Midgley, P.M. (Eds.), Climate Change 2013: The Physical Science Basis. Cambridge University Press, Cambridge, United Kingdom and New York, NY, USA. Contribution of Working Group I to the Fifth Assessment Report of the Intergovernmental Panel on Climate Change.

Demir, I., Yildirim, E., Sermet, Y., Muhammed, A.S., 2018. FLOODSS: Iowa flood information system as a generalized flood cyberinfrastructure. Int. J. River Basin Manag. 16 (3), 393–400. https://doi.org/10.1080/15715124.2017.1411927.

Ebel, E., Beckers, J., 2010. Operational River and Coastal Water Level Forecast using Bayesian Model. http://publications.deltares.nl/1200379_003.pdf. 1200379–003-ZWS-0001, 6 January 2010, final.

European Environment Agency, 2018. Catastrophic Floods Cause Human Tragedy, Endanger Lives and Bring Heavy Economic Losses. https://www.eea.europa.eu/archived/archived-content-water-topic/water-resources/floods.

Fang, Z., Bedient, P.B., Benavidas, J.A., Zimmer, A.L., 2008. Enhanced radar-based flood alert system and floodplain map library. ASCE J. Hydraul. Eng. 13 (10). ISSN 1084-0699/2008/10-926-938.

Fang, Z., Bedient, P.B., Buzcu-Guven, B., 2011. Long-term performance of a flood alert system and upgrade to FAS3: A Houston Texas case study. ASCE J. Hydraul. Eng. 16 (10). ISSN 1084-0699/2011/10-818-828.

Fang, Z., Dolan, G., Sebastian, A., Bedient, P.B., 2014. Case study: flood mitigation and hazard management at the Texas medical center in the wake of tropical storm Allison (2001). ASCE J. Nat. Hazards Rev. 15 (3). ISSN 1527-6988/05014001(11).

Federal Emergency Management Agency, 2019. Flood Risk Communication Toolkit for Community Officials, Communication Plan Guide. https://www.fema.gov/media-library-data/1558444240699-c6447fe036e4fdf97e355e0839abcc59/CX_Toolkit_CommunicationPlan_(508).pdf.

Gochis, D.J., Barlage, M., Cabell, R., Casali, M., Dugger, A., FitzGerald, K., McAllister, M., McCreight, J., RafieeiNasab, A., Read, L., Sampson, K., Yates, D., Zhang, Y., 2020. The WRF-Hydro® Modeling System Technical Description, (Version 5.1.1). NCAR Technical Note, p. 107. https://ral.ucar.edu/sites/default/files/public/WRFHydroV511TechnicalDescription.pdf.

Hydrologic Engineering Center (HEC), Dec. 2013. HEC-HMS, Hydrologic Modeling System User's Manual Version 4.0. U.S. Army Corps of Eng., Davis, CA.

Hydrologic Engineering Center (HEC), Feb. 2016. HEC-RAS, River Analysis System, User's Manual Version 5.0. U.S. Army Corps of Eng., Davis, CA.

Hydrologic Engineering Center (HEC), May 2017. Real-Time Simulation (HEC-RTS) User's Manual Version 3.0. U.S. Army Corps of Eng., Davis, CA.

Intergovernmental Panel on Climate Change, 2013. Climate Change 2013, The Physical Science Basis. Working Group I. Cambridge University Press, London.

Kahn, M., 2005. The death toll from natural disasters: the role of income, geography, and institutions. Rev. Econ. Stat. 87 (2), 271–284.

Krajewski, W.F., Smith, J.A., 2002. Radar hydrology: rainfall estimation. Adv. Water Resour. 25 (8–12), 1387–1394.

Krajewski, W.F., et al., 2017. Real-time flood forecasting and information system for the State of Iowa. Bull. Am. Meteor. Soc. 98, 539–554. https://doi.org/10.1175/BAMS-D-15-00243.1.

Kuligowski, R.J., Li, Y., Hao, Y., Zhang, Y., 2016. Improvements to the goes-r rainfall rate algorithm. J. Hydrometeorol. 2016 (17), 1693–1704.

Liechti, K., Panziera, L., Germann, U., Zappa, M., 2013. The potential of radar-based ensemble forecasts for flash-flood early warning in the southern Swiss Alps. Hydrol. Earth Syst. Sci. 17, 3853–3869. https://doi.org/10.5194/hess-17-3853-2013.

Ly, S., Charles, C., Degré, A., 2013. Different methods for spatial interpolation of rainfall data for operational hydrology and hydrological modeling at watershed scale. Rev. Biotechnol. Agron. Soc. Environ. 17 (2013), 392.

Mallakpour, I., Villarini, G., 2015. The changing nature of flooding across the Central United States. Nat. Clim. Chang. 5, 250–254. https://doi.org/10.1038/nclimate2516.

Michelson, D., 2004. Systematic correction of precipitation gauge observations using analysed metrological variables. J. Hydrol. 290, 161–177. https://doi.org/10.1016/j.jhydrol.2003.10.005.

Milly, P.C.D., Wetherald, R.T., Dunne, K.A., Delworth, T.L., 2002. Increasing risk of great floods in a changing climate. Nature 415, 514–517.

Moore, R.J., Bell, V.A., Jones, D.A., 2005. Forecasting for flood warning. Compt. Rendus Geosci. 337, 203–217.

Mosavi, A., Ozturk, P., Chau, K.W., 2018. Flood prediction using machine learning models: literature review. Water 10, 1536.

National Aeronautics and Space Administration (NASA), 2020a. Global Precipitation Measurement. https://www.nasa.gov/mission_pages/GPM/main/index.html.

National Aeronautics and Space Administration (NASA), 2020b. Geostationary Operational Environmental Satellites—R Series. https://www.goes-r.gov/.

National Weather Service (NWS), 2012. Flood Warning System Manual. https://www.hsdl.org/?view&did=818329/.

National Weather Service (NWS), 2016. Sacramento Soil Moisture Accounting (SAC-SMA) Model. https://www.nws.noaa.gov/oh/hrl/general/chps/Models/Sacramento_Soil_Moisture_Accounting.pdf.

Nielsen, J.P., Norris, J.M., 2007. From the River to You—USGS Real-Time Streamflow Information., p. 4. U.S. Geological Survey Fact Sheet 2007–3043, Also available at: http://pubs.usgs.gov/fs/2007/3043/.

Nikolopoulos, E.I., Anagnostou, E.N., Borga, M., 2013. Using high-resolution satellite rainfall products to simulate a major flash flood event in Northern Italy. J. Hydrometeorol. 14, 171–185. https://doi.org/10.1175/JHM-D-12-09.1.

NOAA National Center of Environmental Information, 2019. NOAA Next Generation Radar (NEXRAD) Level 2 Base Data., https://doi.org/10.7289/V5W9574V.

NOAA National Centers for Environmental Information (NCEI), 2020. U.S. Billion-Dollar Weather and Climate Disasters., https://doi.org/10.25921/stkw-7w73. https://www.ncdc.noaa.gov/billions/.

Office of Water Prediction, 2020. National Water Model. https://water.noaa.gov/about/nwm.

Parker, D., 2017. Flood Warning Systems and Their Performance. Oxford Research Encyclopedia of Natural Hazard Science. Retrieved 9 Jul. 2020, from: https://oxfordre.com/naturalhazardscience/view/10.1093/acrefore/9780199389407.001.0001/acrefore-9780199389407-e-84.

Perera, et al., 2019. Flood Early Warning Systems: A Review of Benefits, Challenges and Prospects. UNU-INWEH Report Series, Issue 08, United Nations University Institute for Water, Environment and Health, Hamilton, Canada.

Perica, S., Pavlovic, S., Laurent, M.S., Trypaluk, C., Unru, D., Wilhite, O., 2018. NOAA Atlas 14, Precipitation Frequency Atlas of the United States. vol. 11 U.S. Department of Commerce, Silver Spring, MD.

Rollason, E., Bracken, L.J., Hardy, R.J., Large, A.R.G., 2018. Rethinking flood risk communication. Nat. Hazards 92 (3), 1665–1686.

Shen, C., 2018. A transdisciplinary review of deep learning research and its relevance for water resources scientists. Water Resour. Res. 54. https://doi.org/10.1029/2018WR022643.

Smith, P.J., Pappenberger, F., Wetterhall, F., Thielen Del Pozo, J., Krzeminski, B., Salamon, P., Muraro, D., Kalas, M., Baugh, C., 2016a. On the operational implementation of the European flood awareness system (EFAS). In: Flood Forecasting: A Global Perspective, pp. 313–348.

Smith, B.K., Smith, J., Baeck, M.L., 2016b. Flash flood–producing storm properties in a small urban watershed. J. Hydrometeorol. 17, 2631–2647. https://doi.org/10.1175/JHM-D-16-0070.1.

The Dallas Morning News, 2017. https://www.dallasnews.com/news/texas/2017/09/01/ut-arlington-flood-expert-helped-keep-houston-hospitals-safe-during-harvey-s-onslaught/.

Today's Earth Developing Group, 2020. Today's Earth Japan Brief Description & Validation Report. https://www.eorc.jaxa.jp/water/TE-japan/documents/TE-Japan_20200309.pdf.

United Nations International Strategy for Disaster Reduction (UNISDR), 2006. The International Early Warning Programme—The Four Elements of Effective Early Warning Systems—Brochure, Platform for the Promotion of Early Warning (PPEW)., p. 4. http://www.unisdr.org/2006/ppew/iewp/IEWP-brochure.pdf.

United Nations Office for Disaster Risk Reduction, 2018. UNISDR Annual Report 2017. https://www.unisdr.org/files/58158_unisdr2017annualreport.pdf.

United States Geological Survey (USGS), 2020. National Water Information System. https://waterdata.usgs.gov/nwis.

Vieux, B.E., Bedient, P.B., 2004. Assessing urban hydrologic prediction accuracy through event reconstruction. J. Hydrol. 299 (3–4), 217–236. https://doi.org/10.1016/j.jhydrol.2004.08.005.

Vieux, B., Vieux, J., 2005. Rainfall accuracy considerations using radar and rain gauge networks for rainfall-runoff monitoring. J. Water Manag. Model. https://doi.org/10.14796/JWMM.R223-17.

Villarini, G., Mandapaka, P.V., Krajewski, W.F., Moore, R.J., 2008. Rainfall and sampling uncertainties: a rain gauge perspective. J. Geophys. Res. 113, D11102. https://doi.org/10.1029/2007JD009214.

CHAPTER

Lifeline infrastructures and hydroclimate extremes climate: A future outlook

7

Shahzaib Khan, Nishant Kamboj, and Udit Bhatia
Indian Institute of Technology Gandhinagar, Gandhinagar, India

Introduction

The world is urbanizing at a swift pace. Indian cities have undergone an unprecedented rate of growth in the past 30 years (Taubenböck et al., 2009). In 2018, around 34% of the total population in India lived in Urban areas (World Urbanization Prospects—Population Division—United NationsDocument, 2018). United Nations predictions show that, by 2025, Delhi would be the most populated city in the world, and Mumbai would be the sixth in the list. The massive growing population necessitated the need for extensive infrastructure, preserving the physical and environmental milieu of the city. The vast scale of these urban systems and their complex networks make them vulnerable to any natural or human-made attacks. India is most imperiled to natural hazards and also not unknown to human-made disasters. Experience attests that any attack on urban infrastructure cripples the city and halts life for days, be it 2012 India Blackout, which left half of the Indian population without electricity, or 2013 Uttarakhand flash floods, which killed more than 1000 people and ruined infrastructure (Bhatia et al., 2015; Bhatt et al., 2013). A similar catastrophe happened in Mumbai in 2005, where the city witnessed one of its worst floods in the history of India—having an area of 437 km^2 and around 12 million population, Mumbai reached to complete halt owing to unparalleled rainfall of 994 mm in just 24 h (Gupta, 2020). The rain paralyzed the city. Almost all the services such as transportation, telecommunications, and power came to an absolute standstill. For the first time in Mumbai's history, all domestic and international air flights were grounded owing to the devastating flooding of the runways for 30 h. The deep-seated vulnerability of Mumbai's poor infrastructure was now all out in the face of the disastrous flood. Weak planning and implementation of the government's disaster mitigation strategy led to a tremendous loss of life, infrastructure, and money.

Specifically, hydroclimate extremes, including precipitation extremes, can severely impact the functionality of infrastructure systems and the overall well-being of the society. Recently, India has witnessed many devastating extreme precipitation events affecting the road networks and human lives. Floods in Mumbai in July 2019 caused the Central Railway to suspend its services (Dhiman et al., 2018). Furthermore, November–December 2015 Floods in Chennai caused by the heavy rainfall killed more than 500 people and displaced over 18 lakhs people with estimates of economic damages of around Rs. 200 billion–1 trillion. Recent studies have shown that precipitation extremes are projected

Climate Change and Extreme Events. https://doi.org/10.1016/B978-0-12-822700-8.00004-4
Copyright © 2021 Elsevier Inc. All rights reserved.

to intensify further (Ali and Mishra, 2017; Mukherjee et al., 2018). Extreme precipitation events directly or indirectly cause flooding, crop damages, health hazard, erosion, and water contamination (Guhathakurta et al., 2011; Rajeevan et al., 2008). Despite these events, policies for critical infrastructure in India are still poorly framed. Thus knowing precipitation extremes can be very beneficial not only for the infrastructure development to prevent flooding but also for water resource management bodies. A better study on precipitation extremes and network science can help the international and regional authorities to frame strategies making the critical infrastructure resilient and perhaps predict any possible anthropogenic or natural calamities.

To have an understanding of these events, climatologists use extreme value theory, a branch of statistics that deals with the tail of the probability distributions. It has multidisciplinary applications, including finance (Gilli and këllezi, 2006), traffic prediction (Uchida, 2004), structural engineering (Schuëller, 1984), ecology (Katz et al., 2005), etc. It is widely used in meteorology to describe the frequency of extremes, intensity, in the evaluation of climate models and to analyze the impacts of projected climate change on tails of the distribution of both temperature and precipitation. For our case study, we have used the Generalized Extreme value distribution given by Jenkinson (Jenkinson, 1955). This approach is called block maxima approach. It got this name because it fits the distribution to the maximum value in a block of equal size. In our study, we investigated the variability of extremes using the stability indicator precipitation extremes volatility index (PEVI), as defined by Khan et al. (2007), and found that nearly 50% of the grid points across the nation exhibit significant volatility, posing new challenges to infrastructure managers in the management of such extremes.

To translate the understanding gained from extreme indicators, understanding the curse of interconnectivity across infrastructure systems at scales is crucial. In this chapter, we discuss the infrastructure relevant extreme volatility indices and motivate the use of network science-based approaches to model infrastructure systems to understand their resilience to compound and multiple hazards.

Organization of the chapter

This chapter is organized into two main sections. The first section discusses various aspects of quantification of risks from extreme precipitation events and associated methodologies in detail, with results demonstrated for India. Part two focuses on the networked perspectives on critical infrastructure, with a case study focused on Indian Railways Network (IRN) spanning throughout India and Mumbai Suburban Railways Network, which serves the daily commute of Mumbai and its adjoining suburban areas. Surrounded on three sides by water and located along the western coast of India, Mumbai is referred to as the "commercial capital of India." However, rapid urbanization and population growth have contributed to severe social, environmental, and infrastructure challenges. As per the census of 2011, some areas of Mumbai city have population densities of 46,000 per km^2—among the highest in the world. Moreover, recent events of flooding in the Mumbai region have been linked to the impact of urban growth and land use changes that, in turn, impact microclimate and extreme precipitation patterns (Pathirana et al., 2014). In addition, the functioning of Mumbai critically depends on its lifeline infrastructure—Mumbai Suburban Railways Network. However, the operations of the Railway network have been severely impacted by disruptions—both natural and human-made (Ranger et al., 2011). The second section of the chapter presents a case study focusing on the Mumbai suburban Railways network in the context of posthazard recovery.

Quantifying risk from extreme events

To quantify and characterize the risk to infrastructures from weather and climate extremes, return levels associated with the design period of infrastructures (50–100 years) are often used in design standardization. However, in the context of inherent nonstationarity and volatility associated with extremes, point estimates of the return level would not help in comprehensive risk assessment, specifically from the infrastructure perspective. Hence we use the measure of relative change in the extremes measured through the PEVI. The term derived from the stock market, volatility in the stock market is an indicator of uncertainty. Also known as the fear index or VIX, using the volatility, investors get to see the condition of the market, whether they have to invest or not. A higher volatility means higher instability of the market. Similarly, in climate, to study the behavior of extreme events, we use a measure of volatility in precipitation extremes, PEVI (Khan et al., 2007). PEVI compares the increase in intensity with the rarity of extreme events. PEVI is defined as the ratio of a higher return level to that of a lower return level. When this ratio equals one, it means that there is less probability of occurrence of an extreme event. When the PEVI increases, uncertainty increases. It can be considered in designing for hydraulic structures that are made for a particular return level. If these structures experience an event of higher return period, then they will collapse; thus the infrastructures built in regions with increasing PEVI need special attention from the policymakers. In our study, PEVI is the ratio of the 100-year return level to the 30-year return level. PEVI values were calculated at each grid points, with a moving window to account for the nonstationarity scenario of PEVI; PEVI was also calculated for the re-gridded observed data and data from seven CMIP5 models for both historical and predicted values, with an RCP 8.5 scenario. A suite of observations and model projections were obtained for India to develop extreme volatility indices. Data are obtained from the Indian Meteorological Department (IMD) (Pai et al., 2015) at 0.25-degree spatial resolution. A period of at least 30 years was used to estimate the return levels that are required for the calculation of extreme volatility indices. To take account of nonstationarity, the period of 1951–2005 with overlapping moving wind 40 years period resulting in 16 blocks is used. Projections of climate for the 21st century were obtained from the Coupled Model Intercomparison Project Phase-5 archives (Taylor et al., 2012). We use seven models in our multimodel ensemble approach. The choice behind these seven models is guided by the reasonable skills in the context of the Indian subcontinent, as shown in the study by Ashfaq et al. (2017). These models (with names of their parent laboratories listed in the parentheses) are BNU-ESM (Beijing Normal University), CANESM2 (Canadian Earth System Model), GFDLESM2M (Geophysical Fluid Dynamics Laboratory), MIROC-ESM (Atmosphere and Ocean Research Institute (The University of Tokyo), National Institute for Environmental Studies and Japan Agency for Marine-Earth Science and Technology), MPI-ESMLR, MPI-ESMMR (Max Planck Institute for Meteorology), and NOR-ESM (Norwegian Climate Centre) for the period of 2005–2100. More details about these models can be found in (Taylor et al., 2012).

Because the spatial resolution of all the models is different from each other, to have consistency, daily observed data were re-gridded to the resolution of BNU-ESM. The analysis was done on Representative Concentration Pathways (RCP 8.5) scenarios. RCP 8.5 scenario corresponds to the pathway with the highest greenhouse gas emissions (Riahi et al., 2011). The main reason for choosing the RCP 8.5 scenario for predicting the precipitation extremes of the future in our study is that the present emission scenarios are following the trail or are very close to the RCP 8.5 (Sanford et al., 2014).

Analyzing extremes

Generalized extreme value distribution

The generalized extreme value (GEV) distribution was proposed by Jenkinson in 1955, often denoted by $G(\mu, \sigma, \xi)$, whose cumulative distribution function is given by

$$G(x;\mu,\sigma,\xi)=\exp\left\{-\left[1+\xi\left(\frac{x-\mu}{\sigma}\right)\right]_{+}^{-\frac{1}{\xi}}\right\} \tag{1}$$

For $\xi = 0$, G is defined as follows:

$$G(x;\mu;\sigma;\xi)=\exp\left\{-\exp\left(\frac{x-\mu}{\sigma}\right)\right\}, \tag{2}$$

where μ or location varies from $-\infty$ to $+\infty$, σ, or scale factor ($\sigma > 0$) and ξ, also known as the scale factor, varies from $-\infty$ to $+\infty$. Depending on the value of the shape parameter, three types of GEV are formed (Coles, 2001):

1. Gumbel Distribution or heavy-tailed distribution ($\xi > 0$)
2. Fréchet Distribution or light-tailed distribution ($\xi = 0$)
3. Weibull Distribution or short-tailed distribution ($\xi < 0$)

By differentiating Eq. (1), we get the probability density function (p.d.f) of GEV as

$$g(x;\mu,\sigma,\xi)=\frac{1}{\sigma}\left[1+\xi\left(\frac{x-\mu}{\sigma}\right)\right]_{+}^{-\frac{1}{1+\xi}}\exp\left\{-\left[1+\xi\left(\frac{x-\mu}{\sigma}\right)\right]_{+}^{-\frac{1}{\xi}}\right\} \tag{3}$$

For $x_1, x_2, x_3, \ldots, x_n$ independent and identically distributed random variables having probability distribution function $g(x, \mu, \sigma, \xi)$, the likelihood function will be

$$L(\theta)=\prod_{i=1}^{n}g(x,\theta) \tag{4}$$

The log-likelihood of GEV will be as follows:

$$l(\mu,\sigma,\xi;x)=-n\log\sigma-\left(1+\frac{1}{\xi}\right)\sum_{i=1}^{n}\log\left[1+\xi\left(\frac{x_i-\mu}{\sigma}\right)\right]_{+}-\sum_{i=1}^{n}\log\left[1+\xi\left(\frac{x_i-\mu}{\sigma}\right)\right]_{+}^{-\frac{1}{\xi}} \tag{5}$$

The parameters of GEV are obtained by maximum likelihood estimation. GEV was fitted by the eva and fevd library in python using rpy2.[a]

Estimation of return levels

An N-year return level is defined as the level expected to be exceeded once in every N years, or having a probability of $\frac{1}{N}$ in any given year. To estimate the N-year return level equate equation 1 to $1-\frac{1}{N}$. The simplest example of estimating an N year return level is shown further.

[a]Link to rpy2: https://rpy2.github.io/doc/latest/html/index.html.

Example 1

Let N be 30

$$P(x > z_{30}) = 1 - \frac{1}{30}$$

$$1 - P(x > z_{30}) = 0.33$$

$$1 - \exp\left\{ -\left[1 + \xi\left(\frac{\hat{z}_{30} - \hat{\mu}}{\hat{\sigma}}\right)\right]_{+}^{-\frac{1}{\hat{\xi}}} \right\} = 0.33$$

$$\exp\left\{ -\left[1 + \xi\left(\frac{\hat{z}_{30} - \hat{\mu}}{\hat{\sigma}}\right)\right]_{+}^{-\frac{1}{\hat{\xi}}} \right\} = 0.67$$

$$\hat{z}_{30} = \hat{\mu} + \frac{\hat{\sigma}}{\hat{\xi}}\left[(-\log(0.67))^{-\hat{\xi}} - 1\right]$$

GevrRl from EVA package was used to estimate the 100-year and 30-year return levels of all the grid points across the nation for the observed high resolution (0.25 degrees gridded) data and also for the observed low resolution (2.7906 × 2.8125 degrees) gridded data. Estimation was done from 1951 to 2005 using a 40-year moving window.

Return levels for CMIP5 models for a historic run and for predicted values were estimated. For the future run, time from 2006 to 2100 with a moving window of 40 years was used. After estimating the return levels, PEVI was calculated.

Precipitation extremes volatility index

PEVI is an indicator that compares the increase in intensity with the rarity of extreme events and can be used to check the vulnerability of infrastructure or hydraulic structures (Khan et al., 2007). PEVI is defined as the ratio of the return levels. In our case, PEVI is the ratio of the 100-year return level to the 30-year return level. The term PEVI is inspired by the stock market volatility index (VIX); it is also called a fear index. When there is high volatility in the market, there is high risk; similarly, higher values of PEVI indicate the instability of a grid point. Thus it can be an indicator of the safety of engineering infrastructures. Hence it will be a good idea of decision-makers to have a glance at PEVI. PEVI values were calculated at each grid points, with a moving window to account for the nonstationarity scenario of PEVI. PEVI was also calculated for the re-gridded observed data and data from seven CMIP5 models for both historical and predicted values with an RCP 8.5 scenario. After obtaining PEVI values for the whole nation, the trend was inspected using the Mann–Kendall test.

Trend analysis

The nonparametric Mann-Kendall test was performed (Kendall, 1948; Mann, 1945) with a 5% significance level on nonstationary PEVI values from 1951 to 2005 for observed, observed re-gridded, and for the historical run of seven CMIP5 models and also for the predicted data from 2006 to 2100. The slope of the trend was obtained using Sen's method (Sen, 1968). After calculating the slope,

we collected the number of grid points, which showed the positive, negative, and no trends. For simple and easy visualization, pie charts were created describing the percent of grid points showing positive, negative, and no trends.

Spatiotemporal variability in volatility

Spatiotemporal variability was analyzed using the PEVI from 1951 to 2005 and from 2006 to 2100 in a nonstationary frame. Highest values of PEVI across the nation in Annual and in June, July, August, and September (JJAS) period were obtained in North of India and North-East India with values going around 3. While in NON-JJAS, most of the values were below 2, but there were two grid points whose value were exceptionally higher. Fig. 1 A, B, D, E, G, and H shows the nonstationarity of PEVI values. Fig. 1A corresponds to the analysis window from 1951 to 1991, and Fig. 1B shows the analysis window

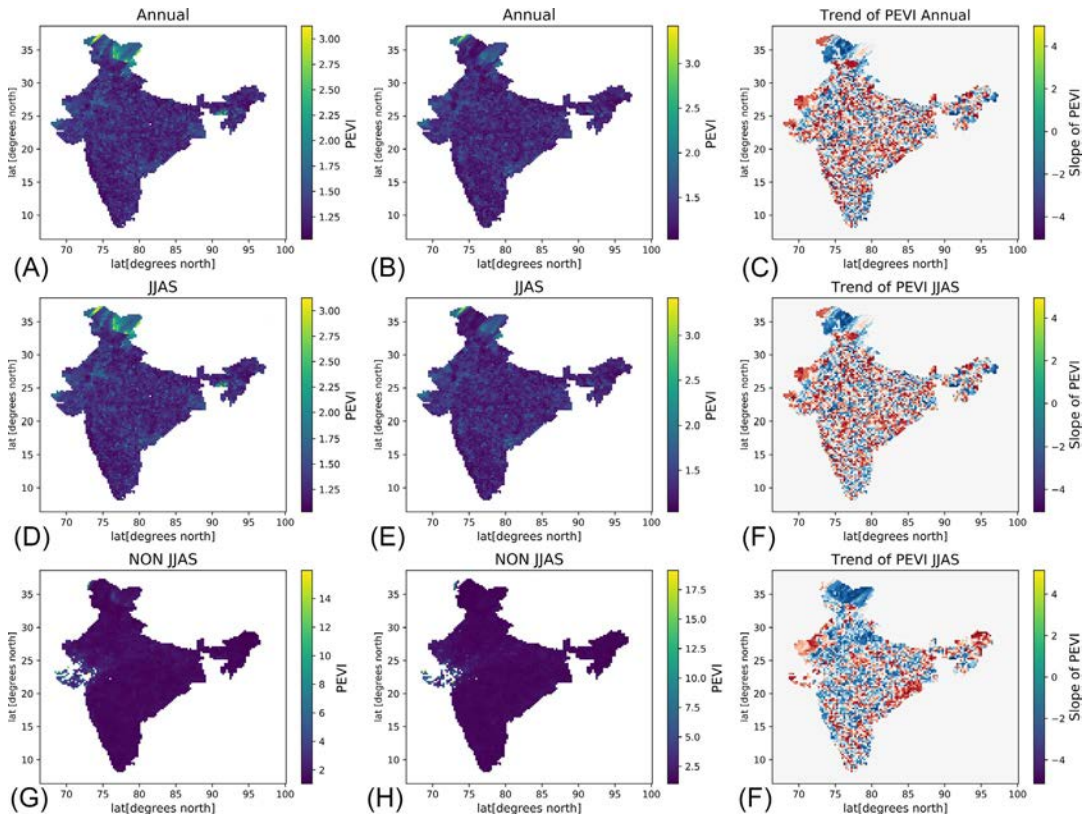

FIG. 1

(A, D, and G) shows the PEVI values for the time window of 1951–91. (B, E, and H) shows the PEVI values for the time window of 1975–2005. (C, F, and I) shows the trend of PEVI values from the time frame of 1951–2005.

from 1975 to 2005. These two figures clearly show there is a change in the PEVI values over time, motivating us to investigate the trend of the PEVI values. Fig. 1C, F, and I shows the slope of the trend of the PEVI values. The blue and the red parts in Fig. 1C show the increasing and decreasing trends, respectively. We also captured grid points showing these trends and found their behavior in terms of percent.

Fig. 2A–C represents the percent of points showing the increasing, decreasing, and no trends. This shows that the nation exhibits around 50% significant volatility. We also analyzed the behavior of grid points through seven CMIP5 models data for historical and predicted values. Our analysis of historical data, as shown in Table 1, and for the predicted data under RCP 8.5 for the time varying from 2006 to 2100 in a nonstationary, the percents are shown in Table 2.

- **BNUESM:** BNUESM model with the resolution of 2.7906 × 2.8125 degrees showed that the trend of the PEVI is increasing as we go from historical data (1951–2005) to predicted data (2006–2100), with a significant jump of 11.2% and 12.2% in grid points in Annual and JJAS periods, respectively, but a decrease of 0.3% in grid points in NON-JJAS period.
- **CANESM2M**: Model with resolution of 2.7906 × 2.8125 degrees showed an increase in trend of PEVI values in grid points in all Annual, JJAS, and NON-JJAS periods, with the increase of 14.7%, 3.4%, and 4.4% respectively.

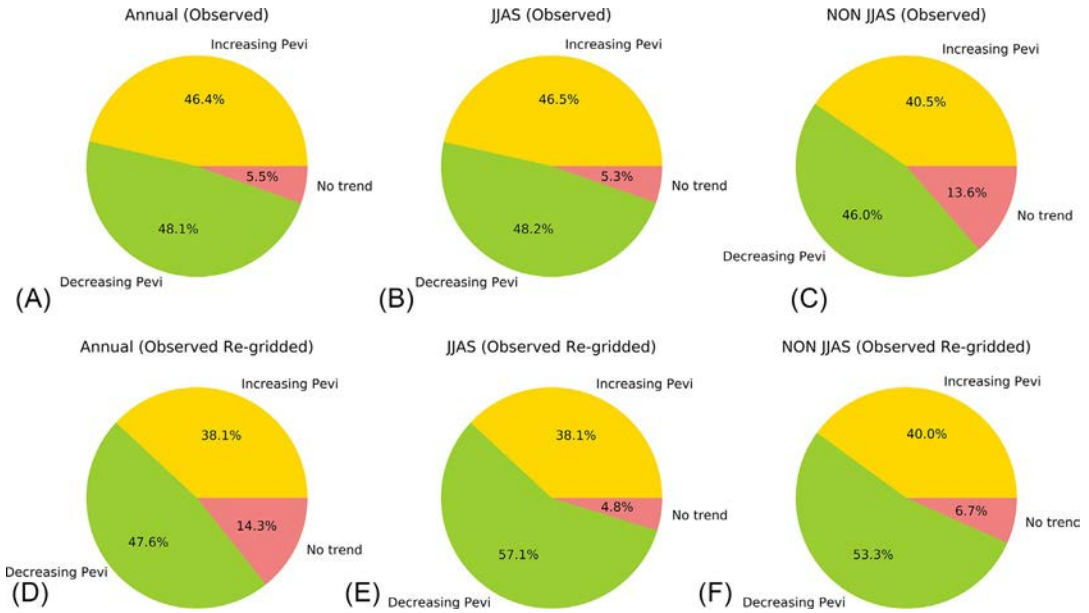

FIG. 2

(A–C) shows the percent of PEVI trend of grid points for the time window of 1951–91, with a resolution of 0.25 × 0.25 degrees. (D–F) shows the percent of PEVI trend of grid points for the time window of 1951–91, with a resolution of 2.7906 × 2.8125 degrees (consistent with other seven CMIP5 models).

Table 1 Historical run of CMIP5 models and analysis of observed data from 1951 to 2005, showing percent of the grid points with increasing, decreasing, and no trends.

S. No.	Model	Annual			JJAS			NON-JJAS		
		Increasing (%)	Decreasing (%)	None (%)	Increasing (%)	Decreasing (%)	None (%)	Increasing (%)	Decreasing (%)	None (%)
1	Observed	46.4	48.1	5.5	46.5	48.2	5.3	40.5	46	13.6
2	BNU_ESM	56.2	43.8	0	55.9	44.1	0	52.9	47.1	0
3	CAN_ESM2	45.3	54.7	0	50	48.9	1.1	41.3	56	2.7
4	GFDL_ESM2	54	46	0	60	38.5	1.5	48.4	51.6	0
5	MIROC_ESM	45.6	53.2	1.3	46.3	52.4	1.2	45.9	54.1	0
6	MPI_ESM_LR	47.5	52.5	0	44.3	55.7	0	46.6	51.7	1.7
7	MPI_ESM_MR	52.2	47.8	0	49.3	50.7	0	47.7	49.2	3.1
8	NORESM	58.6	39.7	1.7	44.1	52.55	3.4	42	56.5	1.4

Table 2 Predicted run of CMIP5 models from 2006 to 2100 showing percent of grid points with increasing, decreasing, and no trends.

S. No.	Model	Annual			JJAS			NON-JJAS		
		Increasing (%)	Decreasing (%)	None (%)	Increasing (%)	Decreasing (%)	None (%)	Increasing (%)	Decreasing (%)	None (%)
1	BNU_ESM	67.4	32.6	0	68.1	31.9	0	52.6	47.4	0
2	CAN_ESM2	60	40	0	53.4	46.7	0	45.7	54.3	0
3	GFDL_ESM2	42.9	57.1	0	40.7	59.3	0	50	46.7	3.3
4	MIROC_ESM	54.3	45.7	0	51.1	48.9	0	48.8	51.2	0
5	MPI_ESM_LR	32.1	64.3	3.6	35.7	60.7	3.6	46.5	53.5	0
6	MPI_ESM_MR	50	50	0	52.8	47.2	0	41.4	58.6	0
7	NORESM	56.8	40.5	2.7	60.5	36.8	2.6	54.8	45.2	0

- **GFDLESM2M**: Model with a resolution of 2.0225 × 2.5 degrees showed that there was an increase of 1.6% in grid points in NONJJAS period but also had a decreasing trend in grid points in both Annual and JJAS periods. To maintain the consistency, GFDLESM2M was re-gridded to BNUESM resolution.
- **MIROCESM**: A model with a resolution of 2.7906 × 2.8125 degrees showed an increasing trend in all periods, with an increase of 8.7%, 4.8%, and 2.9% in grid points in Annual, JJAS, and NON-JJAS periods, respectively.
- **MPIESMLR and MPIESMMR**: Having the resolution of 1.8653 × 1.875 degrees showed a decreasing trend in most of the periods except that MPIESMMR showed an increasing trend in the JJAS period.
- **NORESM**: NORESM model having a resolution of 1.8947 × 2.5 degrees showed an increasing trend in JJAS and NON-JJAS periods, with an increase of 16.4% and 12.8% in grid points, respectively.

Network perspective on critical infrastructure

As our world develops, our societies become more and more connected to each other. Thus any impact on one connection affects the others. We are stepping toward a warmer world, where precipitation extremes will more intensify, with PEVI as an indicator, and network science strategies and more resilience can be introduced into the infrastructure. Let's take the example of floods in Mumbai, where all transportation activities, including the railways, were shut. This not only affects human lives but also the economy of the state. If network-guided recovery strategies are used and policies are framed using this science, a huge amount of money could be saved. Knowledge of network science might help our society to prepare for the worst-case scenarios.

Till June 2020, India has witnessed events such as cyclone Amphan, COVID-19 pandemic, and intensifying heatwaves; alarming us more is yet to come. These events, directly and indirectly, affect our network system. In May 2019, cyclone Fani hit the coast of Orissa, with winds reaching the speed of 200 km/h. Owing to this, millions of households (3.5 million according to NASA) were left without electric power for days, and this created havoc in the state. Fig. 3 shows the lighting in the cyclone affected region of the state before and after the cyclone. As visible from Fig. 3, many sections of the region lost the power, including the area near the Biju Airport, which affected the functioning of the airport. This is a real-world example that exposes the vulnerabilities of interconnected networks.

Fig. 4 takes an example of an electric grid network and shows how failure in this network may cripple other critical infrastructure. Here five critical infrastructure networks are taken: agriculture, transportation, electric grid, oil and natural gas, and water supply network. The left section of the figure shows how the electric grid is involved in the functioning of other networks. The right part of the figure represents the outcomes if the electric grid network is crippled. The supply of drinkable water, pumping and extraction of oil and gas, irrigation, and the whole transportation networks work on the power supply, without which these networks can't function. This clearly demonstrates how dependent these critical infrastructures are on a single network. Failures such as these accompany a huge loss of money and life. Addressing these issues using technology and incorporating solutions in policymaking would prepare us more efficient in dealing with these kinds of situations. These critical infrastructures are closely connected to our daily life, and failures such as these raise questions to the resilience of these networks.

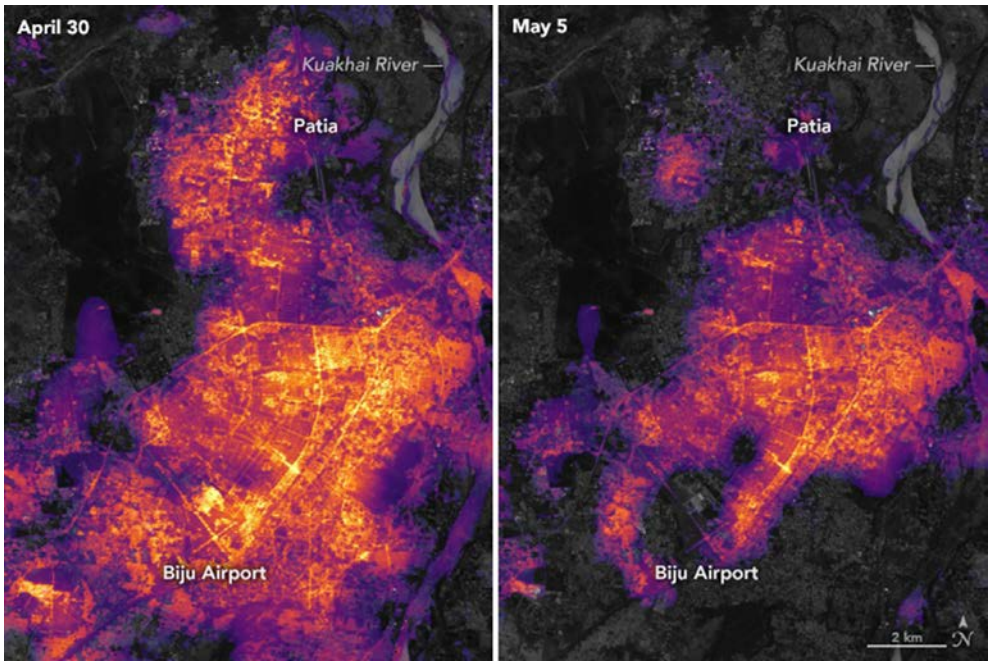

FIG. 3

Lighting in Bhubaneshwar before and after Cyclone Fani ("Lights Out after Cyclone Fani," 2019).

Mitigation analysis on Mumbai and Indian Railway Networks

Gathering network data

Mumbai Railways Network (MRN) was constructed by collecting the data manually. The map of Mumbai Railways was thoroughly analyzed and a datasheet was prepared, which consisted of a list of all the stations with an identity (ID) provided to each station. Then these station IDs were matched with the IDs of stations that have at least one train running between them. Mumbai Suburban Railways has seven lines (Western Line, Central Line, Harbour Line, Trans Harbour Line, Mono Rail, Mumbai Metro, and Indian Railways Line), which contains a total of 148 stations. The network has 169 links that connect these stations. The geographical locations of all the 148 stations were collected using Google Maps and appended in the datasheet. The weight of links, that is, the number of trains running between two stations in either direction, was also collected manually using the train data available on the website: https://indiarailinfo.com/ and on the m-Indicator app. The average revenue generated per train per day from only passenger tickets was calculated by multiplying the total number of passengers traveling every day, which was 0.79 crores, with an average ticket price of Rs. 6. This is divided by total trains running, which is 2342. This makes average revenue generated per train per day in MRN to be Rs. 20,240. During the data collection, every possible effort was made to nullify human error.

IRN data for nodes, edges, weight, and geographical location was already available in a systematic form for the year 2012–13 (Bhatia et al., 2015). IRN generated a total of Rs. 1,237,326 million in

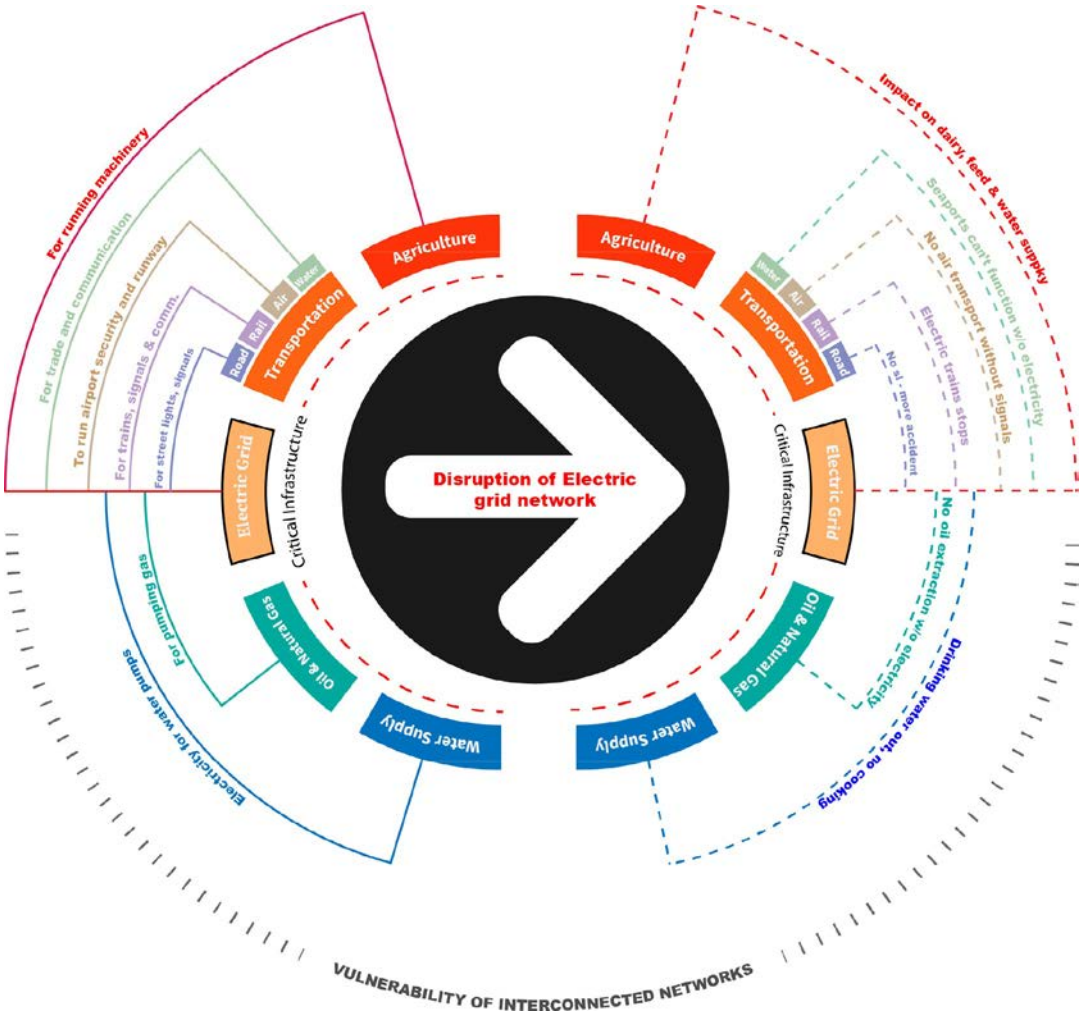

FIG. 4

Visualizing vulnerability of interconnected networks with power grid.

2012–13 from passengers and freight. There were around 19,000 trains (12,000 passenger trains and 7000 freight trains) running in IRN every day ("Ministry of Railways (Railway Board)," n.d.). This makes the average revenue generated by each train every day in IRN to be Rs. 1,78,400.

Visualizing and analyzing networks

Railways are a national asset for any country, and any perturbation leading to failure in this network may lead to a serious catastrophic event. So it is important to understand the network fully before proceeding to recovery. The MRN is a tree-like network with 148 nodes and 169 edges. The degree of a node is defined by the number of nodes it is directly connected to. Here the maximum degree of a node

is 4. The strength of a node is defined by the number of trains passing through that node. To clearly understand the importance of each node, network centralities come into the picture. For this study, betweenness centrality, closeness centrality, degree centrality, and eigenvector centrality have been used. Two stations are said to be connected if there is at least one train running between them. For analyzing the network and for applying the proposed recovery strategies, an adjacency matrix is generated from the network. This is an r matrix where r is the number of nodes, and its entries are 1 and 0. The entry corresponding to the mth row and nth column is 1 if there is an edge between m and n, otherwise 0. In the case of a weighted adjacency matrix, 1 is replaced by the respective weight. There is an almost equal number of trains running between two stations in both directions. That is why the adjacency matrix for the MRN is symmetric, and thus the network is an undirected network.

Quantification of resilience is necessary for analyzing the behavior of a network in the situation of failure and recovery. There are many metrics identified for measuring the critical functionality of a network that shows how a network responds to an attack. The weight of an edge is the amount of flow on that edge in or out and is an important factor in measuring the critical functionality. For this study, we use weighted critical functionality for determining the robustness and recovery state of a network. For the analysis, the giant component is used, which is the largest connected set of nodes in the network (i.e., within the giant component, one could travel from any station to any other station by at least one path) (Bhatia et al., 2015). For MRN, size of the giant component is 148 nodes, and for the IRN, the size is 752 nodes. We define the state of critical functionality (SCF) as WFs/WF_f, where WFs is the cumulative sum of the weight of all the edges in the giant component at a given state where one or more nodes are incapacitated by disruption, and WF_f is the cumulative sum of the edges in the largest giant component. The manner in which any network fails is random, and it is not necessary that the recovery strategy follows the same sequence as of failure. SCF gives a better picture of random or targeted failure states and helps in determining the best possible recovery strategy. For the robustness curve, a random sequence is generated, and SCF is calculated for every state by removing one node at a time. The SCF value goes from 1 to 0 as the network shifts from a fully functional state to a fully disrupted state. For the recovery curve, a strategy is developed for determining the recovery sequence using network attributes. Attributes used here are: Degree Centrality representing connectivity, Betweenness Centrality representing the number of times a station acts as a bridge along the shortest path between two other stations, Closeness Centrality calculated as the inverse of the average network distance of a given station to all other stations, and Eigenvector Centrality representing the importance of stations because of its connections (Bhatia et al., 2015). First, the values of these network attributes are listed for all the nodes, and then these attributes are prioritized. Suppose if betweenness centrality is chosen as the first best attribute, then all the nodes are arranged in the decreasing order of their betweenness centrality values. Now, if there is a tie between some nodes, that is, they all have the same centrality value, then the second best attribute is selected, and those nodes are arranged in decreasing order of that attribute values. This tie-breaking strategy is used until a prioritization sequence for recovery is obtained. The SCF value at the initial state is 0 because all the nodes are disrupted. Now, the SCF values for each step is calculated by recovering one node at a time. When all the nodes are recovered, then SCF becomes equal to 1. Using this algorithm, many different recovery sequences are generated, and the one that gives the best result is selected. Other curves are also generated by using a single network attribute for determining the recovery sequence. Median of the SCF values of 1000 random sequences are taken, and the resulting curve is used as a baseline to compare different strategies.

For the rupee curve, the total number of trains running in the network at a given state of recovery is calculated for every step and is multiplied by the average revenue generated by each train every day.

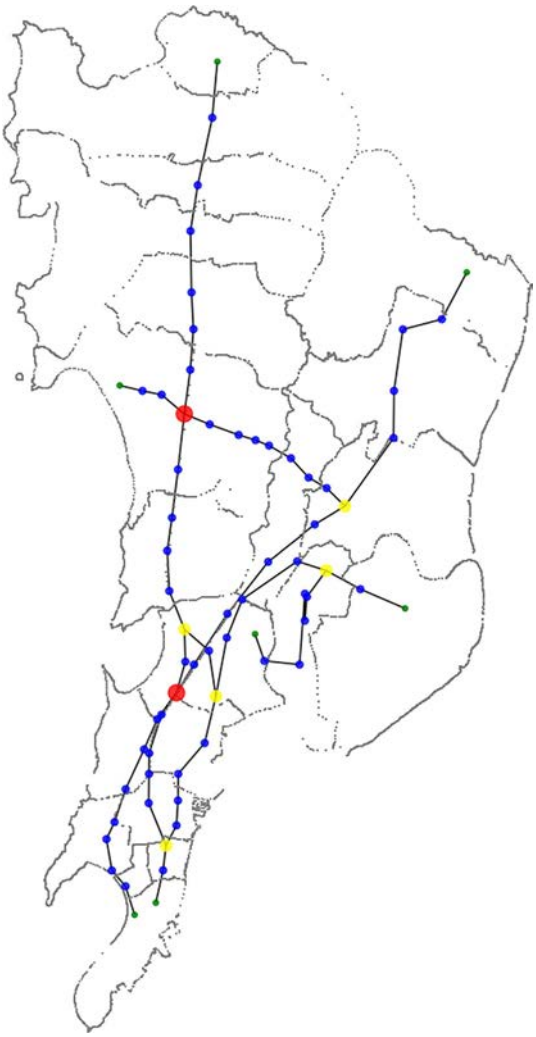

FIG. 5

Network representation of Mumbai Suburban Railways Network with the stations with the largest number of incoming tracks highlighted in *red*. We note that here nodes represent the stations, and two stations are connected if there is a direct train between a pair of nodes.

The values are then normalized, and a rupee vs time curve is generated. The recovery sequence used here is the same as obtained in the recovery curve analysis. Median of the SCF values of 1000 random sequences was taken, and the resulting curve was plotted. The amount of money saved by following different strategies was calculated by taking area between the strategy curve and the random curve multiplied with the total revenue generated (Figs. 5 and 6).

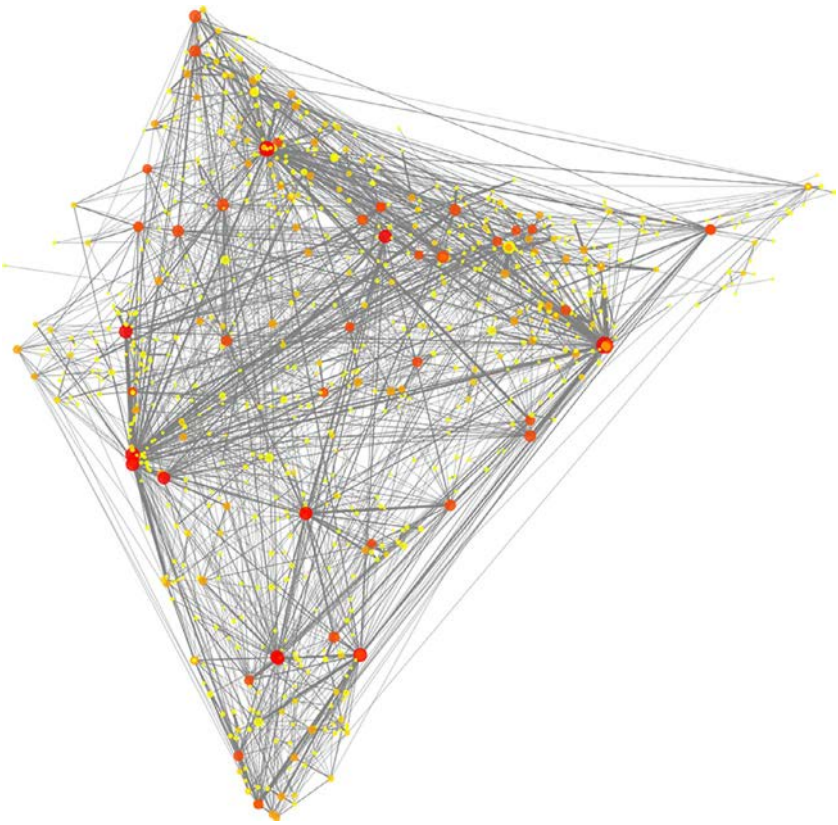

FIG. 6

Network visualization of Indian Railways Network: Here nodes represent the stations, and a pair of stations is considered to be connected by an edge if there is a direct train between them.

Robustness and recovery characteristics

The curves below show the failure and recovery of the MRN and IRN and rupee curve, which represent the money saved while following different strategies compared with random recovery, which is generally followed. The recovery curve and the rupee curve are similar to both these curves that are generated by considering the number of trains in the network. Although the perturbation in the network was random, the random recovery is not the best strategy to be followed. Network centralities provide us with a better and faster recovery plan leading to monetary benefits. As for MRN, the tie-breaking approach (Degree—Eigenvector—Closeness—Betweenness centralities) and for IRN, betweenness centrality provide a better recovery strategy than random recovery. The inferences drawn from this study advance the point that network science-based mitigation analysis can help the policymakers devise a strategy to deal with these uncertain and unavoidable situations more effectively and efficiently (Figs. 7–9).

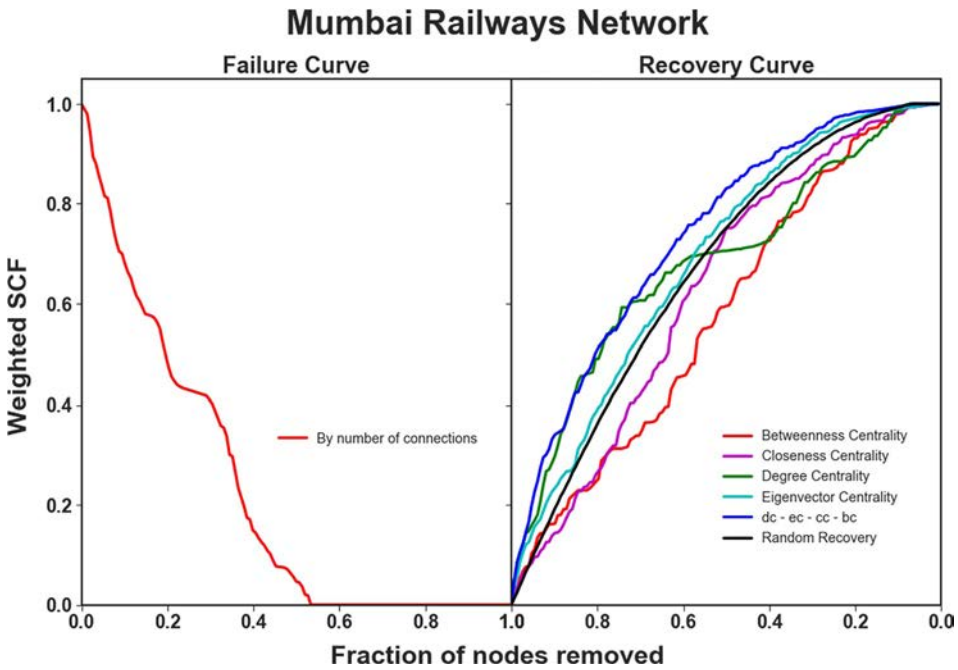

FIG. 7

Failure and recovery curves for the Mumbai Railways Network with 148 nodes. Weighted SCF, that is (number of trains running at the moment)/(total number of trains running), is used to define the functionality of the network. Betweenness, Closeness, Degree and Eigenvector Centralities and a tie-breaking strategy are used for generating sequences for recovery and are plotted on the recovery curve. Here, 1000 randomly generated sequences are used, and their median is taken to get a single random recovery curve.

Conclusion

Our study found that India's grid points have shown significant volatility from 1951 to 2005. All the seven CMIP5 models under the RCP 8.5 scenario, except MPIESMLR, have shown a significant increase in the volatility, going as high up to 16.4% in 2006–2100 when compared with the analysis of 1951–2005. Although projected CMIP5 models are associated with uncertainties, analysis on them can be used as a precaution. Grid points showing the increasing trends of PEVI have higher instability. When this instability exists in regions with high population density, or exists in the location of critical infrastructures or national/human assets, which can be damaged owing to extreme events, it poses a dangerous situation to society in terms of human lives and economy of the state. Thus PEVI needs special attention from policymakers. The structures that are built to withstand a particular return level get damaged when a greater return level strikes; hence PEVI should be considered while designing these structures. The critical infrastructure and network system lying in high PEVI areas should be

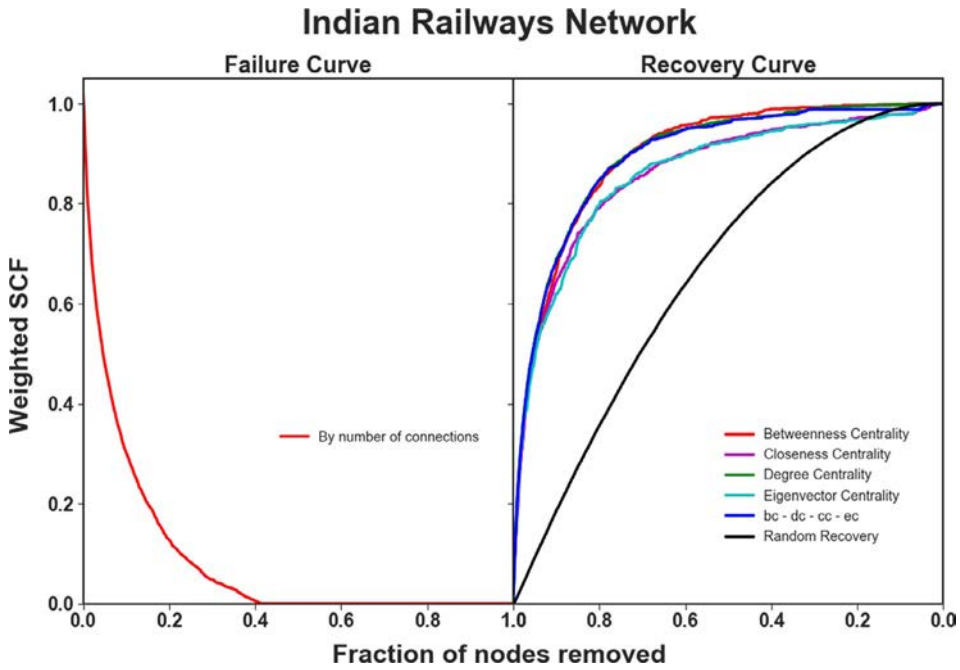

FIG. 8

Failure and recovery curves for the Indian Railways Network with 809 nodes. Weighted SCF, that is (number of trains running at the moment)/(total number of trains running), is used to define the functionality of the network. Betweenness, Closeness, Degree, and Eigenvector Centralities and a tie-breaking strategy are used for generating sequences for recovery and are plotted on the recovery curve. Here, 1000 randomly generated sequences are used, and their median is taken to get a single random recovery curve.

more robust than critical infrastructure and network systems lying in low PEVI areas. Thus the infrastructure should line up with those policies, which make them strong enough to face the calamities, and the networks should also be resilient enough to withstand any perturbations because of these events. Recent advances in network science can predict the damages that a natural or human-made attack could do to a network, and a proper recovery strategy can be devised in case a network collapses as it happened in the case of Mumbai floods. An in-depth study on the network is required to introduce resilience in the lifeline network and make it robust. Robustness is a measure of network functionality, and when a network loses its fraction of nodes, the functionality drops steeply, leading to the ultimate failure of the whole network. The complexity of these lifeline networks makes them more vulnerable to intentional and random attacks. Any delay in the recovery of these networks or following a poor recovery strategy would lead to a huge loss of time and money. With the network science approach, these losses can be predicted and eradicated. Combining both climate science and network science and incorporating the insights gained in the policymaking framework would lead to a resilient infrastructure and make the lifeline networks more robust to perturbation, saving lives, time, and money.

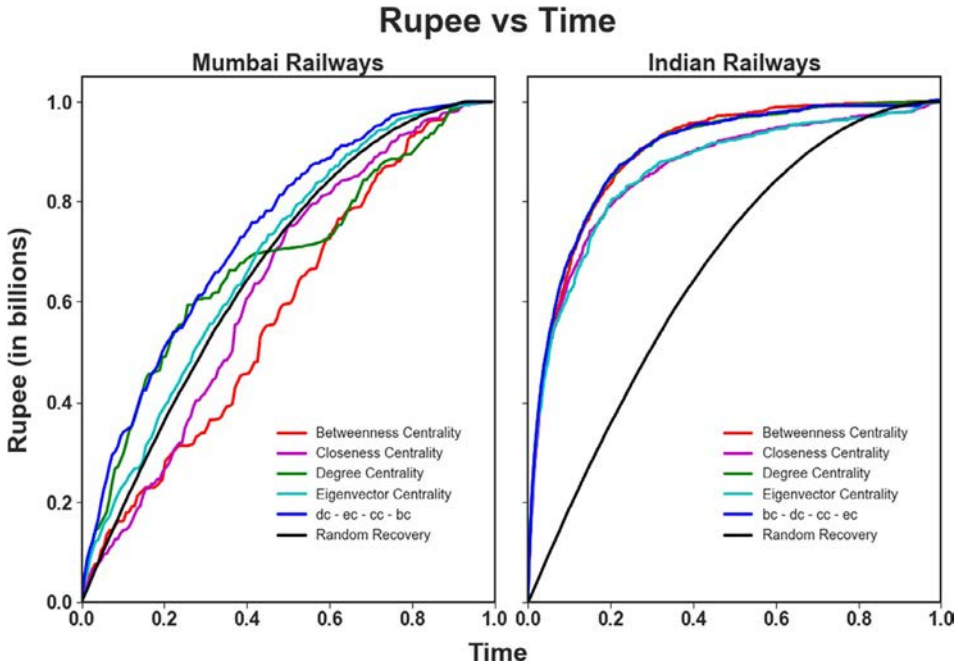

FIG. 9

Rupee vs Time plot of MRN (left) and IRN (right). Different recovery sequences for different strategies were generated, and the average revenue produced by each train was multiplied with the number of trains running at a given step of recovery, and the data were normalized and plotted. For full recovery, the revenue generated by trains in the Mumbai Railways Network is 0.048 billion rupees, and for the Indian Railway Network, it is 1.32 billion rupees.

Acknowledgment

This work was supported by the Indian Institute of Technology, Gandhinagar, through the Internal Research Grant. We are thankful to Dr. Vimal Mishra, IIT Gandhinagar, for data support.

References

Ali, H., Mishra, V., 2017. Contrasting response of rainfall extremes to increase in surface air and dewpoint temperatures at urban locations in India. Sci. Rep. 7, 1228. https://doi.org/10.1038/s41598-017-01306-1.

Ashfaq, M., Rastogi, D., Mei, R., Touma, D., Ruby Leung, L., 2017. Sources of errors in the simulation of south Asian summer monsoon in the CMIP5 GCMs. Clim. Dyn. 49, 193–223. https://doi.org/10.1007/s00382-016-3337-7.

Bhatia, U., Kumar, D., Kodra, E., Ganguly, A.R., 2015. Network science-based quantification of resilience demonstrated on the Indian Railways Network. PLoS One 10, e0141890. https://doi.org/10.1371/journal.pone.0141890.

Bhatt, M.R., Pandya, M., Goh, H.C., 2013. Floods in Uttarakhand: a new deal relief. Econ. Polit. Wkly. 48, 19–22.
Coles, S., 2001. An Introduction to Statistical Modeling of Extreme Values. Springer Series in Statistics, Springer-Verlag, London, https://doi.org/10.1007/978-1-4471-3675-0.
Dhiman, R., VishnuRadhan, R., Eldho, T.I., Inamdar, A., 2018. Flood risk and adaptation in Indian coastal cities: recent scenarios. Appl. Water Sci. 9, 5. https://doi.org/10.1007/s13201-018-0881-9.
Gilli, M., këllezi, E., 2006. An application of extreme value theory for measuring financial risk. Comput. Econ. 27, 207–228. https://doi.org/10.1007/s10614-006-9025-7.
Guhathakurta, P., Sreejith, O.P., Menon, P.A., 2011. Impact of climate change on extreme rainfall events and flood risk in India. J. Earth Syst. Sci. 120, 359. https://doi.org/10.1007/s12040-011-0082-5.
Gupta, K., 2020. Challenges in developing urban flood resilience in India. Philos. Trans. R. Soc. A Math. Phys. Eng. Sci. 378, 20190211. https://doi.org/10.1098/rsta.2019.0211.
Jenkinson, A.F., 1955. The frequency distribution of the annual maximum (or minimum) values of meteorological elements. Q. J. R. Meteorol. Soc. 81, 158–171. https://doi.org/10.1002/qj.49708134804.
Katz, R.W., Brush, G.S., Parlange, M.B., 2005. Statistics of extremes: modeling ecological disturbances. Ecology 86, 1124–1134. https://doi.org/10.1890/04-0606.
Kendall, M.G., 1948. Rank Correlation Methods, Rank Correlation Methods. Griffin, Oxford.
Khan, S., Kuhn, G., Ganguly, A.R., Erickson, D.J., Ostrouchov, G., 2007. Spatio-temporal variability of daily and weekly precipitation extremes in South America. Water Resour. Res. 43. https://doi.org/10.1029/2006WR005384.
Lights Out after Cyclone Fani [WWW Document], 2019. https://earthobservatory.nasa.gov/images/145017/lights-out-after-cyclone-fani (Accessed 31 July 2020).
Mann, H.B., 1945. Non-parametric tests against trend. Econometrica 13, 245–259. https://doi.org/10.2307/1907187.
Ministry of Railways (Railway Board) [WWW Document], n.d. http://indianrailways.gov.in/railwayboard/view_section.jsp?lang=0&id=0,1,304,366,554 (Accessed 31 July 2020).
Mukherjee, S., Aadhar, S., Stone, D., Mishra, V., 2018. Increase in extreme precipitation events under anthropogenic warming in India. Weather Clim. Extremes 20, 45–53. https://doi.org/10.1016/j.wace.2018.03.005.
Pai, D.S., Sridhar, L., Badwaik, M.R., Rajeevan, M., 2015. Analysis of the daily rainfall events over India using a new long period (1901–2010) high resolution (0.25°×0.25°) gridded rainfall data set. Clim. Dyn. 45, 755–776. https://doi.org/10.1007/s00382-014-2307-1.
Pathirana, A., Denekew, H.B., Veerbeek, W., Zevenbergen, C., Banda, A.T., 2014. Impact of urban growth-driven land-use change on microclimate and extreme precipitation—a sensitivity study. Atmos. Res. 138, 59–72. https://doi.org/10.1016/j.atmosres.2013.10.005.
Rajeevan, M., Bhate, J., Jaswal, A.K., 2008. Analysis of variability and trends of extreme rainfall events over India using 104 years of gridded daily rainfall data. Geophys. Res. Lett. 35. https://doi.org/10.1029/2008GL035143.
Ranger, N., Hallegatte, S., Bhattacharya, S., Bachu, M., Priya, S., Dhore, K., Rafique, F., Mathur, P., Naville, N., Henriet, F., Herweijer, C., Pohit, S., Corfee-Morlot, J., 2011. An assessment of the potential impact of climate change on flood risk in Mumbai. Clim. Chang. 104, 139–167. https://doi.org/10.1007/s10584-010-9979-2.
Riahi, K., Rao, S., Krey, V., Cho, C., Chirkov, V., Fischer, G., Kindermann, G., Nakicenovic, N., Rafaj, P., 2011. RCP 8.5—a scenario of comparatively high greenhouse gas emissions. Clim. Chang. 109, 33. https://doi.org/10.1007/s10584-011-0149-y.
Sanford, T., Frumhoff, P.C., Luers, A., Gulledge, J., 2014. The climate policy narrative for a dangerously warming world. Nat. Clim. Chang. 4, 164–166. https://doi.org/10.1038/nclimate2148.
Schuëller, G.I., 1984. Application of extreme values in structural engineering. In: de Oliveira, J.T. (Ed.), Statistical Extremes and Applications. NATO ASI Series, Springer Netherlands, Dordrecht, pp. 221–234, https://doi.org/10.1007/978-94-017-3069-3_15.
Sen, P.K., 1968. Estimates of the regression coefficient based on Kendall's tau. J. Am. Stat. Assoc. 63, 1379–1389. https://doi.org/10.2307/2285891.

Taubenböck, H., Wegmann, M., Roth, A., Mehl, H., Dech, S., 2009. Urbanization in India—spatiotemporal analysis using remote sensing data. Comput. Environ. Urban. Syst. 33, 179–188. https://doi.org/10.1016/j.compenvurbsys.2008.09.003.

Taylor, K.E., Stouffer, R.J., Meehl, G.A., 2012. An overview of CMIP5 and the experiment design. Bull. Am. Meteorol. Soc. 93, 485–498. https://doi.org/10.1175/BAMS-D-11-00094.1.

Uchida, M., 2004. Traffic Data Analysis Based on Extreme Value Theory and Its Applications to Predicting Unknown Serious Deterioration (WWW Document) https://search.ieice.org/bin/summary.php?id=e87-d_12_2654. (Accessed 31 July 2020).

World Urbanization Prospects—Population Division—United Nations [WWW Document], 2018, https://population.un.org/wup/Publications/ (Accessed 31 July 2020).

CHAPTER

Form, function, and nomenclature: Deconstructing green infrastructure and its role in a changing climate

8

Vidya Anderson[a] and William A. Gough[a,b]

Climate Lab, Department of Physical & Environmental Sciences, University of Toronto Scarborough, Toronto, ON, Canada[a] Department of Physical & Environmental Sciences, University of Toronto Scarborough, Toronto, ON, Canada[b]

Introduction

Anthropogenic activities continue to change the atmospheric and surface conditions of the Earth, with a large proportion of global greenhouse gas (GHG) emissions being generated from deforestation, agricultural production, land use development, electrical power and energy systems, transportation, industrial processes, and buildings (Lucon et al., 2014). Over half of the world's population resides in urban areas, and by 2050, virtually all global population growth is expected to occur in urban areas (Lucon et al. 2014). Urban areas contribute approximately 75% of global carbon dioxide emissions, primarily those generated by energy use (Revi et al., 2014).

Approaches to address the impacts of climate change, either through mitigation or adaptation efforts, occur across different disciplines, including land-use planning, environmental management, and public health. Climate change mitigation may be defined as an anthropogenic intervention to reduce the anthropogenic forcing of the climate system, and it includes strategies to reduce GHG sources and emissions and to enhance GHG sinks (IPCC, 2007). Conversely, climate change adaptation may be described as an adjustment in natural or human systems in response to actual or expected climatic stimuli or their effects, which moderates harm or exploits beneficial opportunities (IPCC, 2007). Climate change mitigation and adaptation efforts take place across disciplines but do not occur in a coordinated way that maximizes both environmental and human health co-benefits. In addition, the ability of communities to implement these approaches varies in terms of knowledge, capacity, and resources. These differences present a gap in terms of equity and research. Although many of the efforts to address climate change and its related impacts have occurred through environmental initiatives, an effective action can only occur if climate change is recognized and dealt with as an interdisciplinary and cross-sectoral problem.

The application of green infrastructure delivers a nature-based solution to bridge the gap between climate change mitigation and adaptation. Nature-based solutions have been defined by the International Union for Conservation of Nature (IUCN) as "actions to protect, sustainably manage, and restore

Climate Change and Extreme Events. https://doi.org/10.1016/B978-0-12-822700-8.00005-6
Copyright © 2021 Elsevier Inc. All rights reserved.

natural or modified ecosystems, that address societal challenges effectively and adaptively, simultaneously providing human well-being and biodiversity benefits" (Cohen-Shacham et al., 2016). Nature-based solutions provide an umbrella descriptor for the five categories of ecosystem-based approaches of which green infrastructure is one (Cohen-Shacham et al., 2016, 2019; Seddon et al., 2020). The mainstream implementation of green infrastructure can provide a nature-based solution to bridge the gap between mitigation and adaptation actions and presents a unique opportunity to perform the dual functions of climate change mitigation and adaptation simultaneously. Green infrastructure can function as a complex form of adaptation that both minimizes the most harmful effects of climate change on human health and mitigates GHG emissions that cause climate change. Although there is common agreement that green infrastructure is a good thing and that it may provide a mechanism for addressing climate change, what is missing is a clear understanding of how green infrastructure works as a complex intervention, its characteristics, and the multiple co-benefits that can be leveraged if green infrastructure is strategically applied.

This chapter presents a systematic review of the various types of green infrastructure, characteristics and associated benefits, and mainstream uses by deconstructing its nomenclature. Deconstruction of the nomenclature will facilitate organization of direct and indirect impacts, their complexities, and interconnectivity. The following section provides an overview of the systematic review process undertaken for this chapter. The subsequent sections provide a literature view, key characteristics and classifications of green infrastructure by function, the socioeconomic benefits of green infrastructure, and categorization of the nomenclature.

Systematic review

A systematic review was undertaken to identify relevant studies of ecosystem services provided by different applications of green infrastructure, including green roofs, green walls, urban vegetation and forestry, urban agriculture (UA), and tree-based intercropping (TBI) systems. Ecosystem services of interest for this review included air pollution removal, temperature regulation, and carbon sequestration.

Searches were undertaken using scientific databases, including Medline and Proquest Environmental Sciences and Pollution. Search terms used included: "green roofs"; "green walls"; "green infrastructure"; "urban agriculture"; "urban vegetation"; "forestry"; and "tree-based intercropping." These terms were searched individually and in combination with "air quality"; "temperature"; and "carbon sequestration." Duplicates were manually removed. Abstracts were reviewed to screen papers, and based on relevance, full papers were retrieved to determine inclusion within the review as shown in Fig. 1.

Of the 67 articles reviewed for this literature search, a common theme emerged—the application of green infrastructure technologies, such as green roofing, green walling, and urban vegetative strategies, provides multiple environmental benefits through air pollution abatement, mitigation of GHG emissions, provision of carbon sequestration capacity, energy conservation, reduction in urban heat island effect, increased biodiversity and provision of pollinator habitat, building energy efficiency, and flood attenuation and improvements to water quality.

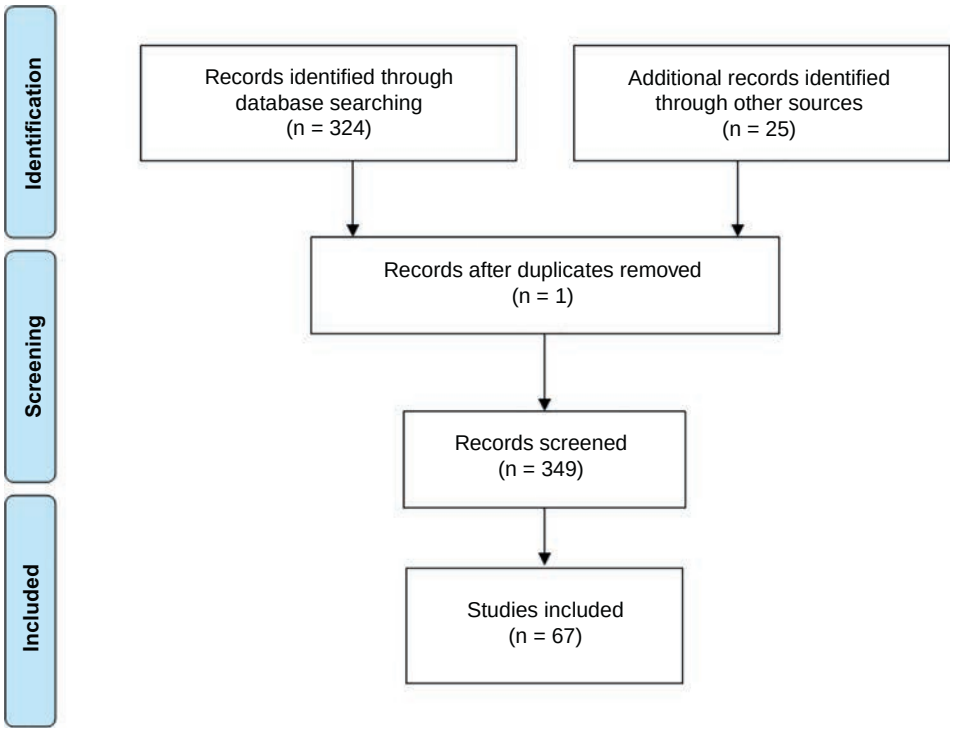
Identification
Screening
Included
Records identified through database searching (n = 324)
Additional records identified through other sources (n = 25)
Records after duplicates removed (n = 1)
Records screened (n = 349)
Studies included (n = 67)

FIG. 1

Overview of studies identified in the steps of the systematic review process derived from the PRISMA flow diagram.

Based on Moher, D., Liberati, A., Tetzlaff, J., Altman, D.G., The PRISMA Group, 2009. Preferred reporting items for systematic reviews and meta-analyses: the PRISMA statement. PLoS Med. 6 (6) e1000097. doi:10.1371/journal.pmed1000097. http://www.prisma-statement.org.

Characteristics of green infrastructure

Green infrastructure may be broadly defined as interconnected networks of natural and engineered green space that provide various ecosystem services. As shown in Fig. 1, applications of green infrastructure can be categorized into five areas: green roofs, green walls, urban vegetation and forestry, urban agriculture (UA) systems, and tree-based intercropping (TBI) systems. Green roofs may be characterized as being extensive, weighing less as a result of shallower depth and also allowing for sloped roof application. Green roofs can also be characterized as being intensive wherein there is substantial depth to the soil layer and greater variety in vegetation (Berardi et al., 2014). Green walls can be characterized as building façades covered by plant growth or vegetated structures fixed to building facades fed by an automatic fertilization and hydration system (Voskamp and Van de Ven, 2014; Marchi et al., 2014). Urban vegetation and forestry includes shrubs, bioswales (e.g., vegetated ditches for stormwater storage, drainage, and infiltration), green permeable pavements (e.g., paved surfaces replaced with

grass or herbs), rain gardens, and trees (Nowak et al., 2006, 2018; Voskamp and Van de Ven, 2014). UA systems include growing roofs, rooftop gardens, market gardens, community gardens, and micro gardens (Thornbush, 2015a,b; Lin et al., 2015). TBI systems can be characterized as agricultural lands where trees or shrubs are intercropped with crops (Thevathasan and Gordon, 2004).

Literature review

Green infrastructure provides a series of complex adaptation interventions to address climate change impacts. In addition, green infrastructure delivers an effective instrument for climate change mitigation by reducing GHG emissions from the built environment and providing carbon sequestration capacity. Tall buildings such as multiunit residential buildings can have negative effect on environmental pollution and air quality with respect to wind flows and green space (Hayati and Sayadi, 2012). Urban desert areas can be defined as areas with little or no green space provision. Such areas often contain higher ratios of multi-unit residential buildings that can be a source of housing stock for vulnerable populations that are more susceptible to the impacts of climate change. In addition, urban deserts contain built infrastructure elements such as tall buildings and impervious surfaces that can contribute to and exacerbate climate change impacts such as flooding and the urban heat island effect. Green infrastructure applications such as green roofing and green walling systems are sustainable building practices that enhance the energy efficiency of buildings, thereby reducing GHG emissions.

Green infrastructure also provides multiple benefits such as creating green space, mitigating urban heat island effect, cooling the environment, and removing air pollutants such as ozone and nitrogen dioxide through absorption and capture (Alexandri and Jones, 2006; Berardi et al., 2014; Feng and Hewage, 2014, Yang et al., 2008; Baik et al., 2012; Bowler et al., 2010). Ambient air pollution is a complex mixture of contaminants, including ground-level ozone (O_3), fine particulate matter ($PM_{2.5}$), nitrogen dioxide (NO_2), sulfur dioxide (SO_2), carbon monoxide (CO), and total reduced sulfur (TRS) compounds. Specific air contaminants have adverse health effects (Health Canada, 2005). Studies have shown that the application of green infrastructure can remove air pollutants, including ozone, nitrogen dioxide, and particulate matter (Yang et al., 2008; Baik et al., 2012; King et al., 2014; Nowak et al., 2006; Rao et al., 2014; Anderson and Gough, 2020).

Green infrastructure can cool the environment actively through evapotranspiration and passively through surface shading, in addition to improving air quality through deposition and immobilization of local air pollutants such as ozone and particulate matter (Kleerekoper et al., 2012; Janhäll, 2015; Nowak et al., 2006; Rao et al., 2014; King et al., 2014). The ability of green infrastructure to provide cool temperatures and reduce urban heat island effect has been demonstrated (Liang et al., 2014; Hall et al., 2011; Susca et al., 2011).

Flooding from extreme weather events is another impact of climate change, and impervious surfaces throughout the built environment exacerbate its effects. Green roofing, urban vegetation, and forestry can effectively manage flood risk by facilitating water absorption and retention, in addition to reducing surface water runoff during rainfall events and related pollution (Voskamp and Van de Ven, 2014; Ellis, 2013; Lennon et al., 2014). In addition, green roofing and urban vegetation provide stormwater management capacity by slowing overland flows, reducing runoff, and increasing permeable surface area.

Urbanization has led to landscape fragmentation and reduced connectivity between green and blue spaces such as forests, rivers, stream, and lakes. This in turn has reduced natural habitat and diminished natural ecosystem functions and biodiversity. Green infrastructure applications can create a network of sites and spaces to provide habitat and increase habitat connectivity and biodiversity (Ellis, 2013; Lin et al., 2015; Williams et al., 2014; Lennon et al., 2014). The application of green infrastructure has been shown to enhance insect and vertebrate diversity and support ecosystem services such as pollination through the provision of pollinator habitat (Lin et al., 2015; Williams et al., 2014).

GHG emission reductions and enhancement of carbon sequestration capacity are integral to mitigating climate change. Studies have shown that green infrastructure applications can reduce GHG emissions from the built environment and lower carbon dioxide concentrations (Berardi et al., 2014; Alexandri and Jones, 2006; Li et al., 2010; Marchi et al., 2014; Bowler et al., 2010; Hall et al., 2011; Anderson & Gough, 2020). Green roofing and green wall technologies have also been shown to reduce air pollutant concentrations and provide urban cooling (Speak et al., 2012; Kessler, 2013; Anderson & Gough, 2020). Urban vegetation strategies like tree and shrub plantings in urban corridors have shown to be effective in the immobilization of particulates, improvement of air quality, and reduction of temperatures (Nowak et al., 2006; Weber et al., 2014; Hall et al., 2011; Anderson & Gough, 2020).

Green infrastructure applications such as UA systems include growing roofs, roof top gardens, and microgardens (Thornbush, 2015a,b). UA systems improve urban biodiversity and provide ecosystem services, including stormwater management and pollination (Lin et al., 2015; Thornbush, 2015a,b). UA systems also capture pollutants and provide carbon sequestration capacity (Thornbush, 2015a,b; Lin et al., 2015). Most importantly, UA systems reduce the food miles and carbon footprint associated with conventional agriculture through local food production and distribution. UA systems also reduce the pressures on conventional agriculture and can improve food security when large-scale agricultural production is affected by weather variation.

Green infrastructure applications, such as TBI, intersperse trees or shrubs with crops on agricultural land. TBI systems improve water quality and reduce emissions associated with conventional agricultural practices by reducing reliance on pesticides and fertilizers and increasing canopy cover (Thevathasan and Gordon, 2004; Wotherspoon et al., 2014). TBI systems also act as a carbon sink by sequestering carbon in the trees and by enhancing soil carbon sequestration capacity through improved soil health (Wotherspoon et al., 2014). In addition, TBI improves soil health and increases bird and insect diversity and earthworm distribution (Thevathasan et al., 2012; Wotherspoon et al., 2014). TBI reduces the ecological impacts of agricultural production and creates more biodiverse and sustainable land-use systems (Thevathasan and Gordon, 2004; Wotherspoon et al., 2014; Thevathasan et al., 2012).

Green infrastructure functions

Green infrastructure provides a comprehensive solution to address key climate change impacts, including air pollution; rising temperatures and extreme heat; flooding; and biodiversity and habitat loss. Green infrastructure also reduces GHG emissions from the built environment and enhances carbon sequestration capacity. In addition, applications of green infrastructure technologies can be used to address adverse health effects associated with extreme heat and air pollution. The implementation of

green infrastructure has multiple environmental and health co-benefits for communities, especially those within urban deserts, where it can reduce the impacts of climate change and the associated burden of illness. In addition, the application of green infrastructure technologies can increase both health and environmental equity across communities in the face of a changing climate.

This review has categorized green infrastructure applications into five areas: green roofs, green walls, urban vegetation and forestry, urban agriculture systems (UA) systems, and tree-based intercropping (TBI) systems. Although the application of green infrastructure provides a mechanism for addressing climate change, each application is a complex climate change intervention with unique characteristics and multiple co-benefits that can be leveraged if strategically applied. There are common functions shared between green infrastructure applications as illustrated in Fig. 2, whereas others are exclusive to particular applications. Key functions include air pollution abatement; temperature regulation; and carbon sequestration. Other functions include increased biodiversity and pollinator support, building energy efficiency, and stormwater management.

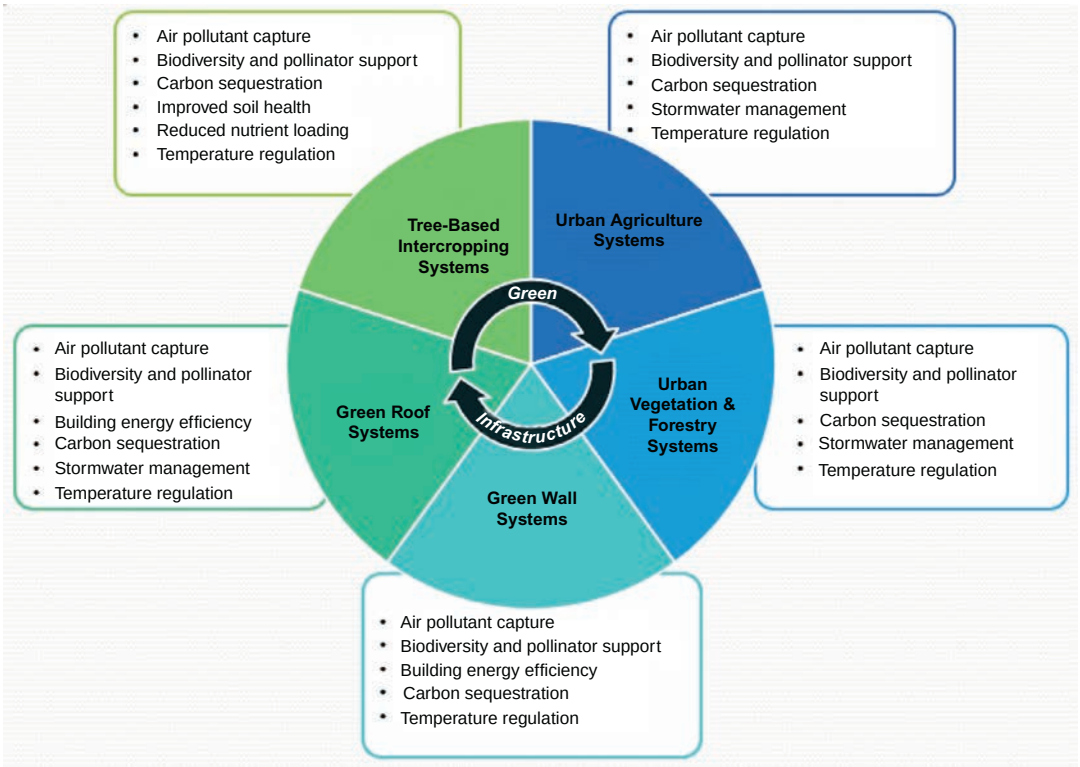

FIG. 2

Green infrastructure form and function.

Reproduced from Anderson, V., 2018. Dissertation: Deep Adaptation: A Framework for Climate Resilience, Decarbonization and Planetary Health in Ontario, University of Toronto. https://tspace.library.utoronto.ca/.

Air pollution abatement

The application of green infrastructure in its various forms can reduce air pollution. Ambient air pollution is a complex mixture of contaminants, including ground-level ozone (O_3), fine particulate matter ($PM_{2.5}$), nitrogen dioxide (NO_2), sulfur dioxide (SO_2), carbon monoxide (CO), and TRS compounds. Various types of vegetation can capture both gaseous and particulate matter pollution (Coutts and Hahn, 2015). Pollution removal of gases occurs through absorption by leaf pores (stomata) and surfaces and by adherence to the surfaces of plants (Hedin, 2000). Particulate matter pollution is removed by deposition on various plant surfaces and can occur through adhesion to the leaf or plant surface at impact or through an adhesive chemical process (Hedin, 2000). Air pollutants can be removed by vegetation through chemical reactions on the surface of a plant when precipitation occurs. Dry deposition occurs when air pollutants are removed by vegetation without precipitation (Coutts and Hahn, 2015). The level of air pollution abatement varies with each green infrastructure application and is influenced by various factors, including location, air flows, physical dimension, type and ratio of vegetation, and seasonal variation.

Green infrastructure affects air quality to varying degrees through deposition and immobilization of local air pollutants such as ozone and particulate matter (Nowak et al., 2006, 2018; Kleerekoper et al., 2012; Rao et al., 2014; King et al., 2014; Gourdji, 2018; Sicard et al., 2018). Studies have shown that the application of green infrastructure can remove air pollutants, including ozone, nitrogen dioxide, and particulate matter (Nowak et al., 2006, 2018; Yang et al., 2008; Baik et al., 2012; King et al., 2014; Rao et al., 2014; Gourdji, 2018; Sicard et al., 2018; Anderson and Gough, 2020). Other applications of green infrastructure, such as urban vegetation strategies like tree and shrub plantings in urban corridors, have also been shown to be effective in the immobilization of particulates and improvement of air quality (Nowak et al., 2006, 2018; Hall et al., 2011; Weber et al., 2014; Abjijith et al., 2017; Abjihith and Kumar, 2019). Although trees have demonstrated the highest uptake of air pollutants, combining green infrastructure applications like tree planting, green roofs, and green walls can be beneficial as they have greater potential to mitigate point source air pollution in industrial areas and require less space than trees (Jayasooriya et al., 2017). In addition, tree size and continuity of form affect performance (Vos et al., 2013; Bottalico et al., 2016; Nowak et al., 2018). The efficacy of a single tree to reduce air pollution is much less than that of an urban forest. Other forms of urban vegetation such as hedgerows have been shown to improve air quality in street canyons and are particularly effective in filtering particulate matter due to proximity to emission sources (Vos et al., 2013; Gromke et al., 2016; Abjijith et al., 2017; Abjihith and Kumar, 2019). Green roofs have been shown to reduce air pollution with extensive implementation (Speak et al., 2012; Tan and Sia, 2005; Abjijith et al., 2017). Green walls have been shown to be quite effective at reducing air pollution (Jayasooriya et al., 2017; Joshi and Gosh, 2014; Abjijith et al., 2017). Factors influencing efficacy of green infrastructure applications include configuration, wind flows, and orientation and geometry of the streetscape (Janhäll, 2015; Abjijith et al., 2017; Nowak et al., 2018; Abjihith and Kumar, 2019; Taleghani et al., 2020).

Temperature regulation

The application of green infrastructure in its various forms can reduce air and surface temperature through shading and evapotranspiration, which occurs when water moves from the earth to the atmosphere as it evaporates from the soil and other surfaces and from plant transpiration. Evaporation occurs

with the movement of water from damp soil and vegetation. Transpiration occurs when water moves through plants along with nutrients. The combined process of evapotranspiration is energy driven and is amplified by temperature, radiation, and airflow. Temperature regulation varies with each green infrastructure application and is influenced by various factors, including location, climate, irrigation, physical dimension, type and ratio of vegetation, and seasonal variation.

Various green roof phenomena work together to regulate temperature. Foliage provides shading, enables thermal heat exchange, and absorbs thermal energy as part of photosynthesis, whereas soil and vegetation promote cooling through evaporation and transpiration (Berardi et al., 2014). Green roofs can also reflect up to 30% of solar radiation and absorb up to 60% through photosynthesis (Berardi et al., 2014). The application of a green roof reduces thermal loading (Li and Yeung, 2014). A key factor in a green roof's ability to regulate temperature is the abundance of vegetation (Weng et al., 2004). Maximizing surface area cover is integral (Morakinyo et al., 2017). Green walls regulate temperature through shading, reducing reflected heat, and evapotranspiration (Alexandri and Jones, 2006; Demuzere et al., 2014; Elgizawy, 2016). Temperature increases can be prevented by the application of green wall technology when significant quantities of solar radiation are transformed into latent heat as a result of evapotranspiration (Sheweka and Mohamed, 2012). During the summer season, the application of a green wall can protect exterior walls from intense solar radiation and can both reflect and absorb up to 80% of radiation within its foliage (Sheweka and Mohamed, 2012). The application of vegetation and foliage to building facades has been shown to decrease surface temperature (Hoelscher, 2016; Schettini et al., 2016). Combining both green roof and green wall applications increases overall efficacy (Alexandri and Jones, 2006). Green roofs and urban vegetation have the capacity to function as an effective urban heat island mitigation strategy through their cooling effect on the urban microclimate (Wang et al., 2016; Berardi, 2016; Jandaghian and Berardi, 2019). Urban vegetation and forestry have been shown to be particularly effective in regulating temperature. Trees provide shade cover that cools the air temperature below (Bowler et al., 2010). Denser tree cover can provide further reductions in temperature (Bowler et al., 2010). Trees also reduce temperature through evapotranspiration. The cooling capacity of a single tree on a sunny day is equivalent to 20–30 kW (Kleerekoper et al., 2012). UA systems can also regulate temperature depending on ratio of vegetation and depth of soil or substrate (Lin et al., 2015).

Carbon reduction and sequestration

The application of green infrastructure in its various forms can provide carbon sequestration capacity, create urban carbon sinks, and reduce the carbon footprint of urbanized and developed landscapes. Green infrastructure removes carbon dioxide from the atmosphere through photosynthesis during daylight hours, whereas there is a subsequent release of carbon dioxide through respiration at nighttime with additional carbon uptake occurring through soil and below ground biomass (Demuzere et al., 2014). Carbon reduction and sequestration varies with each green infrastructure application and is influenced by various factors, including climate, location, air flow, type and ratio of vegetation, depth of soil or substrate, soil health, and landscape management. A green roof can sequester carbon in its vegetated layer and in the organic substrate (Whittinghill et al., 2014). Both intensive and extensive green roofs have been shown to be effective in sequestering carbon using different plant varietals, including herbaceous perennials, grasses, vegetables, and herb plants (Whittinghill et al., 2014). Roofs with deeper substrates sequester more carbon (Whittinghill et al., 2014). A green wall can sequester

carbon in the foliage, plant tissues, and biomass (Marchi et al., 2014). Urban vegetation and forestry sequester the most carbon as the majority is stored in the biomass produced by leaves and greenery, woody branches, and roots (Velasco et al., 2016).

Carbon that is stored in wood can be retained for many years and even centuries in a live tree. Carbon that is stored in leaves, greenery, and fine roots has a much shorter retention time (Velasco et al., 2016). TBI systems have been shown to be effective in providing carbon sequestration capacity in comparison to conventional cropping systems because of their ability to store carbon in permanent tree components and their greater sequestration capacity (Thevathasan et al., 2012). TBI systems act as carbon sinks because of the increased carbon storage in the biomass of the trees, the slower decomposition of litter, and the stabilization of soil organic carbon (Montagnini and Nair, 2004; Peichl et al., 2006). TBI systems demonstrate higher soil-organic carbon content than conventional cropping systems (Wotherspoon et al., 2014).

Stormwater management

The application of green infrastructure in its various forms can manage stormwater, reduce flood risk, and reduce runoff and nutrient loading. Green infrastructure can manage stormwater by providing water storage during rainfall events, reducing overland flows, and preventing sediment erosion and nutrient loading. Stormwater management varies with each green infrastructure application and is influenced by various factors, including location, proximity to impervious surfaces, depth of soil or substrate, and type and ratio of vegetation. Green roofs reduce stormwater runoff from 50% to 100% depending on the depth of the substrate, roof slope, and plant species (Rowe, 2011). Green roofs retain stormwater in the substrate, which evapotranspires back into the atmosphere (Rowe, 2011). Water that is discharged from the green roof is delayed by the time required to fully saturate the substrate and eventually drain. This can reduce the burden on municipal stormwater systems by preventing sewer overflow and potential downstream erosion (Rowe, 2011). Urban vegetation and forestry provide permeable surface for bioinfiltration, which enables both evapotranspiration and groundwater recharge (Ellis, 2013). In addition, urban vegetation and forestry can reduce overland flows and discharges to receiving water bodies (Ellis, 2013). TBI systems provide a buffer to reduce runoff and nutrient loading from agricultural fields to nearby water bodies (Plascencia-Escalante, 2008). UA systems reduce impervious surfaces, retain stormwater, and increase infiltration (Lin et al., 2015).

Biodiversity and pollinator support

The application of green infrastructure in its various forms can enhance biodiversity and provide pollinator habitat which varies with each application and is influenced by different factors. Pollinators are essential in modern industrial agriculture for the production of food. Green infrastructure provides essential habitat to support pollination services specifically provided by bees with an estimated economic value of $15–40 Billion USD annually (Coutts and Hahn, 2015). Provision of biodiversity and pollinator support varies with each green infrastructure application and is influenced by various factors, including climate, location, plant diversity, depth of soil or substrate, and type and ratio of vegetation. TBI systems improve soil health and increase bird and insect diversity and earthworm distribution (Thevathasan et al., 2012; Wotherspoon et al., 2014). TBI also reduces the ecological impacts of agricultural production and creates more biodiverse and sustainable land-use systems (Thevathasan and

Gordon, 2004; Wotherspoon et al., 2014; Thevathasan et al., 2012). Green roofs provide habitat for various insect species, as well as space for nesting birds and native avian communities (Oberndorfer et al., 2007). Green roofs play an increasingly important role in converting underutilized space to supportive habitat for urban wildlife and pollinators (Parkins and Clark, 2015). Green roofs have been shown to provide roosts and foraging habitat for urban bats (Parkins and Clark, 2015). Green roofs with greater plant diversity and proximity to other greenspace within the surrounding landscape have also been shown to provide supportive habitat to native bees (Tonietto et al., 2011). Green walls can provide habitat for birds, bees, and other insects (Francis, 2010). Green wall structure and plant species are factors in constructing hospitable habitat (Francis, 2010). Urban vegetation and forestry provide habitat for various types of wildlife by reducing landscape fragmentation and increasing connectivity to the natural environment. UA systems also support pollinator and bird habitat (Lin et al., 2015). In addition, green infrastructure provides habitat for biological control agents that prey on crop pests wherein plants themselves are used to diversify crops and chemically repel pests (Hillel and Rosenzweig, 2008; Coutts and Hahn, 2015; Rosenzweig, 2015). This is accomplished by visually camouflaging crops and diluting attractive stimuli (Coutts and Hahn, 2015).

Building energy efficiency

The application of green infrastructure in its various forms can increase building energy efficiency. Green infrastructure increases building efficiency by decreasing the cooling and heating loads of buildings through the provision of shade and insulation against temperature extremes and through the combined effect of decreased solar heat gains from urban surfaces and decreased air temperature to reduce the cooling energy demand (Demuzere et al., 2014; Berardi, 2016; Jandaghian and Berardi, 2019). Building energy efficiency varies with each green infrastructure application and is influenced by various factors, including location, climate, irrigation, physical dimension, type and ratio of vegetation, seasonal variation, and building insulation. Green roofs increase building efficiency by improving rooftop insulation, providing shade, cooling the air through evapotranspiration, and reducing energy use through natural cooling and insulation (Jaffal et al., 2012; Demuzere et al., 2014; Cascone et al., 2018). Green walls also increase building efficiency by providing shade, protecting exterior walls from intense solar radiation, and cooling the air through evapotranspiration (Alexandri and Jones, 2006; Sheweka and Mohamed, 2012; Elgizawy, 2016; Hoelscher et al., 2016).

Green infrastructure benefits

Over and above its inherent physical benefits, green infrastructure also provides socioeconomic benefits. Green infrastructure can support physical activity and active participation through the provision of multifunctional greenspace such as nature trails and parklands. Green infrastructure in the form of UA systems can also enhance food security by reducing the food miles associated with conventional agriculture through localized food production and distribution from growing roofs to rooftop, terrace, backyard, and community gardens to food forests. These systems can reduce the pressures on conventional agriculture and can improve food security when large-scale agricultural production is affected by

weather variation. In addition, green infrastructure has demonstrated economic and health benefits. These benefits are significant within the broader context of climate change.

Economic benefits

The application of green infrastructure in its various forms has economic benefits. Green infrastructure can improve property values, in addition to reducing the costs of stormwater management, air pollution, and electricity. Energy savings from green roofs range from 15% to 45% of annual energy consumption from reduced cooling costs (CCAP, 2011; Demuzere et al., 2014; Cascone et al., 2018). Trees and vegetation can increase property values with increases ranging from 30% to 37% (CCAP, 2011). In addition, inclusion of green infrastructure within traditional stormwater asset portfolios can save up to 94% of life cycle costs (Berardi, 2016; Jandaghian and Berardi, 2019; Xu et al., 2019). For example, a cost-benefit analysis of street trees in five US cities found an annual benefit of $2–4 CAD for every dollar spent on tree management (GIO, 2020). An analysis conducted by the TD Bank found a benefit of $1–3 CAD for every dollar spent on urban forestry in Toronto, Ontario, Canada (TD Economics, 2014). The value of air pollution abatement by urban trees in the United States is estimated at $4 Billion USD with the removal of 711,000 metric tons of pollutants annually (Nowak, 2006; Coutts and Hahn, 2015), whereas trees in 86 Canadian cities removed 16,500 tons of air pollution with human health effects valued at approximately $227 Million CAD (Nowak et al., 2018).

Health benefits

The application of green infrastructure in its various forms has health benefits. Green infrastructure provides ecosystem services fundamental to health and well-being, including the provision of clean drinking water, food, breathable air, climate regulation, and natural resources for shelter, clothing, medicine, and energy production. There are also direct health co-benefits that result from the application of green infrastructure. Algae blooms on lakes are becoming an increasingly common sight as is the risk of exposure to cyanobacteria from recreational activities or drinking water from these eutrophic water bodies. Green infrastructure in the form of TBI systems can improve water quality in lakes, rivers, and other tributaries by reducing reliance on pesticides and fertilizers associated with conventional agricultural practices (Thevathasan and Gordon, 2004; Wotherspoon et al., 2014). Green infrastructure applications have also been shown to improve respiratory health outcomes from extreme heat and air pollution (Nowak et al., 2006, 2018; Tzoulas et al., 2007; Susca et al., 2011; Liang et al., 2014; Chen et al., 2014; King et al., 2014; Rao et al., 2014). For example, green roofing and green wall technologies have been shown to reduce air pollutant concentrations and provide urban cooling (Speak et al., 2012; Kessler, 2013; Anderson and Gough, 2020). Exposure to urban vegetation and forestry contributes to improved postoperative outcomes for patients recovering from surgery (Ulrich, 1984). Human panel studies have shown that exposure to urban vegetation and forestry can reduce blood pressure, heart rate, and stress while increasing parasympathetic nerve activity and restoration and improving immune response (Lee et al., 2014; Song et al., 2016; Jo et al., 2019). Various cohort studies have also linked residential green infrastructure to reduced mortality from cardiovascular, respiratory, and other causes (Crouse et al., 2018; James et al., 2016; Vienneau et al., 2017; Villeneuve et al., 2012). Green

infrastructure is also essential in reducing the risk of infectious disease spread by providing habitat for vector and zoonotic reservoir populations (Coutts and Hahn, 2015). There is growing recognition that landscape fragmentation, land-use development patterns, and green infrastructure behave as barriers to or conduits for disease amplification and spread in human, domestic animal, and wildlife populations (Defries et al., 2004; Goldberg et al., 2008; Ostfeld et al., 2008; Gottdenker et al., 2014; Coutts and Hahn, 2015).

Green infrastructure nomenclature

Although a rose by any other name may smell just as sweet, terminology defines how green infrastructure is perceived and how it will be used. Identification has implications for how we understand, adopt, and prioritize the use of green infrastructure. Monikers have implications for resource decisions and mainstream implementation.

Green infrastructure has been broadly identified (albeit vaguely) as a potential approach to address the impacts of climate change. The Intergovernmental Panel on Climate Change (IPCC) has identified green infrastructure as a mechanism for expanding urban carbon sinks and undertaking ecosystem-based adaptation to transform the built environment through phytoremediation (Revi et al., 2014). In addition, the IPCC has even gone so far as to suggest that green infrastructure (specifically green roofs and TBI systems) has the potential to create synergies between mitigation and adaptation (Smith et al., 2014). The IUCN promotes green infrastructure as a means of protecting biodiversity and enhancing nature's ability to provide ecosystem services (URBES, 2014) with a European Union-wide strategy promoting investments in green infrastructure (European Commission, 2013). The US Environmental Protection Agency narrowly identifies green infrastructure under the *Clean Water Act* legislation as a mechanism to address stormwater (US EPA, 2019). In Canada, at the provincial level, *Ontario's Climate Change Strategy* explicitly referenced green infrastructure as a means to restore ecosystems, reduce atmospheric carbon, and protect and expand carbon sinks (MOECC, 2015). The Strategy also identified the need to develop a coordinated approach to reduce emissions from new and existing buildings and to integrate climate change adaptation considerations into infrastructure decision making (MOECC, 2015). The *Ontario Climate Change Action Plan* identified the enhancement of carbon sinks in agricultural and natural systems and the development of low-carbon communities as key priorities (MOECC, 2015). Following a change in the provincial government in Ontario, Canada, in 2018, the new government released *A Made-in-Ontario Environment Plan* to address climate change and other environmental challenges that also highlights the importance of green infrastructure in lowering GHG emissions, reducing pollution, and helping to make community infrastructure more resilient (MECP, 2018). At the federal level, the Canadian government has identified green infrastructure using varied nomenclature (e.g., natural infrastructure, climate resilient infrastructure, and stormwater management technology) as a priority under its $120 Billion CAD infrastructure plan—*Investing in Canada* (GOC, 2016, 2020). Green infrastructure is recognized as a means of preserving the integrity of the environment and promoting sustainable and healthy community development nationwide (GOC, 2016, 2020). In addition, the Investing in Canada Infrastructure Program is a cost-shared infrastructure funding program between the federal government, provinces and territories, and municipalities and other recipients. Under this program, $30 Billion CAD in combined federal, provincial, and other

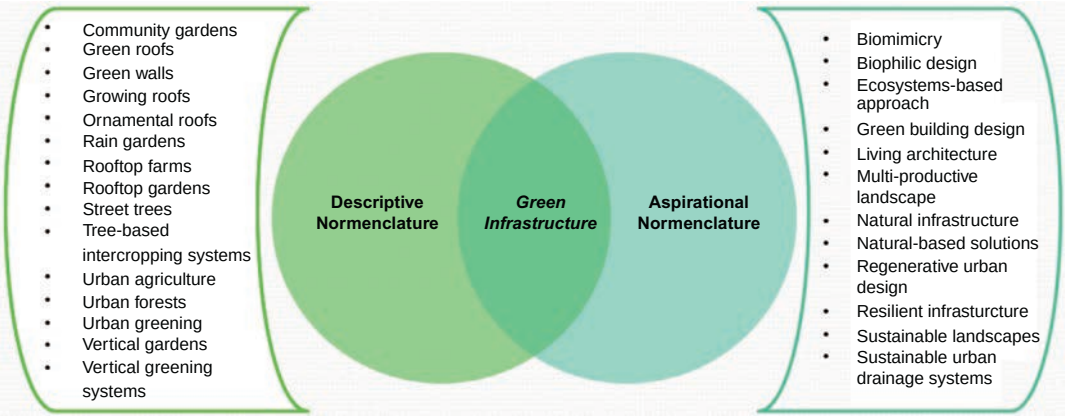

FIG. 3

Examples of green infrastructure nomenclature.

Credit: Anderson, V., 2018. Dissertation: Deep Adaptation: A Framework for Climate Resilience, Decarbonization and Planetary Health in Ontario. University of Toronto. https://tspace.library.utoronto.ca/.

partner funding, has been allocated to four priority areas, including green infrastructure to support the reduction of GHG emissions; enable greater adaptation and resilience to the impacts of climate change and climate-related disaster mitigation; and ensure that communities can provide clean air and safe drinking water (Grant Ontario, 2019).

As this systematic review of green infrastructure was undertaken, it became apparent that green infrastructure terminology is quite variable and follows two different streams of thought. The first stream is descriptive, and the nomenclature is functional and purpose driven. The second stream of nomenclature is aspirational and describes a desired state of being. For the purposes of this review, common green infrastructure terminology has been selected and divided into two distinct categories of either descriptive or aspirational nomenclature. By categorizing the different nomenclature, we can unpack the concept of green infrastructure and how it is translated. Fig. 3 provides examples of the nomenclature and illustrates the different naming conventions.

The descriptive nomenclature for green infrastructure is specific and provides an indication of purpose and function. For example, within the descriptive nomenclature stream, the terms "green walls," "vertical gardens," and "vertical greening systems" can be used interchangeably and describe the shape and type of green infrastructure. The aspirational nomenclature used for green infrastructure is vague, fluid, and may be broadly interpreted. For example, the aspirational moniker 'living architecture' can include green roofs, growing roofs, green walls, ornamental roofs, rooftop farms, rooftop gardens, vertical gardens, and vertical greening systems. The aspirational moniker "sustainable urban drainage systems" is common in the United Kingdom and is also used to describe community gardens, green roofs, green walls, growing roofs, ornamental roofs, street trees, rain gardens, and urban forests (Ellis, 2013; Warwick and Charlesworth, 2013). Table 1 provides a cross-stream translation between descriptive and aspirational nomenclature.

Table 1 Nomenclature comparison.

Descriptive nomenclature	Aspirational nomenclature
Community gardens	Multiproductive landscapes, sustainable landscapes
Green roofs Green walls Growing roofs Ornamental roofs	Biomimicry, biophilic design, ecosystems-based approach, green building design, living architecture, multiproductive landscapes, natural infrastructure, nature-based solutions, regenerative urban design, resilient infrastructure, sustainable landscapes, sustainable urban drainage systems
Rain gardens	Biomimicry, biophilic design, ecosystems-based approach, natural infrastructure, nature-based solutions, regenerative urban design, resilient infrastructure, sustainable landscapes, sustainable urban drainage systems
Rooftop farms	Multiproductive landscapes, sustainable landscapes
Rooftop gardens	Biomimicry, biophilic design, ecosystems-based approach, green building design, living architecture, multiproductive landscapes, natural infrastructure, nature-based solutions, regenerative urban design, resilient infrastructure, sustainable landscapes, sustainable urban drainage systems
Street trees	Ecosystems-based approach, nature-based solutions, regenerative urban design, resilient infrastructure, sustainable landscapes, sustainable urban drainage systems
Urban agriculture	Multiproductive landscapes, regenerative urban design, resilient infrastructure, sustainable landscapes
Urban forests	Ecosystems-based approach, multiproductive landscapes, natural infrastructure, nature-based solutions, regenerative urban design, sustainable landscapes
Urban greening	Ecosystems-based approach, nature-based solutions, regenerative urban design, resilient infrastructure, sustainable landscapes, sustainable urban drainage systems
Vertical gardens	Biomimicry, biophilic design, ecosystems-based approach, green building design, living architecture, nature-based solutions, regenerative urban design, resilient infrastructure
Vertical greening systems	Biomimicry, biophilic design, ecosystems-based approach, green building design, living architecture, nature-based solutions, regenerative urban design, resilient infrastructure
Tree-based intercropping systems	Multiproductive landscapes, sustainable landscapes

Reproduced from Anderson, V., 2018. Dissertation: Deep Adaptation: A Framework for Climate Resilience, Decarbonization and Planetary Health in Ontario. University of Toronto. https://tspace.library.utoronto.ca/.

Conclusions

Without a common lexicon and shared understanding, the pace of uptake and mainstream implementation of green infrastructure will be slow. The differences in nomenclature present a unique challenge for decision makers in whether to adopt green infrastructure as a climate change intervention and allocate resources for its implementation. To facilitate the widespread implementation of green infrastructure, communities and decision makers need guidance and support in evaluating which applications of green infrastructure are most appropriate in addressing the impacts of climate change within individual communities.

Although there is common agreement that green infrastructure is a good thing and that it may provide a mechanism for addressing climate change, what has been missing is a clear understanding of

how green infrastructure works as a complex intervention, its characteristics, and the multiple co-benefits that can be leveraged if green infrastructure is strategically applied. Effective action can only occur if green infrastructure is strategically applied as a complex climate change intervention for mitigation and adaptation. Climate change mitigation as a concept is well-established and mitigation activities are linear. The concept of climate change adaptation is not as well understood. Interventions to moderate harm or exploit beneficial opportunities can be singular, interdependent, or complex such that an activity or intervention may perform the dual function of both adaptation and mitigation. Climate change adaptation actions and interventions range from installing backflow valves to prevent basement flooding, to hardening shorelines against erosion, to heat warning systems to reduce the health impacts of heat waves, to greywater reuse systems for water conservation. Green infrastructure can provide a nature-based solution to bridge the gap between these mitigation and adaptation actions.

Green infrastructure plays a critical role in a changing climate. The impacts of climate change are becoming increasingly apparent across all sectors of society. Finding ways of adapting to and mitigating the impacts of climate change is an issue of concern that transcends geographic, social, and political boundaries. Green infrastructure can provide practical and accessible solutions to address the impacts of climate change on society. The purpose of this chapter is to provide a comprehensive understanding of how green infrastructure works as a complex intervention, its characteristics, the metrics for performance, and the multiple co-benefits that can be leveraged if green infrastructure is strategically applied. The most effective applications of green infrastructure will address multiple issues, including economic costs and human health. With a systematic accounting of the applications, functions, and benefits of green infrastructure, this may stimulate communities and decision makers to adopt green infrastructure as a standard climate change intervention.

References

Abjihith, K.V., Kumar, P., 2019. Field investigations for evaluating green infrastructure effects on air quality in open-road conditions. Atmos. Environ. 201, 132–147.

Abjijith, K.V., et al., 2017. Air pollution abatement performances of green infrastructure in open road and built-up street canyon environments—a review. Atmos. Environ. 162, 71–86.

Alexandri, E., Jones, P., 2006. Temperature decreases in an urban canyon due to green walls and green roofs in diverse climates. Build. Environ. 43, 480–493.

Anderson, V., Gough, W.A., 2020. Evaluating the Potential of Nature-Based Solutions to Reduce Ozone, Nitrogen Dioxide, and Carbon Dioxide through a Multi-Type Green Infrastructure Study in Ontario, Canada. City and Environment Interactions, (in press).

Baik, J., Kwak, K., Park, S., Ryu, Y., 2012. Effects of building roof greening on air quality in street canyons. Atmos. Environ. 61, 48–55. https://doi.org/10.1016/j.atmosenv.2012.06.076.

Berardi, U., 2016. The outdoor microclimate benefits and energy saving resulting from green roofs retrofits. Energy Build. 121, 217–229. https://doi.org/10.1016/j.enbuild.2016.03.021.

Berardi, U., AmirHosein, G.H., Ali, G., 2014. State-of-the-art analysis of the environmental benefits of green roofs. Appl. Energy 115, 411–428.

Bottalico, F., et al., 2016. Air pollution removal by green infrastructures and urban forests in the city of Florence. Agric. Agric. Sci. Procedia 8, 243–251.

Bowler, D.E., Buyung-Ali, L., Knight, T.M., Pullin, A.S., 2010. Urban greening to cool towns and cities: a systematic review of the empirical evidence. Landsc. Urban Plan. 97 (3), 147–155. https://doi.org/10.1016/j.landurbplan.2010.05.006.

Cascone, S., et al., 2018. A comprehensive study in green roof performance for retrofitting existing buildings. Build. Environ. 136, 227–239.

Chen, D., Wang, X., Thatcher, M., Barnett, G., Kachenko, A., 2014. Urban vegetation for reducing heat related mortality. Environ. Pollut. 192, 275–284. https://doi.org/10.1016/j.envpol.2014.05.002.

Cohen-Shacham, E., Walters, G., Janzen, C., Maginnis, S. (Eds.), 2016. Nature-Based Solutions to Address Global Societal Challenges., ISBN: 978-2-8317-1812-5, p. 97, https://doi.org/10.2305/IUCN.CH.2016.13.en. Gland, Switzerland: IUCN. xiii +.

Cohen-Shacham, E., Andrade, A., Dalton, J., Dudley, N., Jones, M., Kumar, C., Maginnis, S., Maynard, S., Nelson, C.R., Renauda, F.G., Welling, R., Walters, G., 2019. Core principles for successfully implementing and upscaling nature-based solutions. Environ. Sci. Policy 98, 20–29.

Coutts, C., Hahn, M., 2015. Green infrastructure, ecosystem services, and human health. Int. J. Environ. Res. Public Health 12 (8), 9768–9798. https://doi.org/10.3390/ijerph120809768.

Crouse, D.L., Pinault, L., Balram, A., Hystad, P., Peters, P.A., Chen, H., van Donkelaar, A., Martin, R.V., Ménard, R., Robichaud, A., et al., 2018. Urban greenness and mortality in Canada's largest cities: a national cohort study. Lancet Planet. Health. 1, e289–e297. https://doi.org/10.1016/S2542-5196(17)30118-3.2.

Defries, R.S., Foley, J., Asner, G., 2004. Land-use choices: balancing human needs and ecosystem function. Front. Ecol. Environ. 2, 249–257. https://doi.org/10.1890/1540-9295(2004)002[0249,LCBHNA]2.0.CO;2.

Demuzere, M., et al., 2014. Mitigating and adapting to climate change: multi-functional and multi-scale assessment of green urban infrastructure. J. Environ. Manag. 146, 107–115. https://doi.org/10.1016/j.jenvman.2014.07.025.

Elgizawy, E., 2016. The effect of green facades in landscape ecology. Procedia Environ. Sci. 34, 119–130.

Ellis, J.B., 2013. Sustainable surface water management and green infrastructure in UK urban catchment planning. J. Environ. Plan. Manag. 56 (1), 26–41.

European Commission, 2013. Green Infrastructure (GI)—Enhancing Europe's Natural Capital. https://eur-lex.europa.eu/resource.html?uri=cellar:d41348f2-01d5-4abe-b817-4c73e6f1b2df.0014.04/DOC_1&format=PDF.

Feng, H., Hewage, K., 2014. Lifecycle assessment of living walls: air purification and energy performance. Clean. Prod. 69, 91–99. https://doi.org/10.1016/j.jclepro.2014.01.041.

Francis, R., 2010. Wall ecology: a frontier for urban biodiversity and ecological engineering. Prog. Phys. Geogr. 35 (1), 43–63.

Goldberg, T.L., Gillespie, T.R., Rwego, I.B., Estoff, E.L., Chapman, C.A., 2008. Forest fragmentation as cause of bacterial transmission among nonhuman primates, humans, and livestock, Uganda. Emerg. Infect. Dis. 14 (9), 1375–1382.

Gottdenker, N.L., Streicker, D.G., Faust, C.L., Carroll, C.R., 2014. Anthropogenic land use change and infectious diseases: a review of the evidence. EcoHealth 11, 619–632. https://doi.org/10.1007/s10393-014-0941-z.

Gourdji, S., 2018. Review of plants to mitigate particulate matter, ozone as well as nitrogen dioxide air pollutants and applicable recommendations for green roofs in Montreal, Quebec. Environ. Pollut. 241, 378–387.

Government of Canada, 2016. Statement Regarding the Government of Canada's Budget 2016 Support for Green Infrastructure. http://news.gc.ca/web/article-en.do?nid=1046989.

Government of Canada, 2020. Investing in Green Infrastructure. https://www.infrastructure.gc.ca/plan/gi-iv-eng.html.

Grant Ontario, 2019. Investing in Canada Infrastructure Program: Green Stream. https://www.grants.gov.on.ca/GrantsPortal/en/OntarioGrants/GrantOpportunities/PRDR020120.

Green Infrastructure Ontario (GIO) Coalition, 2020. An Economic Impact Assessment of the Green Infrastructure Sector in Ontario. https://greeninfrastructureontario.org/app/uploads/2020/07/Economic-Impact-Assessment-of-GI-Sector-in-Ontario_UPDATED_july20-20.pdf.

Gromke, C., et al., 2016. Influence of roadside hedgerows on air quality in urban street canyons. Atmos. Environ. 139, 75–86.
Hall, J.M., Handley, J.F., Ennos, A.R., 2011. The Potential of Tree Planting to Climate-Proof High Density Residential Areas in Manchester, UK. Landscape and Urban Planning.
Hayati, H., Sayadi, M.H., 2012. Impact of tall buildings in environmental pollution. Environ. Skeptics Critics 1 (1), 8–11. Retrieved from http://search.proquest.com/docview/1367489826?accountid=14771.
Health Canada, 2005. Your Health and a Changing Climate.
Hedin, L., 2000. Deposition of nutrients and pollutants to ecosystems. In: Sala, O.E., Jackson, R.B., Mooney, H.A., Howarth, R.W. (Eds.), Methods in Ecosystem Science. Springer-Verlag, New York, NY, pp. 265–276.
Hillel, D., Rosenzweig, C., 2008. Biodiversity and food production. In: Chivian, E., Bernstein, A. (Eds.), Sustaining Life: How Human Health Depends on Biodiversity. Oxford University Press, New York, NY, pp. 325–381.
Hoelscher, M.T., et al., 2016. Quantifying cooling effects of façade greening: shading, transpiration and insulation. Energy Build. 114, 283–290.
IPCC, 2007. In: Solomon, S., Qin, D., Manning, M., Chen, Z., Marquis, M., Averyt, K.B., Tignor, M., Miller, H.L. (Eds.), Climate Change 2007: The physical Science basis. Contribution of Working Group I to the Fourth Assessment Report of the Intergovernmental Panel on Climate Change. Cambridge University Press, Cambridge, United Kingdom and New York, NY, USA. 996 pp.
Jaffal, I., et al., 2012. A comprehensive study of the impact of green roofs in building energy performance. Renew. Energy 43, 157–164.
James, P., Hart, J.L., Banay, R.F., Laden, F., 2016. Exposure to greenness and mortality in a nationwide prospective cohort study of women. Environ. Health Perspect. 124 (9), 1344–1352. https://doi.org/10.1289/ehp.1510363.3.
Jandaghian, Z., Berardi, U., 2019. Analysis of the cooling effects of higher albedo surfaces during heat waves coupling the weather research and forecasting model with building energy models. Energy Build. 207, 109627. https://doi.org/10.1016/j.enbuild.2019.109627.
Janhäll, S., 2015. Review on urban vegetation and particle air pollution—deposition and dispersion. Atmos. Environ. 105, 130–137.
Jayasooriya, V.M., Ng, A.W., Muthukumaran, S., Perera, B.J., 2017. Green infrastructure practices for improvement of urban air quality. Urban For. Urban Green. 21.
Jo, H., Song, C., Miyazaki, Y., 2019. Physiological benefits of viewing nature: a systematic review of indoor experiments. Int. J. Environ. Res. Public Health 16 (23), 4739. https://doi.org/10.3390/ijerph16234739.
Joshi, S., Gosh, S., 2014. On the air cleansing efficiency of an extended green wall: a CFD analysis of mechanistic details of transport processes. J. Theor. Biol. 361, 101–110. https://doi.org/10.1016/j.jtbi.2014.07.018.
Kessler, R., 2013. Urban gardening: managing the risks of contaminated soil. Environ. Health Perspect. 121 (11−12), 326–333.
King, K., Johnson, S., Kheirbek, I., Lu, J., Matte, T., 2014. Differences in magnitude and spatial distribution of urban forest pollution deposition rates, air pollution emissions, and ambient neighborhood air quality in New York City. Landsc. Urban Plan. 128, 14–22.
Kleerekoper, L., van Esch, M., Salcedo, T.B., 2012. How to make a city climate-proof, addressing the urban heat island effect. Resour. Conserv. Recycl. 64, 30–38. https://doi.org/10.1016/j.resconrec.2011.06.004.
Lee, J., et al., 2014. Influence of forest therapy on cardiovascular relaxation in young adults. Evid. Based Complement. Alternat. Med. https://doi.org/10.1155/2014/834360.
Lennon, M., Scott, M., Oneill, E., 2014. Urban Design and adapting to flood risk: the role of green infrastructure. J. Urban Des. 19, 745–758.
Li, W.C., Yeung, K.K.A., 2014. A comprehensive study of green roof performance from environmental perspective. Int. J. Sustain. Built Environ. 3, 127–134.

Li, J., Wai, O.W.H., Li, Y.S., Zhan, J., Ho, Y.A., Li, J., Lam, E., 2010. Effect of green roofs on ambient CO_2 concentration. Build. Environ. 45 (12), 2644–2651. https://doi.org/10.1016/j.buildenv.2010.05.025.

Liang, T.C., Wong, N.H., Jusuf, S.K., 2014. Effects of vertical greenery on mean radiant temperature in the tropical urban environment. Landsc. Urban Plan. 127, 52–64.

Lin, B., Philpott, S.M., Jia, S., 2015. The future of urban agriculture and biodiversity-ecosystem services: challenges and next steps. Basic Appl. Ecol. 16 (3), 189–201. https://doi.org/10.1016/j.baae.2015.01.005.

Lucon, O., Ürge-Vorsatz, D., Zain Ahmed, A., Akbari, H., Bertoldi, P., Cabeza, L.F., Eyre, N., Gadgil, A., Harvey, L.D.D., Jiang, Y., Liphoto, E., Mirasgedis, S., Murakami, S., Parikh, J., Pyke, C., Vilariño, M.V., 2014. Buildings. In: Edenhofer, O., Pichs-Madruga, R., Sokona, Y., Farahani, E., Kadner, S., Seyboth, K., Minx, J.C. (Eds.), Climate Change 2014: Mitigation of Climate Change. Contribution of Working Group III to the Fifth Assessment Report of the Intergovernmental Panel on Climate Change. Cambridge University Press, Cambridge and New York, NY.

Marchi, M., Pulselli, R.M., Marchettini, N., Pulselli, F.M., 2014. Carbon dioxide sequestration model of a vertical greenery system. Ecol. Model.

Montagnini, F., Nair, P., 2004. Carbon sequestration: an underexploited environmental benefit of agroforestry systems. Agrofor. Syst. 61, 281.

Morakinyo, T.E., et al., 2017. Temperature and cooling demand reduction by green-roof types in different climates and urban densities: a co-simulation parametric study. Energy Build. 145, 226–237.

Nowak, D., Crane, D., Stevens, J.C., 2006. Air pollution removal by urban trees and shrubs in the United States. Urban For. Urban Green. 4, 115–123.

Nowak, D.J., Hirabayashi, S., Doyle, M., McGovern, M., Pasher, J., 2018. Air pollution removal by urban forests in Canada and its effect on air quality and human health. Urban For. Urban Green. 29, 40–48.

Oberndorfer, E., et al., 2007. Green roofs as urban ecosystems: ecological structures, functions, and services. BioScience 57 (10), 823–833.

Ontario Ministry of the Environment and Climate Change, 2015. Ontario's Climate Change Strategy. https://docs.ontario.ca/documents/4928/climate-change-strategy-en.pdf.

Ontario Ministry of the Environment, Conservation, & Parks, 2018. A Made-in-Ontario Environment Plan. https://prod-environmental-registry.s3.amazonaws.com/2018-11/EnvironmentPlan.pdf.

Ostfeld, R.S., Keesing, F., Eviner, V., 2008. Infectious Disease Ecology: Effects of Ecosystems on Disease and of Disease on Ecosystems. Princeton University Press, Princeton, NJ.

Parkins, K.L., Clark, J.A., 2015. Green roofs provide habitat for urban bats. Glob. Ecol. Conserv. 4, 349–357.

Peichl, M., Thevathasan, N.V., Gordon, A.M., Huss, J., Abohassan, R.A., 2006. Carbon sequestration potentials in temperate tree-based intercropping systems, Southern Ontario, Canada. Agrofor. Syst. 66, 243–257.

Plascencia-Escalante, F., 2008. An Analysis of some Components of the Nitrogen Cycle as Affected by Land Use Adjacent to the Riparian Zone of a Southern Ontario Stream. Ph.D, University of Guelph, Guelph, ON.

Rao, M., George, L., Rosenstiehl, T.N., Shandas, V., Dinno, A., 2014. Assessing the relationship among urban trees, nitrogen dioxide, and respiratory health. Environ. Pollut. 194, 96–104.

Revi, A., Satterthwaite, D.E., Aragón-Durand, F., Corfee-Morlot, J., Kiunsi, R.B.R., Pelling, M., Roberts, D.C., Solecki, W., 2014. Urban areas. In: Field, C.B., Barros, V.R., Dokken, D.J., Mach, K.J., Mastrandrea, M.D., Bilir, T.E., White, L.L. (Eds.), Climate Change 2014: Impacts, Adaptation, and Vulnerability. Part A: Global and Sectoral Aspects. Contribution of Working Group II to the Fifth Assessment Report of the Intergovernmental Panel on Climate Change. Cambridge University Press, Cambridge and New York, NY, pp. 535–612.

Rosenzweig, M.L., 2015. Green roofs: new ecosystems to defend species diversity. Israel J. Ecol. Evol. 62, 7–14.

Rowe, D.B., 2011. Green roofs as a means of pollution abatement. Environ. Pollut. 159 (8–9), 2100–2110. https://doi.org/10.1016/j.envpol.2010.10.029.

Schettini, E., et al., 2016. Green control of microclimate in buildings. Agric. Agric. Sci. Procedia 8, 576–582.

Seddon, N., Chausson, A., Berry, P., Girardin, C.A.J., Smith, A., Turner, B., 2020. Understanding the value and limits of nature-based solutions to climate change and other global challenges. Philos. Trans. R. Soc. B 375, 20190120. https://doi.org/10.1098/rstb.2019.0120.

Sheweka, S., Mohamed, N.M., 2012. Green facades as a new sustainable approach towards climate change. Energy Procedia 18, 507–520.

Sicard, P., Agathokleous, E., Araminiene, V., Carrari, E., Hoshika, Y., De Marco, A., Paoletti, E., 2018. Should we see urban trees as effective solutions to reduce increasing ozone levels in cities? Environ. Pollut. 243, 163–176.

Smith, K.R., Woodward, A., Campbell-Lendrum, D., Chadee, D.D., Honda, Y., Liu, Q., Olwoch, J.M., Revich, B., Sauerborn, R., 2014. Human health: impacts, adaptation, and co-benefits. In: Field, C.B., Barros, V.R., Dokken, D.J., Mach, K.J., Mastrandrea, M.D., Bilir, T.E., White, L.L. (Eds.), Climate Change 2014: Impacts, Adaptation, and Vulnerability. Part A: Global and Sectoral Aspects. Contribution of Working Group II to the Fifth Assessment Report of the Intergovernmental Panel on Climate Change. Cambridge University Press, Cambridge and New York, NY, pp. 709–754.

Song, C., Ikei, H., Miyazaki, Y., 2016. Physiological effects of nature therapy: a review of the research in Japan. Int. J. Environ. Res. Public Health 13 (8), 781. https://doi.org/10.3390/ijerph13080781.

Speak, A.F., Rothwell, J.J., Lindley, S.J., Smith, C.L., 2012. Urban particulate pollution reduction by four species of green roof vegetation in a UK city. Atmos. Environ. 61, 283–293.

Susca, T., Gaffin, Dell'Osso, G.R., 2011. Positive effects of vegetation: urban heat island and green roofs. Environ. Pollut. 159 (8–9), 2119–2126. https://doi.org/10.1016/j.envpol.2011.03.007.

Taleghani, M., Clark, A., Swan, W., Mohegh, A., 2020. Air pollution in a microclimate; the impact of different green barriers on the dispersion. Sci. Total Environ. 711, 134649.

Tan, P.Y., Sia, A., 2005. A pilot green roof research project in Singapore. In: Proceedings of Third Annual Greening Rooftops for Sustainable Communities Conference, Awards and Trade Show, Washington, DC, May 4–6.

TD Economics, 2014. Urban Forests: The Value of Trees in the City of Toronto. https://www.td.com/document/PDF/economics/special/UrbanForests.pdf.

The Centre for Clean Air Policy (CCAP), 2011. The Value of Green Infrastructure for Urban Climate Adaptation. http://ccap.org/assets/The-Value-of-Green-Infrastructure-for-Urban-Climate-Adaptation_CCAP-Feb-2011.pdf.

Thevathasan, N.V., Gordon, A.M., 2004. Ecology of tree intercropping systems in the north temperate region: experiences from southern Ontario, Canada. Agrofor. Syst. 61, 257–268.

Thevathasan, N.V., et al., 2012. Agroforestry research and development in Canada: the way forward in agroforestry—the future of global land use. In: Advances in Agroforestry. 9. Springer Science, https://doi.org/10.1007/978-94-007-4676-3_15.

Thornbush, M.J., 2015a. Vehicular Air Pollution and Urban Sustainability: An Assessment from Central Oxford, UK. Springer Briefs in Geography.

Thornbush, M.J., 2015b. Urban agriculture in the transition to low carbon cities through urban greening. AIMS Environ. Sci. 2 (3), 852–867. https://doi.org/10.3934/environsci.2015.3.852.

Tonietto, R., et al., 2011. A comparison of bee communities of Chicago green roofs, parks and prairies. Landsc. Urban Plan. 103, 102–108.

Tzoulas, K., Korpela, K., Venn, S., Yli-Pelkonen, V., Kazmierczak, A., Niemela, J., James, P., 2007. Promoting ecosystem and human health in urban areas using green infrastructure: a literature review. Landsc. Urban Plan. 81 (3), 167–178. https://doi.org/10.1016/j.landurbplan.2007.02.001.

Ulrich, R.S., 1984. View through a window may influence recovery from surgery. Science 224, 420–421. https://doi.org/10.1126/science.6143402.

URBES, 2014. Green Infrastructure, a Wealth for Cities. Fact Sheet https://www.iucn.org/sites/dev/files/import/downloads/urbes_factsheet_06_web.pdf.

US EPA, 2019. What is Green Infrastructure? https://www.epa.gov/green-infrastructure/what-green-infrastructure.

Velasco, E., et al., 2016. Does urban vegetation enhance carbon sequestration? Landsc. Urban Plan. 148, 99–107.
Vienneau, D., de Hoogh, K., Faeh, D., Kaufmann, M., Wunderli, J.M., Röösli, M., et al., 2017. More than clean air and tranquillity: residential green is independently associated with decreasing mortality. Environ. Int. 108, 176–184. https://doi.org/10.1016/j.envint.2017.08.0122.4.
Villeneuve, P.J., Jerrett, M., Su, J.G., et al., 2012. A cohort study relating urban green space with mortality in Ontario, Canada. Environ. Res. 115, 51–58. https://doi.org/10.1016/j.envres.2012.03.003.
Vos, P.E.J., Maiheu, B., Jankerkom, J., Janssen, S., 2013. Improving local air quality in cities: to tree or not to tree? Environ. Pollut. 183, 113–122. https://doi.org/10.1016/j.envpol.2012.10.021.
Voskamp, I.M., Van de Ven, F.H.M., 2014. Planning support system for climate change: composing effective sets of blue-green measures to reduce urban vulnerability to extreme weather events. Build. Environ. 83, 159–167.
Wang, Y., Berardi, U., Akbari, H., 2016. Comparing the effects of urban heat island mitigation strategies for Toronto, Canada. Energy Build. 114, 2–19. https://doi.org/10.1016/j.enbuild.2015.06.046.
Warwick, F., Charlesworth, S., 2013. Sustainable drainage devices for carbon mitigation. Manag. Environ. Qual. 24, 123–136.
Weber, F., Kowarik, I., Saeumel, I., 2014. Herbaceous plants as filters: immobilization of particulates along urban street corridors. Environ. Pollut. 186, 234–240.
Weng, Q., et al., 2004. Estimation of land surface temperature–vegetation abundance relationship for urban heat island studies. Remote Sens. Environ. 89, 467–483.
Whittinghill, L.J., et al., 2014. Quantifying carbon sequestration systems of various green roof and ornamental landscape systems. Landsc. Urban Plan. 123, 41–48.
Williams, N.S.G., Lundholm, J., MacIvor, J.S., 2014. Do green roofs help urban biodiversity conservation? J. Appl. Ecol. 51, 1643–1649.
Wotherspoon, A., Thevathasan, N.V., Gordon, A.M., et al., 2014. Carbon sequestration potential of five tree species in a 25-year-old temperate tree-based intercropping system in southern Ontario, Canada. Agrofor. Syst. 88, 631–643. https://doi.org/10.1007/s10457-014-9719-0.
Xu, C., et al., 2019. Benefits of coupled green and grey infrastructure systems: evidence based on analytic hierarchy process and life cycle costing. Resour. Conserv. Recycl. 151, 104478. https://doi.org/10.1016/j.resconrec.2019.104478.
Yang, J., Yu, Q., Gong, P., 2008. Quantifying air pollution removal by green roofs in Chicago. Atmos. Environ. 42, 7266–7273.

Further reading

Moher, D., Liberati, A., Tetzlaff, J., Altman, D.G., The PRISMA Group, 2009. Preferred reporting items for systematic reviews and meta-analyses: the PRISMA statement. PLoS Med. 6 (6), e1000097. https://doi.org/10.1371/journal.pmed1000097.

CHAPTER

Adaptation to climate extremes and sea level rise in coastal cities of developing countries

9

Tu Dam Ngoc Le[a] **and Ripendra Awal**[b]

Faculty of Architecture, MienTrung University of Civil Engineering, Tuy Hoa, Phu Yen, Vietnam[a] *College of Agriculture and Human Sciences, Prairie View A&M University, Prairie View, TX, United States*[b]

Introduction

Coastal communities and settlements are vulnerable to climate hazards and sea level rise (SLR). Exposure to the coast made them frequently attacked by typhoons, storm surges, and flooding, leading to erosion, inundation, loss of habitat and infrastructure, and damages to the ecosystem. Also, current and projected SLR have exacerbated extreme climate impacts. The concentration of population and assets has aggravated the social and economic effects and losses. Annually, up to 119 million people are exposed to tropical cyclone hazards, which cost more than 250,000 fatalities from 1980 to 2000 (Nicholls et al., 2007). Under the scenario of 1-m SLR, an estimation of more than 50 million people in developing countries is likely to displace, accompanied by severe economic and ecological damage (Dasgupta et al., 2009).

In 1990, the Coastal Zone Management Subgroup held workshops to generate information on the available adaptive response (CZMS, 1990). For about 30 years of the aftermath, coastal communities around the world have conducted numerous adaptation measures to protect people, assets, and coastal ecosystems. However, we still lack empirical studies to survey on how coastal cities in developing countries respond to climate change and recurring extreme events.

Despite a large body of literature on coastal climate change adaptation, there is a lack of studies that look at the links between exposure to climate change and adaptation in various countries, especially developing countries. Few studies focus on small and medium cities in developing countries due to lack of data, difficulties in access to their system, and lack of local personnel who conduct studies. This chapter examines the linkages between coastal vulnerability and adaptation and identifies the appropriate adaptation measures for these coastal vulnerabilities. Although adaptation options are context based, analysis from multiple coastal cities will provide a fruitful lesson for cities in finding the suitable adaptation pathways to climate change and SLR. The chapter has twofold: (1) to unpack the state-of-the-art of climate change adaptation in small and medium coastal cities in developing countries through characterizing coastal exposure and impacts of climate change and examining adaptation strategies to those exposures and impacts and (2) to conduct a synthesis of adaptation strategies for coastal cities, especially small and medium cities, which tend to have less capacity to adapt.

Climate Change and Extreme Events. https://doi.org/10.1016/B978-0-12-822700-8.00003-2
Copyright © 2021 Elsevier Inc. All rights reserved.

Typologies of coastal adaptation to climate change

Options for coastal adaptation can be classified into three main categories, including protection, accommodation, and managed retreat (Klein et al., 2001; Wong et al., 2014). These options are described as follows:

- **Protection** is to reduce the risk of the hazards by using "hard" structural or "soft" measures to protect critical infrastructures, such as seawalls, levees, barriers, beach nourishment, or wetland restoration.
- **Accommodation** involves changes in human activities and infrastructure to enhance society's ability to cope with the effects of the events, such as retrofitting buildings, raising floor elevation, or adjustments to land-use management and insurance programs.
- **Managed retreat** involves stepping back from the problem to avoid the catastrophic such as moving away from the coast, allowing tidal seawater to areas previously protected, relocating threatened buildings.

Attack, as classified by Building Futures and ICE (2010), is another type of accommodation but responds more actively to advance and step seaward of the existing coastline by applying several means of building out onto the water, such as stilts, floating structure, or land reclamation.

Methodology

This study focuses on small- and medium-sized cities that have a population below one million in the coastal region in developing countries. The case study consists of 27 cities located along or within 100 km from the coast that is affected by coastal hazards and SLR (Fig. 1). The selected cases cover in 4 regions, including 2 cities in Africa, 17 in Asia, 4 in South America and the Caribbean, and 5 in Oceania.

The study uses the city's climate change planning documents as the primary data sources, including the city's climate change vulnerability assessment, adaptation plan, a climate action plan with the chapter of adaptation, and the city resilience strategy with climate change as the main driver. Appendix shows a list of used documents of all selected cities. From the chosen records, data were collected into two groups to characterize types of coastal hazards and adaptation options using an excel-table format. This is a data-driven process, in which the main themes emerge during the coding process. Following the methodology in Le (2019), data on the type of climate extreme events are analyzed in two rounds, the coding and the ranking process to classify how coastal hazards or climate risks impact the cities. The evaluation of each hazard or climate risk follows a three-level ordinal scale. *Low impact* stands for the hazard having caused or potentially causing a low impact on the city and its citizens. *Moderate* if the hazard causes moderate impacts or damages, and *high* if the hazard causes significant impacts or damages.

From the documents, all the adaptation initiatives are recorded in an excel table for the analysis. These initiatives are coded into the type of climate extreme that is addressed and the typologies of the actions. Only the adaptation measures that address one of the issues relating to climate change, climate extreme events, and SLR are selected to analyze further. Regarding the typologies of adaptation initiatives, first, this study classifies adaptation initiatives into three categories of adaptation

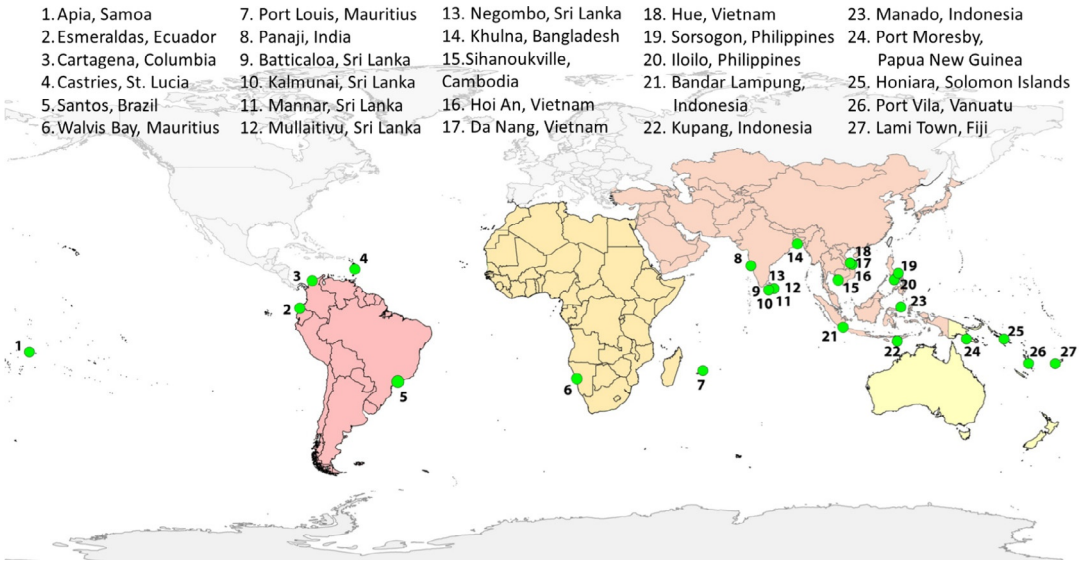

FIG. 1

Map of case studies.

options, that is, protection, accommodation, or retreat. Second, the study follows some other system of classification, such as Biagini et al. (2014), Noble et al. (2014), and USAID (2009) to identify the typologies.

Also, this study used the web-based search engine to learn about the magnitude of coastal hazards that attacked these cities and the adaptation measures that were proposed in these adaptation plans. This study used the search engine to examine whether the measures were indeed applied in those cities. Although the search engine did not yield a complete result of all actions and cities because many cities use non-English languages for their news, it still could provide insight for the researcher to reinforce the findings.

Climate risks in coastal cities of developing countries

The analysis from 27 small- and medium-sized cities shows that flooding, SLR, and storm or typhoon are the most common climate risks in coastal cities of developing countries (Fig. 2). All cities have experienced flooding, either coastal or inland flooding. Along with the rainfall increase in the rainy season and the rising frequency of strong storm and typhoons, cities are increasingly impacted by flooding, storm, or typhoon, leading to coastal or riverbank erosion. More than 50% of the cities are affected by extreme flood events with significant losses and damages. Prolonged heavy rain together with coastal storm caused severe flooding that affected hundreds of thousands of people as well as damages to properties. Storms and typhoons also cause massive damage to coastal cities and regions. For example, in 2013, typhoon Nari damaged the roofs of thousands of houses in Da Nang (Vietnam); also,

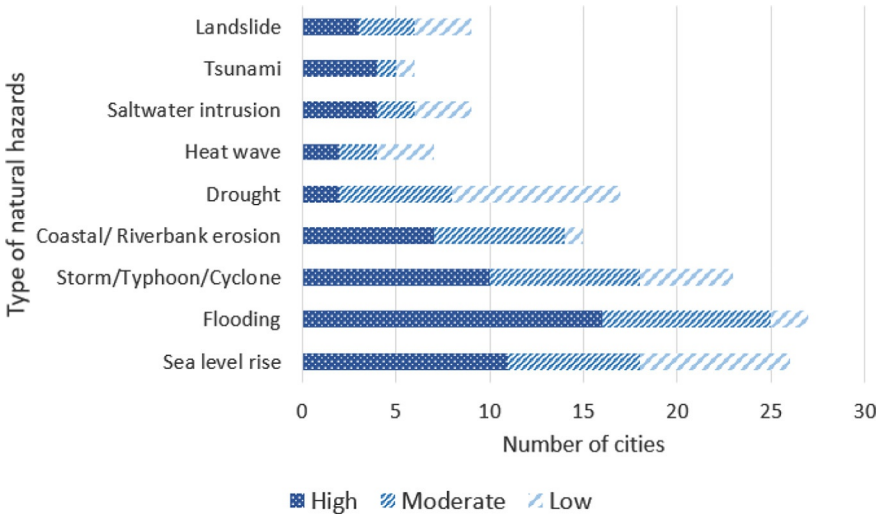

FIG. 2

The number of cities addresses hazard exposure in the planning documents. Impact scale: *High*, the hazard causes significant impacts or damages to the city; *Moderate*, the hazard causes moderate impacts or damages to the city; *Low*, the hazard is mentioned as a threat without detail or at a low impact.

in 2015, cyclone Palm adversely impacted at least 90% of homes in Greater Port Vila or typhoon Haiyan in 2013 that killed more than thousands of people in the coastline of Philippines.

Cities along and near the coast, as a result of SLR, are increasingly impacted. SLR, tidal surge, and strong waves have been causing severe coastal erosion in many places that led to the loss of protective forests along the coast, and the shoreline eroded 10–20 m every year in Hoi An (Vietnam). With the projection of SLR to the mid and end of the century, hundreds of beaches are at risk of erosion and inundation, leading to thousands of people being displaced (such as in Castries, Cartagena, Walvis Bay, Sorsogon, and Negombo). According to the Cartagena Climate Compatible Plan, the projection of 15–20 cm SLR scenario in 2040 and without adaptation can affect 27.5% of the city population and 26.2% of houses, 35% of road infrastructure, 86% of historical heritage, and 70% of mangrove swamp areas are at risk of flooding (Zamora-Bornachera et al., 2014).

The temperature increase due to climate change also leads to drought and extreme heat events. It exacerbates the problem of water shortage during the dry season. It impacts economic activities, such as crops, reduction in fishing production, and whitening of corals that provide economical means for people in many cities in developing countries (Cartagena, Honiara, Da Nang, Hue, Iloilo). Drought coupled with SLR worsens the problem of saltwater intrusion during the dry season that reduces agricultural production, affects aquatic ecosystem, causes infrastructure damages, and affects groundwater (Hoi An, Hue, Negombo, Walvis Bay, Khulna).

The manifestation of climate change and SLR is clear in coastal cities. They exacerbate the impacts of extreme weather events that have frequently attacked coastal regions. The next section aims to explore how coastal cities, especially small- and medium-sized cities in developing countries, where capacity and resources are lacking, respond to these impacts.

Adaptation response to climate extremes and SLR

From the adaptation planning documents in 27 cities, the study analyzes 587 adaptation measures. Among this, 78% of proposed initiatives aim to accommodate, 16% are used for protection, and 6% account for the managed retreat (Fig. 3). This result illustrates that accommodation is still a significant intervention for the cities to adapt to climate change, extreme events, and SLR. It provides ample space for the city and its residents to enhance their capacity to cope with these incidents.

Fig. 4 denotes the frequency of adaptation typologies applied in those cities. The result illustrates the diversity, popularity, and the level of importance of measures in climate change adaptation. Effective adaptation will need a combination of various aspects, from protection to accommodation and

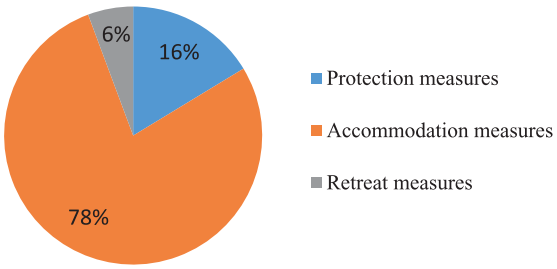

FIG. 3

Coastal adaptation categories.

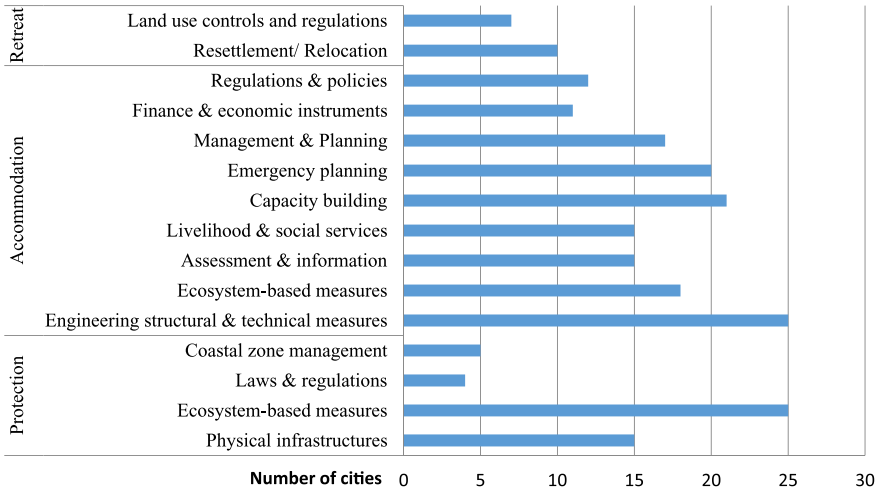

FIG. 4

Different adaptation measures proposed by the number of cities in the planning documents.

retreat. Indeed, it requires a mutual interaction of multiple actions intervened on different aspects, both hard and soft measures, capacity building, management and planning, policies and regulations, and so on (Fig. 4).

All cities plan for different adaptation measures (Table 1). Some cities in Asia (e.g., Iloilo, Kalmunai, Batticaloa, Hoi An, Da Nang, Negombo, Sihanoukville), Africa (e.g., Walvis Bay, Port Louis), and Oceania (e.g., Honiara) are adapting 10 or more different adaptation measures listed in Table 1. All options are not adequate or necessary for all coastal cities. Options that are suitable for a specific region should have positive cost benefits, with fewer negative impacts or favorable consequences (Sinay and Carter, 2020).

Protection measures

This study found that small and medium coastal cities in developing countries rely on both hard and soft measures to respond to extreme coastal events and climate change. Among these adaptation responses, ecosystem-based options are the most preferred in those cities. Twenty-five of twenty-seven cities choose to protect the coastlines and coastal assets basing on ecosystem services. Only eight cities propose protection bylaws and policies, whereas 15 cities propose various hard engineered structures.

Various measures are proposed and applied in the studied cities, as shown in Fig. 4, Tables 1 and 2. Conventional measures consist of the use of hard structural infrastructures such as seawalls, dikes, embankment, revetment walls, bulkheads, windbreakers or water breakers, retrofitting ports, and wharves, and specific flood mitigation infrastructures (Table 2). These infrastructures, however, tend to be costly for construction and maintenance. The cost might go beyond the limited capacity of small and medium cities in developing countries. As an effective alternative, those cities rely more on ecosystem-based measures that are usually cheaper and more environmental friendly than physical infrastructures. The hard and soft structural measures, however, cannot be efficient without the implementation of laws, regulations, and policies, specific regulations to protect coastal and wetland ecosystem, and coastal zone management policies (Table 2).

Accommodation measures

This study found more excessively ample room for accommodation than two other categories (Fig. 4 and Table 3). It illustrates that accommodation cannot be standalone actions on some specific areas but rather a combination of various measures on multiple aspects. To respond to climate change and extreme events, cities will need to conduct a vulnerability assessment and survey to identify their vulnerabilities and limited capacity. From that, the interventions can be on structural aspects such as water source management, drainage and sanitation, urban and building designs, or using ecosystem services such as watersheds or green infrastructure to accommodate cities to adapt to climate change, extreme events, and SLR. In addition, interventions to leverage the livelihood of people, providing insurance and health services, capacity building, improving early warning systems, constructing evacuation centers, and preparedness on evacuation drills are equally crucial to reduce the risk and damage of cities and people in the face of climate change and coastal hazards. Furthermore, as a long-term strategy, management and planning, financial and economic instruments, and regulations and policies will establish a mechanism and pathway for cities and their residents to adapt to climate change and extreme events.

Table 1 Adaptation measures adapted in different cities.

Continent/ geographic region	City	Country	Protection				Accommodation									Managed retreat	
			Physical infrastructures	Ecosystem-based measures	Laws and regulations	Coastal zone management	Engineering structural and technical measures	Ecosystem-based measures	Assessment and information	Livelihood and social services	Capacity building	Emergency planning	Management and planning	Finance and economic instruments	Regulations and policies	Resettlement or relocation	Land use controls and regulations
South America and the Caribbean	Cartagena	Columbia		Y		Y	Y	Y	Y		Y						
	Castries	St. Lucia	Y	Y			Y	Y		Y	Y	Y	Y	Y			
	Esmeraldas	Ecuador		Y			Y		Y	Y	Y				Y	Y	
	Santos	Brazil		Y			Y	Y		Y	Y		Y	Y			
Africa	Port Louis	Mauritius	Y	Y			Y	Y	Y		Y	Y	Y		Y	Y	Y
	Walvis Bay	Mauritius	Y	Y		Y	Y	Y		Y	Y	Y	Y			Y	Y
Asia	Bandar Lampung	Indonesia	Y	Y			Y			Y		Y					
	Batticaloa	Sri Lanka	Y	Y	Y		Y	Y	Y	Y	Y	Y	Y	Y	Y		
	Da Nang	Vietnam	Y	Y			Y	Y	Y	Y	Y	Y	Y	Y		Y	
	Hoi An	Vietnam	Y	Y			Y		Y	Y	Y	Y	Y	Y	Y	Y	
	Hue	Vietnam	Y	Y			Y		Y		Y	Y	Y	Y			
	Iloilo	Philippines	Y	Y	Y	Y	Y	Y		Y	Y	Y	Y		Y	Y	Y
	Kalmunai	Sri Lanka	Y		Y		Y	Y	Y	Y	Y	Y	Y	Y	Y		Y
	Khulna	Bangladesh					Y	Y				Y		Y	Y	Y	
	Kupang	Indonesia	Y	Y			Y	Y	Y	Y	Y	Y	Y				
	Manado	Indonesia		Y			Y										
	Mannar	Sri Lanka	Y				Y	Y		Y	Y	Y		Y	Y		
	Mullaitivu	Sri Lanka		Y			Y	Y		Y	Y	Y					
	Negombo	Sri Lanka	Y	Y	Y		Y	Y	Y		Y	Y	Y		Y		
	Panaji	India		Y			Y		Y			Y	Y				Y
	Sihanoukville	Cambodia	Y	Y			Y		Y	Y	Y	Y	Y			Y	Y
	Sorsogon	Philippines		Y		Y	Y			Y	Y		Y				

Continued

Table 1 Adaptation measures adapted in different cities—cont'd

Continent/ geographic region	City	Country	Protection				Accommodation									Managed retreat	
			Physical infrastructures	Ecosystem-based measures	Laws and regulations	Coastal zone management	Engineering structural and technical measures	Ecosystem-based measures	Assessment and information	Livelihood and social services	Capacity building	Emergency planning	Management and planning	Finance and economic instruments	Regulations and policies	Resettlement or relocation	Land use controls and regulations
Oceania	Apia	Samoa										Y			Y		Y
	Honiara	Solomon Islands		Y		Y	Y	Y	Y		Y	Y	Y	Y	Y	Y	
	Lami Town	Fiji		Y			Y	Y			Y	Y	Y	Y		Y	
	Port Moresby	Papua New Guinea	Y	Y				Y	Y		Y				Y		
	Port Vila	Vanuatu		Y			Y	Y	Y								

Table 2 Protection adaptation measures.

Adaptation typologies	Climate stressors	Adaptation measures	Cities apply the measures
Physical infrastructures			
• Hard engineering infrastructures	Floods, storms, landslides, erosion, sea level rise	• Seawalls, seawalls with patches of stones to prevent wave energy • Dikes, revetment walls, bulkheads rip-rapping along rivers, estuaries, creeks, coastal defense to control floods, landslides, and coastal erosion • Natural and man-made wind breakers and wave breakers • Embankments	Bandar Lampung, Batticaloa, Castries, Da Nang, Hoi An, Iloilo, Kupang, Kalmunai, Mannar, Port Moresby, Port Louis, Sihanoukville, Walvis Bay
• Retrofitting of ports and wharves	Coastal flood, storm, sea level rise	• Retrofitting of ports and wharves and emergency protocol for the occurrence of sea level rise • Raising harbor defenses	Iloilo, Walvis Bay, Port Louis
• Flood mitigation infrastructures	Flood	• Gabion and retention walls • Sluice gate • Flood retention ponds and weirs • Dams and flood walls to capture excess water	Batticaloa, Hue, Kalmunai, Kupang, Negombo, Walvis Bay
Ecosystem-based measures			
• Forest and critical land rehabilitation	Erosion, extreme temperature, landslides	• Rehabilitation of green open spaces, greening of mountains, hills, nature parks, water catchment areas, and river banks • Conserve vegetation and reforest hillside areas and Slope reforestation • Terrace hill-slopes using vetiver or lemongrass to strengthen soil stability, reduce erosion	Bandar Lampung, Da Nang, Esmeraldas, Hoi An, Kupang, Manado, Mullaitivu, Port Moresby, Walvis Bay
• Wetland protection and restoration	Drought, flood, erosion	• Development, management, and conservation of rivers, lakes, and other water resources and basins and micro-basins • Revegetate catchment area, establish natural water corridors and floodwater drainage corridors and floodway plan • Retention of fishponds, temporary reservoir in low-lying bare land	Batticaloa, Cartagena, Da Nang, Esmeraldas, Hue, Iloilo, Manado, Port Vila, Walvis Bay
• Marine ecosystem protection and conservation	Sea warming temperature, sea level rise, wave energy	• Rehabilitation of coral reefs and seagrass beds, fish shelters, seaweed farms • Restore and rehabilitate artificial reefs	Cartagena, Sorsogon, Walvis Bay

Continued

Table 2 Protection adaptation measures—cont'd

Adaptation typologies	Climate stressors	Adaptation measures	Cities apply the measures
		• Preservation and cooperation of the marine and coastal ecosystems	
• Mangrove protection and restoration	Coastal flood, sea level rise, storm surges	• Reforestation of mangrove and watershed areas • Restoration of the ecological structure with emphasis on the mangrove swamp • Protection of mangrove	Batticaloa, Cartagena, Castries, Iloilo, Kupang, Lami Town, Negombo, Port Moresby, Port Vila, Santos, Sihanoukville
• Dune protection and beach nourishment	Coastal flood, storm surges	• Rehabilitation and preservation measures around sand dunes and mangroves • Regeneration of beaches using external supply and direct supply from dredging • Nourishment of the sand spit	Cartagena, Panaji, Port Louis, Walvis Bay
• Green space development	Extreme temperature, excess rainfall	• Community-led tree-planting programs • Development of multipurpose greenbelts and green buffer along the coast • Biological corridors for ecological connectivity • Riverine development along main hydrological canals and lagoons	Batticaloa, Cartagena, Esmeraldas, Honiara, Iloilo, Kalmunai, Mannar, Mullaitivu, Walvis Bay
Laws and regulations			
• Coastal and wetland ecosystem protection bylaws	Flood, storm, erosion, sea level rise	• Prohibit illegal fishing activities • Removal of illegal fish ponds and fish corals • Stop sand mining in coastal areas • Prohibit mangrove destruction • Protect floodway channels from obstructions and illegal structures • Reserve water retention areas in the zoning plan	Batticaloa, Iloilo, Kalmunai, Negombo
Coastal zone management			
• Establishment of coastal protection zone	Coastal hazards, sea level rise	• Coastal protection zone (CPZ) for protecting vulnerable coastal areas and maximizing sustainable social and economic benefits • Coastal asset protection bylaws	Sorsogon, Cartagena, Walvis Bay

Table 2 Protection adaptation measures—cont'd

Adaptation typologies	Climate stressors	Adaptation measures	Cities apply the measures
• Integrated coastal zone management	Coastal hazards, sea level rise, flood	• Integrate ecosystem strategies (ridge to reef) into all planning initiatives • Develop a coastal zone management plan and water catchment protection plan • Reclamation project along the coastlines and foreshores • Integrating flood prevention and mitigation measures in the city's development plans, programs, and policies	Honiara, Iloilo

Table 3 Accommodation adaptation measures.

Adaptation typologies	Climate stressors	Adaptation measures	Cities apply the measures
Engineering structural and technical measures			
– **Water source management**			
• Water supply management	Extreme temperature, drought, water scarcity, water contamination due to flood, saltwater intrusion	• Increased coverage of clean water services and access to clean water for poor households • Prevent water leakage and infiltration of floodwater into the pipelines • Design new water intakes • Increase the impounding reservoir size • Improve the water supply system and diversify water sources	Bandar Lampung, Esmeraldas, Hoi An, Honiara, Khulna, Lami Town, Negombo, Panaji, Sihanoukville
• Water treatment	Salinity, water scarcity	• Brackish water treatment technology and filtration • Managing salinity and seawater desalination plants • Groundwater conservation and quality improvement • Monitoring and supervision of seawater intrusion control	Bandar Lampung, Batticaloa, Manado, Mannar

Continued

Table 3 Accommodation adaptation measures—cont'd

Adaptation typologies	Climate stressors	Adaptation measures	Cities apply the measures
• Water saving promotion	Extreme temperature, water scarcity, flood, drought	• Advocating the inclusion of water-saving devices in buildings • Rainwater harvesting such as making wells and biopori wells • Develop moisture conservation pits for harvesting during times of drought • Greywater recycling from households • Water demand management through progressive water pricing for drinking, cooking, and other purposes	Bandar Lampung, Batticaloa, Castries, Esmeraldas, Iloilo, Kalmunai, Manado, Mullaitivu, Walvis Bay
– **Drainage and sanitation**			
• Maintenance and construction of drainage	Excess rainfall, flood, sea level rise	• Construction of new drainage/improved drainage and sustainable urban drainage system • Improved links to community-driven drainage programs • Remove silt, garbage, and clean existing drains regularly • Incorporation of projected precipitation and SLR levels into drainage systems	Bandar Lampung, Batticaloa, Castries, Honiara, Hue, Iloilo, Kupang, Kalmunai, Lami Town, Manado, Mannar, Mullaitivu, Negombo, Panaji, Khulna, Sihanoukville, Santos
• Integrated drainage	Excess rainfall, flood, sea level rise	• Maintenance and construction of integrated drainage. Integrate wastewater management system into drainage networks. Integrate the drainage network and the canal system • Climate-sensitive and community-led integrated drainage	
• Improved sanitation	Flood, pollution due to floods	• Improved septic tank storage and disposal to ensure that floodwaters are not contaminated with wastewater	Lami Town, Kupang, Sorsogon

Table 3 Accommodation adaptation measures—cont'd

Adaptation typologies	Climate stressors	Adaptation measures	Cities apply the measures
		• Proper waste management and sewage disposal	
– **Urban design, buildings, and infrastructures**			
• Climate-friendly urban design and resilient community	Climate change, flood, storm	• Climate-friendly urban development. Climate-sensitive public open space. Using permeable materials and adequate slope in flood-prone areas. Model of flood resilient community, climate change adaptation neighborhood. Construction of safe housing and community infrastructure	Bandar Lampung, Cartagena, Da Nang, Honiara, Kupang, Iloilo, Mannar, Mullaitivu, Panaji, Sorsogon
• Building designs and structures	Flood, storm/cyclones, strong wind, extreme temperature, sea level rise	• Flood-resistant housing. Houses on stilts, elevation of horizontal and vertical facilities, and infrastructure. Introducing waterproofing measures, waterproof covers, and rain shelters • Storm-resistant housing and tourism facilities • Maintenance and preservation techniques for the ancient and open-air buildings to cope with climate change • Retrofitting of schools and hospitals to adapt to storms and floods • Sustainable housing development using bioclimatic architecture	Batticaloa, Bandar Lampung, Lami Town, Cartagena, Da Nang, Hoi An, Hue, Iloilo, Kalmunai, Kupang, Mullaitivu, Panaji, Port Vila, Sihanoukville, Sorsogon
• Climate-proofing transportation routes and infrastructures	Flood, sea level rise, storm surges, strong winds	• Safeguard transportation routes. Reconstruct the bridges to prevent the area from becoming an "island," elevated roads in low-lying areas	Hoi An, Honiara, Hue, Negombo, Mannar, Mullaitivu, Panaji, Port Louis, Sihanoukville, Walvis Bay

Continued

Table 3 Accommodation adaptation measures—cont'd

Adaptation typologies	Climate stressors	Adaptation measures	Cities apply the measures
		• Materials and technologies in transportation infrastructure to increase durability and tolerance to flood impacts • Accommodate SLR in the design of new coastal structures • Retrofitting of energy infrastructures, towers and cables, airports, and seaports to cope with storm surges and strong winds	
Ecosystem-based measures			
• Watershed management	Flood, drought, erosion	• Dredging of rivers, creeks, and estuaries • Widening of lagoon mouth at the rainy season to ensure smooth flow of water • Tank rehabilitation, creating linkages between water bodies, improving the depths of water bodies	Batticaloa, Iloilo, Kalmunai, Khulna, Lami Town, Mannar, Mullaitivu, Negombo
• Greening space development	Flood, erosion, urban heat, drought, salinity	• Tree preservation, green infrastructure projects. Enhancing the natural vegetation of the city. Street tree planting program and urban forest protection • Planting salinity-resistant trees • Roof gardens to reduce heat. Urban home gardening • Increase permeable surfaces to filtrate water	Batticaloa, Cartagena, Castries, Da Nang, Honiara, Iloilo, Kalmunai, Kupang, Mannar, Negombo, Port Louis, Port Moresby, Port Vila, Santos, Walvis Bay
Assessment and information			
• Vulnerability assessment and survey	Climate change, sea level rise, floods, coastal hazards	• Vulnerability assessment and survey on climate change/sea level rise/ coastal hazard impacts • Inventory of disaster damages	Cartagena, Da Nang, Esmeraldas, Hoi An, Honiara, Hue, Kalmunai, Kupang, Negombo, Panaji, Port Louis, Port Moresby, Port Vila, Sihanoukville

Table 3 Accommodation adaptation measures—cont'd

Adaptation typologies	Climate stressors	Adaptation measures	Cities apply the measures
• Information and database management	Flood, sea level rise, climate change	• Assessment of water source availability and the capacity of drainage systems • Developing local and comprehensive information systems for climate change and information-sharing mechanisms for public reach • Using applications for smartphones with up to date meteorological information • Integrated GIS database with hazard data collection and mapping • Spatial database on land use, thematic information, infrastructure information, locations vulnerable to disasters, natural assets, and shoreline ecosystem	Batticaloa, Cartagena, Da Nang, Esmeraldas, Honiara, Hue, Kalmunai, Kupang, Negombo, Panaji, Port Louis
Livelihood and social services			
– **Livelihood supports**			
• Support to farmers and fishery communities	Livelihood insecurity due to climate change impacts	• Developing crops that can withstand salinity • Improved and varied seasonal crops • Climate-proofed irrigation facility • Sustain and support to farmers and fishery communities • Supporting fisheries tools and infrastructure for coastal community development	Esmeraldas, Hoi An, Iloilo, Mullaitivu, Sorsogon, Sihanoukville, Walvis Bay
• Livelihood diversification		• Diversifying livelihood. Job training • Implementing pilot community livelihood adaptation strategy or plans	

Continued

Table 3 Accommodation adaptation measures—cont'd

Adaptation typologies	Climate stressors	Adaptation measures	Cities apply the measures
– **Insurance and health services**			
• Insurance	Climate change, disaster	• Improving insurance mechanisms, and climate financing for building resilience against climate change, micro-insurance mechanisms for housing damages • Providing affordable health insurance to residents	Bandar Lampung, Castries, Da Nang, Santos, Sorsogon
• Health services	Climate change, disaster	• Developing resilient health service systems: providing mobile health services during a disaster situation and improving the capacity of hospitals • Prevention, controlling, and monitoring of sickness and conditions affecting human health relating to climate change	Batticaloa, Esmeraldas, Kalmunai, Kupang, Mannar, Sihanoukville, Walvis Bay
Capacity building			
• Community capacity building	Climate change, natural hazards	• Strengthening human resources, increasing knowledge and awareness through education, training, information, and awareness-raising campaigns • Creation of spaces for training in climate change • Mainstreaming climate change into school curriculum, vocational training, and educational programs	Batticaloa, Cartagena, Castries, Da Nang, Esmeraldas, Hoi An, Honiara, Hue, Iloilo, Kalmunai, Kupang, Lami Town, Mannar, Mullaitivu, Negombo, Port Louis, Port Moresby, Santos, Sihanoukville, Sorsogon, Walvis Bay
• Institutional capacity building	Climate change, natural hazards	• Training programs for city officers in disaster management, natural disaster forecasting, and early warning • Embed disaster risk reduction personnel within all major ministries at a national level and city-level departments	

Table 3 Accommodation adaptation measures—cont'd

Adaptation typologies	Climate stressors	Adaptation measures	Cities apply the measures
		• Establish a local-level technical committee to make decisions on development initiatives within the city	
Emergency planning			
• Early warning systems	Flood, storm, cyclone, sea level rise	• Improving hazard monitoring, forecasting, and early warning systems, especially flood and cyclone • Developing a community-based warning system through using the SMS gateway for climate information • Screening near-shore reclamation against sea level rise impacts	Apia, Bandar Lampung, Batticaloa, Castries, Da Nang, Hoi An, Honiara, Hue, Iloilo, Kalmunai, Kupang, Khulna, Lami Town, Mullaitivu, Mannar, Negombo, Panaji, Port Louis, Sihanoukville, Walvis Bay
• Evacuation centers, routes, and maps	Flood, storm, hazards, tsunami	• Constructing evacuation center/city shelter plan/ multifunction house • Assessing the coverage of emergency shelters and identify additional shelter sites required to cover 100% of the city's residents • Developing safe and reliable evacuation routes, distributing evacuation maps to all families • Providing disaster preparedness guide books	
Management and planning			
• Disaster risk management	Climate change, natural hazards	• City disaster risk reduction and management plan • Incorporating disaster risk reduction and climate change into city development plan or city land-use plan • Inclusion of the private sector in disaster risk management	Batticaloa, Castries, Da Nang, Iloilo, Kalmunai, Kupang, Lami Town, Honiara, Santos, Sihanoukville, Sorsogon, Walvis Bay

Continued

Table 3 Accommodation adaptation measures—cont'd

Adaptation typologies	Climate stressors	Adaptation measures	Cities apply the measures
		• Applying a crisis management system (CMS) in flood management and response • Community-based risk reduction through community disaster response groups or rapid response task force for assisting hazard-prone communities	
• Integrated planning	Climate change	• Integrating vulnerability assessment, resilience planning, and climate change in institutional framework and plans, acts, rules, bylaws, and building codes • Mainstreaming climate change across all sectors and at all levels of government decision making • Integrate ecosystem services and ecosystem-based adaptation (EbA) actions into water catchment management plans • Applying hybrid EbA and engineered protection measures in coastal management plans	Hoi An, Honiara, Hue, Lami Town, Negombo, Panaji, Port Louis, Sihanoukville, Walvis Bay.
Finance and economic instruments			
• Budget and funding allocation	Climate change, natural hazards	• Establish community-saving groups and a disaster relief fund • Expanding loan supports for the community to build or repair housing resilient to flood and storms • Allocate budget and funding to cope with climate change	Batticaloa, Castries, Da Nang, Hoi An, Honiara, Hue, Kalmunai, Lami Town, Mannar, Santos

Table 3 Accommodation adaptation measures—cont'd

Adaptation typologies	Climate stressors	Adaptation measures	Cities apply the measures
• Economic instruments	Water scarcity	• Progressive water pricing: one for drinking and cooking purposes with higher price tags per liter and one for other uses • Drainage tax. Fine for disposal of garbage in the canal	Khulna, Kalmunai
Regulations and policies			
• Land-use controls and regulations	Climate change, flood, coastal hazards	• Reviewing current land-use regulations in the city considering climate change and the magnitude of disaster impacts • Regulating industrial and service effluents to avoid pollution of water sources • Developing a safe flood discharge process of upstream hydropower to prevent downstream flooding • Developing, enforcing rules, regulations, building codes within disaster-prone areas	Apia, Batticaloa, Esmeraldas, Hoi An, Honiara, Iloilo, Kalmunai, Khulna, Mannar, Negombo, Port Louis, Port Moresby
• Incentive policies	Climate change	• Policy and adequate support to developers, businesses that demonstrate eco-friendly and climate-resilient initiatives	Batticaloa, Esmeraldas, Honiara

Managed retreat

Although the literature proposed various options for managed retreat (CZMS, 1990; Klein et al., 2001; Parry et al., 2007) and increasing attention of scholars on managed retreat because climate change and SLR are inevitable (Abel et al., 2011; Building Futures and ICE, 2010; Gibbs, 2016), this study found that cities pay less attention to managed retreat. Only seven cities propose to manage land use and regulation to direct the development out of risk-prone areas. Ten cities propose relocation of hazard-prone communities and critical infrastructures that are affected by coastal hazards and SLR. However, some cities emphasize that retreat should be the ultimate option to consider when other means cannot be

Table 4 Managed retreat.

Adaptation typologies	Climate stressors	Adaptation measures	Cities apply the measures
Resettlement and relocation	Flood, erosion, salinity	• Resettling residential areas and critical facilities that are located in flooding plain or frequently affected by flood or erosion • Moving the intake point further upstream to avoid the salinity impacts	Da Nang, Esmeraldas, Iloilo, Hoi An, Honiara, Khulna, Lami Town, Port Louis, Sihanoukville, Walvis Bay
Land use controls and regulations	Coastal hazards	• Land use controls and regulations • Managed retreat from high-risk coastal areas • Prohibition of construction of houses and buildings in dangerous zones • Enforcement of coastal regulation zone	Apia, Iloilo, Kalmunai, Panaji, Port Louis, Sihanoukville, Walvis Bay

sufficient to protect the communities (Table 4). It might be due to the cost to relocate large numbers of buildings is too high, and the uncertainty of climate change that hinders the short-term elected politics from implementing these measures (Gibbs, 2016).

Discussions

The results of this chapter have reaffirmed some most common natural hazards in coastal cities. Flood, storm, SLR, erosion, and drought have significantly impacted coastal cities and regions and have captured attention and resources to adapt (Bhat et al., 2013; Sales Jr, 2009; Wong et al., 2014). In addition, other hazards such as landslides, saltwater intrusion, and the tsunami also significantly affect some cities. A city is affected by multiple risks. Therefore cities must plan and allocate resources to address various hazards simultaneously.

A variety of adaptation actions had been proposed and implemented in coastal cities to address climate change, extreme events, and SLR. Consistent with other studies on coastal adaptation such as (CZMS, 1990; IPCC, 2007; Klein et al., 2001), results of this study illustrate that adaptation to climate change, coastal hazards, and SLR happening in three primary ways: protection, accommodation, and retreat. However, as specified by Klein (2011), adaptation to climate change is not just technology but a continuum that requires adaptation integrated with human and economic development efforts. The result of this empirical study, with 78% of proposed adaptation initiatives for accommodation, has supported that argument. In addition to necessary technological and engineering measures, small and medium coastal cities in developing countries apply various

accommodation measures to enhance their capacity to tackle those climate risks such as assessment and information, livelihood, health, and insurance services, and capacity building.

Regarding protection measures, interestingly, the highest number of small- and medium-sized cities relies on ecosystem-based adaptation (EbA). EbA is increasingly recognized to be relevant to communities in developing countries because it promotes the symbiotic relationships between sociocultural and ecological systems (Pedersen Zari et al., 2020). EbA is cost-effective, flexible, and widely applicable to buffering climate change impacts (Munang et al., 2013). Results of this study support advocating the use of ecosystem-based approaches in coastal cities in developing countries.

Only a few cities pay attention to managed retreat. Its application, even in cities in developed countries, faces challenges given the projected scale of climate-induced displacement, the difficulties of resettlement, and social and psychological difficulties (Hino et al., 2017).

Conclusions

This chapter has analyzed the risks to climate change and extreme events and created an inventory of adaptation measures in small and medium coastal cities in developing countries. The study found that flooding, SLR, storm/typhoon, coastal erosion, and drought are among the most impacted natural hazards. As a result, coastal cities use a variety of adaptation measures to respond to these risks in all three categories: protection, accommodation, and retreat. Among the various adaptation measures, physical infrastructures and ecosystem-based adaptation appear to be the most popular measures in those cities. Every action encompasses both pros and cons, such as potential land saving but possible failure and recurring cost of physical infrastructures or the cheaper investment cost but the large land occupation of ecosystem-based measures. The combination of both hard and soft structural measures will take advantage of the benefit of both categories and will help to balance the disadvantages. Furthermore, adaptation implementation should also focus on various aspects such as capacity building, management, and policies and regulations, not just limited to structural measures. Some lessons emerge from these findings.

- Adaptation needs to encompass a wide range of actions on multiple aspects. It should aim simultaneously to protect and accommodate the living of coastal communities and plan for future climate change or extreme event impacts. The action also needs to pay more attention and resources to implement active retreat policies to reduce the effect in the future.
- Adaptation to current climate variability and future climate change needs to be flexible, cost-effective, and broadly applicable alternatives. It is crucial to apply the combination of both hard and soft measures such as physical structures, ecosystem-based adaptation, policies, and regulations to exploit the opportunities and address both short and long-term impacts.

Appendix: List of case studies and documents used as a primary data source

Continent/ region	City	Country	Population (2010)	Area (km^2)	Document
South America and the Caribbean	Cartagena	Columbia	944,481	51.4	• Plan 4C—A competitive and Climate Compatible Cartagena (2014)
	Castries	Saint Lucia	22,111	79	• Climate change adaptation planning in Latin American and Caribbean cities. Final report: Castries, Saint Lucia (2013)
	Esmeraldas	Ecuador	188,694	70.45	• Adaptation to Climate Change in Ecuador and the city of Esmeraldas: An assessment of Challenges and Opportunities (11/2009)
	Santos	Brazil	419,086	281	• Climate change adaptation planning in Latin American and Caribbean cities. Complete report: Santos, Brazil (2012)
Africa	Port Louis	Mauritius	118,042	42.7	• Building Climate Resilience: A Handbook for Port Louis Municipal Council, Mauritius (09/ 2012) • Climate change Projections for Port Louis: Adding value through downscaling (03/ 2012) • Sub-Saharan African Cities: A five-city Network to Pioneer Climate Adaptation through Participatory Research & Local Action. Baseline Study—Port Louis (02/2011)
	Walvis Bay	Namibia	59,940	32.5	• Building Climate Resilience. A handbook for Walvis Bay Municipality, Namibia (2012) • Climate change projections for Walvis Bay: Adding value through downscaling (07/2011)

Continent/ region	City	Country	Population (2010)	Area (km^2)	Document
					• Sub-Saharan African Cities: A five-city Network to Pioneer Climate Adaptation through Participatory Research & Local Action. Baseline Study—Walvis Bay (2011)
Asia	Bandar Lampung	Indonesia	879,651	197.22	• Vulnerability and Adaptation Assessment to Climate Change in Bandar Lampung City (2010) • Bandar Lampung Resilience Strategy 2011–2030 (in Indonesian) (2010)
	Batticaloa	Sri Lanka	85,120	75	• Batticaloa, Sri Lanka: Climate change Vulnerability Assessment (12/2011) • Batticaloa, Disaster Risk Reduction and Preparedness Plan: Towards a Sustainable and Resilience City (2013)
	Da Nang	Vietnam	926,014	1256.54	• Action Plan in Responding to Climate Change and Sea level Rise for Da Nang up to 2020 (in Vietnamese) (08/2012) • Resilience Da Nang 2016
	Hoi An	Vietnam	90,265	61.71	• Hoi An, Vietnam: Climate Change Vulnerability Assessment (2014) • VIE: Urban Environment and Climate Change Adaptation Project (Hoi An City, Quang Nam Province) (2014)
	Hue	Vietnam	310,962	70.67	• Climate Action Plan for Hue City (09/2014)
	Iloilo	Philippines	424,619	78.34	• Iloilo City Local Climate Action Plan 2014–2028 (2014)
	Kalmunai	Sri Lanka	105,264	22.8	• Kalmunai Disaster Risk Reduction and Preparedness Plan: Toward a sustainable and resilience city (2013)
	Khulna	Bangladesh	674,616	50.6	• Adapting to Climate Change: Strengthening the Climate Resilience of the Water Sector Infrastructure in Khulna, Bangladesh (2011)

Continued

Continent/ region	City	Country	Population (2010)	Area (km^2)	Document
	Kupang	Indonesia	315,768	180.26	• Climate Change Vulnerability Assessment Kupang City (06/2015) • Urban Climate Risk Management Plan—City of Kupang (08/2015)
	Manado	Indonesia	394,683	157.26	• City of Manado: Climate Change Vulnerability Assessment (09/2014)
	Mannar	Sri Lanka	73,608	216.94	• Mannar Disaster Risk Reduction and Preparedness Plan: Toward a sustainable and resilient city (2014)
	Mullaitivu	Sri Lanka	32,022	728.6	• Mullaitivu Disaster Risk Reduction and Preparedness Plan: Toward a Sustainable and Resilience city (2014)
	Negombo	Sri Lanka	142,050	31	• Negombo, Sri Lanka: Climate Change Vulnerability Assessment (12/2011) • Formulation of a City Development Strategy for Sri Lankan Cities to Response to Climate Change (Part 2, 3, 4)
	Panaji	India	113,153	76.3	• Climate-resilient infrastructure services. Case Study Brief: Panaji (2014)
	Sihanoukville	Cambodia	234,340	2585	• Sihanoukville, Cambodia: Climate Change Vulnerability Assessment (2012)
	Sorsogon	Philippines	155,144	312.92	• Climate Change Vulnerability Assessment (2010) • Sorsogon City Strategy for Climate Change Resilience (2010)
Oceania	Apia	Samoa	36,936	123.81	• Apia, Samoa: Climate Change Vulnerability Assessment (2014)
	Honiara	Solomon Islands	66,406	22.73	• Honiara, Solomon Islands: Climate Change Vulnerability Assessment (2014) • Honiara Urban Resilience & Climate Action Plan (2016)
	Lami Town	Republic of Fiji	20,989	6.8	• Lami Town, Fiji: Climate Change Vulnerability Assessment (2014)

Continent/ region	City	Country	Population (2010)	Area (km^2)	Document
	Port Moresby	Papua New Guinea	352,416	267.6	• Port Moresby, Papua New Guinea: Climate Change Vulnerability Assessment (2014)
	Port Villa	Vanuatu	66,081	24.3	• Greater Port Villa Climate Vulnerability Assessment—Full Report (2015). • Planning for ecosystem-based adaptation in Port Vila, Vanuatu—Synthesis report (2017)

References

Abel, N., Gorddard, R., Harman, B., Leitch, A., Langridge, J., Ryan, A., Heyenga, S., 2011. Sea-level rise, coastal development and planned retreat: analytical framework, governance principles and an Australian case study. Environ. Sci. Pol. 14 (3), 279–288. https://doi.org/10.1016/j.envsci.2010.12.002.

Bhat, G.K., Karanth, A., Dashora, L., Rajasekar, U., 2013. Addressing flooding in the city of Surat beyond its boundaries. Environ. Urban. 25 (2), 429–441. https://doi.org/10.1177/0956247813495002.

Biagini, B., Bierbaum, R., Stults, M., Dobardzic, S., McNeeley, S.M., 2014. A typology of adaptation actions: a global look at climate adaptation actions financed through the Global Environment Facility. Glob. Environ. Chang. 25, 97–108. https://doi.org/10.1016/j.gloenvcha.2014.01.003.

Building Futures and ICE, 2010. Facing up to Rising Sea-Levels: Retreat? Defend? Attack? London.

CZMS, I., 1990. Strategies for Adaptation to Sea-Level Rise. Report of the Coastal Zone Management Subgroup, Response Strategies Working Group of the Intergovernmental Panel on Climate Change, Ministry of Transport, Public Works and Water Management, The Hague.

Dasgupta, S., Laplante, B., Meisner, C., Wheeler, D., Yan, J., 2009. The impact of sea-level rise on developing countries: a comparative analysis. Clim. Chang. 93 (3), 379–388. https://doi.org/10.1007/s10584-008-9499-5.

Gibbs, M.T., 2016. Why is coastal retreat so hard to implement? Understanding the political risk of coastal adaptation pathways. Ocean Coast. Manag. 130, 107–114. https://doi.org/10.1016/j.ocecoaman.2016.06.002.

Hino, M., Field, C., Mach, K., 2017. Managed retreat as a response to natural hazard risk. Nat. Clim. Chang. 7, 364–370. https://doi.org/10.1038/nclimate3252.

IPCC, 2007. Climate Change 2007: Impacts, Adaptation and Vulnerability. Contribution of Working Group II to the Fourth Assessment Report of the Intergovernmental Panel on Climate Change. Cambridge University Press, Cambridge.

Klein, R.J.T., 2011. Adaptation to climate change: more than technology. In: Christiansen, L., Olhoff, A., Trærup, S. (Eds.), Technologies for Adaptation: Perspectives and Practical Experiences. Springer, Netherlands, pp. 19–25.

Klein, R.J.T., Nicholls, R.J., Sachooda, R., Michele, C., James, A., Buckley, E.N., 2001. Technological options for adaptation to climate change in coastal zones. J. Coast. Res. 17 (3), 531–543.

Le, T.D.N., 2019. Climate change adaptation in coastal cities of developing countries: characterizing types of vulnerability and adaptation options. Mitig. Adapt. Strateg. Glob. Chang. https://doi.org/10.1007/s11027-019-09888-z.

Munang, R., Thiaw, I., Alverson, K., Mumba, M., Liu, J., Rivington, M., 2013. Climate change and ecosystem-based adaptation: a new pragmatic approach to buffering climate change impacts. Curr. Opin. Environ. Sustain. 5 (1), 67–71. https://doi.org/10.1016/j.cosust.2012.12.001.

Nicholls, R.J., Wong, P.P., Burkett, V., Codignotto, J., Hay, J., McLean, R., Arblaster, J., 2007. Coastal systems and low-lying areas. In: Parry, M.L., Canziani, O.F., Palutikof, J.P., van der Linden, P.J., Hanson, C.E. (Eds.), Climate Change 2007: Impacts, Adaptation and Vulnerability. Contribution of Working Group II to the Fourth Assessment Report of the Intergovernmental Panel on Climate Change. Cambridge University Press, Cambridge, pp. 315–356.

Noble, I.R., Huq, S., Anokhin, Y.A., Carmin, J., Goudon, D., Lansigan, F.P., Villamizar, A., 2014. Adaptation needs and options. In: Field, C.B., Barros, V.R., Dokken, D.J., Mach, K.J., Mastrandrea, M.D., Bilir, T.E., White, L.L. (Eds.), Climate Change 2014: Impacts, Adaptation, and Vulnerability. Part A: Global and Sectoral Aspects. Contribution of Working Group II to the Fifth Assessment Report of the Intergovernmental Panel on Climate Change. Cambridge University Press, Cambridge and New York, NY, pp. 833–868.

Parry, M.L., Canziani, O.F., Palutikof, J.P., Van Der Linden, P.J., Hanson, C.E., 2007. IPCC, 2007: Climate Change 2007: Impacts, Adaptation and Vulnerability. Contribution of Working Group II to the Fourth Assessment Report of the Intergovernmental Panel on Climate Change. Cambridge University Press, Cambridge.

Pedersen Zari, M., Blaschke, P.M., Jackson, B., Komugabe-Dixson, A., Livesey, C., Loubser, D.I., Archie, K.M., 2020. Devising urban ecosystem-based adaptation (EbA) projects with developing nations: A case study of Port Vila, Vanuatu. Ocean Coast. Manag. 184, 105037. https://doi.org/10.1016/j.ocecoaman.2019.105037.

Sales Jr., R.F.M., 2009. Vulnerability and adaptation of coastal communities to climate variability and sea-level rise: their implications for integrated coastal management in Cavite City, Philippines. Ocean Coast. Manag. 52 (7), 395–404. https://doi.org/10.1016/j.ocecoaman.2009.04.007.

Sinay, L., Carter, R.W., 2020. Climate change adaptation options for coastal communities and local governments. Climate 8, 7. https://doi.org/10.3390/cli8010007.

USAID, 2009. Adaptation to Coastal Climate Change—A Guidebook for Development Planners. U.S. Agency for International Development (USAID), Washington, DC.

Wong, P.P., Losada, I.J., Gattuso, J.P., Hinkel, J., Khattabi, A., Mclnnes, K.L., Sallenger, A., 2014. Coastal systems and low-lying areas. In: Field, C.B., Barros, V.R., Dokken, D.J., Mach, K.J., Mastrandrea, M.D., Bilir, T. E., White, L.L. (Eds.), Climate Change 2014: Impacts, Adaptation, and Vulnerability. Part A: Global and Sectoral Aspects. Contribution of Working Group II to the Fifth Assessment Report of the Intergovernmental Panel on Climate Change. Cambridge University Press, Cambridge and New York, NY, pp. 361–409.

Zamora-Bornachera, A.P., López Rodríguez, A., Martinez, C., Lacoste, M., 2014. Plan 4C: A Competitive and Climate Compatible Cartagena. Executive Summary. Office of the Mayor of Cartagena de Indias, MADS, Invemar, CDKN and Cartagena Chamber of Commerce. Invemar General Publications Series No. 77, Santa Marta. 24 p.

CHAPTER

Multilevel governance in climate change adaptation: Conceptual clarification and future outlook

10

Asif Ishtiaque

School for Environment and Sustainability, University of Michigan, Ann Arbor, MI, United States

Introduction

The impacts of climate change are evident across the globe through increased extreme weather events, erratic weather patterns, and uncertainties in food security. These impacts do not substantially maintain political or jurisdictional scales and can be observed at multiple levels: global, national, regional, and local (Cash and Moser, 2000; Termeer et al., 2016; Westerhoff et al., 2011). For instance, at the local level, farmers of coastal areas may encounter more frequent tidal flooding due to sea-level rise; however, regionally, the impacts may appear as a threat to food security. Because of the multilevel nature of impacts, engagement of multiple actors in different sectors and at varying levels of governance is indispensable for efficient and effective climate responses (Adger et al., 2005; Amundsen et al., 2010; Eakin and Patt, 2011; Bauer et al., 2012; Chhetri et al., 2019). The term "actor" is used in a general sense in this chapter, and it includes individual, community, and organization. In this chapter, I emphasize on adaptation as a climate response initiative. Adaptation is defined as "process, action or outcome in a system for the system to better cope with, manage or adjust to some changing condition, stress, hazard, risk or opportunity" (Smit and Wandel, 2006).

Local-level disturbances may have regional or even national impacts, whereas national or global policy decisions may influence local-level outcomes. While addressing the impacts of climate change, actors operating at different levels of governance (i.e., local, regional, national, global) interact with each other and form a multilevel network of governance (see Fig. 1). The success of adaptation largely relies on the multilevel interactions that facilitate the governance process (Moser and Boykoff, 2013). However, whether the interactions among actors may facilitate or impair governance processes depend on their nature of interactions, structural arrangements, power asymmetries, and nature of barriers (Bulkeley and Moser, 2007; Keskitalo, 2010; Bauer et al., 2012). Thus, to analyze the efficiency and effectiveness of adaptation actions, it is important to examine the adaptation governance processes *aka* the interaction processes among actors that are involved in adaptation actions and the outcomes these processes generate. In this chapter, I intend to represent the strengths and limitations of the multilevel governance (MLG) concept and how analysis of MLG processes in adaptation actions can help us to understand the adaptation governance better. This will provide insights on interactions among involved actors, which would further be useful to decipher the complexities of adaptation governance.

Climate Change and Extreme Events. https://doi.org/10.1016/B978-0-12-822700-8.00009-3
Copyright © 2021 Elsevier Inc. All rights reserved.

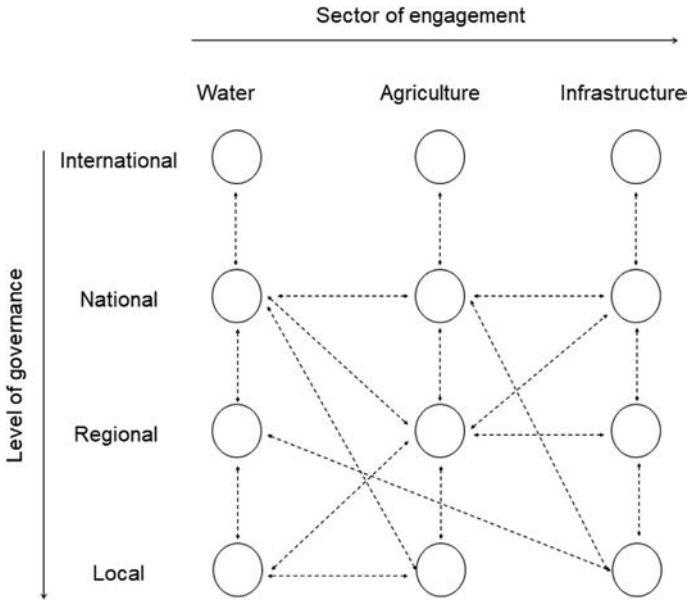

FIG. 1

Multilevel network of governance. The nodes represent actors that operate in different sectors of engagement and at different levels of governance. The arrows represent interactions among actors.

Many adaptation studies use the MLG concept without examining or validating the usability of the concept in their contexts. As such, they often leave us with some fundamental yet important questions: how many levels of governance should be incorporated to use this concept?; would it be all right to consider only horizontal or vertical levels?; is MLG all about government or international entities?; should we focus on the arrangement of multilevel networks or on the processes? In this chapter, I attempted to elucidate these issues by discussing conceptual nuances. I further identified how MLG concept is being used in climate adaptation research and the research gaps.

Multilevel governance—Conceptual clarification

Evolution of the concept

The MLG concept was formulated in a political milieu in which the authorities were dispersed across multiple jurisdictions. The concept was evolved in the early 1990s to capture the transformed governance structure and mechanisms of the European integration process. To enhance political and economic cooperation among member states, the European Economic Community, now known as the European Union (EU), signed the Single European Act in 1986. Later, with the signing of the Maastricht Treaty in 1992, the European nations increased their cooperation scope to domestic and foreign policies. In addition to these treaties, new policy formulation (e.g., cohesion policy) and increase of funds distributed the power and authority from the national governments to the supranational EU

and to other regional government entities (Hooghe, 1996; Tortola, 2017). These transformations brought about significant changes in the EU polity and it no longer could be explained or captured by the dominant European integration theories—neofunctionalism and intergovernmentalism (Marks, 1992, 1993; Marks et al., 1996).

Developed in the late 1950s, the neofunctionalism theory primarily rests upon the "spillover" notion meaning that integration or cooperation in one area creates the conditions or incentives for integration in another policy area. This theory downplays the importance of nationalism or nation-state; instead, it hypothesized that regional integration would be dominated by common needs and interests. On the other hand, intergovernmentalism is characterized by state-centrism. It postulates that national governments of the member states are the primary actors in the European integration process (Cini, 2016). Establishment of a supranational body (i.e., EU) does not weaken the role of national governments; rather, it determines the national governments as the ultimate decision makers in the integration process. As such, intergovernmentalism emphasizes on the national governments and negotiations among them in the integration process (Tsebelis and Garrett, 2001).

However, the new policy configuration in Europe was relatively nonhierarchical, dynamic, uneven, and characterized by continuous negotiations among nested governments at several territorial levels (Marks, 1993; Hooghe, 1996). The MLG concept came into existence to capture this pluralistic and networked polity. The fundamental notion of MLG is decision making in a pluralistic and highly dispersed policymaking milieu where multiple actors participate at various political levels from supranational to national to regional to local (Stephenson, 2013). MLG directs threefold of authority displacement: upward to international actors, downward to local actors, and outward to private and civil actors (Pierre and Peters, 2000). It implies that the actors are mutually dependent through intertwined cross-level decision-making activities. The MLG concept challenges the state-centric intergovernmentalism theory by contending that the national governments have important roles to play in the policymaking and implementation process. Still, their influences should no more be like monopolists because to democratize the governance process, the supranational and subnational actors can have significant influences as well.

Under the MLG concept, actors in a multilevel network can exert influence on the basis of diverse resources, including information, organization, expertise, financial resources, and legitimacy (Marks et al., 1996). State or national governments can no longer act as a "gate-keeper." The increased competencies and the interconnectedness among the actors allow the subnational and/or noncentral actors to open the center-periphery gate (representativeness of peripheral actors in the central policy processes). For instance, because of the interconnectedness, communities were able to engage in climate mitigation policy processes (Awono et al., 2014). This interrelationship also opens the domestic-foreign gate (representation of national or local interest in the international arena). For example, four different South American countries and international development agencies worked together to plan adaptation actions in the Andes mountain region (see Huggel et al., 2015). The inclusions of nongovernment organizations (NGOs), corporations, professional societies, and advocacy groups in the multiactor network open up the state-society gate (prioritization of societal demand as national interest) (Piattoni, 2009). To illustrate, Broto et al. (2015) found that to obtain international climate adaptation-related funds, a city government in Mozambique partnered with NGOs and communities to plan adaptation actions. The globalization process and social mobilization enabled the participation of multiple actors and enhanced intersectoral cooperation throughout the world (Alcantara et al., 2015). For this reason, despite its conception to study the European multiactor governance settings, the MLG

concept has been used to analyze the institutional and policy dynamics of the multiactor governance arrangements in other parts of the world as well.

Inclusiveness of MLG

Before directly applying the MLG perspective to any multiactor governance context, two sets of confusions need to be addressed: *actor-centered* and *process-centered* confusions. The *actor-centered* confusion deals with the issue of which actors should be considered for MLG analysis. More particularly, it addresses the inclusion or exclusion of supranational and nonstate actors. The MLG concept was first conceptualized under the context where a supranational actor—EU was dominant. As such, it was implicit that the presence of a supranational actor would be required to analyze MLG. However, more recent conceptual applications relaxed the supranational requirement and applied the MLG concept to settings as diverse as federations, international cooperation, and unitary states (Tortola, 2017).

On the other hand, the role of nongovernment or nonstate actors has not been treated similarly across the MLG conceptualization. Almost a decade after the advent of the MLG concept, Hooghe and Marks (2001) elaborately talked about the involvement of nonstate and private actors, but they did not specify how these actors should be treated in the MLG network. As a result, although some scholars (e.g., Peters and Pierre, 2004; Piattoni, 2009) stressed on the involvement of nonstate or private actors in their analyses, some others (e.g., Ciaffi, 2001; Bruszt, 2008) relegated the nonstate actors to a secondary role, if not ignored, in their empirical applications. The *process-centered* confusion deals with the issue of focusing on the structural arrangements or the interrelations of actors or both. This confusion arises with the claims that the MLG concept puts too much focus on the structure of the multiactor network. Bache (2008) argued that the MLG concept lacks attention toward the dynamic processes, interrelationships, and power relations across the multiactor network. Although this is true to some extent that Marks (1993) and Hooghe and Marks (2003) put more attention to the structure of the network in the conceptualization, but they also include the involvement of processes in their discussion. The empirical applications have evidence from both structures and processes of MLG networks depending on the purpose of research (Tortola, 2017).

The boundary of MLG

In the applications of MLG concept, the empirical studies might face challenges with defining whether or not MLG or coproduction of policies has occurred (Benz, 2004; Alcantara et al., 2015). The determination of the boundary of governance is tricky because there is a difference between engagement and influence, between a seat at the table and a real voice in crafting policy (Bache, 2008; Norman and Bakker, 2009). The MLG concept takes an inclusive approach to analyze governance processes. It incorporates multilevel actors that interact across and around formal structures of representative government in decision-making processes that transcend beyond formal institutions (Klijn and Skelcher, 2007). Notably, the decision-making process comprises not only policy formulation or coordination processes but also implementation, monitoring, and evaluation processes. Commonly, not all actors will actively participate in every stage of decision-making processes. To adopt the MLG concept, it is not imperative to have a full and sustained relationship among all actors throughout the decision-making processes; the interrelationships can be active or latent at different stages (Alcantara et al., 2015). With this encompassing approach,

the MLG concept gives the researchers the freedom to define the boundary of an MLG network depending on the context.

Approaches of MLG

An MLG network can be examined through one of the two approaches: *system approach* and *instance approach* (Alcantara et al., 2015). The *system approach* emphasizes more on the architecture of the governance—how the actors are structured and interconnected in the MLG network. The system approach analyzes the interactions among governance tiers but keeps its concentration on the MLG structure. In this way, the system approach of MLG captures the traditional relationships among government actors, like in case of federalism or intergovernmentalism, as well as the newly formed relationships with supranational and subnational actors and nonstate actors. This approach views the arrangement of MLG in two ways: Type I and Type II MLG (Hooghe and Marks, 2001, 2003). Type I MLG is characterized by dispersion of authority to a limited number of nonoverlapping jurisdictions in a limited number of levels. The jurisdictions are large enough to carry out or bundle multiple tasks. By supporting a quasipermanent jurisdictional system, Type I MLG bases its argument on federalism, which is concerned with power sharing among a few governance levels. For example, in Canada and the United States, the adoption of indigenous claims took place through the development of MLG in the existing federal structures (Papillon, 2012).

Contrary to the Type I MLG, Type II MLG is characterized by a vast number of jurisdictions operating at diverse territorial scales. The jurisdictions are flexible and territorially overlapping but task specific to respond to changing social demands and functional requirements. Type II MLG has resemblance with FOCJ (functional, overlapping, and competing jurisdictions) governance (Frey and Eichenberger, 1996) and polycentric governance (Ostrom et al., 1961). Type II MLG is generally embedded in Type I governance (Hooghe and Marks, 2003) and can be observed through contractual privatization, outsourcing, and administrative decentralization under the Type I MLG. Also, the formation of task forces, international commissions, or intercity agencies represents the Type II MLG. In this way, Type II MLG can be observed in the boundary of Type I MLG network. For instance, in Australia, Bates et al. (2013) observed that climate adaptation practices are benefitted from creating new forums (i.e., task forces, policy development committees, interagency groups), which may act as boundary objects in the existing governance structure.

The *instance approach*, on the other hand, conceptualizes MLG through episodes or moments of interactions, rather than formal rules or large-scale mechanisms of a political architecture (Alcantara et al., 2015). This approach mainly focuses on the processes of interactions, regular or sporadic, instead of configuration of the governance. As such, the instance approach assumes that MLG is not about having a distinct governance configuration; instead, it can thrive within federal, confederal, or even unitary systems where the dispersion of authority happens. According to this approach, instances can be led by any actor—local government, corporation, taskforce, or private organization that is part of the MLG network. However, this approach requires the presence of at least one nongovernmental actor in an MLG network. For instance, Verkerk et al. (2015) found that the MLG processes could be a discontinuous and nonlinear chain of actions that crosses various governance levels. In instance approach, MLG can appear only through interactions among actors that are constituted at different territorial levels. Therefore, same-level interactions would be considered as governance only, not an MLG.

MLG concept in climate adaptation

In response to climate change impacts, the national governments play key roles in country-specific climate adaptation. However, supranational bodies, such as the Intergovernmental Panel on Climate Change, United Nations Framework Convention on Climate Change, and Global Commission on Adaptation, act as platforms to accelerate, coordinate, and support adaptation efforts. Furthermore, the international development agencies (e.g., the World Bank Group, United Nations Development Program, Bill and Melinda Gates Foundation) are assisting national governments in planning and implementing climate adaptations. National governments also mobilized the local governments in the climate adaptation process. In addition, the participation of NGOs and private sectors increased substantially, particularly in the local-level adaptation, over the years (Keskitalo, 2010; Juhola and Westerhoff, 2011; Haque et al., 2016). In this way, in the governance of climate change, the national governments do not necessarily remain as the only or most important actor. The presence of such constellation of diverse actors in climate change governance has been possible by recognizing the roles of supranational, subnational, and nonstate actors and their entangled connections. This arrangement of actors and the interactions among them in pursuing a collective goal (*aka* climate adaptation) makes the climate adaptation governance a perfect subject for analysis through the lens of the MLG concept.

The initial attempts of using the MLG concept in climate change governance sought to explore the roles of subnational actors in climate policy response processes. With a particular focus on city governments, these studies adopted the MLG concept to analyze the governance configurations and interactions of actors in climate policymaking in transnational governance networks (Betsill and Bulkeley, 2006), in England (Bulkeley and Betsill, 2005), Sweden (Gustavsson et al., 2009), Ireland (McGloughlin and Sweeney, 2011), North America (Rabe, 2007; Lee and Koski, 2015), and East Asia (Schreurs, 2017). These studies found that because of globalization and increasing attention to local-level dynamics, city and municipal governments become important actors in climate policymaking. These local governments can promote a participatory approach in climate policymaking by involving local communities and other stakeholders.

The use of the MLG concept explicitly focusing on climate adaptation began with the work of Keskitalo (2010). Focusing on the European context, they took a system approach and showed that MLG could be embedded in the existing governance structure, be it centralized or decentralized. They also portrayed how MLG could be extended to private sectors. More recently, adopting the instance approach, Verkerk et al. (2015) argued that MLG in climate adaptation is characterized by a discontinuous chain of actions, and it is strengthened by instances of synchronization among multiple actors. However, Fidelman et al. (2013) found that episodic and task-specific ideas about MLG are not sufficient to govern response to a complex, multisectoral issue like climate adaptation. Instead, more stable, continuous, and inclusive interactions among the actors can provide more effective outcomes. The MLG process can be hindered by traditional governance challenges, such as institutional fragmentation, organizational tension. Based on a study in a rain-fed farming system of India, Chaudhari and Mishra (2016) identified that even though MLG is facilitative in mainstreaming climate adaptation in India, the preexisting structural and governance challenges impair the successes. Amundsen et al. (2010) further found that lack of interorganizational relationships can generate barriers in the adaptation planning and implementation processes. Bates et al. (2013) argued that these types of

challenges could be minimized by creating forums—an interorganizational kind of relationship to solve complex mutual problems, which can include industry task forces, policy development committees, interagency groups, and specific climate change committees. Similarly, Lidskog and Elander (2010) argued that local-level horizontal exchange of information, often informal, and transnational networks exchanging experiences would facilitate climate adaptation.

In general, climate adaptation research used the MLG concept to explain and examine the structure and processes of the multiactor network involved in adaptation management. These studies showed the significance of local actors in MLG. Unlike the traditional MLG, in which the authority is dispersed from national governments, in climate adaptation, local governments can initiate policymaking processes by exposing the local needs or by pushing the national government for climate response. Furthermore, climate adaptation studies showed that transnational networks to exchange information and experience facilitate the colearning process in MLG. These studies represent that the involvement of private sectors at the local level and their partnerships with public sectors have a positive influence on climate adaptation. However, the majority of the studies indicated that the national governments are often at the vanguard of climate adaptation as they are the gateway to access climate-related fundings.

Research trends in climate adaptation using MLG and future outlook

The introduction of the MLG concept into climate adaptation research is relatively recent. However, studies addressed various issues in the interactions of actors that are involved in climate mitigation and adaptation for long. Although these studies did not consider the MLG concept explicitly, they analyzed the interactions among actors operating at the same level (i.e., horizontal interactions) or different levels (i.e., vertical interactions). Based on the topical review of the existing literature, I identified three broad themes of MLG of adaptation-related research. These three themes can guide future research directions. It is important to note that studies do not always adhere to a single theme; instead, they often cover more than one topic.

Theme I: Structure and process of MLG

Many adaptation studies focused on analyzing the structural characteristics of the multilevel network of actors and examined the process of interactions. For instance, Huh et al. (2017) presented the MLG network and processes of climate adaptation in South Korea. They concluded that the lack of interactions across sectors at the local level impedes the governance process. Again, Zen et al. (2019) identified how national-level policymaking is translated into local-level implementation in Malaysia using the MLG concept. Studies under this theme are usually concerned with the participation of actors in the decision-making process and their coordination and collaboration in the process. Oftentimes, studies take an embracing approach to address these issues by focusing on multiple actions in a specific context, rather than on a particular action or project.

Studies under this theme examine the participation of various actors in the adaptation governance process. Their analyses provide insights on how participation is facilitated or curtailed by institutional norms and practices, how participation influences the governance process, and how more inclusive governance milieu could be created. For instance, Bates et al. (2013) found that forums, a platform for participation, play a vital role in enhancing the ability of actors to address a range of issues in

climate adaptation. Critical studies of this research area advance our understanding of how participation can be used as an instrument of power and domination. Few et al. (2007), for example, demonstrated that participation of a large number of actors might raise competition for dominance, and it is unlikely to achieve participatory goals in that circumstance. However, ensuring the participation of concerned parties of adaptation actions is crucial. The participation of different actors in different stages of adaptation can lead to higher effectiveness, efficiency, equity, legitimacy, and sustainability (Sherman and Ford, 2014).

Similar to participation-related research, studies under this theme also analyzed collaboration and coordination networks among actors. Collaboration and coordination among actors are core elements of MLG. Studies (e.g., Armitage et al., 2010; Briassoulis, 2011) give us knowledge on what processes lead to collaboration, how collaboration among actors could be enhanced, and how collaborations among actors result in better decision making. However, cooperation and coordination are often dictated by the visions, objectives, and intentions of actors. As an example, Verkerk et al. (2015) argued that a lack of mutual understanding of a problem could lead to stagnation of collaboration while an understanding strengthens their coordination. It may also happen that frequent formal or informal interactions result in a similar understanding of a problem, which ultimately may lead to better coordination. Ishtiaque et al. (2019), for instance, found that a similar understanding of climate vulnerability was possible due to regular interactions among actors (also see Juhola et al., 2011).

Despite these attempts, we need more research under this theme on various issues. Although studies under this theme emphasized on country-, city-, or community-specific adaptation actions to analyze MLG structure and processes, the regional or international partnerships remain less focused (but see Bauer and Steurer, 2014). Also, more studies are required focusing on the complexities of negotiation, mechanisms of convergence and divergence of understanding, intersectoral-, or horizontal-level coordination processes. Studies addressed these issues to some extent, but in most cases, they answered the "what" and "how" questions, whereas the "why" question remained vague. The participation of actors has been studied for long in different research areas, yet in climate adaptation, it remains understudied. More specifically, more research is required on how the participation of involved actors could be ensured efficiently, equitably, and effectively, how institutional capacities influence participation and the effect of participation on the governance process. The climate adaptation studies that used the MLG concept are regionally clustered in Global North, particularly in Europe, perhaps because the MLG concept evolved in the European setting. Therefore, evidence from the Global South is scant. Unlike Global North, in Global South, governance processes are often marred with national and or local politics, and at the same time, inequality, injustice, subjugation, and marginalization are quite prevalent there. Some countries even encounter frequent destabilization of governance processes. Thus it becomes essential to gather evidence from the Global South to understand the MLG of climate adaptation better and provide contextual solutions.

Theme II: Power interplay in MLG

Adaptation studies that are concerned with MLG also focused on power interplay among actors in MLG settings. Often, studies under this theme address *Theme I* (structure and process of MLG) as well because these two themes are overlapping in most cases. Under this theme, these studies emphasized how MLG processes are influenced by power struggles, power inequalities, and power sharing. In this chapter, I define power as the ability of an actor to influence others within a social relationship to carry

out his agenda or will, regardless of resistance (Weber, 1947; Dahl, 1982). Some studies (e.g., Vink et al., 2013; Gordon and Johnson, 2017) under this theme do not directly adopt the MLG concept in their analysis per se, but they analyze the power dynamics among actors that are operating at different levels.

Studies under this theme found that power interplay among actors is often the key to effective adaptation actions. If the power relations among actors are not addressed, measures taken to increase the effectiveness of adaptation may become futile. For instance, Nagoda and Nightingale (2017) found that because of the existing power relations among actors that prohibit contributions of marginalized stakeholders in the adaptation process, participatory approaches are not successful; instead, they reinforce existing vulnerabilities. Power dynamics among actors may determine the objectives of adaptation actions. The actors struggle among themselves for power to establish their understanding of the problem and its solutions. Vij et al. (2018), as an example, demonstrated that the actors use power to convince others to agree with their planning. Power dynamics are evident at all levels of governance. At the national level, actors may use power to obtain funds or to formulating policies according to their objectives. In contrast, at the local level, actors may use power to gather influence or resources. Stock et al. (2020) identified that power interplay among actors impairs coordination at the national level and increases vulnerabilities at the local level.

Power relations analyses further provide us insights on how MLG is taking place and how certain actors are more powerful than others (Marquardt, 2017). These analyses show that how power distribution among actors can defy the formal structural arrangements and regulatory protocols. Studies found that often certain national-level actors or a few local-level actors can overpower others and become absurdly dominant in the decision-making process. They termed it as "elite-capture" of governance process (see Nagoda and Nightingale, 2017; Sova et al., 2017; Stock et al., 2020). The elite-capture nature of governance discourages the creation of an inclusive governance milieu. However, some studies also found an elite-pluralistic nature—a combination of elitism and pluralism in adaptation governance (see Bisaro et al., 2010; Di Gregorio et al., 2019). These two terms also represent top-down and bottom-up processes as well as centralized and decentralized nature. Some studies claimed that top-down or centralized decision making is an effective approach for climate adaptation by arguing that it can facilitate better coordination and, as a result, prevent overlapping authorities, conflicting responsibilities, and duplicating functions (e.g., Tompkins et al., 2010; Bauer and Steurer, 2014). These studies contextualize their analysis in Global North, more particularly in the United Kingdom. However, overwhelming evidence from Global South and other parts of Global North suggests that the disadvantages of centralization outweigh its advantages by prohibiting experimental learning, trust building, and collaborative management and leading to a disregard of local priorities and context sensitivities (e.g., Dannevig and Aall, 2015; Ojha et al., 2016; Nightingale, 2017; Sova et al., 2017).

Power analysis among actors has been addressed quite widely in climate adaptation research. These studies provide insights and understanding of how power interplay leads to tensions, conflicts, elite-capture, and marginalization. They often offer broad policy recommendations to address these issues, but solution-focused studies remain limited. I think specific solution-based studies would be significantly useful in decision making in an MLG setting. At the same time, we need more research on power interplay among actors to understand the opportunities and tradeoffs for potential solutions to power inequities. Furthermore, in climate adaptation management, private actors (i.e., NGOs, communities) play important roles. Although their roles and contributions are addressed by some (e.g., Nagoda and Nightingale, 2017), we are in need of more research on public-private relationships in MLG settings.

Theme III: Barriers to adaptation in MLG

Studies under this theme deal with the barriers to adaptation in MLG settings. In MLG arrangements, actors interact with each other continuously or episodically, and their interactions are often characterized by their ambitions, preferences, responsibilities, and resources. Discrepancies in these attributes among actors may cause numerous challenges to surface during interactions and impair the governance process. These challenges are popularly known as *barriers to adaptation*. Synonymously termed as "hindrances" or "constraints" or "impasses" in the literature, barriers to adaptation can generally be defined as obstacles or challenges that can impede the governance process of planning, implementing, and monitoring adaptation actions (Moser and Ekstrom, 2010; Eisenack et al., 2014).

Even though barriers to adaptation have been discussed widely in adaptation literature, few of them analyzed these barriers from an MLG perspective. An MLG perspective allows analyzing barriers that emerge not only because of same-level interactions or limitations but also interactions or limitations at different levels. It further enables us to understand that these barriers may not be overcome with the resources of the same-level actors and may require multilevel responses. For instance, Juhola (2016) found that the barriers that emerge at the local level from the existing governance structure cannot be solved by the local level alone. She recognizes coordination across levels of governance. Studies also identified that barriers might emerge due to less collaboration, lack of coordination, the divergence of priorities, and political opposition (Amundsen et al., 2010; Walker et al., 2015). The key finding these studies presented is that deliberate and slow-moving collaboration and coordination, although maybe democratic in nature, can also impede swift adaptation.

Barrier-related studies in MLG of climate adaptation are scarce, and we are in dire need of more research. However, considering the barrier-related studies in the overall adaptation process, I think the focus should be on why and how the barriers emerge in the MLG process, rather than on what are the barriers. Because categorizing a factor or process as a barrier reduces complex and highly dynamic decision-making processes into simplified, static, and metaphorical statements about why current outcomes are "incorrect" without sufficient evidence or explanation (Biesbroek et al., 2014). For example, "lack of coordination" among actors has been identified as a barrier to adaptation by many without sufficient explanation on how it comes into play through the interactions among actors. Addressing the barriers in decision-making processes requires explanations of the mechanisms that cause these unintended outcomes or barriers to emerge (Biesbroek et al., 2017). Lately, Ishtiaque et al. (2021) analyzed the barriers to adaptation in a MLG setting and identified key mechanisms that cause emergence of those barriers. However, more studies are required to understand how and why barriers emerge. Unless we know and address these mechanisms, attempts to overcome the obstacles may become futile.

Conclusion

In this chapter, I attempt to clarify the concept of MLG by discussing its evolution, approaches, and boundaries. Despite its development in the European context, the MLG concept could be used for any context where the dispersion of authority took place upward, downward, and sideways. MLG considers not only public actors but also private actors. Furthermore, in MLG, interactions among organizations can be continuous; moreover, they can be task specific and episodic. This inclusive approach enables

researchers to use this concept more widely to analyze the climate adaptation governance process in a variety of contexts. In this chapter, I discussed the key research themes that the existing MLG-related studies addressed. I identified three research themes: structure and process, power interplay, and barriers to adaptation. Under each of these themes, I have discussed the limitations of existing studies and provided the future outlook.

Methodologically, the MLG of climate adaptation-related studies is not innovative. They mostly used the traditional social science methods of interviewing and review. Common methodological approaches include key interview, focus group discussion, case study analysis, stakeholder analysis, institutional analysis, policy review, literature review, etc. Although these are mostly qualitative and indeed practical approaches to address MLG-related issues, I argue that there remain some opportunities to add quantitative methods in this type of analysis. I think social network analysis could be a useful method to address issues related to collaboration and coordination (see, for instance, Lienert et al., 2013; Sayles and Baggio, 2017).

The concept of MLG is proven useful in analyzing multiactor networks and processes. Because of its encompassing nature, the concept can be used in many contexts; however, before applying the MLG concept to a context, one must be certain about authority dispersion and carefully consider the approaches and boundaries of the multiactor network. The use of MLG is relatively recent in climate adaptation research, and there are ample opportunities to use this concept effectively to analyze the adaptation governance. These analyses may provide insights to make adaptation governance more efficient. Also, they can increase our understanding of potential solutions and tradeoffs.

References

Adger, W.N., Arnell, N.W., Tompkins, E.L., 2005. Successful adaptation to climate change across scales. Glob. Environ. Chang. 15 (2), 77–86. https://doi.org/10.1016/j.gloenvcha.2004.12.005.

Alcantara, C., Broschek, J., Nelles, J., 2015. Rethinking multilevel governance as an instance of multilevel politics: a conceptual strategy. Territ. Politic. Gov. 4 (1), 33–51.

Amundsen, H., Berglund, F., Westskogh, H., 2010. Overcoming barriers to climate change adaptation-a question of multilevel governance? Environ. Plan. C Govt Policy 28 (2), 276–289. https://doi.org/10.1068/c0941.

Armitage, D., Berkes, F., Doubleday, N. (Eds.), 2010. Adaptive Co-Management: Collaboration, Learning, and Multilevel Governance. UBC Press.

Awono, A., Somorin, O.A., Atyi, R.E.A., Levang, P., 2014. Tenure and participation in local REDD+ projects: insights from southern Cameroon. Environ. Sci. Pol. 35, 76–86.

Bache, I., 2008. Europeanization and Multilevel Governance: Cohesion Policy in the European Union and Britain. Rowman & Littlefield.

Bates, L.E., Green, M., Leonard, R., Walker, I., 2013. The influence of forums and multilevel governance on the climate adaptation practices of Australian organizations. Ecol. Soc. 18 (4), 62.

Bauer, A., Steurer, R., 2014. Multilevel governance of climate change adaptation through regional partnerships in Canada and England. Geoforum 51, 121–129.

Bauer, A., Feichtinger, J., Steurer, R., 2012. The governance of climate change adaptation in 10 OECD countries : challenges and approaches countries : challenges and approaches. J. Environ. Policy Plan. 14 (3), 279–304. https://doi.org/10.1080/1523908X.2012.707406.

Benz, A., 2004. Multilevel governance—governance in Mehrebenensystemen. In: Governance—Regieren in komplexen Regelsystemen. VS Verlag für Sozialwissenschaften, pp. 125–146.

Biesbroek, G.R., Termeer, C.J.A.M., Klostermann, J.E.M., Kabat, P., 2014. Rethinking barriers to adaptation : mechanism-based explanation of impasses in the governance of an innovative adaptation measure. Glob. Environ. Change 26, 108–118. https://doi.org/10.1016/j.gloenvcha.2014.04.004.

Betsill, M.M., Bulkeley, H., 2006. Cities and the multilevel governance of global climate change. Glob. Gov. 12 (2), 141–160.

Biesbroek, R., Dupuis, J., Wellstead, A., 2017. Explaining through causal mechanisms : resilience and governance of social–ecological systems. Curr. Opin. Environ. Sustain. 28, 64–70. https://doi.org/10.1016/j.cosust.2017.08.007.

Bisaro, A., Hinkel, J., Kranz, N., 2010. Multilevel water, biodiversity and climate adaptation governance : evaluating adaptive management in Lesotho. Environ. Sci. Pol. 13, 637–647. https://doi.org/10.1016/j.envsci.2010.08.004.

Briassoulis, H., 2011. Governing desertification in Mediterranean Europe: the challenge of environmental policy integration in multilevel governance contexts. Land Degrad. Dev. 22 (3), 313–325.

Broto, V.C., Macucule, D.A., Boyd, E., Ensor, J., Allen, C., 2015. Building collaborative partnerships for climate change action in Maputo, Mozambique. Environ Plan A 47 (3), 571–587.

Bruszt, L., 2008. Multilevel governance—the eastern versions: emerging patterns of regional developmental governance in the new member states. Reg. Fed. Stud. 18 (5), 607–627.

Bulkeley, H., Betsill, M., 2005. Rethinking sustainable cities: multilevel governance and the 'urban' politics of climate change. Environ. Politics 14 (1), 42–63.

Bulkeley, H., Moser, S.C., 2007. Responding to climate change: governance and social action beyond Kyoto. Glob. Environ. Politics 7 (2), 1–10. https://doi.org/10.1162/glep.2007.7.2.1.

Cash, D.W., Moser, S.C., 2000. Linking global and local scales: dynamic assessment and management processes. Glob. Environ. Chang. 10, 109–120.

Chaudhari, V.R., Mishra, A., 2016. Multilevel policy responses to mainstream climate adaptation through watershed development in rainfed farming systems of India. Clim. Dev. 8 (4), 324–335.

Chhetri, N., Stuhlmacher, M., Ishtiaque, A., 2019. Nested pathways to adaptation. Environ. Res. Commun. 1 (1), 015001.

Ciaffi, A., 2001. Multilevel governance in Italy: the case of Marche. Reg. Fed. Stud. 11 (2), 115–146.

Cini, M., 2016. Intergovernmentalism. In: Cini, M., Borragan, N.P. (Eds.), European Union Politics, fifth ed. Oxford Press, England.

Dahl, R., 1982. Dilemmas of Pluralist Democracy: Autonomy vs. Control. Yale University Press, New Haven, CT.

Dannevig, H., Aall, C., 2015. The regional level as boundary organization? An analysis of climate change adaptation governance in Norway. Environ. Sci. Pol. 54, 168–175.

Di Gregorio, M., Fatorelli, L., Paavola, J., Locatelli, B., Pramova, E., Nurrochmat, D.R., Kusumadewi, S.D., 2019. Multilevel governance and power in climate change policy networks. Glob. Environ. Chang. 54, 64–77. https://doi.org/10.1016/j.gloenvcha.2018.10.003.

Eakin, H.C., Patt, A., 2011. Are adaptation studies effective, and what can enhance their practical impact? Wiley Interdiscip. Rev. Clim. Chang. 2 (2), 141–153. https://doi.org/10.1002/wcc.100.

Eisenack, K., et al., 2014. Explaining and overcoming barriers to climate change adaptation. Nat. Clim. Chang. 4 (10), 867–872.

Few, R., Brown, K., Tompkins, E.L., 2007. Public participation and climate change adaptation: avoiding the illusion of inclusion. Clim. Pol. 7 (1), 46–59.

Fidelman, P.I.J., Leitch, A.M., Nelson, D.R., 2013. Unpacking multilevel adaptation to climate change in the Great Barrier Reef, Australia. Glob. Environ. Chang. 23 (4), 800–812. https://doi.org/10.1016/j.gloenvcha.2013.02.016.

Frey, B.S., Eichenberger, R., 1996. FOCJ: competitive governments for Europe. Int. Rev. Law Econ. 16 (3), 315–327.

Gordon, D.J., Johnson, C.A., 2017. The orchestration of global urban climate governance: conducting power in the post-Paris climate regime. Environ. Politics 26 (4), 694–714.

Gustavsson, E., Elander, I., Lundmark, M., 2009. Multilevel governance, networking cities, and the geography of climate-change mitigation: two Swedish examples. Environ. Plan. C Govt Policy 27 (1), 59–74.
Haque, M.M., Bremer, S., Aziz, S.B., van der Sluijs, J.P., 2016. A critical assessment of knowledge quality for climate adaptation in sylhet division, Bangladesh. Clim. Risk Manag. https://doi.org/10.1016/j.crm.2016.12.002.
Hooghe, L. (Ed.), 1996. Cohesion Policy and European Integration: Building Multilevel Governance. University Press on Demand, Oxford.
Hooghe, L., Marks, G., 2001. Types of multilevel governance. Eur. Integ. Online Papers 5 (11), 1–26.
Hooghe, L., Marks, G., 2003. Unraveling the central state, but how ? Types of multilevel governance. Am. Polit. Sci. Rev. 97 (2), 233–243.
Huggel, C., Scheel, M., Albrecht, F., Andres, N., Calanca, P., Jurt, C., Silva, Y., 2015. A framework for the science contribution in climate adaptation: experiences from science-policy processes in the Andes. Environ. Sci. Pol. 47, 80–94.
Huh, T., Park, Y., Yang, J.Y., 2017. Multilateral governance for climate change adaptation in S. Korea: the mechanisms of formulating adaptation policies. Sustainability 9 (8), 1364.
Ishtiaque, A., Eakin, H., Chhetri, N., Myint, S., Dewan, A., Kamruzzaman, M., 2019. Examination of coastal vulnerability framings at multiple levels of governance using spatial MCDA approach. Ocean Coast. Manag. 171, 66–79. https://doi.org/10.1016/j.ocecoaman.2019.01.020.
Ishtiaque, A., Stock, R., Vij, S., Eakin, H., Chhetri, N., 2021. Beyond the barriers: an overview of mechanisms driving barriers to adaptation in Bangladesh. Environ. Policy Gov. https://doi.org/10.1002/eet.1925.
Juhola, S., 2016. Barriers to the implementation of climate change adaptation in land use planning: a multilevel governance problem? Int. J. Clim. Chang. Strateg. Manag. 8 (3), 338–355.
Juhola, S., Westerhoff, L., 2011. Challenges of adaptation to climate change across multiple scales: a case study of network governance in two European countries. Environ. Sci. Policy 14 (3), 239–247. https://doi.org/10.1016/j.envsci.2010.12.006.
Juhola, S., Keskitalo, E.C.H., Westerhoff, L., 2011. Understanding the framings of climate change adaptation across multiple scales of governance in Europe. Environ. Politics 20 (4), 445–463.
Keskitalo, E.C.H. (Ed.), 2010. Developing Adaptation Policy and Practice in Europe: Multilevel Governance of Climate Change. Developing Adaptation Policy and Practice in Europe: Multilevel Governance of Climate Change. Springer, https://doi.org/10.1017/CBO9781107415324.004.
Klijn, E.H., Skelcher, C., 2007. Democracy and governance networks: compatible or not? Public Adm. 85 (3), 587–608.
Lee, T., Koski, C., 2015. Multilevel governance and urban climate change mitigation. Environ. Plan. C Govt Policy 33 (6), 1501–1517.
Lidskog, R., Elander, I., 2010. Addressing climate change democratically. Multilevel governance, transnational networks and governmental structures. Sustain. Dev. 18 (1), 32–41.
Lienert, J., Schnetzer, F., Ingold, K., 2013. Stakeholder analysis combined with social network analysis provides fine-grained insights into water infrastructure planning processes. J. Environ. Manag. 125, 134–148.
Marks, G., 1992. Structural Policy in the European Community. Euro-Politics. The Brookings Institution, Washington, DC, pp. 191–224.
Marks, G., 1993. Structural policy and multilevel governance in the EC. Maastricht Debates Beyond 392.
Marks, G., Scharpf, F.W., Schmitter, P.C., Streeck, W., 1996. Governance in the European Union. Sage.
Marquardt, J., 2017. Conceptualizing power in multilevel climate governance. J. Clean. Prod. 154, 167–175.
McGloughlin, J.S., Sweeney, J., 2011. Multilevel climate policies in Ireland. Ir. Geogr. 44 (1), 137–150.
Moser, S.C., Boykoff, M.T. (Eds.), 2013. Successful Adaptation to Climate Change: Linking Science and Policy in a Rapidly Changing World. Routledge.
Moser, S.C., Ekstrom, J.A., 2010. A framework to diagnose barriers to climate change adaptation. Proc. Natl. Acad. Sci. U. S. A. 107 (51), 22026–22031. http://www.pnas.org/content/107/51/22026.full.

Nagoda, S., Nightingale, A.J., 2017. Participation and power in climate change adaptation policies: vulnerability in food security programs in Nepal. World Dev. 100, 85–93.
Nightingale, AJ, 2017. Power and politics in climate change adaptation efforts: struggles over authority and recognition in the context of political instability. Geoforum 84, 11–20.
Norman, E.S., Bakker, K., 2009. Transgressing scales: water governance across the Canada–US borderland. Ann. Assoc. Am. Geogr. 99 (1), 99–117.
Ojha, H.R., Ghimire, S., Pain, A., Nightingale, A., Khatri, D.B., Dhungana, H., 2016. Policy without politics: technocratic control of climate change adaptation policy making in Nepal. Clim. Pol. 16 (4), 415–433. https://doi.org/10.1080/14693062.2014.1003775.
Ostrom, V., Tiebout, C.M., Warren, R., 1961. The organization of government in metropolitan areas: a theoretical inquiry. Am. Polit. Sci. Rev. 55 (4), 831–842.
Papillon, M., 2012. Adapting federalism: Indigenous multilevel governance in Canada and the United States. Publius: J. Federalism 42 (2), 289–312.
Peters, B.G., Pierre, J., 2004. Multi-level governance and democracy: a Faustian bargain? In: Bache, I., Flinders, M. (Eds.), Multi-level Governance. Oxford University Press, Oxford, pp. 75–89.
Piattoni, S., 2009. Multilevel governance: a historical and conceptual analysis. J. Eur. Integr. 31 (2), 163–180. http://www.tandfonline.com/doi/abs/10.1080/07036330802642755.
Pierre, J., Peters, B.G., 2000. Governance, Politics and the State. St. Martin's, New York.
Rabe, B.G., 2007. Beyond Kyoto: climate change policy in multilevel governance systems. Governance 20 (3), 423–444.
Sayles, J.S., Baggio, J.A., 2017. Social–ecological network analysis of scale mismatches in estuary watershed restoration. Proc. Natl. Acad. Sci. 114 (10), E1776–E1785.
Schreurs, M., 2017. Multilevel climate governance in China. Environ. Policy Gov. 27 (2), 163–174.
Sherman, M.H., Ford, J., 2014. Stakeholder engagement in adaptation interventions: an evaluation of projects in developing nations. Clim. Pol. 14 (3), 417–441.
Smit, B., Wandel, J., 2006. Adaptation, adaptive capacity, and vulnerability. Glob. Environ. Chang. 16 (3), 282–292.
Sova, C.A., et al., 2017. Power and influence mapping in Ghana's agricultural adaptation policy regime. Clim. Dev. 9 (5), 399–414.
Stephenson, P., 2013. Twenty years of multilevel governance: where does it come from? What is it? Where is it going? J. Eur. Public Policy 20 (6), 817–837.
Stock, R., Vij, S., Ishtiaque, A., 2020. Powering and puzzling: climate change adaptation policies in Bangladesh and India. Environ. Dev. Sustain., 1–23. https://doi.org/10.1007/s10668-020-00676-3.
Termeer, C.J.A..M., Dewulf, A., Karlsson-Vinkhuyzen, S.I., Vink, M., Van Vliet, M., 2016. Coping with the wicked problem of climate adaptation across scales: The Five R Governance Capabilities. Landsc. Urban Plan. 154, 11–19.
Tompkins, E.L., Adger, W.N., Boyd, E., Nicholson-Cole, S., Weatherhead, K., Arnell, N., 2010. Observed adaptation to climate change: UK evidence of transition to a well-adapting society. Glob. Environ. Chang. 20 (4), 627–635. https://doi.org/10.1016/j.gloenvcha.2010.05.001.
Tortola, P.D., 2017. Clarifying multilevel governance. Eur J Polit Res 56 (2), 234–250.
Tsebelis, G., Garrett, G., 2001. The institutional foundations of intergovernmentalism and supranationalism in the European Union. Int. Organ. 55 (2), 357–390.
Verkerk, J., Teisman, G., van Buuren, A., 2015. Synchronising climate adaptation processes in a multilevel governance setting: exploring synchronisation of governance levels in the Dutch delta. Policy Polit. 43 (4), 579–596.
Vij, S., et al., 2018. Power interplay between actors: using material and ideational resources to shape local adaptation plans of action (LAPAs) in Nepal. Clim. Pol. 19 (5), 571–584. https://doi.org/10.1080/14693062.2018.1534723.

Vink, M.J., Dewulf, A., Termeer, C., 2013. The role of knowledge and power in climate change adaptation governance: a systematic literature review. Ecol. Soc. 18 (4).
Walker, B.J.A., Neil Adger, W., Russel, D., 2015. Institutional barriers to climate change adaptation in decentralised governance structures: transport planning in England. Urban Stud. 52 (12), 2250–2266.
Weber, M., 1947. The Theory of Social and Economic Organizations. Oxford University Press, New York.
Westerhoff, L., Keskitalo, E.C.H., Juhola, S., 2011. Capacities across scales: local to national adaptation policy in four European countries. Clim. Policy 11 (4), 1071–1085.
Zen, I.S., Al-Amin, A.Q., Doberstein, B., 2019. Mainstreaming climate adaptation and mitigation policy: toward multilevel climate governance in Melaka, Malaysia. Urban Clim. 30, 100501.

CHAPTER

11 Is the local fulfilling its promise as the agent and site of global climate change governance? The status of local climate mitigation in the United States

Mark Anthony Ayure-Inga Agana
University of Arkansas, Fayetteville, AR, United States

Introduction and background

On June 1, 2017, President Donald J. Trump made an appearance in the White House Rose Garden, where he announced the United States' withdrawal from the 2015 Paris agreement. In the speech announcing the withdrawal, he said, "I was elected to represent the citizens of Pittsburgh, not Paris" (Mathews, 2017). He had long before becoming president expressed his opposition to climate change countless times through his favorite social media platform, twitter. In one tweet, he described the issue as follows; Trump, Donald (Trump, 2012) (@realDonaldTrump). "The concept of global warming was created by and for the Chinese in order to make U.S. manufacturing non-competitive" Nov 6, 2012, 1:15 p.m. Tweet. Trump had campaigned on revitalizing America's steel, coal, and car manufacturing industries, which were the major employers of the people of the Rust Belt until the late 1980s. Hence his elicitation of the City of Pittsburg appeared to be a show of camaraderie with the people of the Rust Belt, whose vote secured him the Oval Office in the 2016 Presidential elections (though 80% of the vote in Pittsburg went to Hillary Clinton) and, at the same time, an attempt at uniting his decision to pull the United States out of the Paris Agreement with his promise of reindustrialization.

In response to this announcement, the mayor of the City of Pittsburgh tweeted; Peduto, William (Peduto, 2017) (@billpeduto). "The United States joins Syria, Nicaragua & Russia in deciding not to participate with world's Paris Agreement. It's now up to cities to lead." Jun 1, 2017, 2:57 p.m. Tweet. In addition, Climate Mayors, a peer-to-peer network of US mayors, formed in 2014 with the goal of demonstrating leadership in climate change action, released a statement avowing to uphold the goals of the Paris Climate Agreement. The network's membership also increased to more than 400 cities, following the United State's withdrawal from the Paris Agreement (Climate Mayors, 2017).

Twelve years earlier, a similar development unfolded when on February 16, 2005, the Kyoto Protocol entered into force without the United States. Led by the Mayor of Seattle, Mayor Greg Nickels,

Climate Change and Extreme Events. https://doi.org/10.1016/B978-0-12-822700-8.00006-8
Copyright © 2021 Elsevier Inc. All rights reserved.

the US Conference of Mayors came up with the Mayors Climate Protection Agreement (MCPA), seeking to fill the leadership void left by Washington. By the time of the Mayors' Annual Meeting in June 2005, the initial target of 141 cities was exceeded; reaching 500 members by May 2007—there are currently 1060 signatories to the agreement (United States Conference of Mayors, 2018). The US Conference of Mayors, at their annual meeting in June 2017, also rebuked the Trump administration's decision to pull the United States out of the Paris Agreement by reasserting their commitment to climate change mitigation. The MCPA, in addition, welcomed more than 200 new cities to its ranks following the president's action (Kusnetz, 2017).

As shown above, the federal government's inaction has been one of the main driving forces behind the waves of local climate action network memberships in the United States. However, more broadly, there has been an ongoing politics of scale around climate change governance (Bulkeley, 2005). In the local scaling of climate change governance, the "think globally and act locally" conceptualization—a global problem, but requires more local action—is invoked (Betsill, 2001; Betsill and Bulkeley, 2006; Betsill and Bulkeley, 2007; Brown and Purcell, 2005; Bulkeley, 2005; Bulkeley, 2010; Bulkeley and Schroeder, 2012; Easterling et al., 1998). Stakeholders and analysts have produced various desirable reasons why there should be a shift in focus to the "city"/"urban"/"local" scale as the domain of anthropogenic climate change action (for more on this, see Angel et al., 1998; Betsill, 2001; Bulkeley, 2005; C40, 2017; Flynn, 2000; Kates et al., 1998; Lindseth, 2004; Reed and Bruyneel, 2010; Rosenzweig et al., 2010; Rutland and Aylett, 2008; UN-HABITAT, 2011; Wang, 2013).

One of the most effective means through which the local scaling of climate change governance has taken place is the creation of transnational municipal networks (TMN). One of the forerunners in this regard has been the International Council for Local Environmental Initiatives' (ICLEI). Through platforms such as international negotiations, ICLEI has discursively portrayed climate change as a local problem with local solutions (Bulkeley, 2005). Materially, ICLEI's Cities for Climate Protection (CCP) campaign, established in 1993, is perhaps the first driving force of local governments' widespread adoption of climate action efforts globally. ICLEI designed a five-milestone agenda and developed a greenhouse gas (GHG) emissions reduction protocol and software to guide local governments incrementally implement climate mitigation policies (ICLEI, 2018). The TMN approach to mainstreaming climate mitigation policies at the local scale has continued with newer TMNs such as C40 cities, the Carbon Neutral Cities Alliance (or "Alliance"), the World Mayors Council on Climate Change, and the Global Covenant of Mayors among others.

Although the memberships to international and national trans-municipal networks for climate action are on the rise, the actual status of local CAPs in the United States (the extent to which local climate initiatives have moved beyond symbolic agreements to actual action) is still unclear. Most of the earlier studies on local climate mitigation have focused on the structural and functional suitability of the locality, especially the municipality, to address climate change (Broto and Bulkeley, 2013a; Bulkeley and Betsill, 2005; Gustavsson et al., 2009; Schreurs and Tiberghien, 2007; Schreurs, 2008; Tiberghien and Schreurs, 2010). Those that have attempted to evaluate the implementation of local CAPs have largely been case studies or descriptions of the types of practices that localities are deploying in their GHG emissions reduction efforts, with little opportunity for an expansive view (Angel et al., 1998; Broto and Bulkeley, 2013b; Broto, 2017; Bulkeley and Kern, 2006; Bulkeley and Castán Broto, 2013; Corfee-Morlot et al., 2009; Deangelo and Harvey, 1998; Kern and Bulkeley, 2009; Kern and Alber, 2009; Lindseth, 2004; Michaelowa and Michaelowa, 2017; Robinson and Gore, 2005; Rutland and Aylett, 2008; Westman and Broto, 2018). The studies that have sort after a generalizable

perspective have limited their focus to policy innovation using localities' memberships to climate action networks such as ICLEI and the MCPA (Bae and Feiock, 2013; Daley et al., 2013; Homsy and Warner, 2015; Krause, 2011a, b; Krause, 2012; Wang, 2013; Yeganeh et al., 2020; Zahran et al., 2008a, b).

The objective here is to move the conversation beyond the often flaunted attributes of the "local," "urban," and "city" scale, which makes it the suitable or desirable platforms for climate change action, to the real practical world of local climate mitigation efforts. This is also in the spirit of counterbalancing the potential for overromanticizing—perhaps, partly due to the discursive exaggerations of the attributes of the "local," "urban," and "city"—the local scale with respect to climate change governance, without evidence of a commensurate amount of concrete action (Davies and Imbroscio, 2009; Evans et al., 2016; Johnson et al., 2015; Johnson, 2017; Van der Heijden, 2018; Van Der Heijden et al., 2019). The chapter focuses on local governments' CAPs to evaluate the extent to which cities are engaging in GHG mitigation activities. To do this, the chapter relies on descriptive statistics derived from a content analysis of localities' CAPs, along with interviews with local climate managers. The chapter starts by discussing the politics and policy of climate change in the United States, at the national, state, and local levels to establish the relevance of intergovernmental relations to the multilevel context in which local climate actions occur. The chapter then delves into constructing a broad view of local climate mitigation by first giving a spatial image of CAPs with the local political landscape as a backdrop. The chapter proceeds to discuss the mediating factors that motivate localities to innovate CAPs. Finally, the status of local CAPs in the context of their GHG emissions reduction efforts is examined using available pre- and postplan GHG emissions inventory data. The chapter concludes with a discussion of the key findings.

US climate change policy and politics

The national level: Politics over policy

The United States has been a pioneer in scientific research on climate change; however, it has not been similarly proactive in formulating and implementing policies to respond to the scientific understanding generated. President Jimmy Carter is said to be the first American president to address the issue of global climate change (Sussman, 2009; Sussman and Daynes, 2013). However, this was largely in the direction of producing more scientific knowledge. Roger Pielke Jr., in his two-part paper, which reviewed the policy history of the US Global Change Research Program between 1989 and 2000, blames the science-policy gap on the failure to integrate science and policy at the inception of the program (Pielke Jr, 1995; Pielke, 2000a, b).

National Aeronautics and Space Administration (NASA) scientist, Robert Watson, activated the policy aspect of climate change when he testified in Congress in June 1986 (Pielke, 2000a). The increasing congressional interest in climate change policy, following Watson's testimony, led to the Global Climate Protection Act of 1987, signed by President Ronald Regan into law (Pielke, 2000a). It was however observed that a major tactic employed by the Regan-Bush administration was to formally accept legislations but oppose any efforts to put them into practice (Pielke, 2000a).

It was not until NASA scientist, James Hansen, testified in the US Senate in June 1988, that he was "99% certain" that global temperatures were rising due to anthropogenic forces, that the issue of

climate change began to generate public interest (Pielke Jr, 1995; Pielke, 2000a, b). Perhaps, Hansen's testimony was amplified by the severe weather incidents that occurred in the United States the same year. The United States experienced a hot summer with severe drought in the Midwest; the largest forest fire on record in the Yellowstone; and the most powerful hurricane of the century, Gilbert, on the northeast coast of Mexico (Pielke, 2000a).

Climate change then became an issue in the 1988 presidential election. On August 31, 1988, in a campaign speech, George H.W. Bush promised as follows:

Those who think we are powerless to do anything about the "greenhouse effect' are forgetting about the "White House effect." In my first year in office, I will convene a global conference on the environment at the White House.

President Bush organized his promised summit in April 1990 upon winning the election but went on to be adamant against perusing meaningful policy on climate change throughout his administration. At the World Climate Conference in Geneva in 1990, President Bush refused to sign the carbon dioxide emission agreement: making the United States the only developed country to opt out (Vig and Kraft, 1996). Again, when the United Nations Framework Convention on Climate Change was presented for ratification at the UN Earth Summit in Rio de Janeiro, the President only agreed to ratify the convention when the terms were changed from mandatory to voluntary commitment (Pielke, 2000a).

The election of Bill Clinton in 1992 was perceived by the environmental movement as an opening of the policy window for climate action (McCright and Dunlap, 2003); but the "Republican Revolution" happened—the Republican party claimed the majority in the two chambers of Congress in the 1994 midterm elections. President Clinton's first foray into climate change policy was a failed attempt in 1993 to introduce a 4.3-cent per gallon carbon tax on gasoline through congress, which was intended to finance a transition away from fossils fuels to renewable energy (Kibert et al., 2012). The period of the Clinton-Gore presidency was also a period of high anticlimate change activism by the American conservative movement, conservative think tanks, politicians (republican members of congress), and the fossil fuel industries and their business allies (Dunlap et al., 2016; McCright and Dunlap, 2003; McCright and Dunlap, 2010). Their activities largely focused on undermining the scientific authenticity of climate change, to delegitimize any attempts at taking policy action. It was therefore not a surprise that the US' ratification of the Kyoto Protocol was dead on arrival, given that the Senate passed the Hagel-Byrd Resolution on July 25, 1997, blocking its ratification (McCright and Dunlap, 2003). It was argued that the agreement would be detrimental to the US economy, particularly, given that it did not have similar requirements for developing countries (McCright and Dunlap, 2003). The Protocol lay lifeless in the remainder of the Clinton administration and was finally interred when President George W. Bush announced in March 2001 that the United States did not intend to commit to it.

With the entry of George W. Bush into the White House in January 2001, the fertile ground was laid for a continuous attack on the scientific legitimacy of climate change by the conservative movement. The administration itself had been accused of employing a wide range of practices, described as "abusing science," in its antipathy toward climate change (McCright and Dunlap, 2010). The practice involves suppressing scientific information on climate change, dismissing federal scientists, doctoring or hiding scientific findings for government reports, and manipulating the government's science advisory system among others (McCright and Dunlap, 2010; Sussman and Daynes, 2013). The only intervention in favor of climate change during the George W. Bush administration was the US Supreme Court decision in Massachusetts v. Environmental Protection Agency (EPA) in 2007. The state of Massachusetts, joined with 12 other states, argued that they had been put at risk of sea-level rise among

other impacts of climate change because of the federal government's refusal to tag carbon dioxide as an air pollutant under the 1990 Clean Air Act Amendments (Rabe, 2011). The five-to-four majority decision enjoined the EPA to revise its position. It is argued that the significance of the ruling lies in its potential impact on intergovernmental relations in climate change policy; the states, through the court, compelling a federal course of action (Engel, 2009; Rabe, 2011).

As would be expected of a Democratic president, Barack Obama regarded climate change as an issue deserving of the political agenda. In February 2009, the administration attempted and failed to introduce the cap-and-trade system as a GHG emissions reduction mechanism—the bill failed to make it out of the Senate after passing the House (Sussman and Daynes, 2013). Guided by its failure and that of the Clinton Administration in involving the legislature, the presidency fell back on presidential powers (Sussman and Daynes, 2013). As part of the American Recovery and Reinvestment Act (Recovery Act), which was a stimulus package to revive the American economy following the Great Recession, the Energy Efficiency and Conservation Block Grant (EECBG) Program was introduced. The program, through the Office of Energy Resources, awarded $9,593,500 to support cities, communities, states, US territories, and Indian tribes to carry out energy efficiency and conservation programs. Another instrumental climate mitigation-related policy instituted by the Obama Administration was the upping of the Corporate Average Fuel Economy (CAFE) standards of vehicles. Just like the Clinton administration, the Obama era too was accompanied by anticlimate change activities by cohorts of conservatives.

President Donald Trump, even before declaring his intention to run for president, had through his favored medium of communication—twitter—made it abundantly clear which side of the climate change divide he was on. His twitter attacks on climate change have sought to either rebuff the reality of climate change, by directly attacking the science and confusing weather with climate, or arguing that any action on climate change would unfairly put the United States at an economic disadvantage vis-à-vis its rivals.

The new Trump administration did not fall short of the expectation that there would be an immediate and extensive reversal of the Obama-era proclimate change policy actions, as soon as it assumed office. On January 25, 2017, news broke that the Trump administration had removed all references to climate change from the White House's website. An even more egregious action was the president's nomination of Scott Pruitt, who would be confirmed by the US Senate on February 17, 2017, to head the EPA. Mr. Pruitt was a regular litigant of the EPA over environmental regulations. The first major climate policy causality carried out by the Trump administration was the reversal of the Obama administration's decision to incrementally improve the CAFE standards of vehicles. The administration also declared that the United States would no longer regard climate change by name as a national security threat (Greshko et al., 2018). Other anticlimate change policy actions taken under the Trump administration include many budgetary cuts, which for the sake of space cannot all be discussed here (See, Greshko et al., 2018).

Republican administrations have openly expressed their opposition to climate change policy, whereas their Democratic counterparts have often appeared to be more sympathetic to the issue. However, in terms of concrete policy action at the federal level, there seems to be a consensus, particularly in Congress, against enacting any concrete climate change policy. For instance, the senate vote on the resolution blocking the ratification of the Kyoto protocol was one of consensus—a Senate made up of both Republicans and Democrats produced a vote of 0 to 95. Also, President Obama went to the Copenhagen summit adamant about settling for a nonlegally binding agreement. Perhaps, the absence of a

policy venue for minority and radical interests in the US political system is the reason a consensus has formed against policy alternatives that are deemed to contradict the majority ideology of an unfettered market economy. Perhaps, with the recent fortunes of the more progressive wing of the Democratic Party in congressional elections, more radical policy options for climate change mitigation—for example, the Green New Deal—will be part of the conversation. But, in a nutshell, the federal level has generally been characterized by more politics with little policy with respect to climate change.

The state level: Some policy and fewer politics

Perhaps, the Kyoto Protocol becoming international law on February 16, 2005, with Russia's ratification and the United States' absence was the final signal that there needed to be a scalar shift in leadership on climate change policy. Between 2005 and 2009, a record number of US states, either through executive orders by governors or legislative acts by the state legislatures, directed the establishment of climate change advisory committees to examine the opportunities for GHG emissions reduction and to develop CAPs. Categorizing the periods of climate change policy in the United States, Rabe (2011) designated the period between 1998 and 2007 as "state dominance," given that there was no significant climate change policy from the federal government throughout the Clinton and Bush administrations.

It is instructive to note that except for a couple of states, the initial executive orders or legislative acts, which subsequently led to the development of these state CAPs, were for the creation of the climate change advisory committees, and not to set up mandatory CAPs or GHG emissions reduction targets. Currently, 34 states have CAPs of some sort. Most of these plans have been largely symbolic, in that they are sets of recommendations on the type of actions the state can take to reduce GHG emissions (Center for Climate and Energy Solutions, 2020). In a study conducted by Alexander (2020), of 32 state CAPs examined, only eight of them—California, Colorado, Connecticut, Maryland, Massachusetts, Minnesota, New Hampshire, and Oregon—showed strong evidence of concrete implementation (Alexander, 2020).

The little to no progress in the implementation of state CAPs notwithstanding, there are ongoing state-level legislative and policy actions to promote renewable energy, which have the potential of leading to GHG emissions reduction. The major renewable energy mandates pursued by states are the Solar Power Purchase Agreement (SPPA), Net Metering, and Renewable & Clean Energy Standards. SPPA is a financial arrangement that allows residential and commercial consumers to lease out their properties, mostly their rooftops, to renewable energy developers to install solar photovoltaic (PV) (National Renewable Energy Laboratory, 2019). The consumer, who owns the building but not the PV system, in turn, buys the electricity produced by the facility from the energy developer. Currently, 28 States allow third-party power purchase agreements for solar PV (DSIRE, 2019a). The net metering renewable energy mandate allows residential and commercial customers to generate their renewable energy and sell the excess back into the grid (National Renewable Energy Laboratory, 2019). In a net-metered facility, the electricity meter is set to run backward, and the customer is credited, when the facility produces more energy than it consumes. There are currently 40 states with mandatory net metering rules (DSIRE, 2020). With regard to the Renewable & Clean Energy Standards, there are two types—Renewable Portfolio Standards (RPS) and Clean Energy Standard (CES). The goal of RPS is to diversify the energy mix with zero-carbon renewable energy resources. A certain percentage of the electricity sold by utilities is required to be sourced from qualified renewable energy technologies such as wind, solar, and biomass. However, the percent renewable technology requirement varies from state

to state (Cleary et al., 2019). For instance, although the state of New York has an RPS requirement of 50% by 2030, the state of Missouri's is 15% by 2021. There are currently 29 states with mandatory RPS (DSIRE, 2019b). CES, on the other hand, is a technology-neutral way of promoting zero- or low-carbon energy resources; it requires a certain percentage of the energy sold by utilities to come from renewables, nuclear energy, and coal or natural gas fitted with carbon capture among others (National Renewable Energy Laboratory, 2019). There are three states in the United States with CES (DSIRE, 2019b).

These renewable energy policies cut across Republican and Democratic states and, overall, the state level does not appear to be actively engaged in the dual politics that has come to engulf climate change policy at the national level (Hurlburt et al., 2019). However, there is evidence that high participation in renewable energy production is not a proxy for a state's openness to climate change policy, more broadly (Hurlburt et al., 2019). For instance, the states of Texas, Alabama, South Carolina, and Georgia are ranked 3rd, 8th, 9th, and 10th, respectively, in terms of the amount of renewable energy produced, yet with the exception of South Carolina that had a report produced by its Climate, Energy, and Commerce Committee, recommending a voluntary economy-wide goal of reducing GHG emissions by 5% below 1990 levels by 2020, the other three states have no publicized climate action goals (Center for Climate and Energy Solutions, 2020; Hurlburt et al., 2019). In terms of the internal advocacies for renewable energy, an atmosphere of bipartisan coalitions has been observed across states. The success of Nevada's landmark "Solar Bill of Rights" legislation is attributed to the tremendous advocacy work of a coalition of libertarians and environmentalists (Hurlburt et al., 2019). In Florida, one of the main opponents of the restrictions on solar power, whose use of antimonopoly arguments proved effective across states, is the founder of the Florida Tea Party (Hurlburt et al., 2019). In addition, the highly influential Bring Back Solar Alliance is a bipartisan group made up of well-known progressive groups and environmental groups of conservative origin such as Green Tea, Conservatives for Energy Freedom, and the Evangelical Environmental Network (Hurlburt et al., 2019). It is argued that the support for renewable energy, especially among the states, is motivated by economic considerations rather than environmental stewardship. Apart from the potential contribution of the growth in renewable energy to GHG emissions reduction, households get a reliable and relatively cheap supply of electricity, and service provider gets incentives such as tax credits in addition to the revenue from the sale of the electricity (Hurlburt et al., 2019).

Although there is a relatively modest activity in terms of explicit climate change mitigation efforts at the state tier, the renewable energy mandates have served as enabling conditions for climate mitigation efforts at the local level. Community members are informed of the existence of these state-level renewable energy mandates and encouraged and incentivized to take advantage of them, as part of the GHG emissions reduction efforts of local CAPs.

The local level: Policy and some politics

The TMN model has been the driving force behind local climate policy, both discursively and materially. Nationally, this model has been followed by the MCPA and Climate Mayors, among other regional scale networks. However, the most conspicuous local politics of climate change in the public sphere in the United States has been the anti-Local Agenda 21 activism by local conservative individuals and groups, linked to the Tea Party movement, which was more spirited from around 2010 to 2014. They attacked all local climate mitigation and sustainability efforts, by associating them with the UN

Agenda 21, which they disparaged as a globalist agenda meant to derail the highly valued United States ideals of personal liberty and private property ownership.

At the United Nations Conference on Environment and Development, also called the Earth Summit, held in Rio de Janeiro, Brazil, in June 1992, whose purpose was to determine ways of balancing worldwide economic prosperity and environmental protection, the concept of Agenda 21 was birthed. The rationale was that many environmental problems originate from localities and, so, local governments were better positioned to develop and implement policies to address such problems. Local Agenda 21, therefore, provided the guide to drive local governments toward leadership in sustainable development. Around this time, an international organization (ICLEI) with the objective of galvanizing local governments globally, around this idea of sustainable development, was also in the works (ICLEI, 2018). In 1993, ICLEI introduced the CCP campaign, which was the source of the first wave of local governments' adoption of CAPs globally. Most cities that were motivated, for whatever reason, to take action on climate change joined ICLEI, either as part of its CPP campaign or to use the resources it provided (ICLEI, 2018).

The Tea Party anticlimate change activists made ICLEI, as the most dominant network helping localities with their sustainability and climate protection efforts, synonymous with the UN Local Agenda 21. Using rhetoric that portrayed globalization in a negative light—a threat to national culture and identity, decline of national sovereignty, and constraints on national policy discretion—they described the UN Agenda 21, and anything resembling any of its core objectives, as globalist and anti-America (Carey, 2012). This loose coalition of activists made up of thousands of individuals from across the country used avenues, such as local government planning meetings, local government Board of Supervisors meetings, City Council meetings, campaign trails, Tea Party member meetings, and the conservative media, for their campaign. They also spread the content of their propaganda through YouTube videos and the sale of tool kits (Trapenberg Frick et al., 2015).

Cher McCoy, a Tea Party member from Lexington, at a Roanoke, VA Board of Supervisors meeting, in January 2012, described the installation of smart meters in the city in the following manner; "The real job of smart meters is to spy on you and control you—when you can and cannot use electrical appliances" (Kaufman and Zernike, 2012). Judd Saul, a Tea Party activist, at a meeting in Cedar Valley Falls, Iowa, described Agenda 21 as "an elusive enemy that floats in and chokes you gradually." "They want to destroy the middle-class way of life," he added (Carey, 2012). At another Tea Party meeting in Murfreesboro, Tennessee, in April 2012, Jake Robinson told Tea Party members that, "Agenda 21 aims to undermine your property rights and force you to live in cities" (Carey, 2012). For Joe Dugan, leader of the Myrtle Beach Tea Party in South Carolina, Agenda 21 is "nothing short of treason" (Carey, 2012). Dan Maes, the Tea Party-backed Republican nominee for Governor of Colorado in the 2010 election, at a campaign rally, warned voters that his Democratic opponent, Denver Mayor John Hickenlooper, was en route to "converting Denver into a United Nations community" (Osher, 2010). His comments were directed at Denver's B-Cycle bike-sharing program launched by the Mayor earlier, on Earth Day, that year. Maes doubled down, characterizing all of Hickenlooper's environmental programs, including the city's membership to ICLEI, as the proverbial Trojan Horse (Osher, 2010). The ranks of the Republican Party were not left out of the sway of the anti-Agenda 21 movements. Newt Gingrich, the then speaker of the US House of Representatives, at a campaign trail, said, "I would explicitly repudiate what Obama has done on Agenda 21." (Kaufman and Zernike, 2012). In addition, the Republican National Committee passed an anti-Agenda 21 resolution (Kaufman and Zernike, 2012).

Many localities, especially those that are politically conservative, yielded to the pressure of the activism and stopped funding carbon reduction-related programs (Kaufman and Zernike, 2012). Some

cities that had committed to climate protection through their membership to ICLEI's CPP cut their commitment by limiting their climate mitigation efforts to city operations instead of the entire community. According to the Virginia Right! Blog, as of June 1, 2012, in the spate of 18 months, 138 local governments had pulled their ICLEI memberships entirely (White, 2012). In addition to attempting to influence legislation against local sustainability issues, the anti-Agenda 21 movement focused on local planning issues and electoral campaigns to remove elected officials who favored sustainability issues (Trapenberg Frick et al., 2015). They also deemed the public display of their activism as an end in itself; as they believed, it deterred local governments from taking on sustainability-related policies, for fear of attracting negative public attention (Trapenberg Frick et al., 2015).

Data and methods

Data

The foremost data collection objective was to systematically identify and collect information on, as many as possible, localities with CAPs. Given that there is no single source data on localities' climate mitigation efforts, multiple sources were explored to put together the list of localities for the study. Two hundred and fifty unique localities with community-wide CAPs were realized from four sources—the EPA's examples of local CAPs (17) (U.S. EPA, 2015); ICLEI's 2015 study containing a list of local governments with CAPs (116) (ICLEI, 2015); the International City/County Management Association (ICMA) 2010 sustainability survey (74); and ICMA 2015 sustainability survey (181).

The EPA and ICLEI sources were published lists of examples of localities with CAPs. However, the CAPs localities derived from the 2010 and 2015 ICMA surveys were based on answers to the survey questions. The 2010 ICMA survey did not have a direct question on whether a locality had community-wide CAP or not. As a result, localities that answered affirmatively to whether they had set GHG emissions reduction targets for businesses, multifamily residences, and single-family residences were taken as having CAPs. The 2015 ICMA sustainability survey, however, had a direct question on whether a locality had a climate mitigation plan. This process yielded 328 unique localities. A web search was then conducted to find each locality's CAP. Although searches in some cases returned websites and web pages, which hosted localities' CAPs, others' CAPs were found in the form of PDF documents uploaded in the documents section of the local government's website. Consequently, of the list of 328 localities from the four sources, the search yielded 250 community-wide CAPs. As shown in Fig. 1, the breakdown of CAPs localities based on local government type, different forms of local jurisdictions are engaged in climate mitigation efforts.

For the GIS mapping of CAPs localities and the political orientation of localities, the study used the 2012 US presidential elections results data (MIT Election Data and Science Lab, 2017), the TIGER/Line 2012 US county shapefile (US Census Bureau, 2012) and the US states shapefile (cb_2018_us_state_500k.shp) (US Census Bureau, 2018).

Methods

The study required the ready availability of uniform data on a range of areas of localities' climate mitigation efforts, such as GHG emissions reduction targets, base years and target years of the set targets; the strategies and structures put in place to reach the set targets; GHG emissions inventory data; and

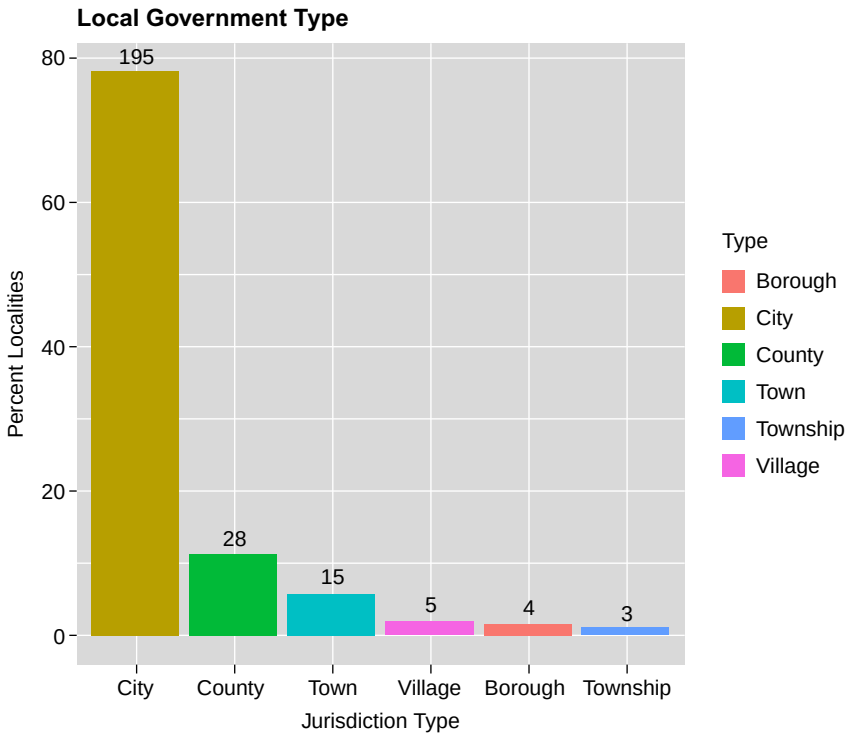

FIG. 1

US localities with CAPs grouped by type of locality.

information related to outcomes of the CAPs. However, given that there is no single data source from which this type of information could be accessed, content analysis was one of the main methods of data collection. In fact, in addition to memberships to various municipal climate action networks, there is hardly a complete list of US localities with CAPs. The study had to adopt a painstaking data collection process, which involved, searching, finding, and going through each locality's climate action information, on websites, web pages, PDFs of action plans, and reports. Another reason why content analysis was important for this study is that climate change mitigation is a continuous process; hence, content analysis afforded the ability to study the process through time by examining initial plans, plan updates, and progress reports, produced over the course of the mitigation efforts.

The chapter further relied on in-depth interviews with CAPs managers to gain insight into the factors that motivate localities to take on climate mitigation. These interviews were conducted as part of a larger study and, thus, involved a broader range of questions on local CAPs. However, for this chapter, the concern was with the question of why localities take up climate mitigation action. The goal of the in-depth study was to gain full insight into the unique intricacies of the various localities' climate protection efforts to generate reliable comparable qualitative data (Russel Bernard, 1988). A semistructured interviewing style was deployed. Using open-ended questions, this interviewing style prevents digression while generating conversational responses (Crang and Cook, 2007). Climate action

managers had the freedom to express their unique experiences. The interviews with the 21 local climate action managers in the United States (18 municipalities and 3 counties) were conducted via telephone from December 2017 to March 2018.

The status of CAPs

The spatial distribution of CAPs

The discussion in the climate change politics section above has shown that the public discourse on climate change in the United States has taken political ideological lines. Although the liberal wing of the political divide, using affiliation with the Democratic Party as a proxy, has been sympathetic to the course of climate change, their conservative counterparts—the proxy being the Republican Party—have openly opposed it. This dynamic is also observed in the spatial distribution of local CAPs.

Fig. 2 shows the distribution of CAPs and the political leaning of the county within which the locality is situated. The map is made up of three layers: US localities with CAPs; the 2012 county-level US presidential election results displayed in graduated colors; and the US states. The county-level election results were categorized into Democratic, Republican, and Swing, based on the percentage points difference between the Democratic and Republic candidates. The common practice, in national

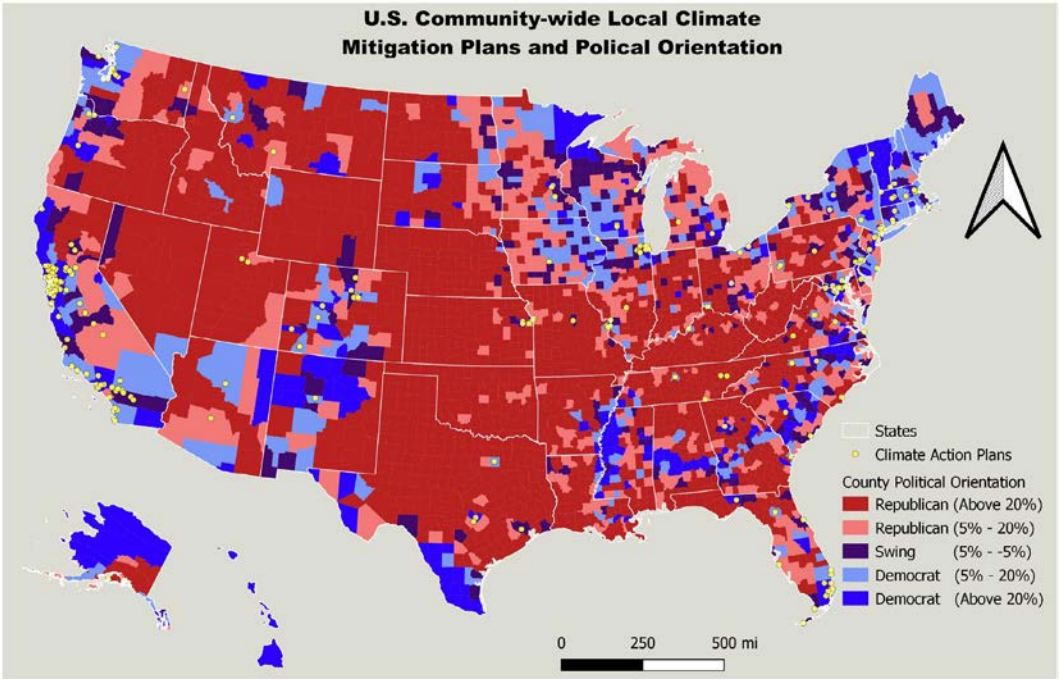

FIG. 2

Map showing the distribution of CAPs in the United States and the county-level political orientation of localities.

election data mapping, of using blue, red, and purple to represent Democratic, Republic, and Swing counties, respectively, was also used in this map. The deeper blue and red colors indicate counties that obtained above 20% points difference between the candidates of the two Political Parties. If the difference was 5% points and below, it was categorized as a Swing county and given the purple color. From a visual inspection of the distribution of CAPs localities and the political landscape, an overwhelming number of localities are associated with blue counties. This finding is consistent with many other studies on the adoption of climate change and sustainability policies at the local level (Hughes et al., 2018; Krause, 2011a; Wang, 2013; Yeganeh et al., 2020; Zahran et al., 2008a, b).

The goal here is to show the relationship between the political orientation of the locality and the adoption of CAPs. The ideal situation would have been, for instance, to use city-level election data if the jurisdiction type is a city. However, even if such data were readily available, it would be difficult to display the data layers on the same map with self-explanatory value; hence, the use of the county-level data to approximate the political learning of the locality irrespective of its type.

Fig. 3 shows the county-level political orientation of the CAPs localities in a bar chart—this shows about 80% of the localities are situated in blue counties, approximately 12% in purple counties, and a little more than 5% in red counties.

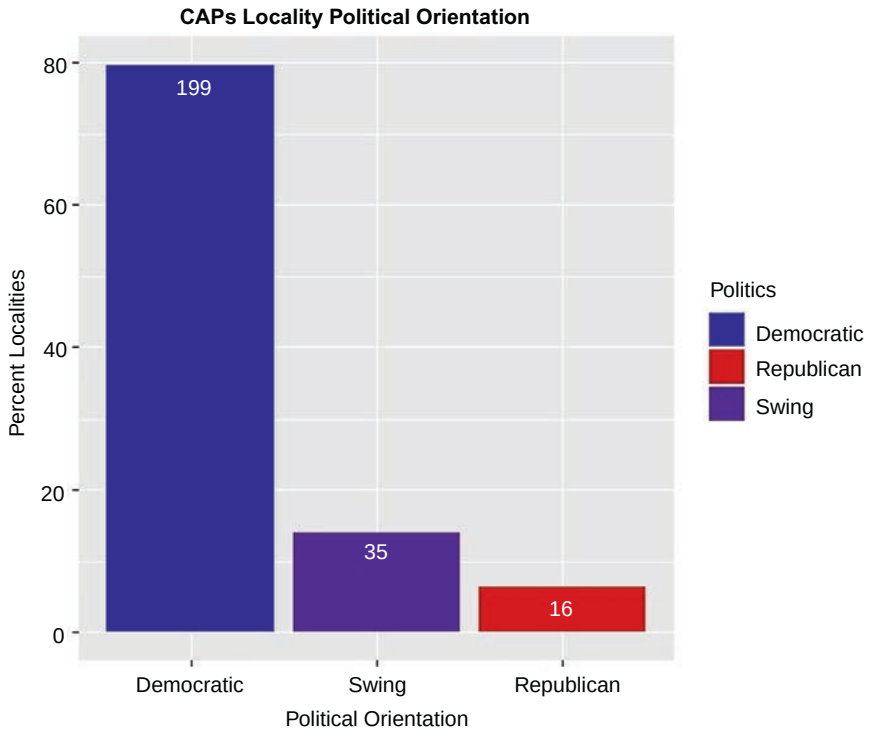

FIG. 3

Bar graph showing CAPs by political orientation.

Why localities take on climate mitigation?

An essential element of the policymaking process is innovation; the question of why certain jurisdictions adopt a policy whereas others do not. It is argued that a jurisdiction's adoption of a policy is influenced by either its internal characteristics or its external interactions (such as influence from neighboring jurisdictions). From the preceding section, there is strong evidence that political orientation is one of the main defining elements of local adoption of CAPs in the United States; however, there may be other mediating factors as well. A number of studies have sought after answers to this question, often deploying the sociodemographic and the structural characteristics of local governments as independent variables and memberships to climate action networks such as ICLEI's CCP and the MCPA as the independent variable (see Zahran et al., 2008a, b; Wang, 2013; Daley et al., 2013; Krause, 2011a, b, 2012). The main challenge of these studies is their use of climate action network memberships, and not actually implemented local CAPs. Also, their application of quantitative methods makes it difficult for contextual and unique factors to be identified. This study, therefore, sought to bring nuance to this question by thoroughly exploring the contextual set of factors that influence localities' decision to innovate CAPs, by relying on actually implemented CAPS, and doing so using qualitative methods—the content analysis of CAPs and in-depth interviews with CAPs managers.

Tables 1 and 2 list the factors collected from the CAPs content analysis and the interviews, respectively. It should be noted that because the information was not collected through a survey, not all the contents of CAPs examined overtly stated reasons for the decision to innovate. It is also the case that in both the content analysis and interviews, some localities stated more than one reason for their decision to act; hence the tally is not one to one. Most of the 21 CAPs managers that were interviewed mentioned that they were not in their current position at the time the decision was made to implement the CAP but nevertheless proceeded to give their reasons for the local government's initial adoption of the CAP.

From the examination of the contents of CAPs, the idea of local co-benefits emerged as one of the most stated reasons for CAPs innovation. Some of the co-benefits cited include: decreased traffic and congestion; improved air quality; better access to parks and green spaces; cost savings, through energy efficiency projects; improved public health; and promotion of economic vitality. Betsill (2001) and Lindseth (2004) had made this point in the context of strategizing for the successful implementation of CAPs. They argued that for CAPs to generate community-wide appeal and be successful, the goals of climate mitigation should be aligned with compelling local problems; to serve as "hooks on which to hang the issue of climate change" (Betsill, 2001, p. 398). In addition, Rutland and Aylett (2008)

Table 1 Factors motivating CAPs innovation from content analysis.

Factors motivating CAPs innovation	
Motivating factors	**Number of localities**
Co-benefits	53
State CAP	24
A history of environmentalism	14
Ecotourism sensitivity	11
Risk of extreme weather	8

Table 2 Factors motivating CAPs innovation from interviews.

Factors motivating CAPs innovation	
Motivating factors	**Number of localities**
Mayoral leadership	8
Progressive community	5
Ecological and environmental wealth	4
History of environmentalism	2
Co-benefits	2
Vocal and additive environmental activist	1
State CAP	1

attributed Portland, Oregon's successful GHG emissions reduction from its 1993 CAP to the alignment of its GHG emissions reduction goals with the city's energy crisis and spiraling utilities cost at the time (the 1980s) (Rutland and Aylett, 2008).

Krause's 2011 application of a multilevel modeling method to ascertain the probability that a local government will adopt local initiatives to mitigate climate change revealed that neither the presence of a CAP at the state level nor the political and economic factors within the state had an impact on the local adoption of CAPs. However, from a review of the CAPs for this study, the issue of state policy influence emerged frequently. The caveat, however, is that it appeared solely among localities in the State of California. Given that other states have CAPs, yet none of their localities cited their state CAP as a motivation for their CAP innovation, it is likely that the State of California's climate policy is unique. As part of the State of California's Global Warming Solutions Act (AB 32), the California Air Resources Board developed a Climate Change Scoping Plan, explicitly directing municipalities to adopt their own GHG emissions reduction goals. Hence, phrases, such as "in line with the goals of AB 32," "consistent with the direction of the State of California," "alignment with California's Climate Change Action Plan," and "to support California's ambitious emissions reductions goals," used in the various localities' CAPs capture the influence of the state's CAP on local CAPs innovation.

One of the assumptions for several quantitative studies of the determinants of local adoption of CAPs is the presence of sensitive ecosystems and coastal proximity. These are often discussed in the context of risks to the impacts of climate change. Eco-sensitivity measures the percent of a locality's land area covered by forests and wetlands (Zahran et al., 2008a, b). Coastal proximity, on the other hand, is measured in terms of the percent of a locality's area that is within the EPA-defined at-risk coastal lands—areas below 3.5 m above sea level (Zahran et al., 2008a, b). However, from the content analysis, ecological and coastal impacts of climate change emerged in the context of risks to tourism and recreational activity; hence, what I refer to as ecotourism sensitivity. The City of Roanoke cites the risks to the Blue Ridge Mountains, the Roanoke River, the Blue Ridge Parkway, the Smith Mountain Lake, the Carvins Cove, and the more than 50 parks to the impacts of climate change as one of its motivations to act. The cities of Nashville; Charleston, North Carolina; and Cincinnati state the need to protect their scenic beauty for tourist attraction as their motivation to act. In the case of Park City, Utah, it is the potential impact of climate change

on the Park City Mountain Resort and the Utah snow sports industry that motivates its action. The issue of coastal proximity appeared to be peculiar to localities in Florida; predominantly, stated in the context of the risks of climate change impacts on tourism—particularly the subtropical climate and beaches.

Taking action on climate change based on the sheer risk of extreme weather, on its face, is a no brainer. The assumption is that local governments are rational actors and, so, localities that are environmentally at most risk of the impacts of climate change will be more likely to take on mitigation. Based on this assumption, some quantitative studies have examined climate risk variables such as precipitation above normal, natural hazard casualties in terms of numbers of injuries and fatalities, and projected temperature change. Precipitation above normal and expected temperature change have been consistently found to be insignificant in a number of studies (Zahran et al., 2008a). These findings notwithstanding, a locality such as the city of Kansas City states its location in the middle of the country and its susceptibility to extreme heat, cold, and precipitation as a motivation for taking action. The city of Louisville and Sullivan County also cite their histories of extreme weather events and the potential of that worsening with climate change as the motivation for their CAP innovation.

A recognition of the locality's ecological and environmental wealth also came up as a key motivation. The following quotes from the interviews with CAPs managers capture this point:

> … where Burlington is situated, we are very much in touch with our natural environment, we see the lake and beautiful view, so being very connected to these aspects, I think, makes a community prone to protection.
>
> **(CAP Manager, City of Burlington, January 19, 2018)**

> … many residents choose to live in Fort Collins because of its natural beauty and their enjoyment of an active outdoor lifestyle and therefore will continue to support increased pedestrian and bicycling transportation options and access.
>
> **(CAP Manager, City of Fort Collins, CO, January 26, 2018)**

Having a long-standing foundation of environmental stewardship appeared in the document analysis as well as the interviews. Localities such as the City of Kirkland, Town of Lexington, City of Missoula, City of Naperville, County of San Mateo, and the City of Phoenix state their long-standing traditions of environmental awareness and stewardship as their motivation to act on climate change mitigation. The Town of San Anselmo recalls the 1973 plan on the conservation of open space, the 1974 passage of the requirements for recycling, the 1975 advocacy for the reduction of automobile emissions, and the 1978 recognition of solar as a viable source of energy, to demonstrate its history of environmentalism. For the city of Charleston, South Carolina, they used the word "sustainable" long before the concept's current popularity and have been involved in the movement as far back as 1931, with the passage of the city's first historic preservation ordinance.

Being a progressive community was mentioned in the interviews as one of the key reasons for localities' motivation to innovate CAPs. Some of the indicators of a progressive locality derived from the interviewees include having a major university, a highly educated populace, and ethnic and racial diversity. The city of Boulder mentioned its highly educated population and the presence of many federal laboratories that do a lot of climate science work. The following quote from the CAP manager of Montgomery County, MD, sums this point up.

> … because we are located next to DC, we have a lot of federal agencies, and in the community, we have a lot of people working for the government and local universities. It's a very educated community, I think we have more individuals with PhDs and other graduate degrees than any jurisdiction in the nation, or something like that. We are very well educated so as a result of that we are also a very progressive county, we have been at the forefront of a lot of different things. We are very active in the environmental area but also, we are a sanctuary community, so we have something like about 152 different languages spoken in the county, we are very diverse, we welcome immigrants, they have been a big part of our community growth. So, people have always been interested in environmental issues and climate change is obviously the biggest environmental issue we face. I think that is what motivates the community to get involved.
>
> **(CAP Manager, Montgomery County, MD, January 31, 2018)**

This factor also appeared in the context of the political leaning of the local government's leadership. In the interview with the CAPs manager of the City of Charlottesville, it was revealed that the Tea Party had tried and failed to convince their local council to abandon their climate protection efforts completely. However, the surrounding Albemarle County conceded to their pressure due to the political calculations of its political leadership at the time:

> At some point along the way, our elected officials wanted to get away from kind of the international large-scale efforts and to focus on local action (as they put it). And so, we were directed as staff to kind of focus on operational goals, meaning municipal sector emissions, and so, we never created a Climate Action Plan (CAP) for the community.
>
> **(CAP Manager, Albemarle County, February 14, 2018)**

Over the years as the county leadership shifted back to independent and later to democratic, strides have been made to advance community-wide climate mitigation efforts.

Mayoral leadership as a motivation for CAPs adoption does not come as a surprise. Most of the pioneering local CAPs originated from local governments' memberships to climate action networks such as ICLEI and the MCPA, led by their mayors. This is consistent with Bae and Feiock (2013) finding that although the council-manager form of local government influences the number of sustainability actions directed at city operations, the mayor-council form influences community-wide initiatives (Bae and Feiock, 2013).

Some local governments mentioned the presence of environmental civil society groups, within the locality, as the main factor that led them to adopt climate mitigation measures.

> We have lots of vocal and additive environmental activists in the city, they participate a lot in local government, so they vote the commissions, they help council members get elected, they lobby the council members, that is the first thing and that was back in 2007 and it's the same thing now...
>
> **(CAP Manager, City of Austin, February 9, 2018)**

> So, the story that people tell about how things happened in Evanston was that there was a lot of community support. I think there are 13 different sought of coalitions that were concerned about environment and sustainability and they really pushed the city to take action and also hire a staff person…
>
> **(CAP Manager, City of Evanston, IL, January 12, 2018)**

In quantitative studies of local climate policy innovation, variables such as environmental cause participation and presence of the environmental nonprofit organization in localities have been tested and found to significantly affect innovation of local climate policy (Bae and Feiock, 2013; Wang, 2012; Yeganeh et al., 2020; Zahran et al., 2008a, b).

Progress of GHG CAPs

The nature of CAPS

Most of the CAPs took place between 2006 and 2015 as can be seen in Fig. 4. The majority of the CAPs were completed in 2009. This also happens to be the same year that the Department of Energy's EECBG Program was instituted as part of the American Recovery and Reinvestment Act (Recovery Act).

CAPs typically have an emissions reduction target, a target year, and a base year for the target. The base year is the year to which future years' GHG emissions are compared to ascertain progress. The emissions reduction target is usually a percentage of the base year's emissions. Finally, the target year

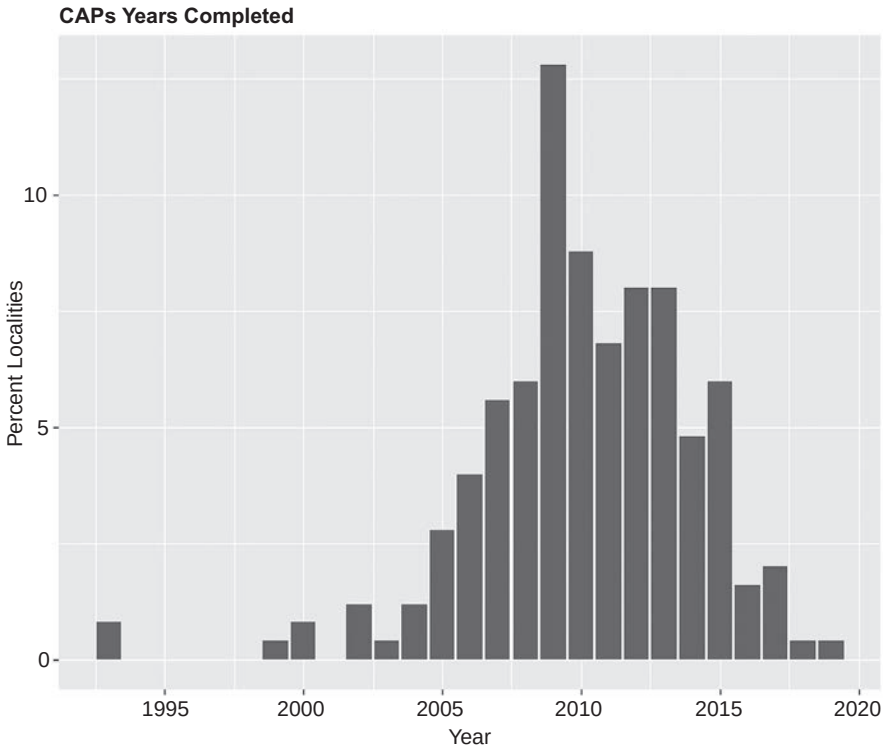

FIG. 4

Years localities' first CAPs where completed.

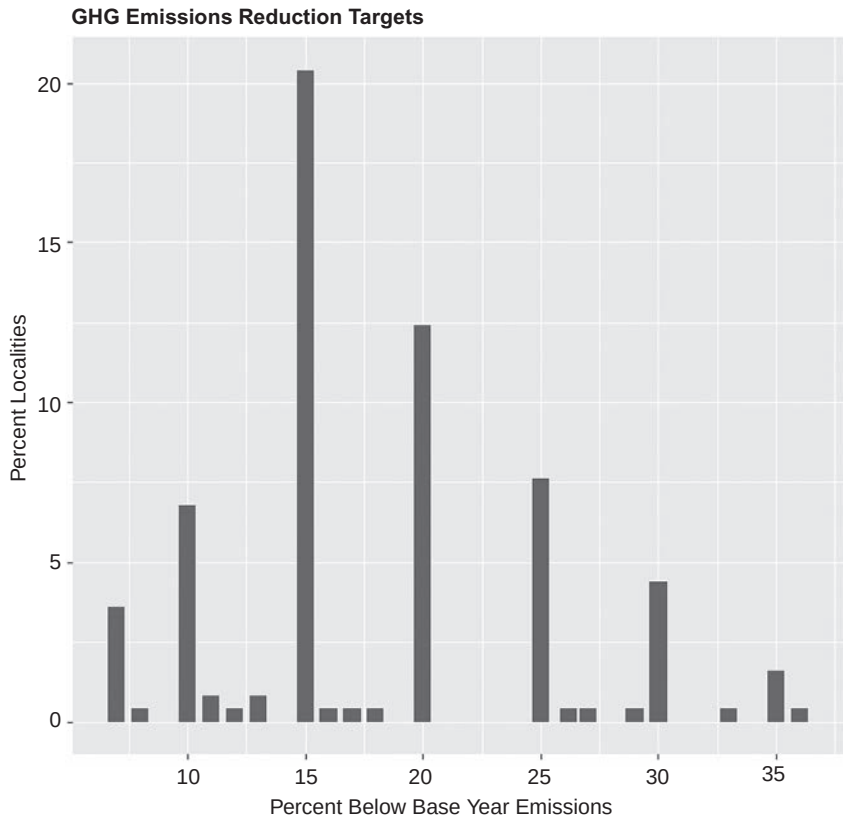

FIG. 5

GHG emissions reduction targets.

is the year by which the programs and strategies of the CAPs are expected to yield the set emissions reduction target. Fig. 5 shows the various target years of the CAPs. The most adopted emissions reduction targets in descending order are 15%, 20%, 25%, 10%, and 30% below base-year emissions. Most localities chose 2005 as the base year for their GHG emissions reduction target as shown in Fig. 6. Also, Fig. 7 shows the year 2020 as the most adopted target year for the CAPs.

GHG emissions reduction

Of the 250 localities with CAPs, 92 of them, representing 36.8%, had postplan GHG emissions inventory data. Of this number, 83 recorded reductions in their GHG emissions, whereas nine recorded increases. The following bar chart shows the distribution of GHG emissions change (Fig. 8)

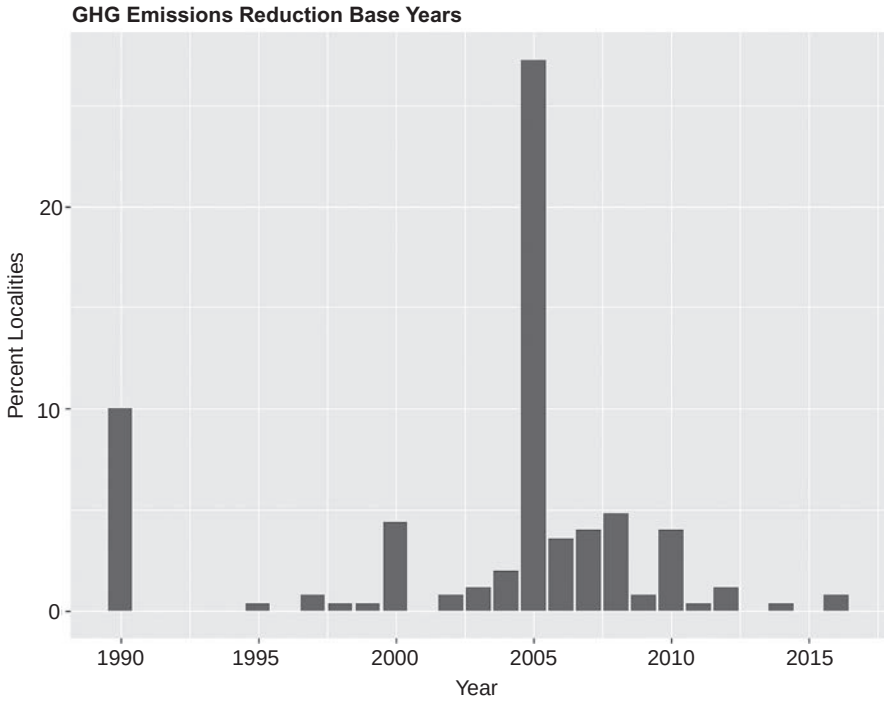

FIG. 6

GHG emissions reduction base years.

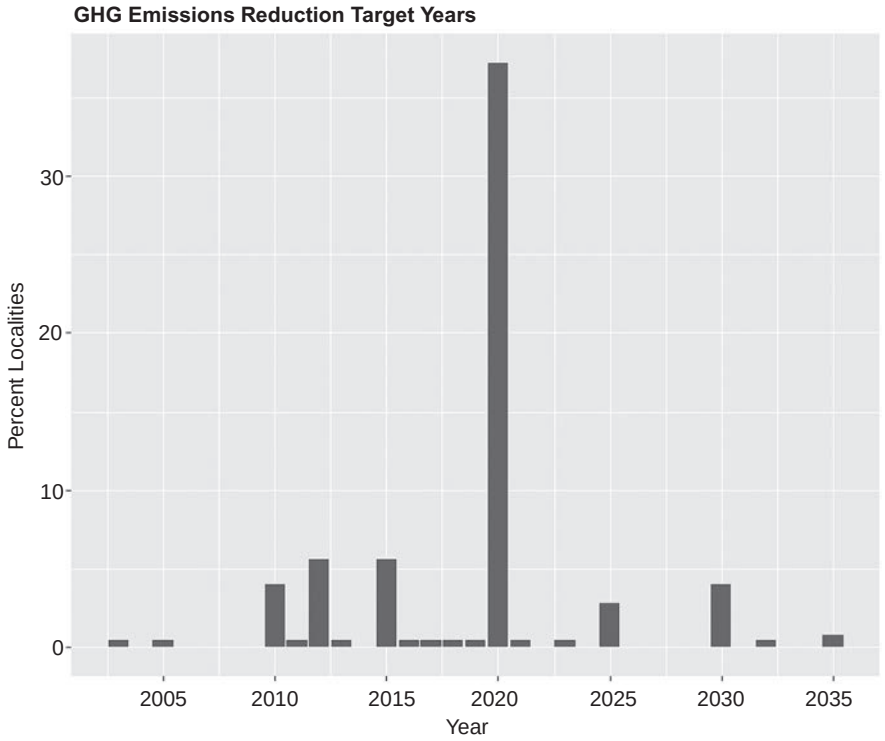

FIG. 7

GHG emissions reduction target years.

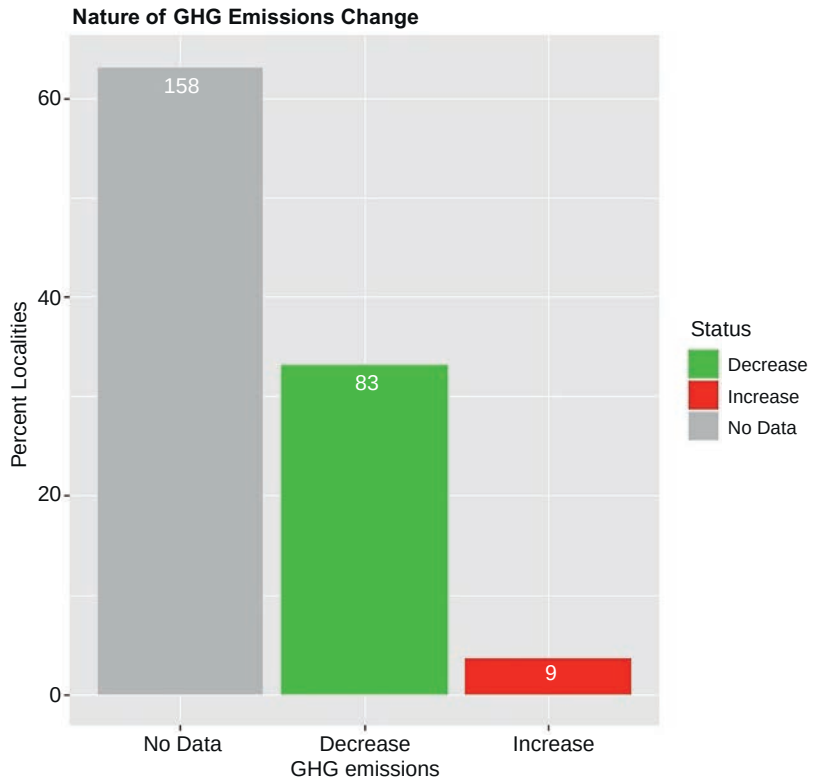

FIG. 8

The nature of GHG emissions change of CAPs.

The majority of the localities that had data on their GHG emissions recorded reductions in emission. All the localities that reported emissions reduction either met or exceeded the Kyoto requirement for the United States—7% below 1990 levels by the year 2012. The majority of the localities' GHG emissions reductions were between 10% and 20% below their respective base-year emissions.

However, there is still a data problem. A total of 63.2% of the localities with CAPs did not have any pre- and postinventory data to make the examination of emissions reduction progress possible. In addition, most of the localities do not consistently record their GHG emissions. Furthermore, the protocols used in reporting the data differ among the localities. Given that the data are not consistent or based on a common, orderly source of inventories, the study simply took the latest available data on the locality's GHG emissions and compared it against its base-year emissions to get the change in emissions. This issue of data is not only a challenge for this type of study but also local climate mitigation effort itself. In fact, some of the GHG inventory data and, consequently, the observed GHG emissions reductions for most of the localities were obtained from their CAPs updates; signaling the importance of monitoring and evaluation to the success of CAPs (Fig. 9).

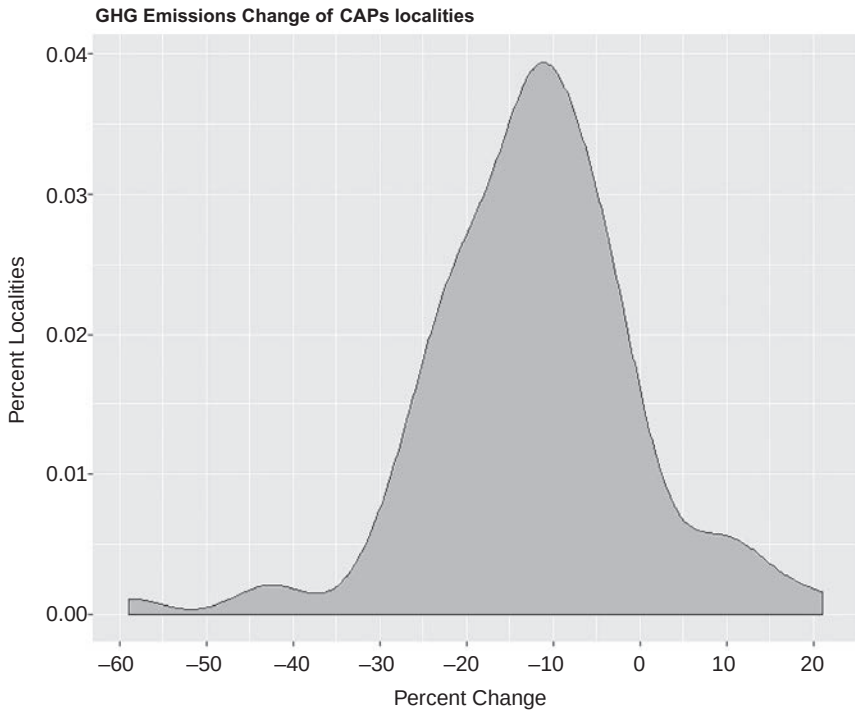

FIG. 9

Change in GHG emissions based on the latest available GHG inventory data.

Discussion and conclusion

The material outcome of the ongoing local scaling of climate change governance, discussed in the introduction, has not been a uniform adoption of CAPs across the United States. As visibly displayed in the GIS mapping, the spatiality of CAPs is consistent with the general politics of climate change in the United States. With regard to this policy issue, it is the outlying dual politics—the conservative versus liberal ideologies and moralities—of the American political space that has generally dictated its direction.

However, beyond the much broader influence of the outlying political context within which localities exist, other more utilitarian considerations have been observed to influence local CAPs innovation. In the CAPs content analysis and interviews for this study, factors such as local co-benefits, the state of California's CAP, ecotourism sensitivity, and the risk of extreme weather (though not stated by a lot of localities) appeared as motivations for localities' decision to innovate. Also, the decision to act based on an acknowledgment of the locality's ecological and environmental wealth could constitute a risk-based consideration. Having a long-standing foundation of environmental stewardship may appear to be ideologically rooted, but it may be historically founded on a locality's past environmental risks. Yet, even at this narrower resolution, ideologically founded motivations, such as having a progressive

mayor, the presence of environmental civil society groups, and being a progressive community, feature prominently. Based on this observation, the assertion that localities with a conservative political orientation are less likely to adopt CAPs is strongly supported. Hence if the local scale is expected to occupy a dominant role in global climate change governance, this bifurcated nature of local CAPs innovation would have to be bridged.

Perhaps, one way would be to single out the conservative localities with CAPs and examine their motivations for innovation. This might reveal a unique set of factors that would inform how to achieve widespread adoption of climate mitigation initiatives among conservative localities. Also, taking seriously Betsill (2001) and Lindseth's (2004) early on idea of "framing" the issue of climate change in a manner that will generate community-wide appeal might be another way, even if it means climate change mitigation becomes a byproduct of programs meant to deal with more conspicuous local problems (which also contribute meaningfully to GHG emissions reduction) (Betsill, 2001; Lindseth, 2004). Also, lessons can be taken from the state level, where renewable energy policies are popular with little to no politicization. Yet, at the same time, there is the risk of over concentrating on the transformative benefits of proxy practices—green jobs, cheap electricity, and smart cities among others—to the neglect of the broader goal of global climate change mitigation (Hayden, 2014; Hodson and Marvin, 2014; Van Der Heijden et al., 2019).

One key revelation of the study, but which does not come as a surprise, is the fact that the majority of the CAPs were completed in 2009; the year the EECBG Program, funded by the federal government, was rolled out. This is a signal that the EECBG funding may have gone into the creation of local CAPs. This observation is in tune with the multilevel governance (MLG) framework—the vertical and lateral interaction of different spheres of authority. For example, Granberg and Elander, in their research, point out the fact that the Swedish government enabled local climate mitigation efforts through funding (Granberg and Elander, 2007). In fact, this multilevel interplay between localities and higher-tier jurisdictions is also apparent in the outcome of the federal government's act of inaction on climate change; as it prompted bouts of memberships to local climate action networks and agreements.

All the localities that reported emissions reduction either met or exceeded the Kyoto requirement for the United States—7% below 1990 levels by the year 2012. This implies that if all localities in the country were taking similar actions, their individual contributions, fitted like a jigsaw puzzle, will make up the national GHG emissions reduction requirement for the United States. However, there are several reasons this may not be entirely accurate or would be a tall order. GHG reductions may be due to changes that are exogenous and not the direct result of actions associated with the CAP. For instance, as shown in the discussion on state actions, a number of state policies, particularly those associated with renewable energy mandates such as the RPS, contribute to the GHG emissions reduction reported in local GHG inventories. Also, from a critical examination of the contributions to global GHG emissions from agriculture, deforestation, heavy industries, high energy-consuming households, and power plants in the outlying rural areas, David Satterthwaite asserts that the assignment of 75%–80% of global GHG emissions to cities (in support of a shift in focus of climate action to the local scale) is an overestimation (Satterthwaite, 2008). He argues the actual contribution of cities to the accumulated GHGs is less than half of all anthropogenic GHG emissions. Hence, the activities of local CAPs alone (which are typically in Urban areas) may not be enough to make up the required emissions reduction for the United States, even if all localities adopt CAPs. Situating this in the context of the global need for GHG emissions reduction, Bansard et al. (2017) found that local climate networks mainly focus on urban areas and the western hemisphere (Bansard et al., 2017).

Zooming out of the successful GHG emissions reductions to all the localities studied, an even higher number of localities had no inventory data to assess their progress in emissions reduction. Similarly, in the study by Bansard et al. (2017) that examined the contribution of TMNs to global climate change mitigation, it was revealed that only a few networks commit to quantified emissions reduction targets and an even fewer number have stringent monitoring and evaluation mechanisms. Conducting inventories regularly and tracking GHG emissions is fundamental to climate change mitigation effort; hence, the lack of data, in itself, is a measure of performance. In fact, all the cities that reported a reduction in their emissions updated their CAPs at least once. This position is also supported by Krause et al. (2019) whose study found a positive effect of regular inventory updates on climate mitigation efforts (Krause et al., 2019).

Joining climate change mitigation agreements, or even passing resolutions to act and setting emissions reduction targets, is a long way from actual action and success. Some scholars are of the view that a locality's membership to a climate action network signals more of a declaration of intention to take action on climate change mitigation rather than actual action itself (Pitt and Bassett, 2014). Betsill and Bulkeley (2007, p. 448) describe this as the "stubborn gap between the rhetoric and reality of local climate policy." For instance, 1060 localities are currently signed onto The US Conference of Mayors' Climate Protection Agreement, "vowing to reduce carbon emissions in their cities below 1990 levels" (United States Conference of Mayors, 2018). Although it cannot be said definitively how many of those localities have gone ahead to develop plans, implement them, and monitor their progress, this study undertook a painstaking systematic approach to identifying localities with community-wide CAPs and came up with only 250 localities. It is a fact that the number of actually implemented CAPs across the United States is more than 250, but the number would not be anything close to the number of localities that have symbolically joined climate action networks or signed onto climate mitigation agreements. Krause's (2011b) study of Indiana municipalities revealed that although 20% established GHG emissions reduction goals, only 5% moved forward in terms of conducting GHG emissions inventory, developing an emissions reduction plan, and including climate change mitigation in their budget (Krause, 2011b).

The above observation is not meant to downplay the role of local action in the global goal of GHG emissions reduction, but to better understand its practical position in the effort. Although the geographical-institutional arrangement (Swyngedouw, 2004) of the locality presents a practical medium for climate mitigation to be initiated and maintained, the presentation of the "city"/"urban"/"local" scale as though it were a uniform platform across the globe, with already existing "willing" and "capable" attributes to completely cure global climate change, needs to be rethought. Local climate action should neither be seen as a straightforward matter nor a replacement for national and global actions (Van Der Heijden et al., 2019). This is illuminated in this study by the observed horizontal gaps in the innovation, implementation, and progress of CAPs and the vertical intergovernmental relations that constitute the practical realities of CAPs.

References

Alexander, S.E., 2020. Harnessing the opportunities and understanding the limits of state level climate action plans in the united states. Cities 99, 102622.

Angel, D.P., Attoh, S., Kromm, D., Dehart, J., Slocum, R., White, S., 1998. The drivers of greenhouse gas emissions: what do we learn from local case studies? Local Environ. 3 (3), 263–277.

Bae, J., Feiock, R., 2013. Forms of government and climate change policies in US cities. Urban Stud. 50 (4), 776–788.
Bansard, J.S., Pattberg, P.H., Widerberg, O., 2017. Cities to the rescue? assessing the performance of transnational municipal networks in global climate governance. Int. Environ. Agreem.: Polit. Law Econom. 17 (2), 229–246.
Betsill, M., 2001. Mitigating climate change in US cities: opportunities and obstacles. Local Environ. 6 (4), 393–406.
Betsill, M., Bulkeley, H., 2006. Cities and the multilevel governance of global climate change. Glob. Gov. 12 (2), 141–159.
Betsill, M., Bulkeley, H., 2007. Looking back and thinking ahead: a decade of cities and climate change research. Local Environ. 12 (5), 447–456.
Broto, V.C., 2017. Urban governance and the politics of climate change. World Dev. 93.
Broto, V.C., Bulkeley, H., 2013a. A survey of urban climate change experiments in 100 cities. Glob. Environ. Chang. 23 (1), 92–102.
Broto, V.C., Bulkeley, H., 2013b. A survey of urban climate change experiments in 100 cities. Glob. Environ. Chang. 23 (1), 92–102.
Brown, J.C., Purcell, M., 2005. There's nothing inherent about scale: political ecology, the local trap, and the politics of development in the Brazilian Amazon. Geoforum 36 (5), 607–624.
Bulkeley, H., 2005. Reconfiguring environmental governance: towards a politics of scales and networks. Polit. Geogr. 24 (8), 875–902.
Bulkeley, H., 2010. Cities and the governing of climate change. Annu. Rev. Environ. Resour. 35.
Bulkeley, H., Betsill, M., 2005. Rethinking sustainable cities: multilevel governance and the 'urban' politics of climate change. Environ. Polit. 14 (1), 42–63.
Bulkeley, H., Castán Broto, V., 2013. Government by experiment? global cities and the governing of climate change. Trans. Inst. Br. Geogr. 38 (3), 361–375.
Bulkeley, H., Kern, K., 2006. Local government and the governing of climate change in germany and the UK. Urban Stud. 43 (12), 2237–2259.
Bulkeley, H., Schroeder, H., 2012. Beyond state/non-state divides: global cities and the governing of climate change. Eur. J. Int. Relat. 18 (4), 743–766.
C40, 2017. About. Retrieved 11/21, 2017, from: http://www.c40.org/about.
Carey, N., 2012. Tea Party Versus Agenda 21: Saving the U.S. or Just Irking It? Reuters.
Census Bureau, U.S., 2018. Cartographic Boundary Files—Shapefile.
Center for Climate and Energy Solutions, 2020. U.S. State Climate Action Plans. Retrieved 07/10, 2020, from: https://www.c2es.org/document/climate-action-plans/.
Cleary, K., Palmer, K., Rennert, K., 2019. Clean Energy Standards No. 19-01. Resources for the Future.
Climate Mayors, 2017. Home. Retrieved 005/10, 2018, from: http://climatemayors.org/.
Corfee-Morlot, J., Kamal-Chaoui, L., Donovan, M.G., Cochran, I., Robert, A., Teasdale, P., 2009. Cities, climate change and multilevel governance. In: OECD Environment Working Papers. vol. 14. 0_1.
Crang, M., Cook, I., 2007. Doing Ethnographies. Sage.
Daley, D.M., Sharp, E.B., Bae, J., 2013. Understanding city engagement in community-focused sustainability initiatives. Cityscape, 143–161.
Davies, J.S., Imbroscio, D.L., 2009. Theories of Urban Politics. Sage.
Deangelo, B.J., Harvey, L.D., 1998. The jurisdictional framework for municipal action to reduce greenhouse gas emissions: case studies from Canada, the USA and Germany. Local Environ. 3 (2), 111–136.
DSIRE, 2019a. In: NC Clean Energy Technology Center (Ed.), 3rd Party Solar PV Power Purchase Agreement (PPA).
DSIRE, 2019b. In: NC Clean Energy Technology Center (Ed.), Renewable & Clean Energy Standards.

DSIRE, 2020. In: NC Clean Energy Technology Center (Ed.), Net Metering.
Dunlap, R.E., McCright, A.M., Yarosh, J.H., 2016. The political divide on climate change: partisan polarization widens in the US. Environ. Sci. Policy Sustain. Dev. 58 (5), 4–23.
Easterling, W.E., Polsky, C., Goodin, D., Mayfield, M.W., Muraco, W.A., Yarnal, B., 1998. Changing places, changing emissions: the cross-scale reliability of greenhouse gas emission inventories in the US. Local Environ. 3 (3), 247–262.
Engel, K.H., 2009. Whither subnational climate change initiatives in the wake of federal climate legislation? Publius 39 (3), 432–454.
Evans, J., Karvonen, A., Raven, R., 2016. The Experimental City. Routledge.
Flynn, B., 2000. Is local truly better? some reflections on sharing environmental policy between local governments and the EU. Eur. Environ. 10 (2), 75–84.
Granberg, M., Elander, I., 2007. Local governance and climate change: reflections on the swedish experience. Local Environ. 12 (5), 537–548.
Greshko, M., Parker, L., Howard, B., Stone, D., 2018. A Running List of How President Trump Is Changing Environmental Policy. National Geographic.
Gustavsson, E., Elander, I., Lundmark, M., 2009. Multilevel governance, networking cities, and the geography of climate-change mitigation: two Swedish examples. Environ. Plann. C: Govern. Policy 27 (1), 59–74.
Hayden, A., 2014. When Green Growth Is Not Enough: Climate Change, Ecological Modernization, and Sufficiency. McGill-Queen's Press-MQUP.
Hodson, M., Marvin, S., 2014. After Sustainable Cities? Routledge.
Homsy, G.C., Warner, M.E., 2015. Cities and sustainability: polycentric action and multilevel governance. Urban Aff. Rev. 51 (1), 46–73.
Hughes, S., Miller Runfola, D., Cormier, B., 2018. Issue proximity and policy response in local governments. Rev. Policy Res. 35 (2), 192–212.
Hurlburt, H., Byrd, K., Souris, E., 2019. Prospects for Climate Change Policy Reform.
ICLEI, 2015. Measuring Up 2015: How US Cities Are Accelerating Progress Toward National Climate Goals.
ICLEI, 2018. Five Milestones of Emissions Management. Retrieved 03/26, 2018, from: http://icleiusa.org/programs/emissions-management/5-milestones/.
Johnson, C.A., 2017. The Power of Cities in Global Climate Politics: Saviours, Supplicants or Agents of Change? Springer.
Johnson, C., Toly, N., Schroeder, H., 2015. The Urban Climate Challenge: Rethinking the Role of Cities in the Global Climate Regime. Routledge.
Kates, R.W., Mayfield, M.W., Torrie, R.D., Witcher, B., 1998. Methods for estimating greenhouse gases from local places. Local Environ. 3 (3), 279–297.
Kaufman, L., Zernike, K., 2012. Activists fight green projects, seeing U.N. plot. The New York Times, 1.
Kern, K., Alber, G., 2009. Governing climate change in cities: Modes of urban climate governance in multi-level systems. In: The International Conference on Competitive Cities and Climate Change, Milan, Italy, 9–10 October, 2009, pp. 171–196.
Kern, K., Bulkeley, H., 2009. Cities, Europeanization and multi-level governance: governing climate change through transnational municipal networks. J. Common Market Stud. 47 (2), 309–332.
Kibert, C.J., Thiele, L., Peterson, A., 2012. The Ethics of Sustainability.
Krause, R.M., 2011a. Policy innovation, intergovernmental relations, and the adoption of climate protection initiatives by US cities. J. Urban Aff. 33 (1), 45–60.
Krause, R.M., 2011b. Symbolic or substantive policy? measuring the extent of local commitment to climate protection. Environ. Plann. C: Govern. Policy 29 (1), 46–62.
Krause, R.M., 2012. Political decision-making and the local provision of public goods: the case of municipal climate protection in the US. Urban Stud. 49 (11), 2399–2417.

Krause, R.M., Park, A.Y.S., Hawkins, C.V., Feiock, R.C., 2019. The effect of administrative form and stability on cities' use of greenhouse gas emissions inventories as a basis for mitigation. J. Environ. Policy Plan. 21 (6), 826–840.
Kusnetz, N., 2017. U.S. Mayors Back 100% Renewable Energy, Vow to Fill Climate Leadership Void. Inside Climate News.
Lindseth, G., 2004. The cities for climate protection campaign (CCPC) and the framing of local climate policy. Local Environ. 9 (4), 325–336.
Mathews, D., 2017. Donald Trump Has Tweeted Climate Change Skepticism 115 Times. Here's All of It. Vox.
McCright, A.M., Dunlap, R.E., 2003. Defeating Kyoto: the conservative movement's impact on US climate change policy. Soc. Probl. 50 (3), 348–373.
McCright, A.M., Dunlap, R.E., 2010. Anti-reflexivity the American conservative movement's success in undermining climate science and policy. Theory Cult. Soc. 27 (2-3), 100–133.
Michaelowa, K., Michaelowa, A., 2017. Transnational climate governance initiatives: designed for effective climate change mitigation? Int. Interact. 43 (1), 129–155.
MIT Election Data and Science Lab, 2017. U.S. President 1976–2016. MIT Election Data and Science Lab.
National Renewable Energy Laboratory, 2019. Net Metering. Retrieved 07/10, 2020, from: https://www.nrel.gov/state-local-tribal/basics-net-metering.html.
Osher, C., 2010. Bike Agenda Spins Cities Toward U.N. Control, Maes Warns. The Denver Post.
Peduto, W., 2017. The United States Joins Syria, Nicaragua & Russia in Deciding Not to Participate With World's Paris Agreement. It's Now Up to Cities to Lead. [Tweet]. Retrieved from: https://twitter.com/billpeduto/status/870368663693660162.
Pielke, R.A., 2000a. Policy history of the US global change research program: part I. Administrative development. Glob. Environ. Chang. 10 (1), 9–25.
Pielke, R.A., 2000b. Policy history of the US global change research program: part II. Legislative process. Glob. Environ. Chang. 10 (2), 133–144.
Pielke Jr., R.A., 1995. Usable information for policy: an appraisal of the US global change research program. Policy. Sci. 28 (1), 39–77.
Pitt, D., Bassett, E., 2014. Innovation and the role of collaborative planning in local clean energy policy. Environ. Policy Gov. 24 (6), 377–390.
Rabe, B., 2011. Contested federalism and American climate policy. Publius 41 (3), 494–521.
Reed, M.G., Bruyneel, S., 2010. Rescaling environmental governance, rethinking the state: a three-dimensional review. Prog. Hum. Geogr. 34.
Robinson, P.J., Gore, C.D., 2005. Barriers to Canadian municipal response to climate change. Canadian J. Urban Res. 14 (1), 102–121.
Rosenzweig, C., Solecki, W., Hammer, S.A., Mehrotra, S., 2010. Cities lead the way in climate-change action. Nature 467 (7318), 909–911.
Russel Bernard, H., 1988. Research Methods in Cultural Anthropology. Sage.
Rutland, T., Aylett, A., 2008. The work of policy: actor networks, governmentality, and local action on climate change in Portland, Oregon. Environ. Plan. D Soc. Space 26.
Satterthwaite, D., 2008. Cities' contribution to global warming: notes on the allocation of greenhouse gas emissions. Environ. Urban. 20 (2), 539–549.
Schreurs, M.A., 2008. From the bottom up local and subnational climate change politics. J. Environ. Dev. 17 (4), 343–355.
Schreurs, M.A., Tiberghien, Y., 2007. Multi-level reinforcement: explaining European Union leadership in climate change mitigation. Global Environ. Polit. 7 (4), 19–46.
Sussman, G., 2009. The science and politics problem: Policymaking, climate change and hurricanes. In: Elsner, J. B., Jagger, T.H. (Eds.), Hurricanes and Climate Change. Springer, New York, pp. 387–411.

Sussman, G., Daynes, B.W., 2013. US Politics & Climate Change: Science Confronts Policy. Lynne Rienner Publishers.

Swyngedouw, E., 2004. Globalisation or 'glocalisation'? Networks, territories and rescaling. Camb. Rev. Int. Aff. 17 (1), 25–48.

Tiberghien, Y., Schreurs, M.A., 2010. Climate leadership, Japanese style: Embedded symbolism and post-2001 Kyoto protocol politics. In: Global Commons, Domestic Decisions: The Comparative Politics of Climate Change, p. 139.

Trapenberg Frick, K., Weinzimmer, D., Waddell, P., 2015. The politics of sustainable development opposition: state legislative efforts to stop the United Nation's agenda 21 in the United States. Urban Stud. 52 (2), 209–232.

Trump, D., 2012. The Concept of Global Warming Was Created by and for the Chinese in Order to Make U.S. Manufacturing Non-Competitive. [Tweet]. Retrieved from: https://twitter.com/realDonaldTrump/status/265895292191248385?ref_src=twsrc%5Etfw%7Ctwcamp%5Etweetembed%7Ctwterm%5E265895292191248385%7Ctwgr%5E&ref_url=https%3A%2F%2Fwww.motherjones.com%2Fenvironment%2F2016%2F12%2Ftrump-climate-timeline%2F.

U.S. Census Bureau, 2012. TIGER/Line Shapefile, 2012, Nation, U.S., Current County and Equivalent National Shapefile.

U.S. EPA, 2015. Climate and Energy Resources for State, Local and Tribal Governments. Retrieved 12/20, 2016, from: www.epa.gov.

UN-HABITAT, 2011. Hot Cities: Battle-Ground for Climate Change. (Cities and Climate Change: Global Report on Human Settlements 2011).

United States Conference of Mayors, 2018. Mayors Climate Protection Center. Retrieved 05/10, 2018, from: https://www.usmayors.org/mayors-climate-protection-center/.

Van der Heijden, J., 2018. The limits of voluntary programs for low-carbon buildings for staying under 1.5 C. Curr. Opin. Environ. Sustain. 30, 59–66.

Van Der Heijden, J., Patterson, J., Juhola, S., Wolfram, M., 2019. Advancing the role of cities in climate governance—promise, limits, politics. J. Environ. Plan. Manag. 62.

Vig, N.J., Kraft, M.E., 1996. Environmental Policy in the 1990s.

Wang, R., 2012. Leaders, followers, and laggards: adoption of the US conference of Mayors climate protection agreement in California. Environ. Plann. C: Govern. Policy 30 (6), 1116–1128.

Wang, R., 2013. Adopting local climate policies what have California cities done and why? Urban Aff. Rev. 49 (4), 593–613.

Westman, L., Broto, V.C., 2018. Climate governance through partnerships: a study of 150 urban initiatives in china. Glob. Environ. Chang. 50, 212–221.

White, T., 2012. Agenda 21—ICLEI Update: 138 ICLEI Members Quit ICLEI in 18 months! We Got 'em on the Run!. Message posted to: https://www.varight.com/news/agenda-21-iclei-update-138-iclei-members-quit-iclei-in-18-months-we-got-em-on-the-run/.

Yeganeh, A.J., McCoy, A.P., Schenk, T., 2020. Determinants of climate change policy adoption: a meta-analysis. Urban Clim. 31, 100547.

Zahran, S., Brody, S.D., Vedlitz, A., Grover, H., Miller, C., 2008a. Vulnerability and capacity: explaining local commitment to climate-change policy. Environ. Plann. C: Govern. Policy 26 (3), 544–562.

Zahran, S., Grover, H., Brody, S.D., Vedlitz, A., 2008b. Risk, stress, and capacity: explaining metropolitan commitment to climate protection. Urban Aff. Rev. 43 (4), 447–474.

CHAPTER

12 The risk of the electrical power grid due to natural hazards and recovery challenge following disasters and record floods: What next?

Enrico Zio[a,b,c] **and Romney B. Duffey**[d,*]

Energy Department, Politecnico di Milano, Milano, Italy[a] *MINE ParisTech, PSL Research University, CRC, Sophia Antipolis, France*[b] *Eminent Scholar, Department of Nuclear Engineering, College of Engineering, Kyung Hee University, Seoul, Republic of Korea*[c] *Private, Idaho Falls, ID, United States*[d]

The electrical power grid is a critical infrastructure: What can happen, and how can it fail?

The electrical power grid is one of the most critical infrastructures (CIs) in many developed and developing countries. As such, it needs to be planned, operated, maintained, and managed in an attentive way to ensure reliable, secure, and resilient (electrical power) service supply.

In general, CIs such as the electrical power grid, transport network, water distribution, and Internet (Fig. 1) are highly mutually dependent, either physically, or geographically, or logically, or through a host of information and communication technologies (the so-called cyber-based systems) (Rinaldi et al., 2001; Kroger and Zio, 2011; Zio, 2016). Although interdependencies can improve CI operational efficiency, they may also bring new vulnerabilities by opening new paths for the propagation of failures from one CI system to another, resulting in intersystems cascading failures (Buldyrev et al., 2010; Fang et al., 2016). Understanding the fragility induced by system interdependencies is one of the major challenges in the design of resilient infrastructures (IRGC, 2006; Vespignani, 2010; Ouyang, 2014; Pescaroli and Alexander, 2016; Zio, 2016).

The importance of the interdependency cannot be overstated: "The risk posed by a catastrophic power outage … is not simply a bigger, stronger storm. It is something that could paralyze entire regions, with grave implications for the nation's economic and social well-being" (NIAC, 2018). For this reason, it is recommended to: "(1) design a national approach to prepare for, respond to, and recover from catastrophic power outages that provide the federal guidance, resources, and incentives needed to take action across all levels of government and industry and down to communities and individuals; and (2) improve our understanding of how cascading failures across CI will affect restoration and survival."

*Romney Duffey retains copyright to the original images in the Contribution.

Climate Change and Extreme Events. https://doi.org/10.1016/B978-0-12-822700-8.00008-1
Copyright © 2021 Elsevier Inc. All rights reserved.

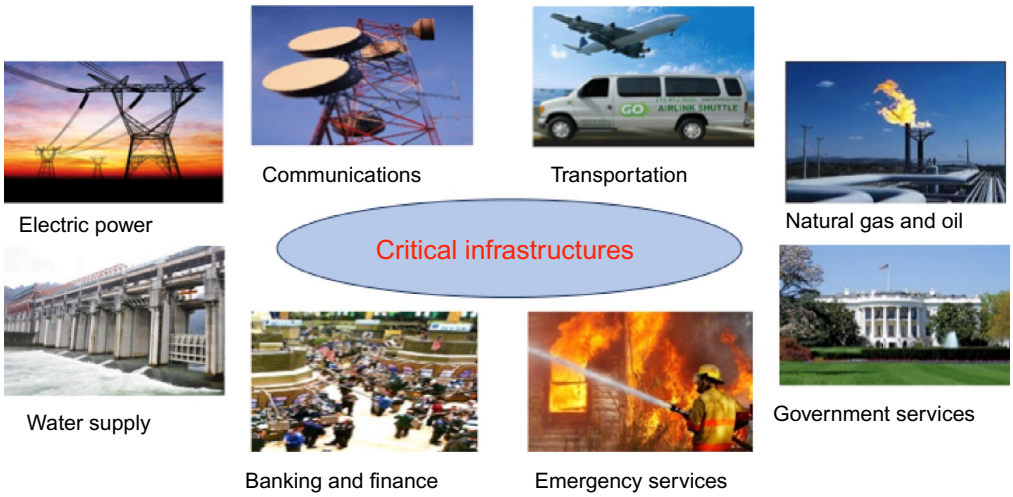

FIG. 1

Critical infrastructures—many interdependent and/or interconnected.

The need to evaluate the risk due to massive unexpected events and disasters is not new. The Government's job is, indeed, to equip society to be prepared for the worst, limiting the potential consequences and the damage extent of disasters, while speeding recovery. However, despite their intentions, Governments do not actually manage the weather; nor do they generally control the entire national and local infrastructure.[a]

The vulnerability of CIs and hazards to which they are exposed

Threats to CIs include severe massive natural disasters (affecting physical structures and systems), cyber (Wang et al., 2017), and electromagnetic attacks (on cabling, communication, and computer networks), or terrorist/extremist actions (on vulnerable targets). Recent years have seen many disruptions of different CIs caused by natural disasters (i.e., floods, ice and wind storms, fires, tsunamis, earthquakes, etc.), with substantial impact on human livelihoods and economic properties (Montz et al., 2017). The costs and number of yearly deaths due to natural hazards (NHs) are rising (see, e.g., EM-DAT, 2014). Just in the United States, 219 major weather and climate disasters have cost more than $1500 billion from 1980 to 2017 (see NOAA, 2019), with the annual impact of weather-related power blackouts ranging from $20 to $55 billion (Campbell, 2012). The trend of such events shows that their frequency has increased over the last 30 years, with a marked increase in the 2000s (Panteli and Mancarella, 2015). Also, there is a justified concern that the number and severity of extreme weather events will increase in the future as a result of global warming and climate changes (Cutter et al., 2015). This calls for frameworks, methodologies, techniques, and tools capable of

[a]The one important exception is the Netherlands flood control system protecting 17 million with over 3800 km of fully integrated levees, barriers and automated gates, periodically upgraded with funding from national and regional taxes.

assessing the risk from NH on interdependent CIs, in support of decision makers for investments in system protection and resilience. This is hardly a new problem, and we have consistently underestimated the threats, remaining unbelieving and unprepared.[b] This is despite the "alerts" from national and international bodies, which continue to study and issue general guidance, policies, and procedures for massive floods and power outages and coping with the associated consequences (e.g., UK EA, 2009; DHS, 2008, 2017, 2018; NIAC, 2018; Hegger et al., 2016; Matczak et al., 2016; COMRISK, 2006; and wetten.overheid.nl).

Climate change potential additional stress on the CI: The flood case

Is climate change a real threat to CIs and, in particular, to the reliable power supply?

This question of the impact of changing weather patterns is now receiving international attention, especially for the overall energy sector in the broader context of global electric power systems and energy supply (IAEA, 2019). The classic and exceptional case is that of the Netherlands where specific numerical risk targets have been set. For overtopping or overloading of the complex Dutch flood barrier systems, the "flood prevention levels" imply an average design failure rate range, $0.000001 < \lambda < 0.0001$ per hour for about 200 levee sections and more than 90 flood zones (Schweckendiek, 2013; and wetten.overheid.nl). A "local individual" or personal risk standard for all citizens of 0.00001 per year has now replaced this system failure rate (Jorissen et al., 2016). This change is specifically driven by the need for considerations of climate change over the next 200 years causing gradual sea-level rise and increased river discharges (Delta Commission, 2008.). Meanwhile, any rise in sea levels may cause many cities to face the same challenges of Holland, where much of the country is below sea level; or the threat like for the historic city of Venice, where periodic flooding is almost normal; and the "paradise" country of Singapore, which could also be placed in great danger. In addition, because of increased precipitation and runoff from extreme storms, there is also a possible increase in the probability of dam overtopping or failure that could lead to extensive flooding of CIs. Thus climate change adds additional stress literally on top of the other "normal stresses" that challenge our CIs (see Fig. 2).

A comprehensive recent analysis has shown that both large flood magnitude and frequency have increased in Europe in the period 1985–2009 (Kundzewicz et al., 2012). The US National Academies Presidents have stated: "The atmosphere and the Earth's oceans are warming, the magnitude and frequency of certain extreme events are increasing, and sea level is rising along our coasts" (McNutt et al., 2019).

One authoritative overview (Kundzewicz et al., 2012, 2013) of flooding locations "shows a clear link between flood reporting and concentrations of the population" but was not able to link changes in flood patterns solely to changing climate. Even more important, they express "low confidence in numerical projections of changes in flood magnitude or frequency resulting from climate change," so we cannot trust model predictions. In addition, Bonnin et al. (2006) also importantly state: "The current practice of precipitation (and river height and flow) frequency analysis makes the implicit assumption that past is prologue for the future…Furthermore, if the climate changes in the future, there is no guarantee that the characteristics extracted are suitable for representing climate during the future lifecycle of projects being designed." This fact was also pointed out by De Gaetano (2009) due to global and local changes in climate and precipitation patterns. For coastal regions, there are similar statistical

[b]In popular terminology, the new records are "unknown knowns."

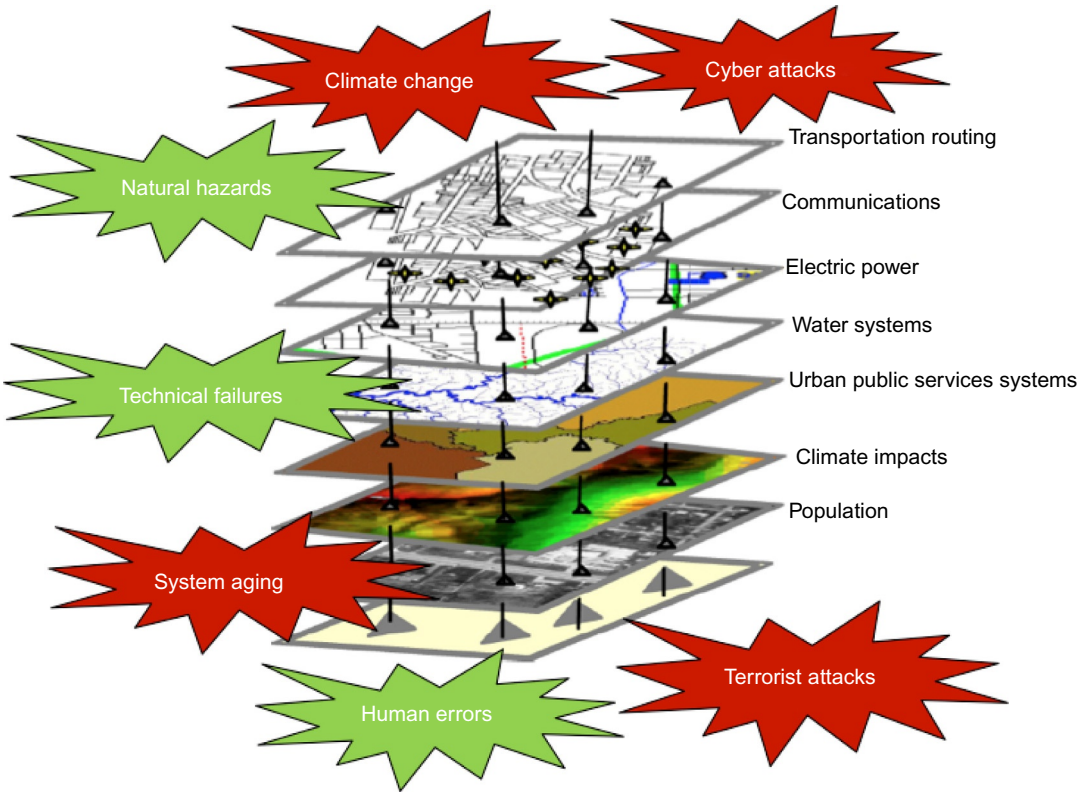

FIG. 2

Hazards and threats for interdependent critical infrastructures now include the impact and stress of potential climate change.

approaches and concerns about the uncertainty of predicting flood and storm surges (see, e.g., Matczak et al., 2016; Emanuel, 2017; ACE, 2006; COMRISK, 2006). For one recent storm surge model, "Many parts ….cannot be separately calibrated or validated using observed historical data because the model produces statistical projections of flood depth and damage risk spanning a wide range of plausible events" (Fischbach et al., 2017).

Both natural and man-made disasters can cause massive damage sufficient to lose power systems for several weeks over large urban or statewide areas, exhaust the capabilities of mutual aid and emergency response plans, and affect many millions, but still not meet the arbitrary NIAC (2018) criteria of 50 million outages lasting months to qualify as a "catastrophic power outage" of national interest. If we consider for a moment a major unexpected event such as Hurricane Katrina's impact on New Orleans and the outage duration, we can only imagine the consequences of such a defined "catastrophe," which is "beyond modern experience." In addition, many dependent systems can be crippled: "Since communications systems rely on electricity, any incident that causes long-term power outages will create a challenging environment for telecommunications and public messaging" (DHS, 2017).

Extensive power outage and restoration data exist as a direct result of many severe NH events, for example, storms, ice storms, fires, hurricanes, cyclones, and floods, causing outages lasting from 24 to 800 h over a wide range of urban and regional scales (Duffey, 2019a). Because of the grid causing past fires in California, the risk and financial liability have now lead to blackouts by deliberate power shut-off to millions of customers. The NH outage data were collected from the public websites and outage trackers of the affected local power companies as the events occurred in real time and reflect both the reporting and updating intervals, varying from every 15 min to few hours. In all cases, the affected power companies, emergency management organizations, and government agencies deployed vast numbers (sometimes many thousands) of emergency staff, specialized repair crews, equipment, and procedures to address power recovery, evacuate people, and repair damage. Essentially restoration only can and does proceed "as fast as humanly possible," limited by damage, access, and social disruption issues caused by flooding, storms, fires, wind, ice, and snow, and as stated (DHS, 2018), "the restoration of the grid is generally the same across all hazards."

The question is how to account for this in the framework of risk assessment and handle this in the framework of risk management.

Risk assessment and complexity: Limitations and development

Vulnerability and risk assessment and management are foundational concepts, and associated analytic disciplines have been developed that are solidly rooted in a structured and systematic approach, which should be deeply ingrained in the practical application of CI protection and resilience. The reason for this is that by identifying and understanding the hazards and vulnerabilities of CI, one can identify the proper measures to implement for its protection and resilience (see Fig. 3). But in practice, the complexity of the CIs brings significant difficulty in the analysis of the vulnerabilities and the assessment of the risks, in a confident and comprehensive way (Zio, 2016).

As for any technological system or human endeavor, there are two complementary but distinct ways to view, model, and quantify the complexity of CI, being: (a) bottom-up, from how the detailed components of the system(s) are physically designed, constructed, and operated; and (b) top-down, from how the overall system(s) are managed and interlinked. In both cases, the degree of complexity derives from known and unknown, explicit, or implicit relationships embedded in the CI. As adapted from Zio (2016), there exists:

- Heterogeneity across different technological domains due to increased integration among systems—a system is not exactly the same as any other (Gheorghe and Schlapfer, 2006).
- Scale and dimensionality of connectivity through a large number of components (nodes)—so there are just many points and opportunities for interaction and interference (Popov, 2009; Rinaldi et al., 2001; Bloomfield et al., 2009, Chou and Tseng, 2010; D'Agostino et al., 2010; Fioriti et al., 2010; Luiijf et al., 2009).
- Dependencies, or one-way, unidirectional relationships—so one component or system depends upon another through a link, but this other one does not depend upon the former through the same link.
- Interdependencies or bidirectional links—here two or more components or systems inherently depend upon each other.

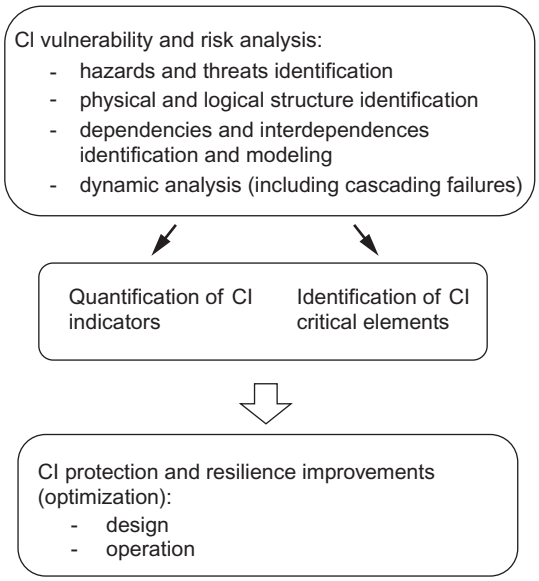
CI vulnerability and risk analysis:
- hazards and threats identification
- physical and logical structure identification
- dependencies and interdependences identification and modeling
- dynamic analysis (including cascading failures)
Quantification of CI indicators
Identification of CI critical elements
CI protection and resilience improvements (optimization):
- design
- operation

FIG. 3

Generalized risk analysis framework as applied to CIs (Zio, 2016).

The issue of interdependency among CIs has been prioritized by the European Reference Network for Critical Infrastructure Protection and a Thematic Area has been launched to address it systematically, and its importance underlined by the several research works (Svendsen and Wolthusen, 2007; Utne et al., 2011; Bobbio et al., 2010; Brown et al., 2004; Johansson and Hassel, 2010) and European Union projects on the subject (e.g., Klein, 2011).

Remaining with the risk of flooding, there is no general form of statistical distribution that fits all prior or past flood, stream flow, or precipitation data—they are location and regionally different and specific and require "regional skewness estimators" (see, e.g., the excellent summaries by Bonnin et al., 2006; Perica et al., 2013; Franz and Sorooshian, 2002). The figures in Bonnin et al., 2006 also illustrate the difficulty—indeed the impossibility—of extrapolating beyond the data interval, whereas having a long interval of reliable data is itself quite rare. Indeed, it is clearly stated that: "As a rule of thumb, statistical methods should not be used to estimate recurrence intervals in years that are more than twice the number of years of available homogeneous data" (FEMA, 2019, pp. 4–6).

Constituting the "fat" or "right" tail of any distribution of the number of events, record floods, and extreme precipitation cannot be described by the statistical distributions derived from our usually or most often experienced occurrences. The usual statistical 'goodness of fit' methods and measures traditionally adopted are heavily influenced by the majority of "normal" data, and barely at all, by the few rare records at the "tail."

Here, we define "higher than designed" as a new record event, which in the insurance industry is categorized as an "Act of God" (IRMI, 2019). Extensive flooding due to storms can cause sufficient

damage to lose power systems for several weeks. Emergency measures should include backup pumping as well as backup power, because as stated for the massive but entirely local Hurricane Katrina flooding: "While the pumping stations have not been considered as an integral part of the hurricane protection system, they should have been" (ACE, 2006, Vol. VI).

Assessing flood and outage risk based on past events

There are many key references on the topic of the statistical and computer models used worldwide for the frequency and magnitudes of flooding caused by storms, surges, and streamflows, and on systematic changes in precipitation patterns (as a sample, see, e.g., Bonnin et al., 2006; Perica et al., 2013; England Jr. et al., 2018; De Gaetano, 2009; Wing et al., 2018; Shukla and Trivedi, 2010; Sandoval and Raynal-Villaseñor, 2008; Emanuel, 2017; Fischbach et al., 2017). By simply counting the number of all prior floods or flows of a given amount in any selected interval, the best statistical fits of the resulting frequency (per unit time interval) all have essentially similar coefficients of determination or "goodness of fit" parameters (e.g., Alam et al., 2018; Langat et al., 2019).

There are wonderfully detailed maps available online (water.weather.gov) of the greater than and equal (50%) chance of having a flood in any 3-month time interval in the United States. The recurrence period or "one-in-so-many-years" flood or "annual exceedance probability" is often used as a standard for assessing flood risk. Although society should exercise forethought and care, we do not, building where we should not and exposing ourselves to undue risk. Issuing flood insurance is often avoided by the private insurance industry and backed in the United States through the Federal Emergency Management Agency (FEMA) National Flood Insurance Program. The reason is simply the uncertainty coupled with the magnitude of the financial (claim) risk. The past cost of flooding risk has been estimated as $90 billion and more than 700 deaths from 2004 to 2014 (NAS, 2019.). Using complex geographic-hydrographic-socioeconomic computer modeling, it has been estimated that about 40 million people and $3 trillion are at future potential risk to the once-in-a-hundred-year floods in the United States alone (Wing et al., 2018). In Louisiana alone, assets totaling about $1.2 billion are currently at risk, with electrical systems about 30% of all the CIs possibly inundated (Fischbach et al., 2017, Fig. 13 and Table 21). In England, there are about 5 million properties at risk of any type of flooding, with an annual insurance cost of more than $3 billion, and 14% or 7000 sites of the electrical infrastructure at risk (UK EA, 2009). The year 2012 was the "wettest winter for 250 years," but despite this new record, the UK flood zones for "planning" are still artificially defined by yearly occurrence[c] (UK EA, 2009) and flood risk delineated in distinct but completely arbitrary categories:

- High risk means that each year…a 3.3% chance or greater
- Medium risk means that each year…between a 1% and 3.3% chance
- Low risk means that each year…between a 0.1% and 1% chance
- Very low risk means that each year…less than 0.1% chance

But there is a completely new problem outside the historical data, identified as responding to "a catastrophic power outage of a magnitude beyond modern experience" (NIAC, 2018). This is a coupled risk

[c]Equivalently, a 0.1% chance in a year is a frequency of 10^{-3}/year or the apocryphal one-in-a-thousand years event.

problem, as it includes the chance of having an even larger event than previously seen, and the chance of a "new record" initiating cause, like a more massive flood, hurricane, ice storm, fire, or earthquake.

The link of flooding extent to infrastructure damage is obvious, but a precise quantitative relation is not available. We have compared the probability of flooding shown by river gauges for Hurricane Florence in the United States with the probability of power outages and found a simple empirical correlation. The best fit to the data from Fig. 4 for the probability of a power outage due to flooding, with an $R^2 = 0.94$, is

$$P(F^*) = P_0^* e^{-\beta^*(h-h_0)} = 0.25\, e^{-0.022(h-h_0)}$$

This implies of course that a maximum of some 25% of the persistent outages is directly attributable to the difficulties caused by flooding. Lacking other evidence or alternative relation, this relation—or something similar—is assumed to be generally applicable to any power system susceptible to flooding, with the parameters being geographically, topologically, and regionally dependent for any given power CI.

Resilience definition, quantification, and concept

In a topical and almost philosophical terminology, many high-level reports (e.g., NIAC, 2018; DHS, 2018; NAS, 2019) now stress the desirability of systems having some unquantified "resilience" or "agility." It is even described as being some "capacity to resist, capacity to absorb, and the capacity

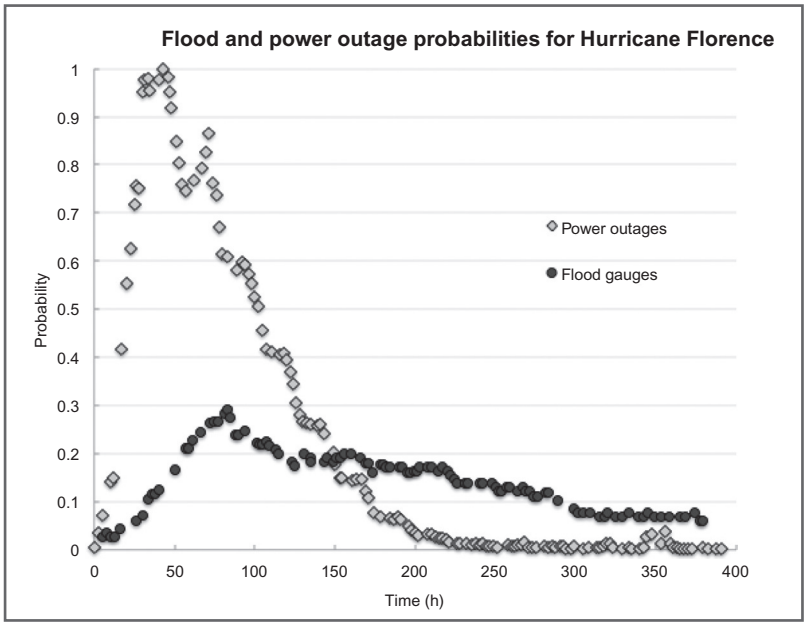

FIG. 4

The observed relation between the probability of river gauge flooding and power outage probability.

to adapt" (Hegger et al., 2016); or "the ability of a system to respond to, absorb and recover from perturbations" (Fisher, 2013). These are all surely desirable attributes and tautological policies, but importantly after an eminent and massive review, "based on the existing literature and research efforts, community meetings, and examination of other resilience programs, the committee found that no single measurement of resilience exists for all elements of resilience for all communities" (NAS, 2019).

A far more precise definition and measure for the real CI system "resilience" is as follows.

For some kth CI network, a quantitative expression, of the resilience, R^k, to a NH is the ratio of the cumulative performance under disruption and restoration over the period, P_{real}, to the target cumulative performance with no disruption, P_{target}, over that same period.

For power loss, the performance parameter is focused on the dynamic probability of successful restoration, $1-P(NR)$. The target performance or "perfect" resilience is actually attaining complete or "perfect" restoration, being, $P(NR)=0$, at or by some required times. By implication, the "resilience" is, then, actually the conventional reliability of the restoration process, $R(t)$; so straightforwardly,

$$R^k(NR) = 1 - P(NR)$$

This treatment of failure and definition of resilience using reliability is well known to systems engineers and risk analysts. What is then also provided in Fang and Zio (2019) is a novel adaptive robust optimization (ARO)-based mathematical framework for resilience enhancement of interdependent CI systems against NHs. In this framework, the potential impacts of a specific NH on infrastructure are first evaluated in terms of failure and recovery probabilities of system components; these are, then, fed into a two-stage ARO model to determine the optimal planning of resilience strategies under limited investment budget, anticipating the most likely worst realization of the uncertainty of component failures under the NH. For its exact solution, a decomposition method based on simultaneous column-and-constraint generation is adopted. This approach has been applied to the resilience of interdependent power and gas networks subject to (simulated) windstorms. The numerical results demonstrate the effectiveness of the proposed framework for the optimization of the resilience of interdependent CIs under hazardous events; this provides a valuable tool for making informed prehazard preparation decisions (Zio, 2016). The value of coordinated prehazard planning that takes into account CI interdependencies is highlighted.

Resilience to damage of CIs fights power system outages

Let us continue considering the NH of flooding and its impact on power outages.

Because of their inherently low probability of occurrence, new rare record floods are treated as random outcomes or events, subject to statistical error and their probability estimated, for example, based on hypergeometric sampling (Jaynes, 2003). Specific example case studies include flooding from New Zealand and US rivers, recent major US hurricanes, Harvey, Irma, and Florence, and the repetitive quasi-periodic tides in the Venice Lagoon. A quantitative link is clearly shown to exist between flooding extent and power outage duration.

In considering this limit, the problem is that the classical methods of the system vulnerability and risk analysis cannot capture the (structural and dynamic) complexities of CIs; the analysis of these systems cannot be carried out with classical methods of system decomposition and logic modeling.

A framework is needed for the integration of methods capable of viewing the problem from different perspectives (topological and functional, static, and dynamic), suitable for coping with the high complexity of the system and the related uncertainties (Kroger and Zio, 2011). Several researchers have addressed this problem, introducing new perspectives and methods of analysis and applying them for the protection and resilience of CIs (Wang et al., 2011; Ouyang, 2014 for some reviews of methods and Yao et al., 2019 for a technological solution of transportable energy storage to make more resilient power distribution systems with multiple microgrids). The complexity of CIs is presented here as a challenging characteristic, which calls for an integrated framework of different types of analyses and methods of vulnerability and risk assessment, for application to CI protection and resilience. The concepts of vulnerability, risk, and resilience are discussed in detail and analyzed with respect to their characterization in CI, and the challenges therein. Recent new perspectives on these concepts and their applications are also discussed with their applicability for analyzing CI vulnerability and risk in view of decision making for protection and resilience.

In the electric power grid, adaptive learning is a challenge–response property, which results from the tradeoff between consumer involvement and control by the central authority in the energy management process. On one side, intense consumer involvement can initiate chaotic behavior in the electrical system; on the opposite side, strong control by the central authority renders the system rigid, missing opportunities for service efficiency and for exercising system "resilience" and adaptation capacity. This raises the question of how much adaptive learning can be expected or should be imparted in the future "smart" grids and on the related feedback mechanisms.

What we have learned from data analysis and intercomparisons show the probability of nonrestoration of power lines and distribution systems is:

(a) First, essentially identical for power outages *without* additional damage due to extreme events (in urban areas or after a major snowstorm) and then slower with difficult weather conditions;
(b) Sometimes, slower for smaller storms where, after any given time, the probability of outage restoration for most of southern Ireland was the same as for restoring 32,000 power outages over the length of the Florida Keys; and
(c) A maximum limit of 20 times slower when additional major *external* or regional damage occurred because of severe events like massive hurricanes (e.g., Sandy also in New York, Harvey, and Irma in Florida) or extreme wildfires (e.g., in California).

The chance of an outage larger than any before depends on what has happened before and rare or extreme events. Statistically, this leads into the arena of the so-called extreme value distribution, which are fits to data with long tails (commonly called extreme value distribution, Gumbell, Weibull and Pearson Types III and IV, with three or more fitting parameters).

We do not need an exact estimate, simply some informed chance. A graph exists for the United States 1984–2000 (IRGC, 2006; Talukdar et al., 2003) for the probability of any given power outage magnitude,[d] without stating the causes, with an average or "normal" outage size $\overline{Q}$ =95MW(e) (i.e., 50% of the events are larger) obtained by transcribing the curve directly from the published graph. By inserting only this average outage into a simple "extreme value" double-exponential distribution

[d]In e-mail correspondence with Professor J. Apt in 2019, we have requested use of and access to the actual data or files, but unfortunately these are not publically available from the NERC.

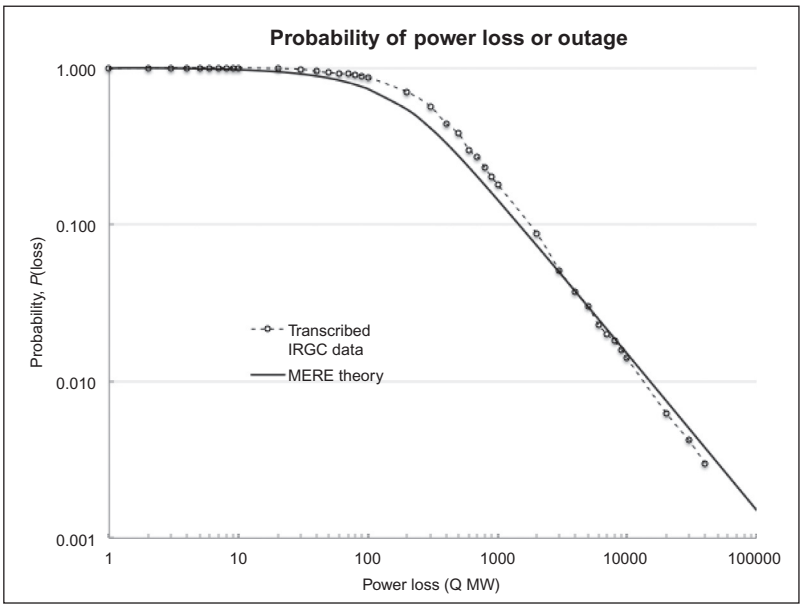

FIG. 5

The chance of a power outage exceeding any given size in the United States.

Derived from data plot in IRGC, 2006. Managing and Reducing Social Vulnerabilities From Coupled Critical Infrastructures, White Paper #3, Geneva, Switzerland: International Risk Governance Council.

derivable from learning theory (see, e.g., Duffey and Saull, 2008), the probability of exceeding any power loss scale, Q, is with $k=1$ (Fig. 5):

$$P_i(loss) = 1 - e^{-\frac{\overline{Q}}{kQ}\left\{1-e^{-\frac{kQ}{\overline{Q}}}\right\}}$$

Although this fit is not perfect, the agreement in the trends is sufficient for making a probability risk estimate within ±20% uncertainty. Numerically, the chance of exceeding a 40,000-MW(e) outage is of order 0.003, or one in 300 outages, which is practically identical to that using the arbitrary Talukdar et al. (2003) "power law," of $P(loss) = 280/(\mathrm{MW}^{1.08})$, that was fitted to just the large loss data for $Q > 500$ MW(e).[e]

To illustrate the problem of making predictions, by extrapolating the present new fit, the probability of exceeding 100,000 MW(e) is 0.002, twice that from extrapolating the Talukdar et al. (2003) limited range "power law." Moreover, the new formula allows the prediction, say if the *average* outage is increased 10 times to 1000 MW(e) about the size of large modern power plants, then the probability of

[e]This numerical agreement validates the accuracy of the transcription from the lines in the original plot, at least for the key "tail" of rare large losses.

exceeding 40,000 MW(e) rises to 0.02. We must indeed be prepared in the future for such large outages and to be able to recover from them quickly, because we may expect them to be up to 10 × more likely than solely past experience suggests.

The rate of restoration by emergency crews learning to repair and restore the *entire system* is observed to be directly proportional to the number of customer outages, n, independent of the event, so that to a good approximation, $\frac{dn}{dt} \propto n = -\beta n$. For CI system design and *recovery* planning purposes, we define the power outage due to extreme events like flooding, wind, fire, and hurricanes as (see Fig. 6) in categories of increasing complexity and degree of difficulty:

- Type 0: Ordinary, which we may classify as "every day" outage restorations that are relatively easy, with simpler equipment replacement, line repairs, and/or reconnection due to an effectively instantaneous initial outage.
- Type 1: Normal baseline, $\beta \sim 0.2$, when outage numbers quickly peak due to finite but relatively limited additional CI damage. Repairs are still fairly straightforward and all outages are restored over timescales of 20 to about 200 h.

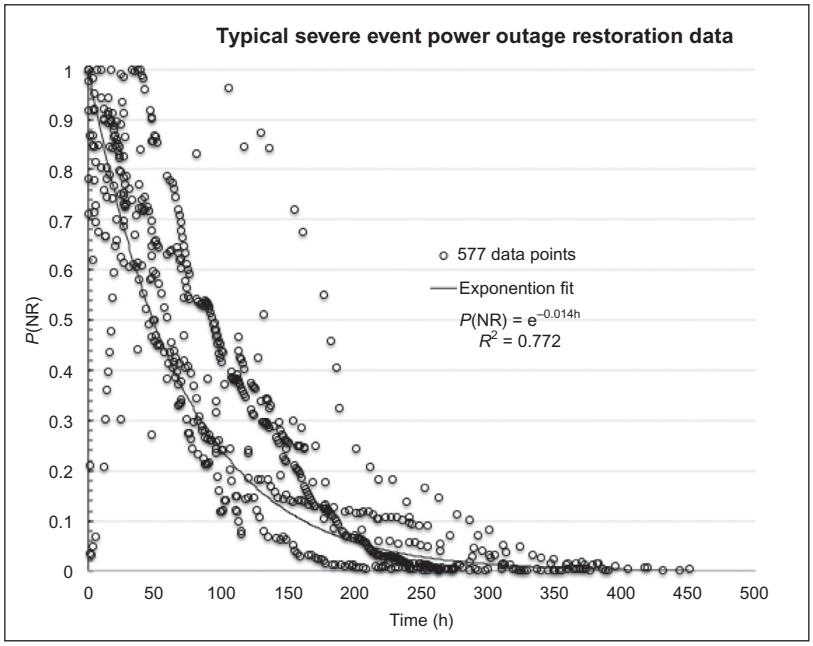

FIG. 6

The universal exponential power restoration trend for outages caused by Hurricanes Harvey, Michael, Irma, and Florence, an ice storm in New Hampshire and wildfires in California.

Data from Duffey, R.B., 2019a. Power restoration prediction following extreme events and disasters, Int. J. Disast. Risk Sci. 10(1), 134–148, https://doi.org/10.1007/s13753-018-0189-2 and Duffey, R.B., 2019b. The risk of extended power loss and the probability of emergency restoration for severe events and nuclear accidents, J. Nucl. Eng. Rad. Sci., NERS-18-1122, https://doi.org/10.1115/1.4042970.

- Type 2: Delayed, $\beta \sim 0.1$–0.02, progressively reaching peak outages in 20 plus hours, as extensive but repairable damage causes lingering repair timescales of 200–300 h before almost all outages are restored.
- Type 3: Extended, $\beta \sim 0.01$, with perhaps 50 or more hours before outage numbers peak due to continued damage and significant loss of CIs, and restoration/repair timescales take 300–500 h or more.
- Type 4: Extraordinary, $\beta \sim 0.001$ or less, for a cataclysmic event with the electric distribution system being essentially destroyed completely and not immediately repairable (e.g., Haiti, Costa Rica, and the NIAC "catastrophic outages").

Typical power nonrestoration probability data are shown in Fig. 6 for many severe Type 3 events (after Duffey, 2019a). Compared with the above learning theory, with time after the peak outages in hours, h, the simplest exponential fit (with $R^2 = 0.722$) is given by:

$$P(NR) = e^{-0.014h} + 0.007$$

Analyses and appropriate fits for many less severe events are given elsewhere (Duffey, 2019a, b). Note that there is a small but finite probability ~ 0.007 of power CIs not being completely restored until after 500 h (3 weeks), being simply too damaged; and, by definition, the probability of an outage not being restored is $P_i(loss) \times P(NR)$. For example, the risk of having a massive power outage of >40,000 MW (e) that is not completely restored for >500 h is $0.02 \times 0.007 = 0.0001$, or once in 10,000 outage events comparable to many other rare event risks.

Emergency response and system recovery

What is remarkable and unprecedented is that it is now possible to directly compare many disparate events and derive the range of needed failure rates for designing and implementing effective emergency backup and recovery systems. Hence *the theory and data show how emergency systems reliability, effective deployment timescale, and severe event nonrestoration rates are intrinsically linked together*. This is an important result, as it illustrates the influence of the failure rates at both the macroscopic engineered system and the detailed emergency response and restoration levels.

The new results also show that the probability of emergency systems failure and recovery follows the same general trends. Independent of the details and type of the severe event itself, they share the common issues of restoration delays caused by extensive damage, access problems, and the degree of difficulty. Hence, even the so-called catastrophic power outages will follow the same trends, independent of what they are or how they occur (DHS, 2018). This knowledge directly impacts the NIAC (2018) recommendation to "Develop a federal design basis and the design standards/criteria that identify what infrastructure sectors, cities, communities, and rural areas need to reduce the impacts and recover from a catastrophic power outage." The range of the emergency failure rate has been determined for real disasters, including all engineered systems, human actions, access issues, restoration governance, and procedural decisions.

As stated (ACE, 2006, Vol. VI, p. 47), "The continued operation of all pumping stations before, during, and after a hurricane is essential to prevent, control and eliminate flooding in the protected areas. An availability of 90% is a reasonable figure to use for modeling future system responses

assuming the stations are not rendered inoperative due to being flooded or abandoned. This percentage has been often exceeded during hurricanes which have struck South Florida's Water Management District which is similar in size and complexity to New Orleans' pumping system." So a key question is how often is "often exceeded," and what is the actual or achieved reliability of the backup pumping systems in a real event.

Following engineering reliability and risk analysis, the basic method combines the time-dependent nonrestoration probability of the failed critical system, $P(NR)$, with the dependent failure probability, $P(ES)$, to successfully deploy or actuate any or all emergency or backup systems. With an assumed overall engineering systems average failure rate, λ, and probability density, $dP(ES)/dt$, conventionally,

$$p(ES) = \frac{dP(ES)}{dt} = \lambda e^{-\lambda t}$$

This rate includes all engineered systems, human actions, access issues, and restoration and procedural decisions during emergency recovery and disaster response. At any elapsed time, t, noting that $P_m \ll 1$, and can be neglected, the probability, $P(EF)$, of extended failure or system outage is,

$$P(EF) = \int_0^t \frac{P(EF)}{dt}\, dt = \int_0^t P(NR)_t \frac{dP(ES)}{dt}\, dt = \int_0^t \left(P_0^* e^{-\beta t}\right) \lambda e^{-\lambda t}\, dt$$

Integrating by parts over any emergency restoration time, t,

$$P(EF) = P_0^* \left(\frac{\lambda}{\beta + \lambda}\right) \left[1 - e^{-(\beta+\lambda)t}\right]$$

Or in an elegant nondimensional form (Duffey, 2019b),

$$P(EF) \equiv P(ELP) = \psi P_0^* \left[1 - e^{-t/t^*}\right]$$

Derived above as the quantitative dynamic measure of the emergency response "resilience," the conventional reliability or chance of restoration is the complement, $R(t) = 1 - P(EF)$. The important failure rate ratio, $\Psi = \lambda/(\beta + \lambda)$, and the key characteristic time, or e-folding timescale, $t^* = 1/(\beta + \lambda)$. The role of the ratio of the key failure rate parameters is now self-evident, with recovery timing depending on which failure rate dominates.

The short- and long-timescale limits also intersect at the characteristic time, $t = t^*$, being the critical timing for an emergency system being effective or not in reducing the probability of extended loss.

Emergency system failure rates for Hurricane Katrina and the Fukushima nuclear events

We apply the method using two parallel and well-known NH Type 3 cases of "extended" long outage duration of national importance and major societal impact.

The first example is the inundation of New Orleans by Hurricane Katrina (CAT 4) in 2005, causing extensive record flooding and infrastructure damage (ACE, 2006). As stated elsewhere (GAO, 2017): "Hurricane Katrina became the single largest, most destructive natural disaster in our nation's history causing over 1800 deaths and an estimated $108 billion in damage."

The full reports (ACE, 2006) show the common causes of emergency system failures were the overwhelming of the flood prevention and pumping systems, including overtopping of levees and barriers. Several hundred flood prevention pumps were distributed in various locations, but many became inoperable, themselves failing due to flooding, power loss, backflows, and/or forced evacuation.

The overall or *integrated systems* failure rate, λ, of the flood prevention systems and the backup emergency pumps to operate has been estimated by analyzing the emergency pump outage/operability information reported daily for August 28 to September 21, 2005, (ACE, 2006, Vol. VI, Figs. 12, 16, 19 and 22). The calculated dynamic probability of successful overall emergency pump system operation, $P(ES)_t$, correcting for the running total, with t measured in hours, h, after the Katrina event started, is (see Fig. 7),

$$P(ES)_t = 0.8\, e^{-0.003\, h}$$

Hence, for these diverse flood prevention and emergency backup pumping systems, the implied integral average failure rate is $\lambda \sim 0.003$ per hour. This effective failure rate is not restricted to just the pumps and/or levees, but encompasses the whole CI backup system, including *all* design features, human decisions/actions, equipment issues, and overall system performance during the entire disaster.

We know that the data show $\beta \sim 0.01$ per hour for humans to restore power systems as fast as possible following severe flooding, fire, hurricanes, and ice storms, which cause damage and access problems, being independent of the initiating event type.

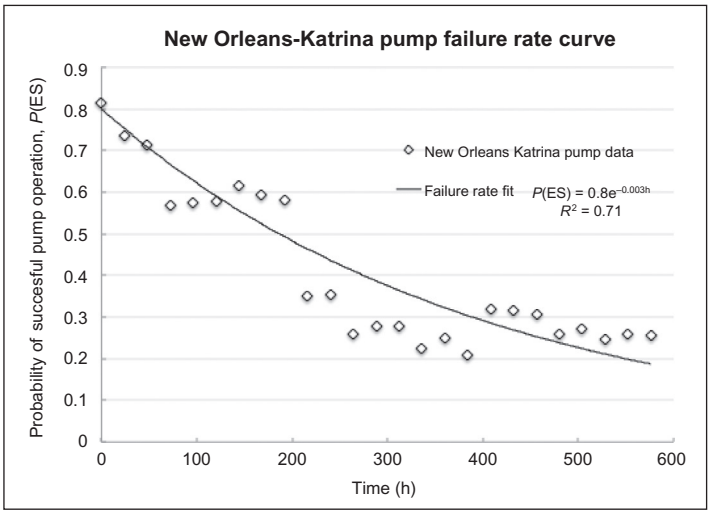

FIG. 7

Reliability curve fitted to data for the emergency flood pump failures in New Orleans over the long term (Type 3) following Hurricane Katrina.

Taking these β and λ rate values as typical for any severe event, the critical time, $t^*=1/(\beta+\lambda) = 1/(0.01+0.003) \sim 77$ h, dominated by the restoration difficulty; while at long times, $P\text{-}(EF)_{t\to\infty} \to \psi = 0.003/0.013 \sim 0.23$, or about a 25% chance of extended systems failure or nonrecovery even with emergency restoration. Hence, for major events, we should expect power and pumping outage durations lasting at least several days, even with multiple backup systems available.

The second example is the unprecedented nuclear plant damage caused by the Great NE Japan offshore earthquake and the resulting record tsunami. For the nine nuclear reactors at Fukushima, the full reports (TEPCO, 2012; ASME, 2012) show the common causes of engineered system failures were power line damage and unexpected overtopping of sea walls and flood barriers, resulting in extended loss of power (LOSP/LOOP), failure of emergency cooling systems, and damage to backup systems and pumps. Emergency efforts were simultaneously made to resupply grid power from offsite, provide power onsite, and use whatever backup, battery, pump, mobile, or other systems that could be deployed to enable control and cooling, and once again, the restoration took many days.

In Fig. 8, the predicted probability of extended systems failure, $P(EF)$, for the Fukushima Units is directly compared with Hurricane Katrina using the actual emergency pump failure rate. Also shown are the calculated effects of a wider range of better ($\lambda=0.001$) or worse ($\lambda=0.01$) emergency or backup systems failure rates that encompass that actually observed. In contrast, the shorter timescale Type 1 "normal" nuclear plant SBO results ($\beta=0.22$) *without* additional damage/difficulty have an emergency system failure rate of $\lambda \sim 0.091$ derivable from the published calculations of Ma et al. (2018). Therefore, it is confirmed that the difficulties caused by the actual Type 3 severe events delay emergency restoration timescales to CIs by at least a factor of ten.

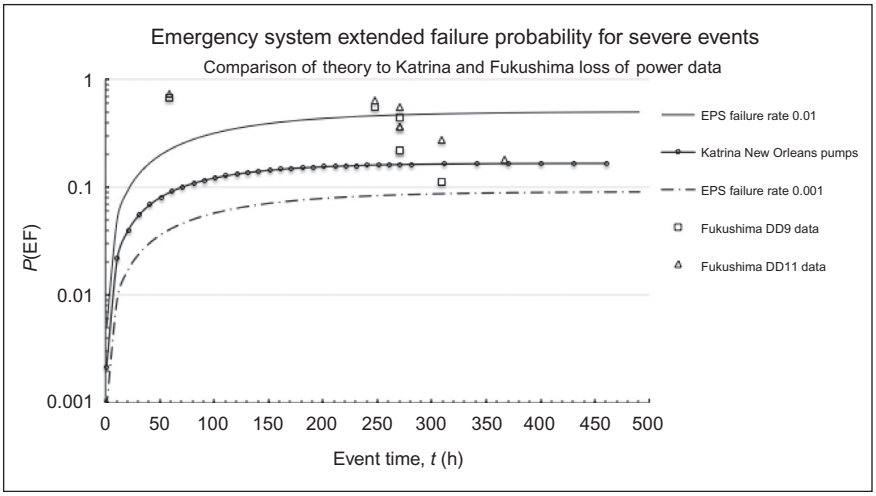

FIG. 8

Probability of extended systems failure, $P(EF)$, for assumed emergency system (ES) failure rates, and comparison to failure to restore data from Hurricane Katrina, and the Fukushima reactor accidents.

Based on the data for the emergency and engineered system failures occurring in the disasters of Hurricane Katrina and the Fukushima nuclear reactors, the implications are now discussed for emergency planning and backup power and pumping systems. Note the emergency "resilience" is quantified using the reliability, but now including all human decisions, emergency actions, systems restoration, and social disruption as occurring in real events.

Enhancing power grid "resilience"

Systematic consideration of vulnerability and risk of CIs must take into account the inherent complexities of these systems. Specifically, the framework of vulnerability and risk analysis has been examined here in relation to its application for the protection and resilience of CIs. It is argued that the complexity of these systems is a challenging characteristic, which calls for the integration of different modeling perspectives and new approaches of analysis. Examples provided to support this conclusion include the relation between the Internet and, particularly, the electric power grid, as representative of CIs with associated complexities. The integration of different types of analyses and methods of system modeling is put forward for capturing the inherent structural and dynamic complexities of CIs and eventually evaluating their vulnerability and risk characteristics. Decisions can then be taken on protections and resilience actions with the required confidence.

What we have learned from the past real events that we have discussed in this chapter has national as well as systems engineering implications.

The so-called hardening of electric power distribution systems has been promoted to achieve "resilience" (NIAC, 2018; DHS, 2019). However, the resilience improvement claims associated with such hardening are based on reduced average restoration times and undamaged pole count for Hurricane Irma, not for regions or outages with worst access and a high degree of restoration difficulty issues. In fact, such improvement claims are not confirmed by the full probabilistic results and the published analysis of regional (*not* average) variation, which states (Duffey, 2019a): "The least initially damaged cities and less flooded regions with easier access were fully restored by 200–300 h, except for the heavily inundated Naples/Collier region, which confirms that damage and access difficulty dominates recovery."

Along these lines, there is also a recent recommendation to develop "adaptable communications systems" (NIAC, 2018). However, despite having a new National Joint Information Center (DHS, 2017) and the DOE GIS EAGLE images (https://eagle-i.doe.gov), apparently nowhere is there a dynamic national power outage tracking system. The plethora of existing interwoven governmental emergency and commercial responsibilities (e.g., in the United States alone, they include DHS, FEMA, EEI, NERC, NARUC, DOE, DOD, DOT, APPA, and NEI) need a national outage data-tracking center and enhanced and extended outage *prevention and restoration* initiatives to help ensure effective emergency management response.

When considering more distributed generation or alternate backup power systems, one key question is whether the size or scale of the electrical distribution system affects restoration time and/or probability. Intuitively, it might be expected that smaller systems are more easily repaired and/or bigger systems should take longer. If true, there are the possibility to subdivide the power system into smaller subregions or "distributed" networks with more limited connectivity and less reliance on central power

generation and supply. We have examined all the data to determine whether such "scale" effects exist, which might help the distribution system design for customers needing or considering installing their own backup power, or if an optimal degree of system subdivision exists for ensuring faster restoration after extreme events.

These data for events covering the range from over 1 million to 8000 outages show that having a smaller number of outages following an extreme event did not systematically or proportionally reduce the timescale for complete restoration over this wide range of systems and regional scale. There is a hint that smaller outage numbers actually take longer times to *completely* restore, but physically based fits (linear, exponential, power-law, etc.) were not statistically significant ($R^2 < 0.2$). Just splitting up a large system into sets of smaller systems or regions apparently does not enhance restoration when there is extensive associated societal disruption and damage.

The inundation of New Orleans by Hurricane Katrina (CAT 4), in 2005, caused an extensive record of flooding and infrastructure damage. Despite several hundred flood prevention pumps being distributed in multiple locations, many failed to provide the service because of being "inaccessible, inoperable, or without electrical power" due to overtopping and failure of barriers and levees. Simply adding more and more distributed backup pumps is not an effective strategy.

Managing the response and improving the systems: What next?

Government agencies, private businesses, and emergency organizations will learn from these previous disasters (Duffey and Saull, 2008; Thompson, 2012), including the improvement of storm and fire damage mitigation measures. The FEMA provides overall emergency support in the United States but building, operating, securing, and protecting CIs like the power grid and power plants are the role and licensed responsibility of the private sector, or some separate quasi-governmental or authorized entity (DHS, 2008; FEMA, 2016; ESB, 2017). The current allocation of management responsibilities between electric utility investments, local government emergency preparedness, and federal government national disaster response works well most of the time but should be further refined.

The current demonstration is that all extreme events have similar restoration trends, which must be attributed to their possessing identical overall CI physical repair mechanisms and processes, engineering design, and learning behavior. There seems to be a fundamentally human limit on the restoration rate. Therefore, urban emergency planning, "smart" grids, and backup power systems need to expect and be able to withstand the probability of highly extended outages for the cases with major external damage from extreme events. This does not just mean adding diversity or redundancy of supply, but also considering the extent and frequency of occurrence of the disaster events.

Cost-benefit analysis as a basis for risk improvements cannot work across such diverse entities and interests. To improve outage risk management due to extreme events and disasters and optimize the local, business, and national investments, the suggested focus and "smart grid" priorities, including emergency planning for cities and utilities, should be:

- Increasing diversity and robustness of supply and delivery;
- Designing for ease and rapidity of restoration;
- Managing emergency system response capability;

- Improving communications and emergency planning;
- Removing or reinforcing vulnerable structures and facilities;
- Revising existing extreme event occurrence criteria;
- Enhancing flood barriers and controls on all vulnerable regions;
- Reducing major fire and flooding risk exposure; and
- Revisiting national preparedness arrangements and agreements.

Some managerial insights can be drawn from specific case studies, including:

(1) Investment in prehazard resilience strategies, for example, transmission line hardening and DG placement, can effectively improve the resilience of interdependent Power and Gas Networks against typhoons; however, the optimal set of lines to be hardened is sensitive to the amount of investment budget. Thus, the DM should evaluate carefully the available budget to obtain the optimal plan for implementation.
(2) Considering the combination of different resilience strategies can be more effective for system resilience enhancement.
(3) When the investment budget is relatively small, it is significant to protect different CIs as a whole and consider their interdependency to achieve a globally optimum resilience enhancement plan against NH.

What have we learned and what should happen next? Key future questions include: how high and reliable to build flooding defenses (e.g., for a Dutch-style flood defense strategy around Florida and England); how to enhance backup power systems for all CI fail-safe interconnections; and establishing markedly increased investment. What next must and can only be better systems, improved reliability, more effective emergency management, through decision making guided by quantified risk and resilience.

References

ACE, 2006. Performance evaluation of the New Orleans and Southeast Louisiana Hurricane Protection System, Volumes I to VIII, Engineering and Operational Risk and Reliability Analysis. US Army Corps of Engineers, Interagency Performance Evaluation Task Force. All volumes available at US ACE Digital Library, usace.contentdm.oclc.org/digital/collection/p266001coll1/id/2844/.

Alam, M.A., Emura, K., Farnham, C., Yuan, J., 2018. Best-fit probability distributions and return periods for maximum monthly rainfall in Bangladesh. Climate 6, 9. https://doi.org/10.3390/cli6010009. 16 pp www.mdpi.com/journal/climate.

ASME, 2012. Forging a New Safety Construct. American Society of Mechanical Engineers, Presidential Task Force, New York.

Bloomfield, R., Chozos, N., Nobles, P., 2009. Infrastructure Interdependency Analysis: Introductory Research Review. Adelard LLP, London. Report D/422/12101/4, CPNI, TSB and EPSRC, contract NSIP/001/0001—Feasibility Study on Interdependency Analysis www.adelard.com/assets/files/docs/d422v10_review.pdf. (Accessed 4 November 2020).

Bobbio, A., Bonanni, G., Ciancamerla, E., Clementi, R., Iacomini, A., Minichino, M., Scarlatti, A., Terruggia, R., Zendri, E., 2010. Unavailability of critical SCADA communication links interconnecting a power grid and a Telconetwork. Reliab. Eng. Syst. Saf. 95 (12), 1345–1357.

Bonnin, G.M., Martin, D., Bingzhang, L., Parzybok, T., Yekta, M., Riley, D., 2006. NOAA Atlas 14, Precipitation-Frequency Atlas of the United States, Volume 2 Version 3.0: Delaware, District of Columbia, Illinois, Indiana, Kentucky, Maryland, New Jersey, North Carolina, Ohio, Pennsylvania, South Carolina, Tennessee, Virginia, West Virginia. U.S. Department of Commerce, National Oceanic and Atmospheric Administration, National Weather Service, Silver Spring, Maryland. 2004 revised 2006, Library of Congress Classification Number GC 1046 .C8 U6 no.14 v.2.

Brown, T., Beyeler, W., Barton, D., 2004. Assessing infrastructure interdependencies: the challenge of risk analysis for complex adaptive systems. Int. J. Crit. Infrastruct. 1 (1), 108–117.

Buldyrev, S.V., Parshani, R., Paul, G., Stanley, H.E., Havlin, S., 2010. Catastrophic cascade of failures in interdependent networks. Nature 464 (7291), 1025–1028. https://doi.org/10.1038/nature08932.

Campbell, R.J., 2012. Weather-Related Power Outages and Electric System Resiliency. Congressional Research Service, Library of Congress, Washington, DC.

Chou, C.C., Tseng, S.M., 2010. Collection and analysis of critical infrastructure inter- dependency relationships. J. Comput. Civ. Eng. 24 (6), 539–547.

COMRISK, 2006. Common Strategies to Reduce the Risk of Storm Floods in Coastal Lowlands. EU project, Accessed at: www.umweltbundesamt.de/en/topics/climate-energy/climate-change-adaptation/adaptation-tools/project-catalog/comrisk.

Cutter, S.L., Ismail-Zadeh, A., Alcantara-Ayala, I., Altan, O., Baker, D.N., Briceno, S., Gupta, H., Holloway, A., Johnston, D., McBean, G.A., 2015. Global risks: pool knowledge to stem losses from disasters. Nature 522 (7556).

D'Agostino, G., Bologna, S.V., Fioriti, E., Casalicchio, E., Brasca, L., Ciapessoni, E., Buschi, S., 2010. Methodologies for inter-dependency assessment. In: Proceedings of the 5th International Conference on Critical Infrastructure(CRIS), pp. 1–7.

De Gaetano, A.T., 2009. Time-dependent changes in extreme-precipitation return-period amounts in the continental United States. J. Appl. Meteorol. Climatol. 48, 2086–2099. https://doi.org/10.1175/2009JAMC2179.1.

Delta Commission, 2008. Findings 2008: Working Together With Water: A Living Land Builds for Its Future. Hollandia Printing, The Netherlands. www.deltacommissie.com.

DHS, 2008. United States, National Response Framework. Department of Homeland Security, Washington, DC. https://www.fema.gov/pdf/emergency/nrf/nrf-core.pdf. (Accessed 23 October 2017).

DHS, 2017. Power outage incident annex (POIA) to the response and recovery federal interagency operational plans. In: Managing the Cascading Impacts from a Long-Term Power Outage. US Department of Homeland Security. Final, Accessed at: www.fema.gov/media-library-data/1512398599047-7565406438d0820111177a9a2d4ee3c6/POIA_Final_7-2017v2_(Compliant_pda)_508.pdf.

DHS, 2018. Strengthening the Cyber Security of Federal Networks and Critical Infrastructure, Section 2(e): Assessment of Electricity Disruption Incident Response Capabilities. Accessed at: www.dhs.gov/sites/default/files/publications/EO13800-electricity-subsector-report.pdf.

Duffey, R.B., 2019a. Power restoration prediction following extreme events and disasters. Int. J. Disast. Risk Sci. 10 (1), 134–148. https://doi.org/10.1007/s13753-018-0189-2.

Duffey, R.B., 2019b. The risk of extended power loss and the probability of emergency restoration for severe events and nuclear accidents. J. Nucl. Eng. Rad. Sci. https://doi.org/10.1115/1.4042970. NERS-18-1122.

Duffey, R.B., Saull, J.W., 2008. Managing Risk. John and Wiley and Sons, ISBN: 978-0-470-69976-8.

Emanuel, K., 2017. Assessing the present and future probability of Hurricane Harvey's rainfall. Proc. Natl. Acad. Sci. U.S.A. 114 (48), 12681–12684. https://doi.org/10.1073/pnas.176222114.

EM-DAT, 2014. The OFDA/CRED – International Disaster Database. Centre for Research on the Epidemiology of Disasters (CRED), IRSS Université catholique de Louvain, Belgium. www.emdat.be.

England Jr., J.F., Cohn, T.A., Faber, B.A., Stedinger, J.R., Thomas, W.O., Veilleux, A.G., Kiang, J.E., Mason Jr., R.R., 2018. Guidelines for determining flood flow frequency—Bulletin 17C. In: U.S. Geological Survey Techniques and Methods, p. 148, https://doi.org/10.3133/tm4B5. Book 4, Chapter B5.

ESB, 2017. Eire Supply Board Distribution System Operator License. doc.# DOC-291111-BJK https://www.esbnetworks.ie/who-weare/about-esb. (Accessed 29 October 2017).

Fang, Y.-P., Zio, E., 2019. An adaptive robust framework for the optimization of the resilience of interdependent infrastructures under natural hazards. Eur. J. Operat. Res. 276 (3), 1119–1136. https://doi.org/10.1016/j.ejor.2019.01.052.

Fang, Y., Pedroni, N., Zio, E., 2016. Resilience-based component importance measures for critical infrastructure network systems. IEEE Trans. Reliab. 65 (2), 502–512.

FEMA, 2016. The Federal Emergency Management Agency. Publication 1, Washington, DC https://www.fema.gov/media-library-data/1462196227387-c10c40e585223d22e2595001e50f1e5c/Pub1_04-07.pdf. (Accessed 23 October 2017).

FEMA, 2019. Academic emergency management and related courses (AEMRC) for the higher education program. In: Floodplain Management: Principles and Current Practices. FEMA Emergency Management Institute. Chapter 4 Flood Risk Assessment, Federal Emergency Management Agency, Accessed at: training.fema.gov/hiedu/aemrc/courses.

Fioriti, V., D'Agostino, G., Bologna, S., 2010. On modeling and measuring inter- dependencies among critical infrastructures. In: Proc. Complexity in Engineering: COMPENG, pp. 85–87.

Fischbach, J.R., Johnson, D.R., Kuhn, K., Pollard, M., Stelzner, C., Costello, R., Molina, E., Sanchez, R., Syme, J., Roberts, H., Cobell, Z., 2017. 2017 Coastal Master Plan Modeling: Attachment C3-25: Storm Surge and Risk Assessment. Version Final, Coastal Protection and Restoration Authority, Baton Rouge, Louisiana, p. 219. Accessed at: coastal.la.gov/resources/library.

Fisher, L., 2013. Preparing for Future Catastrophes. International Risk Governance Council (IRGC), Lausanne, ISBN: 978-2-9700772-3-7. Accessed at: irgc.org/wpcontent/uploads/2018/09/CN_Prep.-for-Future-Catastrophes_final_11March13.pdf.

Franz, K.J., Sorooshian, S., 2002. Verification of National Weather Service Probabilistic Hydrologic Forecasts, Final Report. Department of Hydrology and Water Resources, The University of Arizona, Tucson, Arizona. Grant Number 40-AA-NW-217447.

GAO, 2017. Report to congressional addressees GAO-18-472. In: 2017 Hurricanes and wildfires, Initial Observations on the Federal Response and Key Recovery Challenges, p. 3.

Gheorghe, A.V., Schlapfer, M., 2006. Ubiquity of digitalization and risks of inter- dependent critical infrastructures. In: Proceedings of the IEEE International Conference on Systems, Man, and Cybernetics. vols. 1–6, pp. 580–584.

Hegger, D.L.T., Driessen, P.P.J., Bakker, M.H.N. (Eds.), 2016. A View on More Resilient Flood Risk Governance: Key Conclusions of the STAR-FLOOD Project. STAR-FLOOD Consortium, Utrecht, The Netherlands, ISBN: 978-94-91933-13-4.

IAEA, 2019. Adapting the Energy Sector to Climate Change. International Atomic Energy Agency Report STI/PUB/1847, Vienna, Austria, ISBN: 978-92-0-100919-7.

IRGC, 2006. Managing and Reducing Social Vulnerabilities From Coupled Critical Infrastructures. White Paper #3, International Risk Governance Council, Geneva, Switzerland.

IRMI, 2019. International Risk Management Institute Inc., Dallas, Texas. Accessed 6/2019 at: www.irmi.com/term/insurance-definitions/act-of-god.

Jaynes, E.T., 2003. In: Bretthorst, G.L. (Ed.), Probability Theory: The Logic of Science. Cambridge University Press. ISBN 0-521-59271-2.

Johansson, J., Hassel, H., 2010. An approach for modeling interdependent infrastructures in the context of vulnerability analysis. Reliab. Eng. Syst. Saf. 95 (12), 1335–1344.

Jorissen, R., Kraaij, E., Tromp, E., 2016. Dutch flood prevention policy and measures based on risk assessment. In: Proceedings of the 3rd European Conference on Flood Risk Management, E3S Web of Conferences. vol. 7, p. 20016, https://doi.org/10.1051/e3sconf/20160720016. Open access article.

Klein, R., 2011. The EU FP6 integrated project IRRIIS on dependent critical infrastructures—summary and conclusions. In: Xenakis, C., Wolthusen, S.D. (Eds.), Proceedings of the 5th International Workshop, CRITIS 2010. Springer, Athens, Greece, pp. 26–42.

Kroger, W., Zio, E., 2011. Vulnerable Systems. Springer Science & Business Media, ISBN: 978-0-85729-655-9, p. 204.

Kundzewicz, Z.W., Pińskwar, I., Brakenridge, G.R., 2012. Large floods in Europe, 1985–2009. Hydrol. Sci. J. https://doi.org/10.1080/02626667.2012.745082.

Kundzewicz, Z.W., Kanae, S., Seneviratne, I., Handmer, J., Nicholls, N., Peduzzi, P., Mechler, R., Bouwer, L.M., Arnell, N., Mach, K., Muir-Wood, R., Brakenridge, G., Kron, W., Benito, G., Honda, Y., Takahashi, K., Sherstyukov, B., 2013. Hydrological Sciences Journal: flood risk and climate change: global and regional perspectives. Hydrol. Sci. J. https://doi.org/10.1080/02626667.2013.857411.

Langat, P., Langat, K., Kuma, L., Koech, R., 2019. Identification of the most suitable probability distribution models for maximum, minimum, and mean streamflow. Water 11, 734. https://doi.org/10.3390/w11040734. 24 p, Accessed at: www.mdpi.com/journal/water.

Luiijf, E., Nieuwenhuijs, A., Klaver, M., van Eeten, M., Cruz, E., 2009. Empirical findings on critical infrastructure dependencies in Europe. In: Setola, R., Geretshuber, S. (Eds.), Critical Information Infrastructure Security. Springer, Berlin Heidelberg, pp. 302–310.

Ma, Z., Parisi, C., Zhang, H., Mandelli, D., Blakely, C., Yu, J., Youngblood, R., Anderson, N., 2018. Plant-level scenario-based risk analysis for enhanced resilient PWR – SBO and LBLOCA. Report INL/EXT-18-51436. U.S. Department of Energy, Office of Nuclear Energy.

Matczak, P., Wiering, M., Lewandowski, J., Schellenberger, T., Trémorin, J.-B., Crabbé, A., Ganzevoort, W., Kaufmann, M., Larrue, C., Liefferink, D., Mees, H., 2016. Comparing flood risk governance in six European countries: strategies, arrangements and institutional dynamics (report no. D4.1). STAR-FLOOD Consortium, Utrecht, The Netherlands.

McNutt, M., Mote, C.D., Dzau, V.J., 2019. National Academies Presidents Affirm the Scientific Evidence of Climate Change. Washington, DC.

Montz, B.E., Tobin, G.A., Hagelman III, R.R., 2017. Natural Hazards: Explanation and Integration. Guilford Publications, New York, NY, ISBN: 9781462529179, p. 445.

NAS, 2019. US National Academies of Sciences, Engineering, and Medicine, Building and Measuring Community Resilience: Actions for Communities and the Gulf Research Program. The National Academies Press, Washington, DC, https://doi.org/10.17226/25383.

NIAC, 2018. Surviving a Catastrophic Power Outage. President's National Infrastructure Advisory Council, Washington, DC. Accessed at: www.dhs.gov/national-infrastructure-advisory-council.

NOAA, 2019. U.S. Billion-Dollar Weather & Climate Disasters 1980–2017. https://www.ncdc.noaa.gov/billions/accessed.

Ouyang, M., 2014. Review on modeling and simulation of interdependent critical infrastructure systems. Reliab. Eng. Syst. Saf. 121, 43–60.

Panteli, M., Mancarella, P., 2015. Influence of extreme weather and climate change on the resilience of power systems: impacts and possible mitigation strategies. Electr. Power Syst. Res. 127, 259–270.

Perica, S., Martin, D., Pavlovic, S., Roy, I., St, M., Laurent, C., Trypaluk, D., Unruh, M.Y., Bonnin, G., 2013. Rainfall frequency Atlas of the United States for Durations from 30 minutes to 24 hours and return periods from I to 100 years, NOAA Atlas 14. In: Precipitation-Frequency Atlas of the United States, Volume 9 Version 2.0: Southeastern States (Alabama, Arkansas, Florida, Georgia, Louisiana, Mississippi). U.S. Department of Commerce, National Oceanic and Atmospheric Administration, National Weather Service, Silver Spring, Maryland. Technical paper no. 40.

Pescaroli, G., Alexander, D., 2016. Critical infrastructure, panarchies and the vulnerability paths of cascading disasters. Nat. Hazards 82 (1), 175–192.

Popov, P., 2009. PIA: 2009, FARA (Probabilistic Interdependency Analysis: Framework, Data Analysis and On-Line Risk Assessment). City University, London. http://www.city.ac.uk/centre-for-software-reliability/research/research-projects/piafara-probabilistic-interdependency-analysis-framework-data-analysis-and-on-line-risk-assessment.

Rinaldi, S.M., Peerenboom, J.P., Kelly, T.K., 2001. Identifying, understanding, and analyzing critical infrastructure interdependencies. IEEE Control. Syst. 21 (6), 11–25.

Sandoval, C.E., Raynal-Villaseñor, J., 2008. Trivariate generalized extreme value distribution in flood frequency analysis. J. Hydrol. Sci. 53 (3), 550–567. https://doi.org/10.1623/hysj.53.3.550.

Schweckendiek, T., 2013. Dutch Approach to Levee Reliability and Flood Risk, PFHA Workshop. Deltares & Delft University of Technology, Washington DC. US NRC access # ML13057A730.

Shukla, R.K., Trivedi, M.K., 2010. On the proficient use of GEV distribution: a case study of subtropical monsoon region in India. Ann. Univ. Tibiscus Comp. Sci., 81–92. Anale. Seria Informatică. Vol. VIII fasc. I—2010 Annals. Computer Science Series. 8th Tome 1st Fasc. Accessed at: arxiv.org/pdf/1203.0642.pdf.

Svendsen, N.K., Wolthusen, S.D., 2007. Connectivity models of interdependency in mixed-type critical infrastructure networks. Inf. Secur. Tech. Rep. 12 (1), 44–55.

Talukdar, S., Apt, J., MIlic, D., Lave, B., Morgan, M.G., 2003. Cascading failures: survival versus prevention. Electr. J., 25–31. https://doi.org/10.1016/j.tej.2003.09.003.

TEPCO, 2012. Fukushima nuclear accident analysis report. In: Japanese Government Report to IAEA Ministerial Conference on Nuclear Safety, Vienna, Austria. Tokyo Electric Power Company, Tokyo, Japan.

Thompson, D.D.P., 2012. Leveraging learning to improve disaster management outcomes. Int. J. Disast. Risk Sci. 3 (4), 195–206.

UK EA, 2009. Flooding in England: A National Assessment of Flood Risk. Bristol UK www.environment-agency.gov.uk. Accessed at: assets.publishing.service.gov.uk/government/file/292928.

Utne, I.B., Hokstad, P., Vatn, J., 2011. A method for risk modeling of interdependencies in critical infrastructures. Reliab. Eng. Syst. Saf. 96 (6), 671–678.

Vespignani, A., 2010. Complex networks: the fragility of interdependency. Nature 464 (7291), 984–985.

Wang, S., Hong, L., Chen, X., Zhang, J., Yan, Y., 2011. Review of interdependent infrastructure systems vulnerability analysis. In: Intelligent Control and Information Processing (ICICIP), pp. 446–451.

Wang, C., Ten, C., Hou, Y., Ginter, A., 2017. Cyber inference system for substation anomalies against alter-and-hide attacks. IEEE Trans. Power Syst. 32 (2), 896–909.

Wing, O.E.J., Bates, P.D., Smith, A.M., Sampson, C.C., Johnson, K.A., Fargione, J., Morefield, P., 2018. Estimates of present and future flood risk in the conterminous United States. Environ. Res. Lett. 13. https://doi.org/10.1088/1748-9326/aaac65, 034023.

Yao, S., Wang, P., Zhao, T., 2019. Transportable energy storage for more resilient distribution systems with multiple microgrids. IEEE Trans. Smart Grid 10 (3), 3331–3341.

Zio, E., 2016. Challenges in the vulnerability and risk analysis of critical infrastructures. Reliab. Eng. Syst. Saf. 152, 137–150.

Further reading

Asquith, W., Kiang, J., Cohn, T., 2017. Application of At-Site Peak-Streamflow Frequency Analyses for Very Low Annual Exceedance Probabilities. Scientific Investigations Report 2017-5038, US Geological Survey, https://doi.org/10.3133/sir20175038.

Barthélemy, M., 2011. Spatial networks. Phys. Rep. 499 (1), 1–86.

Espinoza, S., Panteli, M., Mancarella, P., Rudnick, H., 2016. Multi-phase assessment and adaptation of power systems resilience to natural hazards. Electr. Power Syst. Res. 136, 352–361. https://doi.org/10.1016/j.epsr.2016.03.019.

Lee, R.M., Assante, M.J., Conway, T., 2016. Analysis of the Cyber Attack on the Ukrainian Power Grid: Defense Use Case, E-ISAC Report. Electricity Information Sharing and Analysis Center, Industrial Control Systems, Washington, DC. Accessed at: ics.sans.org/media/E-ISAC_SANS_Ukraine_DUC_5.pdf.

Index

Note: Page numbers followed by *f* indicate figures and *t* indicate tables.

A

Adaptive robust optimization (ARO)-based mathematical framework, 223
Air pollution abatement, 131
American Recovery and Reinvestment Act, 191
Asynchronous Regional Regression Modeling (ARRM), 16–17
Atmosphere-ocean general circulation models (AOGCMs), 13
Atmospheric angular momentum (AAM), 47

B

BNUESM model, 111

C

CANESM2M model, 111
Catastrophic power outages, 227
CIs. *See* Critical infrastructures (CIs)
Clean Energy Standard (CES), 192–193
Climate Action Plans (CAPs), United States, 5
  content analysis, 199, 199*t*
  data collection, 195
  GHG emissions, 203–206, 207*f*
  interviews, 199, 200*t*
  localities' climate mitigation methods, 195–197
  nature, 203–204
  spatial distribution, 197–198
  status, 197–206
Coastal city's climate change adaptation
  accommodation measures, 150–162, 155–163*t*
  climate risks, 147–148
  managed retreat, 163–164, 164*t*
  methodology, 146–147, 147*f*
  protection measures, 150, 153–155*t*
  typologies, 146, 149, 149*f*, 151–152*t*
Convection heat, 28
Convection-permitting dynamical downscaling, 42–44
Convective available potential energy (CAPE), 39
Coordinated Regional Climate Downscaling Experiment (CORDEX) program, 13
Cost-benefit analysis, 232–233
Coupled model intercomparison project phase five (CMIP5), 14–15
Critical infrastructures (CIs)
  climate change, 217–219
  emergency response and system recovery, 227–228
  flood and outage risk, 221–222
  interdependencies, 215, 216*f*
  management responsibilities, 232–233
  network perspective, 113
  resilience
    definition, 222–223
    improvement claims, 231–232
    power outages, 223–227
    quantification, 222–223
  risk assessment and complexity, 219–221, 220*f*
  risk improvements, 232–233
  vulnerability, 216–217

D

Damaging convective wind gusts. *See* Severe convective storms (SCSs)
Deterministic models, 30–31
Drought, 58
Dynamical downscaling, 17–18

E

Earth Summit, 194
Earth system models, 13
Electrical power grid. *See* Critical infrastructures (CIs)
El-Niño Southern Oscillation (ENSO), 45
Emergency system (ES) failure rates, 228–231, 230*f*
Empirical models, 30–31
Energy balance models, 12
Energy Efficiency and Conservation Block Grant (EECBG) Program, 191
Ensemble modeling, 14–15
Environmental Protection Agency (EPA), 190–191
European Reference Network for Critical Infrastructure Protection and a Thematic Area, 220
Extreme climatic events, 1, 59–61, 60*t*
eXtreme Gradient Boosted (XGBoost) DT models, 97
Extremely hot weather. *See* Temperature extremes

F

Federal Emergency Management Agency (FEMA) National Flood Insurance Program, 221
Flood alert, 85, 85*f*
Flood Early Warning Systems (FWS), 3
Flood monitoring system, 91–92
Flood warning system (FWS), 84
  challenges and future, 99–100
  communications, 99
  data-driven (DD) approaches, 97–98

Flood warning system (FWS) *(Continued)*
gauge network hardware and software, 86–87
hydrologic and hydraulic modeling, 88–91
methodology, 85–91
precipitation measurements, 87–88
radar-based, 92–97
Fraser River, Canada, 31
Fukushima nuclear events, 228–231

G

General circulation models, 13
Generalized extreme value (GEV) distribution, 108
GFDLESM2M model, 113
Global circulation model (GCM), 26–27, 30
Global climate models (GCMs), 12–13
Global Climate Protection Act of 1987, 189
Global warming, 1, 3–4
Greenhouse gas (GHG) emissions, 1, 125
Green infrastructure
benefits, 134–136
biodiversity and pollinator support, 133–134
building energy efficiency, 134
carbon reduction and sequestration, 132–133
characteristics, 127–129
economic benefits, 135
functions, 129–134
health benefits, 135–136
nomenclature, 136–137
stormwater management, 133
temperature regulation, 131–132

H

Heat Source model, 31
Hot-dry events, 26, 32
Hurricane Katrina (CAT 4) nuclear events, 220–221, 228–232
Hybrid models, 30, 32
Hydroclimate extremes, 105–106
Hydrological modeling, 3–4

I

Indian Railways Network (IRN)
network data gathering, 114–115
robustness and recovery characteristics, 118
visualizing and analyzing networks, 115–117
Integrated assessment models (IAMs), 14
Integrated systems failure rate, 229
International Council for Local Environmental Initiatives (ICLEI), 188
Iowa flood information system (IFIS), 93–94
Island of Oahu, Hawaii, 1

K

Kyoto Protocol, 187–188, 191–192

L

Large hail. *See* Severe convective storms (SCSs)
Latent heat, 28
Localized Constructed Analogs (LOCA), 17
Longwave radiation fluxes, 27

M

Machine Learning Flood Warning System, 97, 98*f*
Madden-Julian oscillation (MJO), 45–47
Mayors Climate Protection Agreement (MCPA), 187–188
MIROCESM model, 113
MLG. *See* Multilevel governance (MLG)
MPIESMLR model, 113
MPIESMMR model, 113
Multilevel governance (MLG), 171–172, 172*f*
approaches, 175
boundary, 174–175
climate adaptation, 176–177
barriers, 180
power interplay, 178–179
research trends, 177–180
structure and process, 177–178
concept, 172–174
framework, 208
inclusiveness, 174
Mumbai Railways Network (MRN)
network data gathering, 114–115
robustness and recovery characteristics, 118
visualizing and analyzing networks, 115–117

N

National water model (NWM), 93
National Weather Service (NWS), 85
Natural Flow Paradigm Approach, 26
Nature-based solutions, 125–126
Net metering renewable energy mandate, 192–193
Net primary productivity (NPP), 60–61
global change drivers, 71–72
interannual timescales, 61–67
intra and interannual interactions, 69–70
intraannual timescales, 67–70
plant community dynamics, 70–71
recovery dynamics, 71
uncertainties, 70–72
within-ecosystem responses, 64–67
Next Generation Weather Radar (NEXRAD) system, 87
NOAA's Storm Prediction Center (SPC), 48
NORESM model, 113

P

Paris Climate Agreement, 187
Precipitation (PPT) extremes
  carbon cycling, 58–59
  changes to, 57
  characteristics, 70
  cross-site distributed experiments, 72–73
  definition, 59–61
  ecosystem models with ecological experiments, 73–74
  net primary productivity (NPP)
    global change drivers, 71–72
    interannual timescales, 61–67
    intra and interannual interactions, 69–70
    intraannual timescales, 67–70
    plant community dynamics, 70–71
    recovery dynamics, 71
    uncertainties, 70–72
    within-ecosystem responses, 64–67
Precipitation extremes volatility index (PEVI), 106, 109
Probability of extended systems failure, 230, 230*f*

R

Radiative convective models, 12
Regional circulation model (RCM), 26–27
Regional climate model (RCM), 13–14
Renewable Portfolio Standards (RPS), 192–193
Return levels, 108–109
River temperature extremes
  fisheries management, 25–26
  heat fluxes, 26, 27*f*
  past and current trends, 29–30
  thermal modeling, 30–34

S

Salmonids, 25–26
Sea level rise (SLR), 145. *See also* Coastal city's climate change adaptation
Sensible heat, 28
Severe convective storms (SCSs)
  climate change, 41–44, 48–49
  convection-permitting dynamical downscaling, 42–44
  environments, 41
  forecasting, 48
  interannual variability, 44–48
  losses, 39, 40*f*
  observations, 40–41
  trends, 40–41
Simple regression models, 31
Solar Power Purchase Agreement (SPPA), 192–193
Spatiotemporal variability, 110–113
Statistical downscaling, 15–17
Stormwater management, 133
Streambed heat flux, 28

T

Tea Party movement, 193–194
Temperature extremes
  downscaling techniques, 15–18
  impacts, 10
  metrics and indices, 11
  mitigation and adaptation strategies, 19–21
    strategy evaluation, 19–21
  observational analysis, 11–12
  temperature projection, 12–18
Texas Medical Center-Rice University flood alert system, 94–97
Today's Earth Japan (TE-Japan), 84–85
Tornadoes. *See* Severe convective storms (SCSs)
Trend analysis, 109–110

U

United Nations Conference on Environment and Development, 194
United States climate change policy and politics
  CAPs
    content analysis, 199, 199*t*
    data collection, 195
    GHG emissions, 203–206, 207*f*
    interviews, 199, 200*t*
    localities' climate mitigation methods, 195–197
    nature, 203–204
    spatial distribution, 197–198
    status, 197–206
  local level, 193–195
  national level, 189–192
  state level, 192–193
Unweighted ensemble simulation, 15

W

Water temperature extremes. *See* River temperature extremes
Weather parameters, 2–3
Weather-related natural catastrophes, 1
Weighted ensemble simulation, 15